


1990

Excited state structure, energy and electron transfer dynamics of photosynthetic reaction centers: a hole burning study

Deming Tang
Iowa State University

Follow this and additional works at: <https://lib.dr.iastate.edu/rtd>

 Part of the [Biochemistry Commons](#), and the [Physical Chemistry Commons](#)

Recommended Citation

Tang, Deming, "Excited state structure, energy and electron transfer dynamics of photosynthetic reaction centers: a hole burning study" (1990). *Retrospective Theses and Dissertations*. 9414.
<https://lib.dr.iastate.edu/rtd/9414>

This Dissertation is brought to you for free and open access by the Iowa State University Capstones, Theses and Dissertations at Iowa State University Digital Repository. It has been accepted for inclusion in Retrospective Theses and Dissertations by an authorized administrator of Iowa State University Digital Repository. For more information, please contact digirep@iastate.edu.

01

00502

U·M·I

MICROFILMED 1990

INFORMATION TO USERS

The most advanced technology has been used to photograph and reproduce this manuscript from the microfilm master. UMI films the text directly from the original or copy submitted. Thus, some thesis and dissertation copies are in typewriter face, while others may be from any type of computer printer.

The quality of this reproduction is dependent upon the quality of the copy submitted. Broken or indistinct print, colored or poor quality illustrations and photographs, print bleedthrough, substandard margins, and improper alignment can adversely affect reproduction.

In the unlikely event that the author did not send UMI a complete manuscript and there are missing pages, these will be noted. Also, if unauthorized copyright material had to be removed, a note will indicate the deletion.

Oversize materials (e.g., maps, drawings, charts) are reproduced by sectioning the original, beginning at the upper left-hand corner and continuing from left to right in equal sections with small overlaps. Each original is also photographed in one exposure and is included in reduced form at the back of the book.

Photographs included in the original manuscript have been reproduced xerographically in this copy. Higher quality 6" x 9" black and white photographic prints are available for any photographs or illustrations appearing in this copy for an additional charge. Contact UMI directly to order.

U·M·I

University Microfilms International
A Bell & Howell Information Company
300 North Zeeb Road, Ann Arbor, MI 48106-1346 USA
313/761-4700 800/521-0600



Order Number 9100502

**Excited state structure, energy and electron transfer dynamics
of photosynthetic reaction centers: A hole burning study**

Tang, Deming, Ph.D.

Iowa State University, 1990

U·M·I

**300 N. Zeeb Rd.
Ann Arbor, MI 48106**



**Excited state structure, energy and electron transfer dynamics
of photosynthetic reaction centers: A hole burning study**

by

Deming Tang

**A Dissertation Submitted to the
Graduate Faculty in Partial Fulfillment of the
Requirements for the Degree of
DOCTOR OF PHILOSOPHY**

**Department: Chemistry
Major: Physical Chemistry**

Approved:

Signature was redacted for privacy.

In ~~Charge~~ of Major Work

Signature was redacted for privacy.

For the Major Department

Signature was redacted for privacy.

For the Graduate College

**Iowa State University
Ames, Iowa**

1990

TABLE OF CONTENTS

| | Page |
|--|------|
| EXPLANATION OF DISSERTATION FORMAT | vi |
| GENERAL INTRODUCTION | 1 |
| <i>Photosynthesis</i> | 1 |
| <i>Hole Burning Spectroscopy</i> | 7 |
| REFERENCES | 13 |
| SECTION I. PHOTOCHEMICAL HOLE BURNING STUDIES OF BACTERIAL PHOTOSYNTHETIC REACTION CENTERS | |
| | 16 |
| INTRODUCTION | |
| | 17 |
| EXPERIMENTAL METHODS | |
| | 23 |
| <i>Sample Preparation</i> | 23 |
| <i>Cryogenic Equipment</i> | 24 |
| <i>Experimental Techniques</i> | 24 |
| PAPER I. STRUCTURED HOLE BURNED SPECTRA OF THE PRIMARY DONOR STATE ABSORPTION REGION OF <i>Rhodopseudomonas Viridis</i> | |
| | 29 |
| ABSTRACT | |
| | 31 |
| INTRODUCTION | |
| | 32 |
| EXPERIMENTAL | |
| | 36 |
| <i>Sample Preparation</i> | 36 |
| <i>Measurements</i> | 36 |
| RESULTS | |
| | 39 |
| <i>Transient Photochemical Hole Burning</i> | 39 |
| <i>Chemically Reduced Reaction Centers</i> | 48 |
| DISCUSSION | |
| | 54 |

| | |
|--|-----|
| <i>Broad Structure in the Transient Hole Spectra of P960</i> | 54 |
| <i>The Zero-phonon Hole in the Transient Hole Spectra of P960</i> | 57 |
| <i>Dynamical Implications of the Zero-phonon Hole</i> | 59 |
| <i>Earlier Related Studies</i> | 62 |
| CONCLUDING REMARKS | 65 |
| ACKNOWLEDGEMENT | 67 |
| REFERENCES | 68 |
| | |
| PAPER II. STRUCTURE AND MARKER MODE OF THE PRIMARY ELECTRON DONOR STATE ABSORP- TION OF PHOTOSYNTHETIC BACTERIA: HOLE BURNED SPECTRA | 72 |
| ABSTRACT | 74 |
| INTRODUCTION | 75 |
| EXPERIMENTAL | 78 |
| <i>Sample Preparation</i> | 78 |
| <i>Measurements</i> | 78 |
| RESULTS AND DISCUSSION | 81 |
| <i>Transient Hole Burned Spectra of P870 and P960</i> | 84 |
| <i>Zero-phonon Holewidths</i> | 95 |
| <i>Site Excitation Energy Correlation Effects in the Transient Spectra</i> | 97 |
| FURTHER DISCUSSION | 102 |
| ACKNOWLEDGEMENT | 105 |
| REFERENCES | 106 |
| | |
| PAPER III. PRIMARY DONOR STATE MODE STRUCTURE AND ENERGY TRANSFER IN BACTERIAL REAC- TION CENTERS | 109 |
| ABSTRACT | 111 |
| INTRODUCTION | 112 |
| EXPERIMENTAL | 115 |
| RESULTS | 116 |

| | |
|--|-----|
| <i>Simulations and Temporal Evolution of the P870 and P960 Hole Profiles</i> | 116 |
| <i>Transient Spectra for Excitation into Accessory Pigment Bands,</i> | |
| <i>Absence of Line Narrowing</i> | 125 |
| DISCUSSION | 132 |
| CONCLUSION | 137 |
| ACKNOWLEDGEMENT | 138 |
| REFERENCES | 139 |
| | |
| CONCLUSIONS | 142 |
| REFERENCES | 144 |
| | |
| SECTION II. PHOTOCHEMICAL HOLE BURNING STUDIES | |
| OF REACTION CENTER OF PHOTOSYSTEM | |
| II | 148 |
| INTRODUCTION | 149 |
| EXPERIMENTAL METHODS | 153 |
| <i>Sample Preparation</i> | 153 |
| <i>Cryogenic Equipment</i> | 154 |
| <i>Experimental Techniques</i> | 154 |
| | |
| PAPER IV. TRANSIENT AND PERSISTENT HOLE BURNING | |
| OF REACTION CENTER OF PHOTOSYSTEM II | 160 |
| ABSTRACT | 162 |
| INTRODUCTION | 163 |
| EXPERIMENTAL | 166 |
| <i>Preparation of the PS II Reaction Center Complex</i> | 166 |
| <i>Measurements</i> | 167 |
| RESULTS | 170 |
| DISCUSSION | 178 |
| CONCLUDING REMARKS | 184 |
| ACKNOWLEDGEMENT | 186 |
| REFERENCES | 187 |

| | |
|--|------------|
| PAPER V. EXCITED STATE STRUCTURE AND ENERGY TRANSFER DYNAMICS OF TWO DIFFERENT PREPARATIONS OF THE REACTION CENTER OF PHOTOSYSTEM II: A HOLE BURNING STUDY | 190 |
| ABSTRACT | 192 |
| ACKNOWLEDGEMENT | 205 |
| REFERENCES | 206 |
| | |
| PAPER VI. EFFECTS OF DETERGENT ON THE EXCITED STATE STRUCTURE AND RELAXATION DY- NAMICS OF THE PHOTOSYSTEM II REACTION CENTER: A HIGH RESOLUTION HOLE BURNING STUDY | 209 |
| ABSTRACT | 211 |
| INTRODUCTION | 212 |
| EXPERIMENTAL | 215 |
| RESULTS | 218 |
| DISCUSSION | 229 |
| <i>Effects of Detergent</i> | <i>229</i> |
| <i>Other Aspects of the Hole Burned Spectra</i> | <i>231</i> |
| ACKNOWLEDGEMENT | 233 |
| REFERENCES | 234 |
| | |
| CONCLUSIONS | 237 |
| REFERENCES | 240 |
| | |
| ACKNOWLEDGEMENTS | 244 |

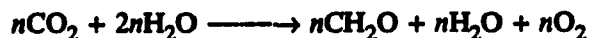
EXPLANATION OF DISSERTATION FORMAT

This dissertation contains the candidate's original work on spectral hole burning of bacterial photosynthetic reaction centers and green plant Photosystem II reaction center. It is arranged in two sections. Section I contains three published papers which describe the transient photochemical hole burning experiment performed on the purple bacterial reaction centers of *Rhodospseudomonas viridis* and *Rhodobacter sphaeroides*. Section II contains also three published papers which report the spectroscopic study on the reaction center of Photosystem II by both persistent and transient hole burning techniques. Each section contains an introduction, experimental methods, three papers and additional results. The references for the introduction, experimental methods and additional results are located at the end of that section. The references for each paper are found at the end of that paper.

GENERAL INTRODUCTION

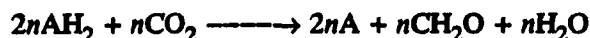
Photosynthesis

Photosynthesis is a process in which light energy is converted to chemical energy by green plants, algae and certain bacteria for synthesis of biological material. In plants, algae and the cyanobacteria, such events can be described by a simple chemical equation,



The importance of such events is most significant as they are directly related to the carbon assimilation and oxygen evolution processes. As our natural energy resources such as coal, oil, etc., diminished and global climate changes, inexorably mediated in part, by the increasing concentration of carbon dioxide, understanding the basic principles of such naturally occurring event is becoming a major task and challenge in the current scientific research.

Other bacteria are also capable of conducting photosynthesis which does not evolve oxygen. The overall process in these bacteria can be written as



where AH_2 represents an oxidizable agent such as hydrogen sulfide (H_2S). Perhaps, as many scientists believe, such events may have prehistorical significance for transforming earth from an anaerobic and "dry" environment into today's oxygen-rich and water-abundant biosphere. An important evolutionary link between the photosynthetic mechanisms of bacteria and green plants is believed to exist. Due to the simplicity in structure of single cell bacteria, the

photosynthetic mechanism of many bacterial species is being studied to a great extent.

The photosynthetic process is initiated through the absorption of light by chlorophyll type molecules (also named antenna molecules) [1,2,3] which are associated with certain protein complexes called light harvesting complexes in the thylakoid membrane of chloroplast [4]. The chlorophyll type molecules, of which there are at least nine different kinds, have rather similar structures (see Figure 1 for the structure of chlorophyll *a* molecule). These molecules play a significant role in light absorption by broadening their absorption band to increase the probability of capturing energies from photons [5-8].

The structures of the antenna molecules are uniquely organized with the assistance of the protein environment such that the energy absorbed through the excitation of antenna molecules is efficiently transferred with almost unity quantum yield [9-11]. Such a process is generally believed to be the result of excitons created by absorption of photons of interacting chromophores and their subsequent migration governed by a non-radiative resonance transfer mechanism [12]. Phonons, which include low frequency protein and pigment intramolecular modes, are also considered as important mediators in promoting such excitation transfer [12-15].

Charge separation occurs in a photosynthetic reaction center which serves as a "chemical trap" by collecting the excitation energy transferred from a nearby light harvesting antenna complex [2,3]. Contrary to bacterial reaction centers, green plants have two reaction centers, photosystem I (PS I) and photosystem II (PS II) [2,3,16] with each one performing a different function in the photosynthetic process. A Z-scheme which was originally proposed by Hill and Bendall [17], as shown in Figure 2, gives us a good overview of the functionality of two photosystems with their inter-connection in green plants. The primary process in

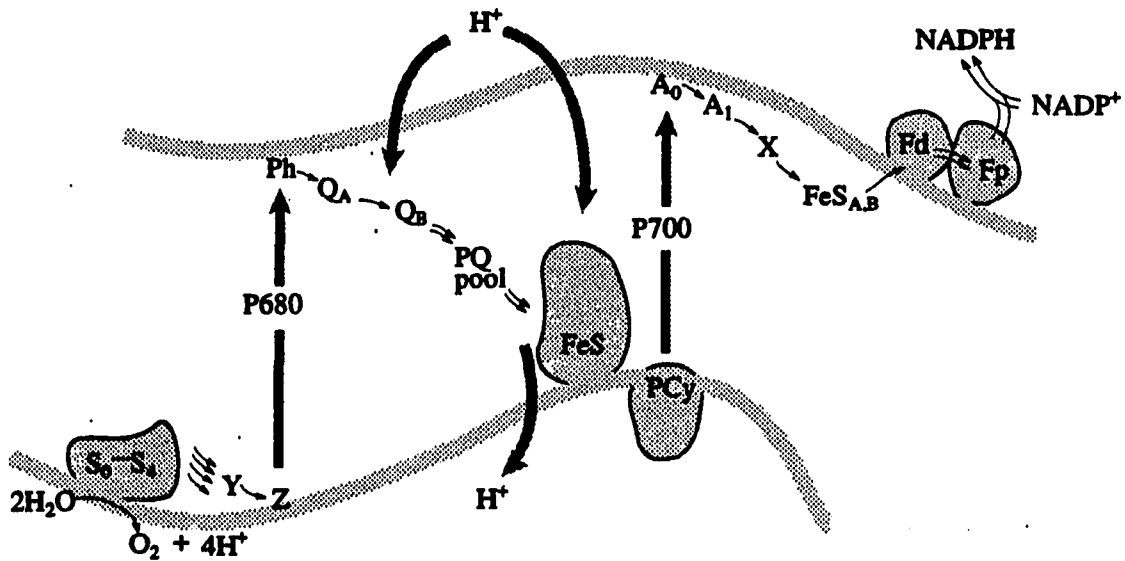


Figure 2.

A modified Z-scheme originally proposed by Hill and Bendall. Energy conversion by two step light reactions acting in series are thought to occur in chloroplasts from higher plants and oxygen-evolving organisms. Photosystem I uses a PED (P700) to transfer an electron to a low reduction potential monomer chlorophyll molecule (A₀) that quickly transfers it through a series of electron carriers, including several iron sulfur proteins (X, FeS_{A,B}, Fd) to NADP⁺ on the outside of the thylakoid membrane (thick shaded line). Photosystem II has a PED (P680) that receives electrons from a high potential tyrosine molecule (Z), an intermediate complex (Y), a Mn-containing water-splitting complex (S₀...S₄) and ultimately from water itself, which is oxidized and O₂ and H⁺ are released at the inside of thylakoid surface. Electrons donated from PS II through pheophytin (Ph) to bound quinones Q_A and Q_B are accumulated by a plastoquinone (PQ) pool. An iron sulfur (FeS) center associated in a complex with cytochrome *f* and b₆ was reduced subsequently, which in turn reduces soluble plastocyanin (PCy) that re-reduces P-700⁺. Associated with this intermediate electron transfer is the translocation of H⁺ from the outside to the inside of the thylakoid membrane. Several components (Q_B, Fp) are known to accumulate electron pairwise, and the water-splitting complex (S₀...S₄) accumulates four oxidizing equivalents

the reaction center, for many years, has stimulated discussions in its kinetics and functionality, specifically its connection with the spatial arrangement of the primary electron donor (PED). Important model systems consisting two Chl *a* molecules with C_2 symmetry were proposed by several authors [18-20] and received a great amount of attention [21]. With recent determination of structures for purple bacteria *Rhodospseudomonas viridis* (*Rps. viridis*) [22,23] and *Rhodobacter sphaeroides* (*Rb. sphaeroides*) [24,25], a pair of strongly interacting but not covalently connected bacteriochlorophyll molecules were found to constitute the PED. The PEDs are generally labeled by their room temperature absorption maximum such as the P960 of *Rps. viridis*, P870 of *Rb. Sphaeroides*, P700 of PS I and P680 of PS II. Figure 3 presents examples of low temperature absorption spectra of several reaction centers with their PED labeled. The interest of this thesis will focus onto the understanding of excited state structure of the PED and its decay kinetics in the reaction center. Such understanding is necessary as it provides a foundation for future research of mimicking photosynthesis by chemically synthesized molecular systems. The question of pigment assignments will be discussed in the papers presented in next two sections.

Charge separation in a photosynthetic reaction center occurs following the transfer of excitation from a nearby light harvesting antenna complex to a PED of the reaction center. The electrons created by the PED during the process are quickly transferred to a pheophytin molecule to constitute the primary electron transfer. The secondary electron/hole transfer is followed by such that other complexes in the membrane, which lacks photosynthetic pigments, process the holes and electrons to carry out important biochemical reactions. Those reactions in turn produce the ATP and NADPH required for carbon dioxide fixation and other metabolic processes. Unlike oxygen-evolving organisms such as green plants, purple and green

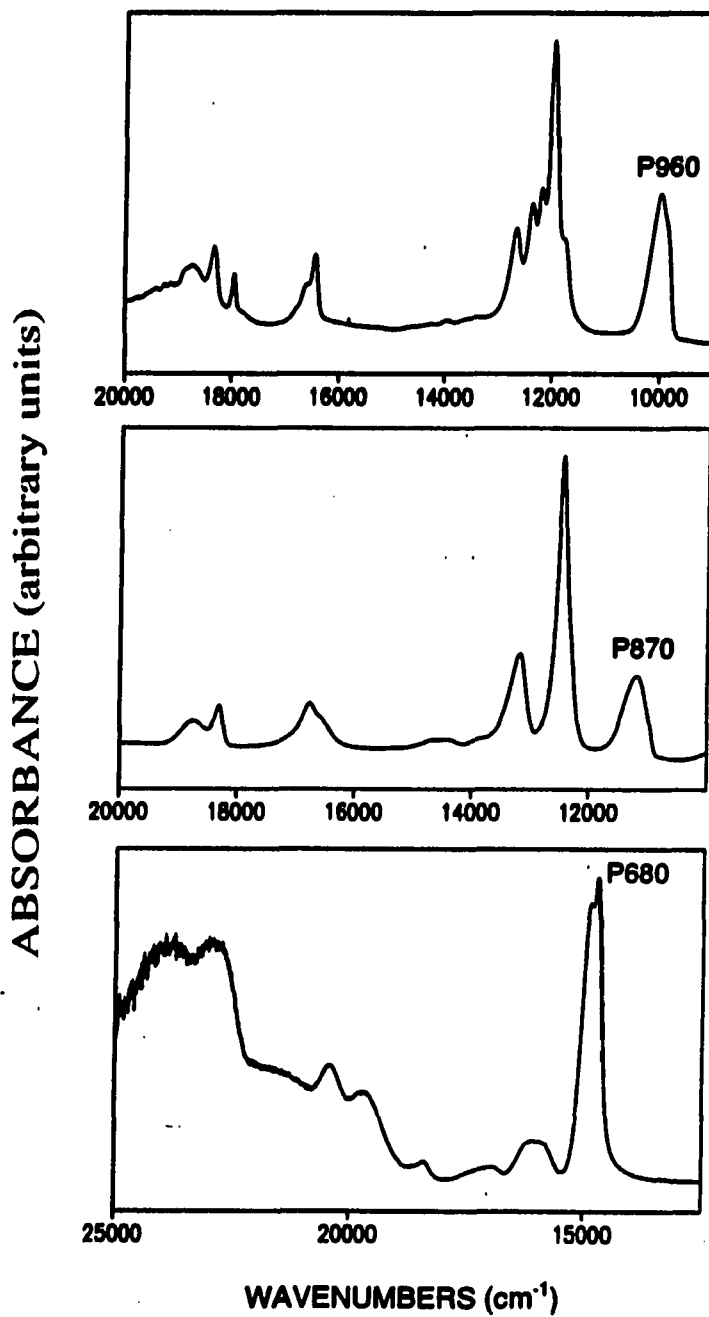


Figure 3. Absorption spectra of *Rps. viridis* (top), *Rb. sphaeroides* (middle) and Photosystem II RC (bottom)

photosynthetic bacteria have only one photosystem, but were suggested to produce the necessary ATP and NADH in a rather similar manner [26].

Hole Burning Spectroscopy

The task of this thesis is to study the primary process involving charge separation by PED, electronic excitation transport and electron transfer dynamics. Thus, important information such as excited state relaxation time, inter- and intramolecular vibration frequencies, low energy lattice (in this case protein) vibration (phonon) frequencies must be obtained in order to describe and understand the nature of the excited state structure and dynamics [27]. Conventional absorption and fluorescence spectroscopy are not adequate to study a complicated system such as reaction center due to the inhomogeneous broadening of its absorption spectrum induced by various factors such as temperature, protein environment, and solvent interaction.

A spectroscopic method which enables one to obtain information about a single site in an inhomogeneous broadened spectrum was first introduced in 1974 [28-30] and was named hole burning spectroscopy. The principle of this method is based on the interactions between host and guest molecules (also called impurity molecules). By doping impurity molecules into a perfect matrix as presented graphically in the Figure 4, extremely sharp absorption lines (equal to its homogeneous line width Γ_H) of the impurity molecules can be obtained due to the uniform microscopic environment surrounding the guest molecules. In contrast, if an amorphous host was used, a large degree of disorder is created because of the change of local environment of each impurity molecule (see Figure 4). Such a change gives rise to the

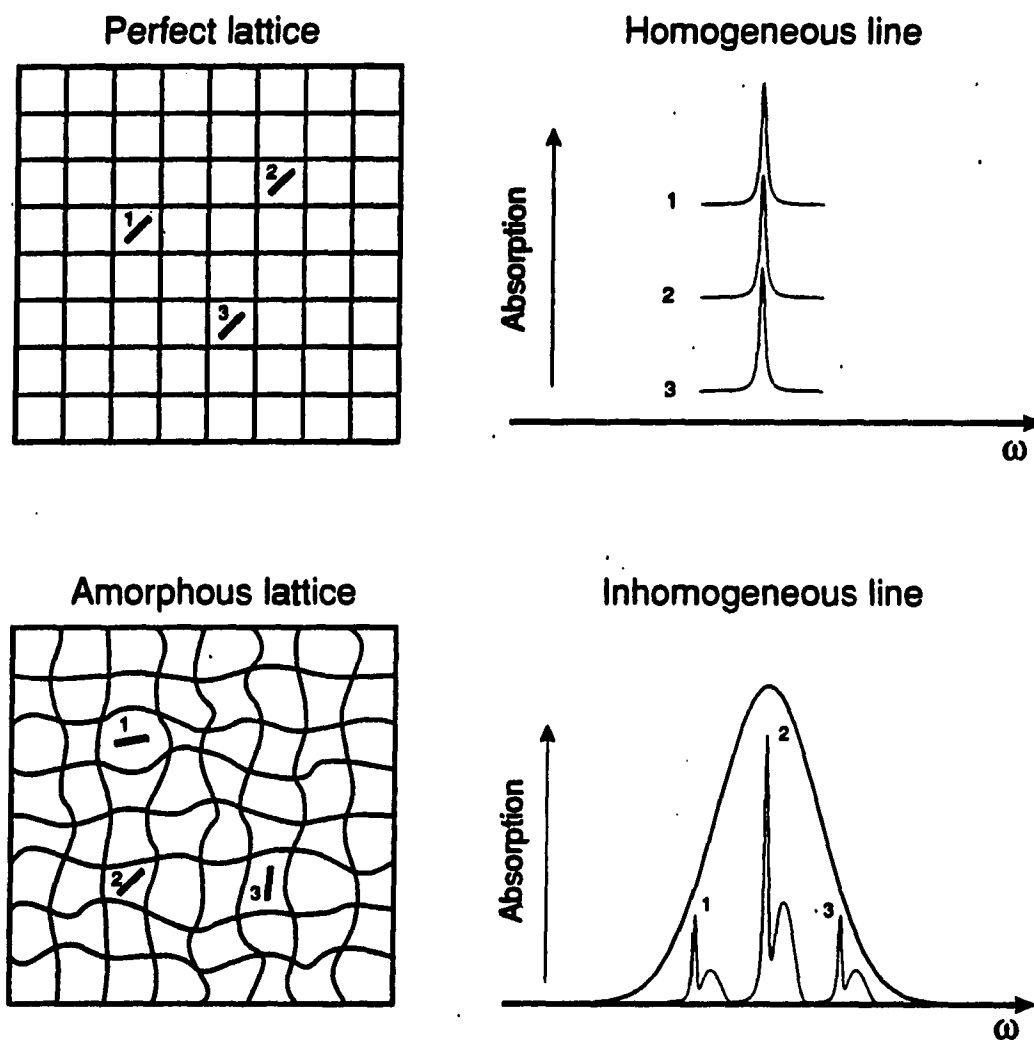


Figure 4. Optical absorption lines of three identical guest molecules in: (Top) an assumed perfect crystal, and (Bottom) an amorphous host. The broad sidebands represent phonon spectra of those molecules.

broadening of the guest molecules' absorption spectra (line width is described by Γ_p) due to the inhomogeneous distribution resulted from such disorder. If a narrow band laser (less than the homogeneous line width of the impurity molecule studied) is irradiated (or "burned") onto this broad absorption spectrum, a small dip (or "hole") corresponding to the laser frequency can be created. Because only an isochromat (subset of impurity sites whose homogeneous absorption profiles overlap the laser profile) of the impurity molecules are excited due to the narrow width of the laser, the hole thus carries the important information such as homogeneous line width.

The mechanism by which the hole was created varies. It can be generally categorized as either photochemical or nonphotochemical (sometimes also called photophysical). Photochemical hole burning, as the name implies, typically involves a reversible or irreversible photochemical reaction such as the electron transfer in RC of photosynthetic bacteria [31-34], PS II, [35-37] and the two photon photochemistry of dimethyl-*s*-tetrazine [38,39]. Unlike photochemical hole burning, nonphotochemical hole burning only involves the modification of the microscopic environment of the impurity molecules. The energies of the products created through this process (also called "anti-hole") are typically located very close to the burn frequency ($< 100 \text{ cm}^{-1}$) whereas in the case of photochemical hole burning, the products are located quite further away from the absorption profile [40,41] (typically greater than several hundred cm^{-1} , see Figure 5).

The homogeneous line width measured can be directly related to the excited state life time by the following expression [41,42],

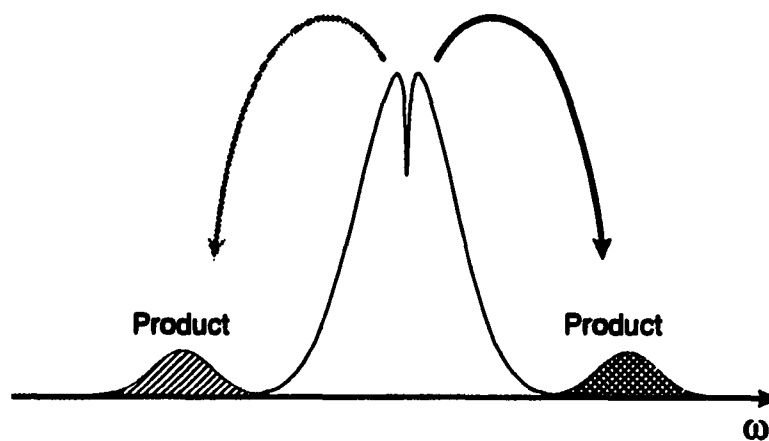
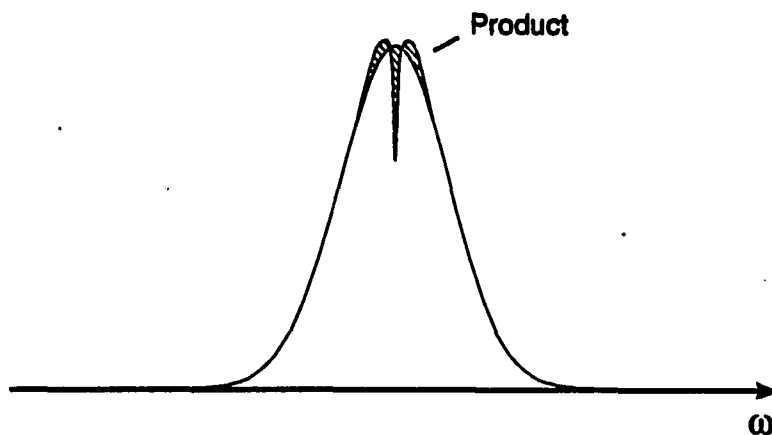
Photochemical Hole Burning (PHB)**Non-photochemical Hole Burning (NPHB)**

Figure 5. Spectral distribution of the photoproduct after photochemical (PHB) and non-photochemical (photophysical) (NPHB) hole burning

$$\frac{1}{T_2} = \frac{1}{2T_1} + \frac{1}{T_2^*}$$

where T_2 is the overall dephasing time for a homogeneous transition and can be described by equation $T_2 = \frac{1}{2\pi c\Gamma_h}$ (where c is the speed of light, Γ_h is the homogeneous line width which equals half of the full width at half maximum of the hole burned). T_1 is the excited state population decay time (or homogeneous life time) and T_2^* is a temperature dependent term governed by pure dephasing and spectral diffusion processes in the system. Extensive literature on spectral hole burning of π -molecular systems indicates that, at 1.6 K, the contribution of those processes to the holewidth is very small (typically $< 0.02 \text{ cm}^{-1}$) [42] and thus can be neglected if the hole burned is relatively broad. This is especially true in the case of hole burning on the photosynthetic reaction centers where hole widths of several wavenumbers were observed.

Holes can be also burned persistently or transiently depending on the characteristics of the system being studied. Persistent hole burning causes a phototransformation from which a new ground state configuration is produced. Depending on the lifetime of the new ground state, the hole burned in this case can last indefinitely at low temperature. If the new configuration is created by a radiationless process to a metastable state such as a triplet state, the process is considered transient since the hole will have to be measured before the relaxation of the metastable state to the ground state occurs. Both persistent and transient phenomena were observed and studied in this thesis.

In this thesis, hole burning spectroscopy was utilized in determining and understanding various processes such as the decay time and the structure of the primary donor state of the

several photosynthetic reaction centers as well as their coupling to the low frequency phonons of the protein-pigment complex. Brief literature reviews on this subject can be found in the introductions of Section I and II. Several other topics such as the study of energy transfer and effect of detergent on excited state electronic structure were also addressed.

REFERENCES

1. Emerson, R.; Arnold, W. J. *Gen. Physiol.* 1932, 15, 391;
Emerson, R.; Arnold, W. J. *Gen. Physiol.* 1932, 16, 191.
2. Govindjee; Govindjee, R. in *Bioenergetics of Photosynthesis*, Govindjee, Ed.; Academic Press: New York, 1975, p. 1.
3. Lawlor, D. W. in *Photosynthesis: Metabolism, Control, and Physiology*; Longman Scientific & Technical: New York, 1987.
4. Knox, R. S. in *Primary Molecular Events in Physiology* (NATO Advanced Study Institute, Badia Fiesolana, A. Ceccucci, R. A. Weale, Eds.), Elsevier: Amsterdam, 1973, pp. 45-77.
5. Seely, G. R., *J. Theor. Biology* 1973, 40, 173.
6. Glazer, A. N. *Annu. Rev. Biochem.* 1983, 52, 125.
7. Davis, R. C.; Ditson, S. L.; Fentiman, A. F.; Pearlstein, R. M. *J. Am. Chem. Soc.* 1981, 103, 6823.
8. Maggoria, L. L.; Maggoria, G. M. *Photochem. Photobiol.* 1984, 39, 847.
9. Lien, S.; San Pietro, A. in *An Inquiry into Biophotolysis of Water to Produce Hydrogen*; A report sponsored by NSF under RANN Grant G140253, 1976.
10. Sauer, K. in *Bioenergetics of Photosynthesis*, Govindjee, Ed.; Academic Press: New York, 1975, p. 115-181.
11. Staehelin, L. A.; Arntzen, C. J. *J. Cell Biol.* 1983, 97, 1327.
12. Sauer, K. in *Encyclopedia of Plant Physiology*, L. A. Staehelin, C. J. Arntzen, Eds.;

Springer-Verlag: Berlin, 1986, Vol. 19, pp. 85-97 and literature cited therein.

13. Gillie, J. K.; Fearey, B. L.; Hayes, J. M.; Small, G. J. *Chem. Phys. Lett.* 1987, 134, 316.
14. Hayes, J. M.; Gillie, J. K.; Tang, D.; Small, G. J. *Biochim. Biophys. Acta* 1988, 932, 287.
15. Gillie, J. K. Ph.D dissertation, Iowa State University, 1989.
16. Mauzerall, D.; Greenbaum, N. L. *Biochim. Biophys. Acta* 1989, 974, 119.
17. Hill, R.; Bendall, F. *Nature* 1960, 186, 136.
18. Shipman, L. L.; Cotton, T. M.; Norris, J. R.; Katz, J. J. *Proc. Natl. Acad. Sci. USA* 1976, 93, 1791.
19. Boxer, S. G.; Closs, G. L. *J. Am. Chem. Soc.* 1976, 98, 5406.
20. Fong, F. K. *Proc. Natl. Acad. Sci. USA* 1974, 71, 3692.
21. Fong, F. K. *J. Theo. Biol.* 1974, 46, 407.
22. Deisenhofer, J.; Epp, O.; Miki, K.; Huber, R.; Michel, H. *J. Mol. Biol.* 1984, 180, 385.
23. Deisenhofer, J.; Epp, O.; Miki, K.; Huber, R.; Michel, H. *Nature (London)* 1985, 318, 618.
24. Allen, J. P.; Feher, G.; Yeates, T. O.; Rees, D. C.; Deisenhofer, J.; Michel, H.; Huber, R. *Proc. Natl. Acad. Sci. USA* 1986, 83, 8589.
25. Chang, C. H.; Tiede, D.; Tang, J.; Smith, U.; Norris, J.; Schiffer, M. *FEBS Lett.* 1986, 205, 82.
26. Wraight, C. A. in *Photosynthesis: Energy Conservation by Plants and Bacteria*, Vol. I, Govindjee, ed., Academic Press: London/New York, 1982, pp. 17-61.
27. Johnson, S. G.; Lee, I.-J.; Small, G. J. in *Chlorophyll*, H. Scheer, ed.; CRC Press:

Boca Raton, in press.

28. Gorokhovskii, A. A.; Kaarli, R. K.; Rebane, L. A. *JETP Lett.* 1974, 20, 216.
29. Kharlamov, B. M.; Personov, R. I.; Bykovskaya, L. A. *Opt. Commun.* 1974, 12, 191.
30. Rebane, L. A.; Gorokhovskii, A. A.; Kikas, J. V. *Appl. Phys.* 1982, 29B, 235 and literature cited therein.
31. Tang, D.; Johnson, S. G.; Jankowiak, R.; Hayes, J. M., Small, G. J.; Tiede, D. M. in *Perspective in Photosynthesis*, J. Jortner and B. Pullman, Eds.; Kluwer: Dordrecht, 1990, pp. 99-120.
32. Johnson, S. G.; Tang, D.; Jankowiak, R.; Hayes, J. M.; Small, G. J.; Tiede, D. M. *J Phys. Chem.* 1989, 93, 5953.
33. Boxer, S. G.; Middendorf, T. R., Lockhart, D. J. *FEBS Lett.* 1986, 200, 237.
34. Meech, S. R.; Hoff, A. J.; Wiersma, D. A. *Proc. Natl. Acad. Sci. USA* 1986, 83, 9464.
35. Jankowiak, R.; Tang, D.; Small, G. J.; Seibert M. *J. Phys. Chem.* 1989, 93, 1649.
36. Tang, D.; Jankowiak, R.; Yocum, C. F.; Seibert, M.; Small, G. J. *J. Phys. Chem.* 1990, submitted.
37. Tang, D.; Jankowiak, R.; Small, G. J.; Seibert, M. *Photosynth. Res.* 1990, submitted.
38. de Vries, H.; Wiersma, D. A. *Phys. Rev. Lett.* 1976, 36, 91.
39. Hochstrasser, R. M.; King, D. S. *J. Am. Chem. Soc.* 1975, 97, 4760.
40. Jankowiak, R.; Small, G. J. *Science* 1987, 237, 618 and literature cited therein.
41. Friedrich J.; Haarer, D. *Angew. Chem. Int. Ed. Engl.* 1984, 23, 113.
42. Völker, S. *Annu Rev. Phys. Chem.* 1989, 40, 499.

SECTION I.

**PHOTOCHEMICAL HOLE BURNING STUDIES OF
BACTERIAL PHOTOSYNTHETIC REACTION CENTERS**

INTRODUCTION

Reaction center (RC) is a highly organized transmembrane protein-pigment complex responsible for the primary process in photosynthesis which involves charge separation and a series of rapid electron transfers. The nature of its excited electronic structure and early time dynamics has been the subject of interest for many years. The recent pioneering achievement by Budil et al. [1] and Deisenhofer et al. [2-3] in determining the structure of *Rps. viridis* at 3 Å resolution has provided us detailed information about the spatial arrangement of chromophores within the protein. As the result of their work which was awarded the Nobel Prize in 1988, the structure of another species, *Rb. Sphaeroides*, was subsequently determined at a resolution of 2.8 Å by two other research groups [4-10].

The RCs of both species consist of a special pair bacteriochlorophyll dimer (P), two accessory bacteriochlorophylls (B), two bacteriopheophytins (H) and two quinones (Q). In the case of *Rps. viridis*, one quinone molecule perhaps was lost during the isolation procedure. A non-heme iron was found to be situated between the two quinone molecules in the RC of *Rb. Sphaeroides*. The structure of *Rps. viridis* is shown in Figure 1. *Rb. Sphaeroides* possesses similar structural characteristics except that *a*-type pigments (BChl *a*, BPheo *a*) were the building blocks, while in *Rps. viridis* they are of the *b*-types. A tightly bound cytochrome molecule was also (and only) found in *Rps. viridis*. Three different polypeptides (~ 30-40 kDa) called L, M and H (stands for light-, medium-, and heavy-weight) protein subunits tightly bind the chromophores in a hydrophobic environment. In the structures, a approximate C₂-rotation axis can be observed by relating two pigment branches. A detailed description

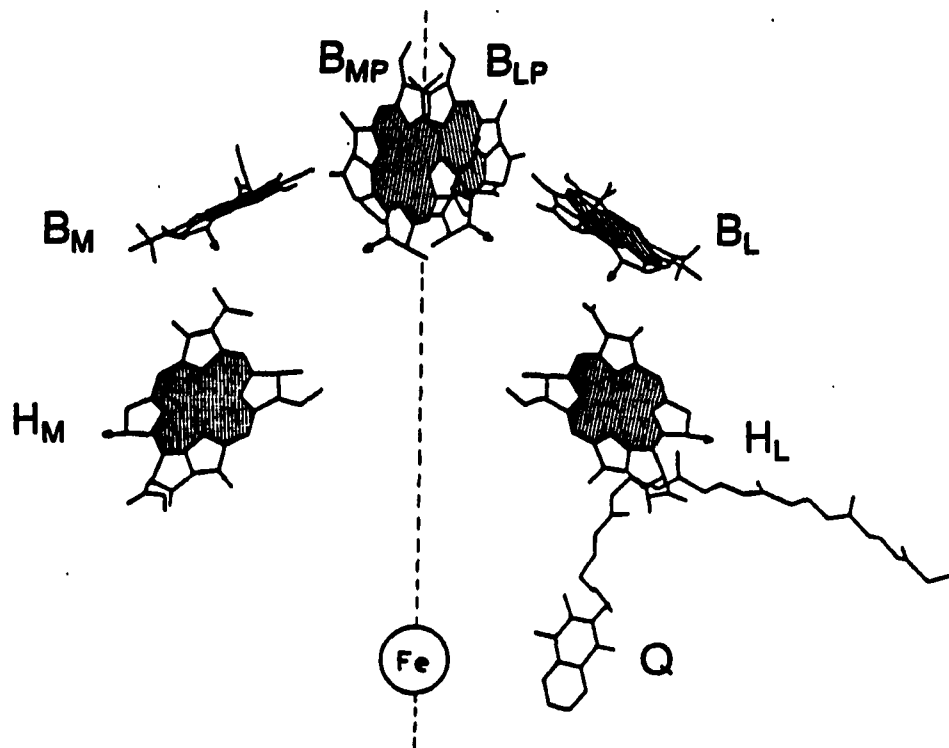


Figure 1. Structure of the reaction center of *Rps. viridis* containing four bacteriochlorophyll *b* (B_{LP} , B_{MP} , B_L , B_M), two bacteriopheophytin molecules (H_L , H_M) and a menaquinone (Q). The molecules are arranged in two branches, L and M forming an approximate C_2 -symmetry

of the spatial arrangement of pigments of both types of RC can be found elsewhere [1-10].

The charge separation occurs from P, comprised of a BChl dimer called special pair where initial excitation energy are trapped upon. It is also called PED because of its function as a primary electron donor. Remarkably, it was found that the rapid electron transfer occurs only via the L branch despite structural symmetry [3]. Such a phenomenon has been attributed to the difference in their protein environment, more specifically due to the difference in the specific amino acid-pigment interactions [3,11,12]. It was also suggested that various charge transfer states might also contribute to a directionality of charge separation which in turn causes the uni-directional electron transfer [3,11,12]. Experiments have been performed by modifying or removing BChl on either side through chemical treatment to monitor the change of electron transfer kinetics [13,14]. More recently, site-directed mutagenesis has been applied to many different types of RC to investigate the role of protein environment surrounding the chromophores within the RC [15-18].

The circular dichroism spectra of those reaction centers have indicated that the pigment molecules are strongly coupled [19,20]. The subsequent electron transfer kinetics for both *Rps. viridis* and *Rb. sphaeroides* has been studied by ultrafast experiments [19-21]. Experimental results indicate that the electron moves from PED to a BPheo_L (bacteriopheophytin molecule on L branch) in less than 3 ps and then to a quinone in approximately 200 ps at room temperature (see Figure 2). The kinetics of electron transfer from PED to BPheo_L, have been found to accelerate as the temperature is reduced. Time constants of 0.7 ps for *Rps. viridis* [20,21] and 1.2 ps for *Rb. Sphaeroides* [20,21] at 10 K with 100 fs time resolution have been reported. Again, no evidence of the involvement of BChl_L (bacteriochlorophyll molecule on L branch) as an intermediate acceptor was observed. The role of BChl_L is

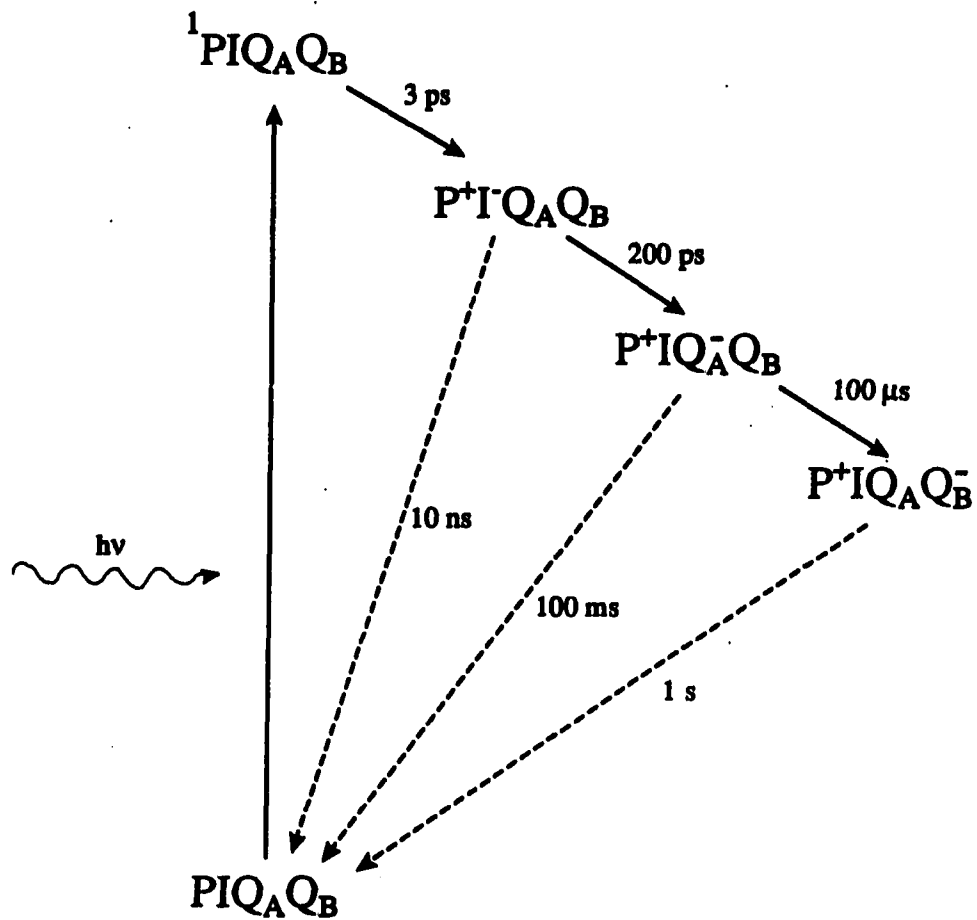


Figure 2. Reaction Scheme of primary processes in the reaction center of *Rps. viridis* at room temperature. P is equivalent to P960, a primary electron donor. I stands for a intermediate acceptor, in this case, a bacteriopheophytin molecule. Q_A and Q_B are the quinone molecules on L and M side, respectively. Experimental evidences have suggested these processes taken place only along the L branch

currently the subject of controversy [22-29]. The increase of electron transfer rate with decreasing temperature indicates, perhaps, that the rate determining step for electron transport to BPheo_L is barrierless. Chekalin et al. [28], however, have argued that the time domain data obtained for *Rb. Sphaeroides* are consistent with the bleaching of the Q_y transition of BChl_L. Recent results presented by Holzzapfel et al. [29] have highlighted such an argument. It was reported that two time constants of 3.5 ps and 0.9 ps were measured for *Rb. Sphaeroides* at room temperature (at a resolution of 80 fs) instead of approximately 3 ps which was measured previously by other groups [19,20]. Nevertheless, such phenomena of electron transfer are not adequately understood and have been the subject of intense theoretical and experimental investigation.

Photochemical hole burning experiments were first independently performed by Boxer et al. and Meech et al. on *Rps. viridis* [30,31] and *Rb. sphaeroides* [32,33], respectively. Both studies observed the formation of featureless broad holes (~ 400 cm⁻¹ FWHM, but varies with burn wavelength) by exciting into lower exciton component of PED. Several burn wavelengths were employed in some experiments [30-32]. In the case of *Rps. viridis*, no obvious burn-wavelength dependence of the broad hole maxima was observed [30,31]. However, careful examination of the results obtained by Boxer et al. on *Rps. viridis* (difference absorption spectra, in PVOH film) does reveal a trend in which the hole width is narrowed and becomes more asymmetric upon burning at longer wavelength (~ 1013 nm). In the data obtained by Meech et al. (difference transmission spectra, in 2:1 glycerol/H₂O), a shoulder was clearly discernible despite the poor signal-to-noise ratio of their spectrum. In the case of *Rb. Sphaeroides*, only the shift of the broad hole maxima was observed by Boxer et al. [30]. Meech et al. [31] presented only one hole burned spectrum and therefore no shift

of the broad hole maxima was reported.

Since the zero phonon hole (ZPH) was absent, the broad hole was interpreted as being homogeneously broadened. Such interpretation provides a life time of ~ 20 fs [30-33] and can be viewed as the ultrafast decay of the excited PED, P^* , into a charge transfer state that precedes population of the charge separated state $|P^+BH^- \rangle$ [30-33].

Two theoretical models have been proposed in order to explain the structureless broad hole and the absence of the ZPH [34-37]. In the theoretical calculations by Won and Friesner [34,35] the absence of ZPH was explained by coupling of the P^* vibronic manifold to a nearby charge transfer state. Hayes et al. [36,37], however, argued that such result can be readily explained by the theory of strong linear electron-phonon coupling and inhomogeneous line broadening [37] and with the displacement of the excited state in a charge transfer complex.

In this section, transient photochemical hole burning experiments, with improved signal-to-noise ratio, performed on RCs of both *Rps. viridis* and *Rps. Sphaeroides* in various hosts are reported [38-42]. By correcting the misinterpretation caused by the earlier unfaithful representation of the obtained ΔT spectra [38,39], our results indicate that a ZPH can be measured and satisfactorily understood in terms of inhomogeneous broadening and the Franck-Condon principle without invoking a charge transfer state [40-42]. The results of theoretical calculation utilizing theory of Hayes and Small [36,37] with modification have shown to be quite adequate in explaining the obtained hole burned spectra.

EXPERIMENTAL METHODS

Sample Preparation

Reaction centers from *Rps. viridis* were prepared by suspending the chromatophores in 5% lauryl dimethylamine-N-oxide (LDAO), 10 mM Tris, pH 8 and loading onto a sucrose gradient (0.1 M - 1 M sucrose, 0.1% LDAO, 10 mM Tris) following the centrifugation at 160,000 xg overnight. The reaction center (RC) band was then collected and placed on a DEAE sephadex column. Purified reaction centers were eluted with a salt gradient (0 - 0.15 M NaCl, 0.1% LDAO, 10 mM Tris, pH 8). The labile LDAO detergent was replaced by n-nonyl- β -D-glucopyranoside (NGP) for carrying out the photochemical trapping of Pheo⁻ at low reduction potentials, which involves the addition of sodium dithionite to the sample and irradiation with white light. First, the RC were dialyzed against 0.1% LDAO, 10 mM Tris, and then placed on a DEAE Sephadex column and washed with several column volumes of 0.3% NGP, 10 mM Tris. RCs were eluted with 0.15 M NaCl, 0.3% NGP, 10 mM Tris, dialyzed versus the same buffer without salt and then frozen for storage.

The RCs from *Rb. spheroides* were isolated with the detergent LDAO following a similar procedure [43]. The RCs were grown from polyethylene glycol [44]. The fresh RC samples were made by dissolving crystals in several suitably buffered hosts. The hosts used were glycerol:H₂O (2:1) with 0.8% LDAO, glycerol:H₂O (2:1) with 0.3% NGP and ethylene-glycol:H₂O (2:1) with 0.3 NGP in 10 mM Tris, 1 mM EDTA (pH = 8.0). Polyvinyl alcohol film (PVOH) was also used as a host during the experiment. The optical density of the

primary donor state absorption band was adjusted to approximately 0.5 during this study. Care was taken to minimize light exposure during the sample preparation.

Cryogenic Equipment

Samples were placed in NMR tubes (path length ~ 0.5 cm) or polystyrene tubes (path length ~ 1.0 cm) in a brass holder and cooled in a Janis Research Model 8-DT Super Vari-Temp liquid helium immersion cryostat equipped with an optical access tail section. The 4.2 K temperature was achieved by raising the liquid helium level just below the sample holder. The sample temperatures were monitored by a Lakeshore Cryotronics DTC-500K calibrated silicon diode.

Experimental Techniques

The standard absorption spectra of the RC in various glasses were obtained with a Bruker IFS 120 HR Fourier-transform infrared (visible) spectrometer operating at a resolution of 4 cm^{-1} . The visible-NIR source consisting of a tungsten lamp (range $3,000 - 25,000\text{ cm}^{-1}$) was used in conjunction with a Si-photodiode detector and a matching beam splitter. The spectra obtained were typically the average of 25 scans covering the spectral range 500-1110 nm to increase signal-to-noise ratio.

The absorption spectra for the chemically reduced RC (PBHQ^-) were obtained by irradiating the sample at 4.2 K (in the presence of sodium dithionite) with white light from the 75 W tungsten-halogen lamp of the FT-IR spectrometer and an additional 600 W tungsten-

halogen lamp (with a 10 cm water filter). The selective reduction utilizing laser excitation was performed by irradiating sample at 1023 nm with a narrow-band laser for 90 min with a peak intensity of $\sim 64 \text{ mW/cm}^2$ at a laser pulse repetition of 45 Hz.

For the transient hole burning experiment, the apparatus as shown in Figure 3 was designed. A 600 W tungsten-halogen lamp was used as the probing source which was dispersed by a 1 m McPherson 2061 monochromator ($F=7.0$) with a linear dispersion of 0.833 nm/mm. The slit width was adjusted to achieve the resolution for the experiment. The probing light, after being dispersed by the monochromator, is focused onto the sample situated in the cryostat. A set of two lenses and a mechanical shutter with rise time of $\sim 1.6 \text{ ms}$ (Uniblitz 26L, Vincent Associate Inc.) were used for focusing and gating. For the experiment performed in PAPER I, a thermo-electric cooled Hamamatsu R406 photomultiplier tube (with S-1 photo cathode) was used for detection. A Hamamatsu R316-02 photomultiplier tube with enhanced S-1 response was employed for the experiment performed in PAPER II and PAPER III.

An excimer (Lambda Physik EMG 102) pumped dye laser (Lambda Physik FL-2002) was utilized with a linewidth of 0.2 cm^{-1} and a pulsewidth of 10 ns. The dye laser (with Coumarin 540A dye for *Rps. viridis* and DCM dye for *Rb. spheroides*) was Raman shifted (H_2 gas) to provide tunable radiation in the 947-1023 nm (for *Rps. viridis*) and 850-920 nm (for *Rb. spheroides*) region. LDS 722 dye was used without Raman shifting for pheophytin hole burning experiments. Appropriate dielectric coated infrared reflecting mirrors and cut off filters were utilized to eliminate the pre-Raman shifted primary beam. Pulse energies (after Raman shifting) were typically between 0.1 – 0.4 mJ focused onto a 0.3 cm diameter or 0.3 cm x 1.0 cm spot. The excimer laser was operated with XeCl (output at 306 nm) at a

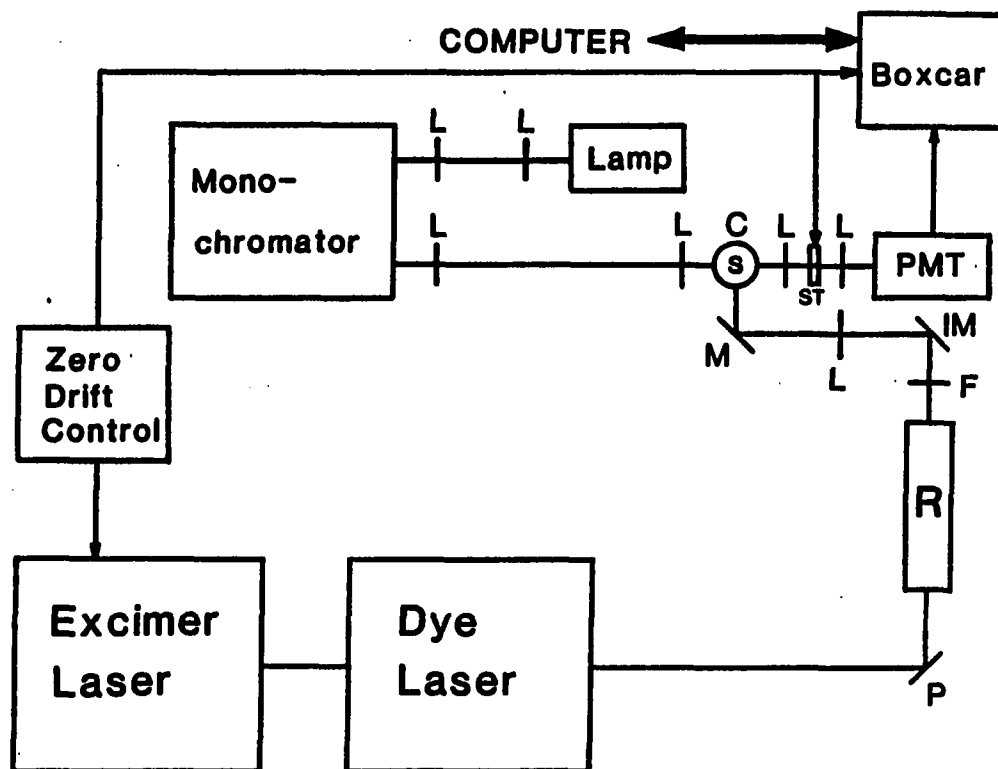


Figure 3. Block diagram of the the experimental setup. L=lens, M=mirror, IM=infrared mirror, ST=mechanical shutter, R=Raman shifter, S=sample, C=liquid helium cryostat, F=filter, P=prism, PMT=photomultiplier tube (S-1 response)

pulse repetition of 10-20 Hz.

For the experiment presented in PAPER I, the output of the photomultiplier tube was fed into an EG&G Model 162 boxcar averager equipped with two Model 164 processor modules for Channel A and B detection. For channel A of the boxcar, an aperture delay and aperture width of 1.6 ms and 5 ms were used. The corresponding values for channel B were 30 ms and 5 ms (the mechanical shutter was adjusted to have a 40 ms aperture and the 10 Hz repetition rate provided a 90 ms duty cycle). Operation of the boxcar in the A-B mode directly provided the transient difference transmission spectra. For the later experiments reported in PAPER II and PAPER III, improvement was made by interfacing a Stanford Research SR250 boxcar averager (with built-in integrator) directly to a Proteus 386 personal computer via IEEE-488. Both shutter and boxcar averager were triggered with a single pulse from the zero drift control module of the excimer laser. The 16 Hz and 20 Hz pulse repetition rate (for *Rb. Spheroides* and *Rps. viridis*, respectively) provided a duty cycle of 40-55 ms which are sufficient to accommodate the charge recombination time for both *Rps. viridis* and *Rb. spheroides* P^+BHQ^- state (8 ms and 21 ms at 4.2 K, respectively). The gate delay for the boxcar was ~ 2 ms and the gatewidth was 150 μ s. The ΔT (delta transmission) spectra were obtained by subtracting laser-on and laser-off spectra. The ΔA (delta absorbance) spectra were obtained during the post data processing by subtracting the logarithms of laser-on and laser-off transmission spectra. By varying the gate delay it was possible to determine the life time of the charge separated bottleneck state P^+BHQ^- for both *Rps. viridis* and *Rb. Spheroides*.

Interference from the laser was eliminated by the gating of the boxcar and the mechanical shutter between the sample and the photomultiplier tube. In addition, any laser

scatter would be detected as a broad range baseline deviation and thus will not result in any sharp feature.

The change of optical density was adjusted to be within 20% of the change of transmittance for both *Rps. viridis* and *Rb. Spheroides* although changes of more than 80% can be achieved by utilizing higher burn power.

Data were analyzed on either a 16 MHz or a 20 MHz 386 IBM compatible personal computer equipped with a 10 MHz 287 math coprocessor by using the program SpectraCalc (Galactic Industry, Inc.) and a HP 7475A plotter (Hewlett Packard Co.) was utilized for data graphing.

**PAPER I. STRUCTURED HOLE BURNED SPECTRA OF THE PRIMARY
DONOR STATE ABSORPTION REGION OF *Rhodospseudomonas*
*Viridis***

**STRUCTURED HOLE BURNED SPECTRA OF
THE PRIMARY DONOR STATE ABSORPTION REGION
OF *Rhodopseudomonas Viridis***

**Deming Tang, Ryszard Jankowiak, Gerald J. Small
and David M. Tiede**

Chemical Physics 1989, 131, 99

ABSTRACT

Structured hole burned spectra for P960 of *Rps. viridis* are reported which, for appropriate burn wavelengths, exhibit four holes (including a zero-phonon hole). Burn wavelength-dependent spectra and other factors indicate that the hole structure is not contributed to by reaction center heterogeneity or impurity. The data are consistent with there being two adiabatic states, $|Z\rangle^*$ and $|X\rangle^*$, which contribute significantly to the P960 absorption profile, with $|X\rangle^*$ defined as the lower energy state (by $\approx 300\text{ cm}^{-1}$). The zero-phonon hole can be assigned as a feature belonging to the hole associated with $|X\rangle^*$ and possesses a width of 10 cm^{-1} at 4.2 K. The width yields a decay time of 1 ps for $|X\rangle^*$ and, consequently, a connection with time domain studies of the primary electron donor state. A number of models for the existence of the two absorbing states are considered. The following two models for $|X\rangle^*$ and $|Z\rangle^*$ appear to be plausible: that they are admixtures of the neutral exciton state and an intra-dimer charge transfer state of the special pair(P) or they are admixtures of P^* and a charge transfer state between P and the bacteriochlorophyll monomer on the active side.

INTRODUCTION

The problem of understanding the primary charge separation in the reaction centers (RC) of photosynthetic units has recently received increased attention [1] as a result of the crystal structure determinations for the RC of *Rps. viridis* [2-4] and *Rb. sphaeroides* [5,6]. In the structures, two pigment branches (related by an approximate C_2 -rotation axis) extend from the special bacteriochlorophyll pair or dimer (P), each containing a BChl monomer (B) followed by a bacterio-pheophytin monomer (H) and a quinone molecule (Q). The excited singlet state that gives rise to the 870 and 960 nm absorption bands of *Rb. sphaeroides* and *Rps. viridis*, respectively, is the primary electron donor state, which is generally denoted by P^* . We adopt this assignment for the purposes of introduction. It has been known for several years now that, upon excitation of P^* , electron transfer to a bacteriopheophytin occurs in just a couple of picoseconds at room temperature [1]. Questions of current interest include what is the electronic structure of P^* (and other low lying states) [1,7,8] and why does electron transfer from P^* occur predominantly along the L branch rather than the M branch [1,9]. Although symmetry breaking by specific amino acid-pigment interactions appears likely to play an important role in the "one-sided" electron transfer [1], electronic structure calculations are still too approximate to allow firm conclusions to be drawn about the mechanistic details. It will prove convenient to designate the ground state of the L branch as $|PBH\rangle$ while realizing that at least six pigments and their intermolecular couplings must be taken into account for a proper description of the excited states and even, perhaps, the ground state. A third important question pertains to the role of intermediation for B in the formation of the

charge separated state $|P^+B^-H\rangle^*$. Two possibilities, which have been considered and debated, are that $|P^+B^-H\rangle^*$ serves as a real intermediate state [10] or as a virtual state in a superexchange mechanism [11]. Of course, utilization of state descriptors like $|P^+B^-H\rangle^*$ implies that inter-pigment couplings are sufficiently weak for a diabatic description of electron transfer to be valid. Maslov et al. [12] and Shuvalov and ~~Nov~~ [13] had argued earlier that $|P^+B^-H\rangle^*$ serves as a real intermediate state although Kirmaier and coworkers [14] concluded that the evidence for this was not convincing. Very recently, however, experiments with ≈ 100 fs resolution have been performed in order to determine whether bleaching of the Q_y transition of B occurs on a subpicosecond time scale in *Rps. viridis* [15-18] and *Rb. sphaeroides* [17-19]. When P^* was directly excited, the bleaching was not directly apparent. On the basis of an approximate model, Breton et al. [17] and Martin et al. [18] concluded that if $|P^+B^-H\rangle^*$ is a real intermediate state, it must undergo decay in a time substantially shorter than 100 fs. The same conclusion would hold for $|PB^+H^-\rangle^*$, which has also been suggested as a real intermediate state [20]. The time domain data do not exclude that the above charge-transfer states could serve as virtual states in superexchange. Time domain data obtained following excitation of the Q_x transition of the bacteriochlorophylls appear to be more difficult to interpret [17], although Chekalin et al. [21] have argued that such data obtained for *Rb. sphaeroides* are consistent with bleaching of Q_y transition of B. In consideration of these opposing views, the high degree of complexity associated with the interpretation of transient spectra for a coupled pigment system should be appreciated.

At present, the nature of the excited electronic states involved and role of the protein in primary charge separation are poorly understood. The importance of the interplay between

time and frequency domain spectroscopic experiments and more refined theoretical computations for an adequate understanding of electron transfer in RC is apparent. Recently, photochemical hole burning (PHB) has been successfully applied to the primary donor (P^*) states P870 [22,23] and P960 [24,25] of *Rb. sphaeroides* and *Rps. viridis*, respectively. Exceedingly broad holes ($\approx 400 \text{ cm}^{-1}$) were observed. A sharp zero-phonon hole was not observed. Such a hole might be expected if the dephasing time of P^* is just twice its population decay time. Recent measurements at 10 K have led to the conclusion that the P^* decay times are 1.2 and 0.7 ps for *Rb. sphaeroides* and *Rps. viridis* [16,17]. Two theoretical models have been put forth to explain the appearance of the structureless broad hole and the apparent absence of a zero-phonon hole. From this laboratory it was proposed that [26,27] the broad hole profiles may be the consequence of strong linear electron-phonon coupling and site inhomogeneous line broadening, Γ_{inh} . That is, the holewidth is not viewed as a manifestation of an ultrafast ($\approx 20 \text{ fs}$) decay of P^* that precedes population of the charge separated state $|P^+BH^- \rangle^*$. Rather, it is a consequence of an absorbing state (P^*) whose absorption profile is dictated by a long progression in phonons which builds on the zero-phonon transition which, itself, is subject to a distribution defined by Γ_{inh} . The strong electron-phonon coupling or large Huang-Rhys factor (S) was argued [25,26] to be consistent with the *absorbing* P^* state possessing significant charge transfer character, perhaps of the intra-dimer type predicted theoretically by Warshel and Parson [7]. Such character would endow P^* with a significant permanent dipole moment. Recent Stark measurements on *Rps. viridis* are consistent with this notion [28-30].

In contrast with the above model are those of Meech and coworkers [25] and Won and Friesner [31] which attribute, respectively, all or a significant fraction of the holewidth to

ultrafast decay or dephasing of P^* into some type of charge-transfer state(s). This decay would precede formation of $|P^+BH^- \rangle^*$.

Since the observation of weak but relatively sharp (several cm^{-1}) zero-phonon hole would be important for distinguishing between the above models [27], a series of more detailed transient hole burning experiments on *Rps. viridis* were undertaken. At the present time only the model of Hayes and co-workers [26,27] appears to allow for the existence of such a zero-phonon hole. The results, reported herein, show that the hole spectra in the region of P960 are quite highly structured and that a zero-phonon hole can be observed when appropriate burn wavelengths are used. These results led to companion laser and white light bleaching experiments on the chemically reduced RC ($PBHQ^-$). The results of both types of experiment are discussed in terms of current theories for the excited electronic state structure of and primary charge separation in the RC. Possible interpretations for the structured hole spectra are considered. A preliminary account of some of the results has appeared [32].

EXPERIMENTAL

Sample Preparation

Reaction centers from *Rps. viridis* were prepared with the detergent lauryl dimethylamine-N-oxide (LDAO) as described previously [33]. Briefly chromatophores were suspended in 5% LDAO, 10 mM Tris, pH 8 and loaded onto a sucrose gradient (0.1 M - 1 M sucrose, 0.1% LDAO, 10 mM Tris) and spun at 160,000xg overnight. The reaction center band was collected and placed on a DEAE Sephadex column. Purified reaction centers were eluted with a salt gradient (0 - 0.15 M NaCl, 0.1% LDAO, 10 mM Tris, pH 8). In order to carry out photochemical trapping of $H^{\cdot-}$ (Pheo $^{\cdot-}$) at low reduction potentials, the labile LDAO was replaced with n-nonyl-b-D-glucopyranoside (NGP). First, the reaction centers were dialysed against 0.1% LDAO, 10 mM Tris, and then placed on a DEAE Sephadex column and washed with several column volumes of 0.3% NGP, 10 mM Tris. Reaction centers were eluted with 0.15 M NaCl, 0.3% NGP, 10 mM Tris, dialysed versus the same buffer without salt and then stored frozen. Reaction centers were thawed, and diluted to 60% glycerol or ethylene glycol as needed. Chemical reduction with sodium dithionite of the RC to PBHQ $^{\cdot-}$ was carried out following the method of refs. [34-36].

Measurements

Samples were mounted and cooled to 4.2 K in a Janis model 8-DT Super Vari-Temp liquid helium cryostat. Standard absorption spectra of the RC in various glasses were

obtained with a Bruker IFS 120 HR Fourier-transform infrared (visible) spectrometer operating at a resolution of 4 cm^{-1} . The peak absorbance of P960 was typically ≈ 0.6 . At a resolution of 4 cm^{-1} , spectra averaged over 25 scans and covering the spectral range 500-1110 nm could be obtained in $\approx 30\text{ s}$. Absorption spectra for the chemically reduced (dithionite) RC (PBHQ⁻) were obtained in the same way. White light irradiation for 150 min with the 75 W tungsten-halogen lamp of the FTIR spectrometer and an external 600 W tungsten-halogen lamp (with a 10 cm water filter) was used to further reduce PBHQ⁻ at 4.2 K. The degree of reduction was determined by monitoring the bleaching of the Q_y absorption band of the H_L at $\approx 808\text{ nm}$. The white light reduction was performed with the cryostat tail-section aligned with the optical axis of the spectrometer. The tail-section was fixed in the same position as that used for recording the spectrum of PBHQ⁻. Reduction to PBHQ⁻ was also performed in a selective manner using narrow band laser excitation (see below) at 1023 nm (irradiation time = 90 min; intensity $\approx 64\text{ mW/cm}^2$ at a laser pulse repetition of 45 Hz).

For the transient hole burning experiments, an excimer (Lambda Physik EMG 102) pumped dye laser (Lambda Physik FL-2002) was utilized with a linewidth of 0.2 cm^{-1} (pulse width 10 ns). With Coumarin 540 A the dye laser output was Raman shifted (H₂ gas) to provide tunable radiation in the 947-1023 nm region. The excimer laser was operated with XeCl at a pulse repetition rate of 10 Hz. Raman shifted pulse energies utilized were $\approx 0.1\text{ mJ}$ (focused to a 0.3 cm diameter spot) and produced P* transmission changes of $\approx 10\text{-}15\%$. Transmission measurements were made using a 1 m focal length McPherson 2061 monochromator ($F = 7.0$) which provided a reciprocal linear dispersion of 0.833 nm/mm. A monochromator bandpass of 2 cm^{-1} was utilized. Probe light was from a 500 W tungsten-halogen lamp passed through the monochromator. A cooled Hamamatsu R406 photomultiplier

tube (S-1 response) was used for detection. The output of the photomultiplier was fed to an EG&G Model 162 boxcar averager equipped with two Model 164 processor modules for channel A and B detection. Operation of the laser at 10 Hz ensured that the charge separated species P^+BHQ^- had relaxed to PBHQ between shots. The relaxation time at 4.2 K is ≈ 7 ms [24]. To exclude the burn laser from the detection system, a mechanical shutter (Uniblitz 26L, Vincent Assoc. Inc.) was used. Both shutter and boxcar averager were triggered off of the laser pulse. The rise time of the mechanical shutter was ≈ 1.6 ms. For channel A of the boxcar, an aperture delay and aperture width of 1.6 ms and 5 ms were used. The corresponding values for channel B were 30 ms and 5 ms (the mechanical shutter aperture was greater than 40 ms). Operation of the boxcar in the A-B mode directly provided the transient difference transmission spectra. The optical setup was such that any interfering laser scatter would impinge directly on the PMT (rather than indirectly through the monochromator) and would add, therefore, a background signal which is independent of the monochromator scan wavelength. However, such direct scattering was totally eliminated by the gated detection and mechanical shutter as routinely determined by comparison of the outputs of channel B with the laser blocked and unblocked.

RESULTS

Transient Photochemical Hole Burning

Experiments were performed on the RC of *Rps. viridis* imbedded in glycerol/H₂O [with LDAO], glycerol/H₂O [with NGP] and ethylene glycol/H₂O [with NGP] glasses. For brevity, these glasses will be referred to as I, II and III, respectively. At 4.2 K, the P960 absorption maximum occurs at 995.9, 1000.5 and 998.9 nm for glasses I, II and III. The respective bandwidths are 430, 410 and 420 cm⁻¹. For each glass, a large number of burn frequencies were used which ranged from the high to low energy sides of the P960 absorption profile. Only a fraction of the data are presented here.

The P960 absorption profiles for the three glasses are similar and only slightly shifted relative to each other. Chemical reduction to PBHQ⁻ produces only a small red shift. Thus, the upper absorption spectrum of Fig. 1 can be used to gauge the location of the burn wavelength, λ_B , within the absorption profile for all three glasses. The low-energy shoulder of the absorption profile in Fig. 1 is also *clearly* discernible in the spectra for the nonreduced RC. 4.2 K absorption spectrum of glass II and I covering the 714-1111 nm region is shown in Fig. 2. An incorrect glass I spectrum was inadvertently published in ref. [32].

For glass I, transient hole spectra of PBHQ were measured for 20 burn wavelengths in the range between 947 and 1023 nm. Figure 3 shows the results for $\lambda_B = 1019.8$ nm (trace (1)) and $\lambda_B = 1006.2$ nm (trace (2)). In this figure the hole intensities increase in the upward vertical direction. Three holes, labeled X, Y, Z, are readily discernible in trace 1.

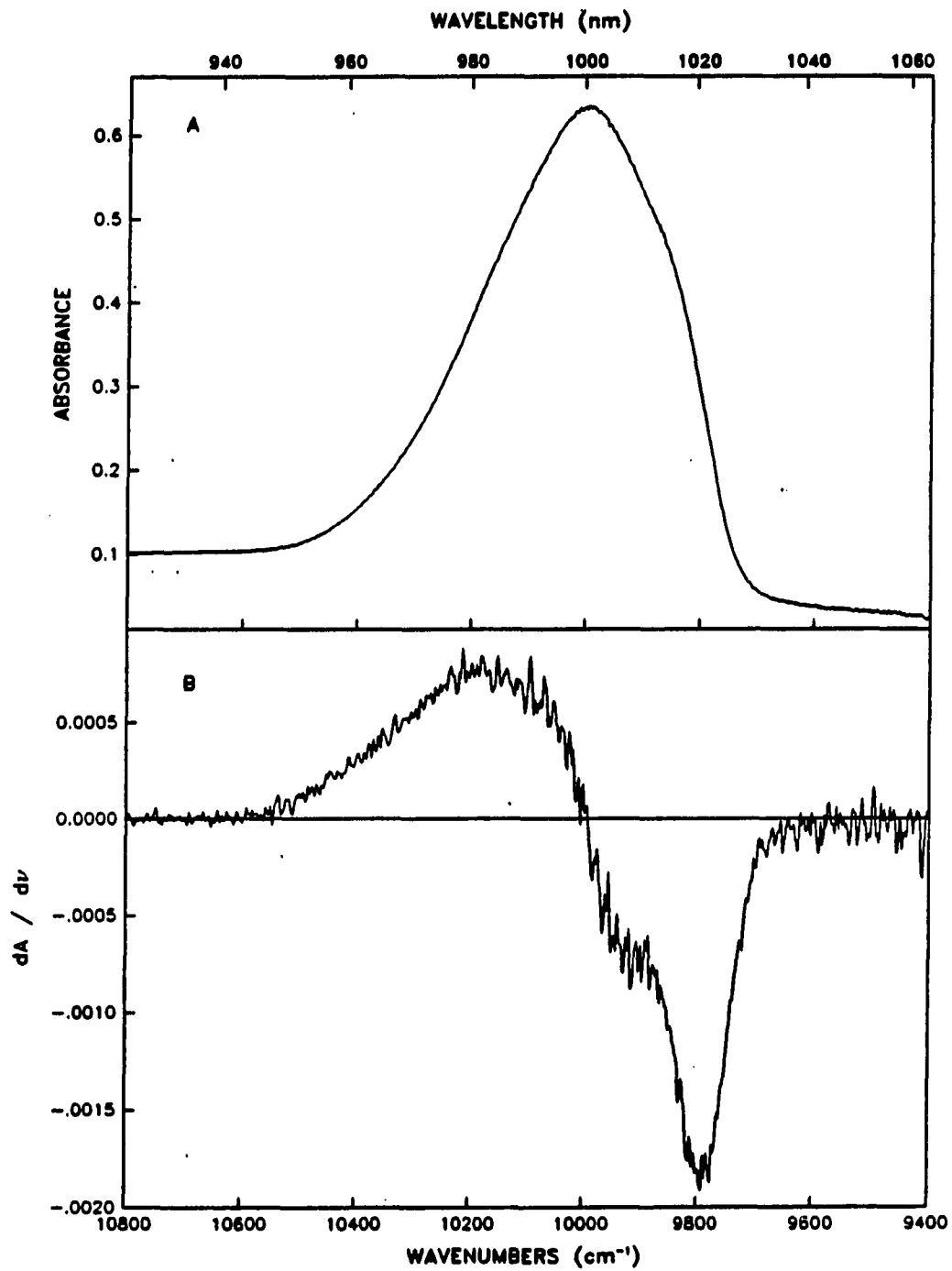


Figure 1. P960 absorption profile of the chemically reduced reaction center of *Rps. viridis* in glass II, $T \sim 4.2$ K (A). Bottom window (B) shows the first derivative of the spectrum shown in (A)

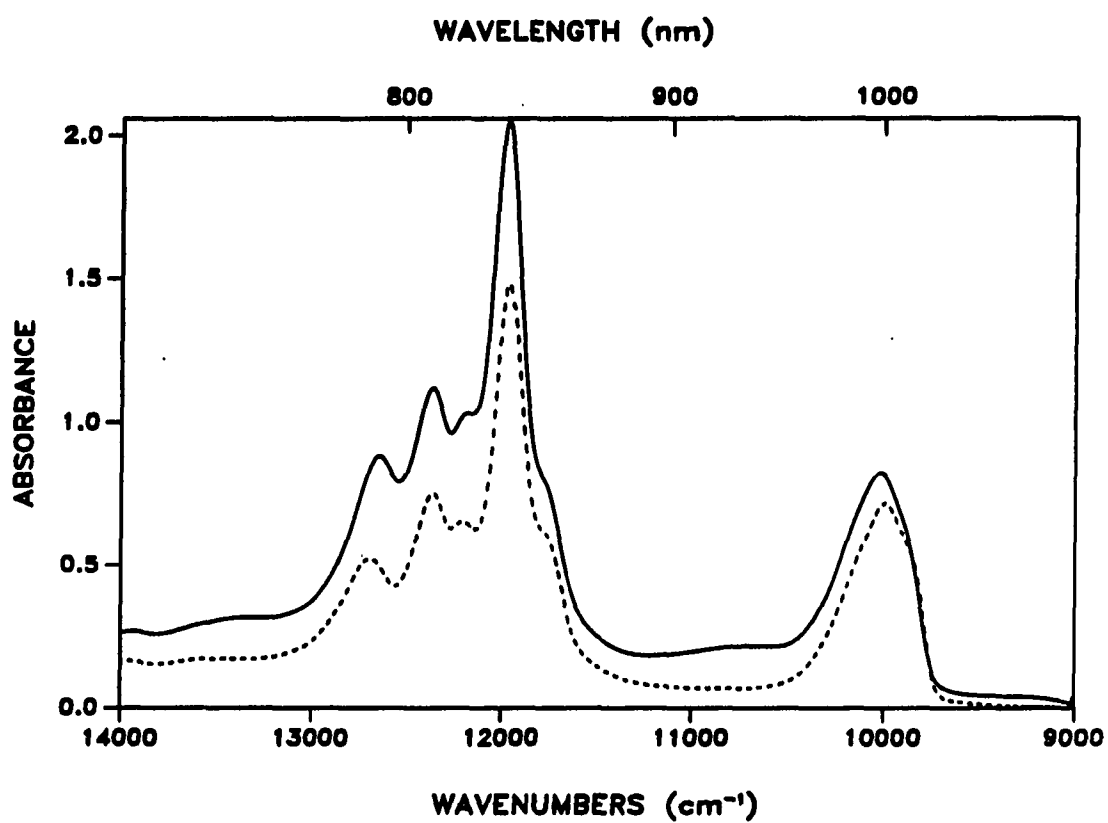


Figure 2. Absorption spectrum of *Rps. viridis* reaction center in glass II (broken line) and glass I (solid line), $T \sim 4.2$ K

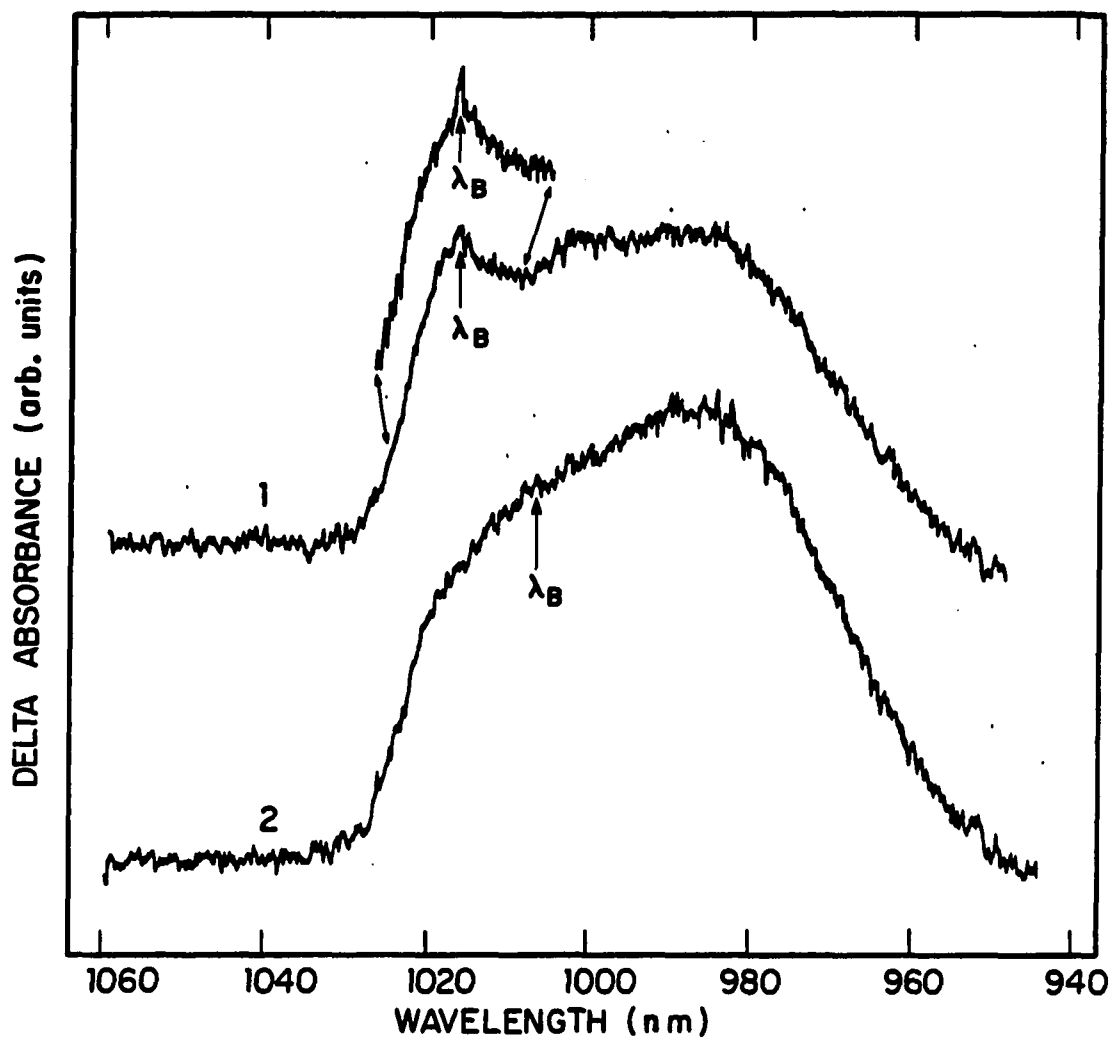


Figure 3. Transient hole burned spectra of P960 in glass I, $T \sim 4.2$ K. Trace 1: $\lambda_B = 1019.8$ nm; Trace 2: $\lambda_B = 1006.2$ nm. Hole intensities increase in upward vertical direction. Read resolution was 2 cm^{-1}

This triplet structure is present in all spectra for which $\lambda_B \geq 1006$ nm. As λ_B decreases from $\lambda_B = 1019.8$ nm the X and Y holes gradually broaden. For $\lambda_B = 1006.2$ nm, the hole Y is no longer resolvable (trace (2)). Importantly, the hole spectra obtained with $\lambda_B < 1006.2$ nm differ very little from trace (2) of Fig. 2. For $\lambda_B = 947$ nm (the lowest wavelength used), the excitation is well into the high energy side of the P960 absorption, Fig. 1. The relative intensities of holes X, Y, Z obtained with $\lambda_B > 1019.8$ nm do not differ significantly from those shown in trace (1) of Fig. 2 [32]. For $\lambda_B = 1023$ nm the excitation is located in the low energy tail of the P960 absorption profile, Fig. 2.

The triplet hole structure shown in spectrum (1) of Fig. 3 has also been observed for glasses II and III for λ_B -values that are located on the low energy side of the P960 absorption profile. The relative intensities of hole X, Y, Z are similar to those observed for glass I. For the glycerol/H₂O glass it is observed that the displacement between holes X and Z appears to be smaller for the NGP detergent than for LDAO (glass I). The observation made for glass I that the hole spectrum is not significantly dependent on λ_B when λ_B is less than a certain value was made for the other two glasses. For all three glasses the separation between holes X and Y is ≈ 120 cm⁻¹. The position of hole Z depends weakly on λ_B . Comparison of our results for the glycerol/water glasses with those of Meech and coworkers [25] establish that hole Z can be correlated with the hole they assign to P*. Although not commented on, their spectrum (obtained with lower S/N than in Fig. 3) possesses the unresolved X-Y structure evident in trace (2) of Fig. 1. Utilizing the high energy side of hole Z leads to a holewidth of ≈ 400 cm⁻¹ for glasses I-III. This value compares reasonably well with those measured by Meech et al. [25] and Boxer and coworkers [24], the latter workers having used polyvinyl alcohol films.

Hole X appears to correlate with the low energy shoulder of the P960 absorption profile. The possibility that hole Y is a vibronic or phononic feature associated with hole X is considered later. Comparison of spectrum (1) of Fig. 3 with the absorption profile establishes that line narrowing is observed by hole burning. Fig. 4 shows the glass I spectra for hole X obtained for $\lambda_B = 1020.0$ (trace (1)), 1018.3 (trace (2)) and 1017.3 nm (trace (3)). Ignoring, for the moment, the weak but relatively sharp zero-phonon hole coincident with λ_B , it can be seen that the peak frequency of hole X does depend on λ_B and that it is not generally coincident with λ_B . For $\lambda_B \geq 1013$ nm, the position of hole X is insensitive to variations in λ_B . The zero-phonon holes coincident with λ_B are just discernible in traces (1)-(3). The low signal-to-noise ratio precludes an accurate measurement of the holewidths. Nevertheless, an average value obtained from several scans is $\approx 10 \text{ cm}^{-1}$. When λ_B was tuned to a sufficiently low value the zero-phonon hole was not discernible. This is illustrated in Fig. 5 for glass II and in Fig. 6 for glass III. The upper trace of Fig. 6, like trace (1), was obtained with $\lambda_B = 1016.4$ nm but with a shorter time constant than that used to obtain trace (1).

In summary, the transient photochemical hole burned spectra associated with the P960 absorption region of *Rps. viridis* exhibit a four hole structure consisting of a zero-phonon hole and three relatively broad holes (X, Y, Z).

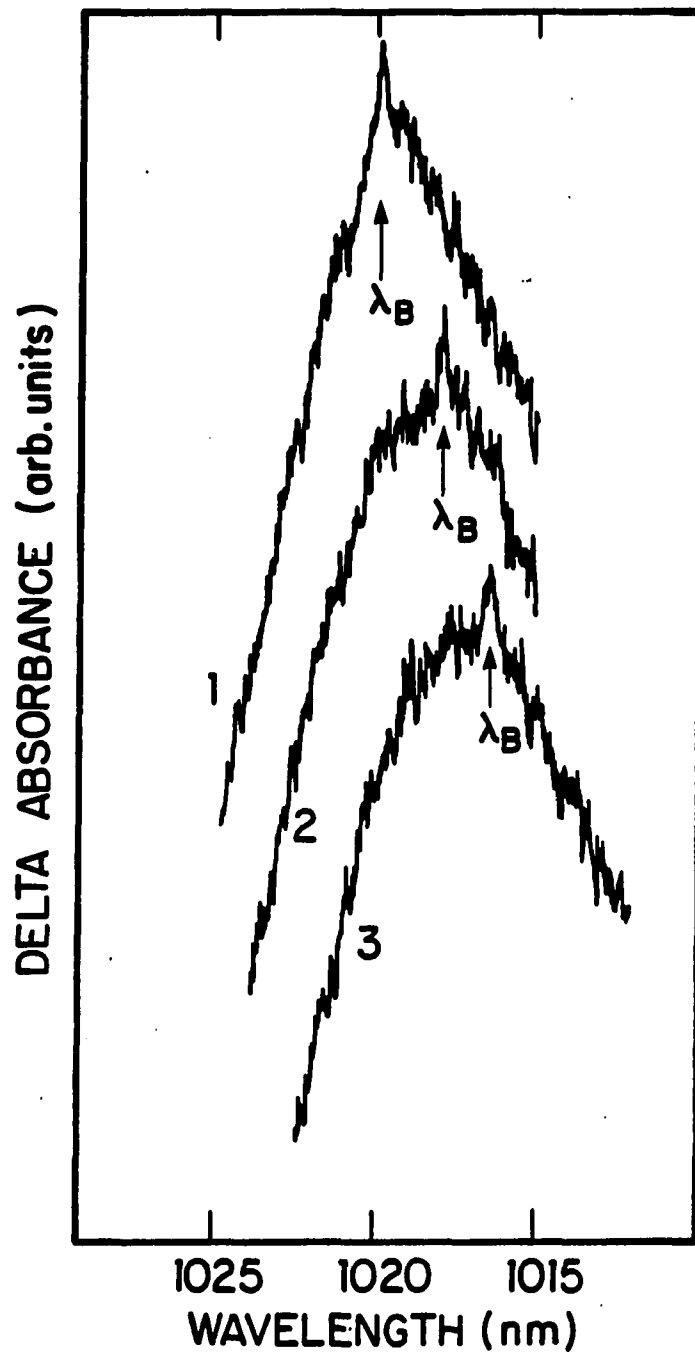


Figure 4. Spectra for hole X of Fig. 3 obtained for (1) $\lambda_B = 1020.0$ nm, (2) 1018.3 nm, (3) 1017.3 nm. Read resolution of $\sim 1 \text{ cm}^{-1}$ with a shorter time constant than used to obtain the spectra of Fig. 3

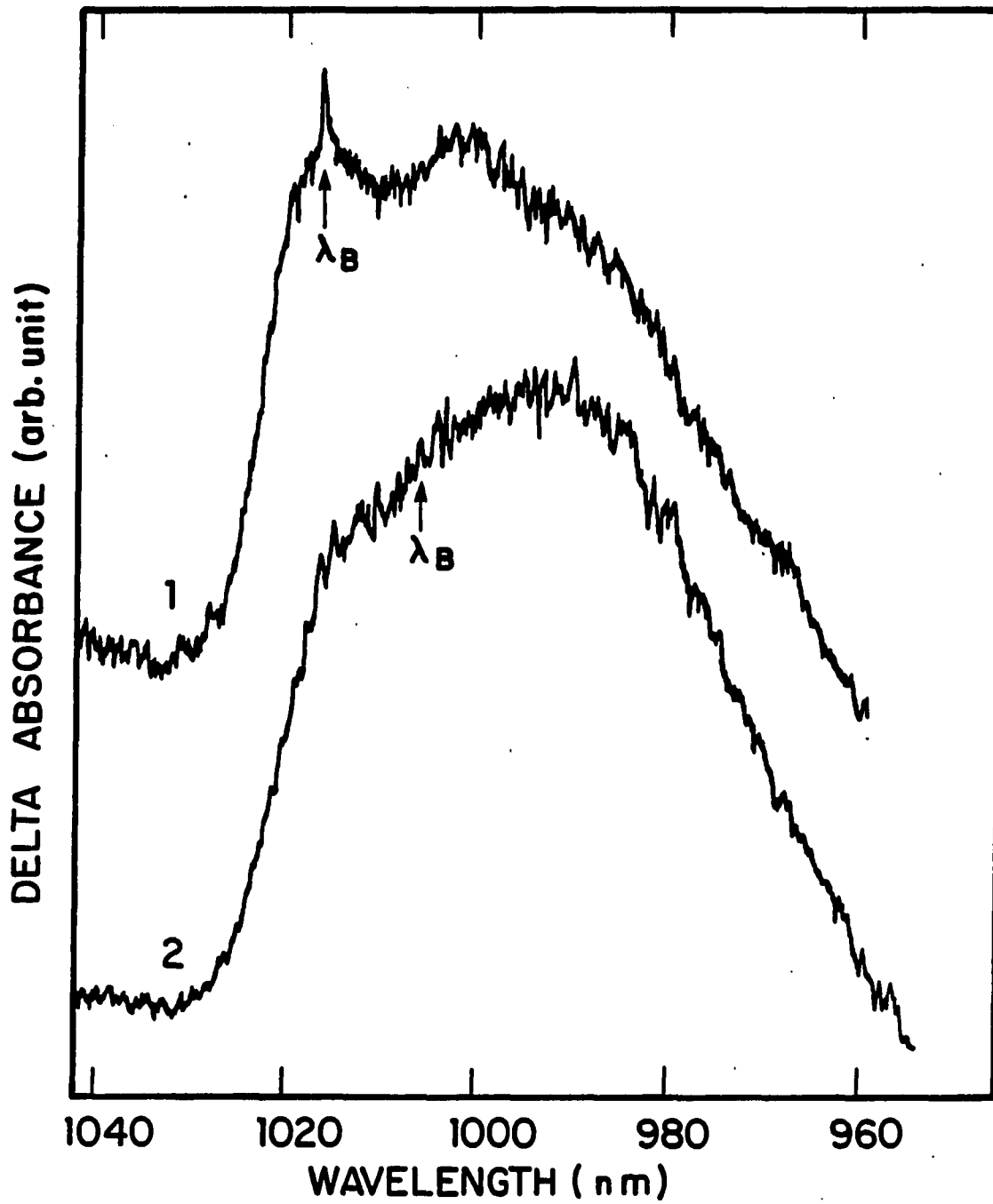


Figure 5. Transient hole burned spectra of P960 in glass II, $T \sim 4.2$ K: (1) $\lambda_B = 1016.4$ nm, (2) $\lambda_B = 1006.2$ nm Zero-phonon hole is discernible in 1) but not (2)

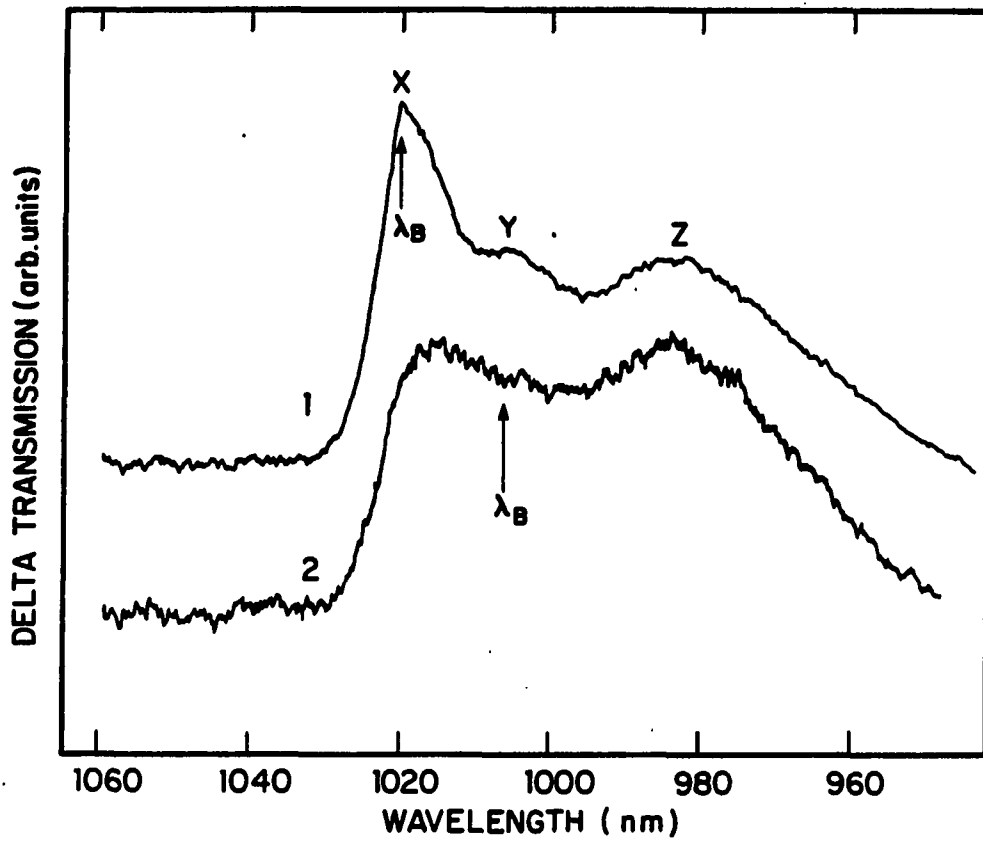


Figure 6. Transient hole burned spectra of P960 in glass II, $T \sim 4.2$ K: (1) $\lambda_B = 1016.4$ nm, (2) $\lambda_B = 1006.2$ nm. The truncated and expanded upper spectrum was obtained with $\lambda_B = 1016.4$ nm and a shorter time constant than used for spectrum (1).

Chemically Reduced Reaction Centers

In order to obtain additional information on the nature of the states associated with the structure of the transient hole spectra, a series of experiments were performed on the chemically reduced RC, PBHQ^- , in the glycerol/ H_2O glass (with NGP). The derivative of the absorption spectrum of this species shown in Fig. 1 establishes that there are two contributing absorption bands. This is also the case for the unreduced RC in glasses I-III (data not shown).

It is well known that white light irradiation of the chemically reduced species at low temperatures (≤ 100 K) leads to the formation of the stable PBH^-Q^- species [37], a cytochrome serving as the secondary donor for its production. The upper spectrum of Fig. 7 is the ΔA absorbance ($\text{PBHQ} - \text{PBH}^-\text{Q}^-$) observed following 150 min of white light irradiation, see Experimental section. The percentage conversion to PBH^-Q^- was $\approx 25\%$ as determined from the bleaching of the Q_y transition of H_L . The experimental ΔA spectrum of Fig. 7 is reasonably well accounted for by a simulation which involves a ≈ 20 cm^{-1} blue electrochromic shift for the absorption spectrum of PBHQ^- . Studies established that there is a linear relationship between the magnitude of the electrochromic shift and the signal amplitude or percentage conversion to PBH^-Q^- . The lower trace of Fig. 7 is the ΔA calculated as the unshifted spectrum of PBHQ^- minus the spectrum of PBHQ^- blue shifted by 20 cm^{-1} . Aside from the fact that the shoulder near 9930 cm^{-1} is better resolved in the simulated spectrum, the two spectra of Fig. 7 are very similar. Recall that Fig. 1 establishes that there are at least two components to the absorption profile of PBHQ^- . Thus, the simulated spectrum assumes that the two major components undergo identical electrochromic

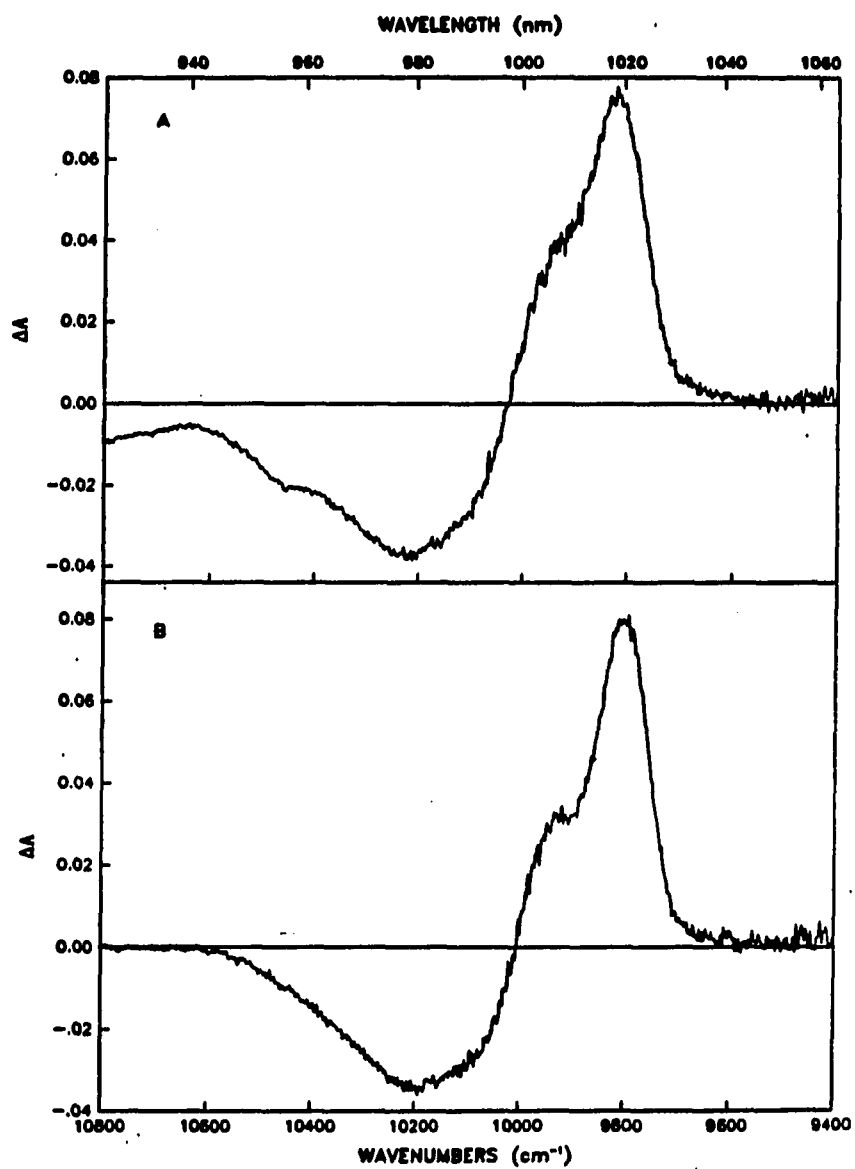


Figure 7. (A) 4.2 K difference absorption spectrum of chemically reduced RC (PBHQ^-) minus that of PBHQ^- exposed to white light irradiation in glass II at ~ 4.2 K, see section II and section III.B for details. White light reduction to PBHQ^- is not complete, see text. (B) Simulated difference spectrum produced by a 20 cm^{-1} blue electrochromic shift of the PBHQ^- spectrum

shifts. Fig. 7 establishes that they are similar but allowance for a slight difference could drive the spectra into better agreement.

The results of the type shown in Fig. 7 indicate that the underlying structure of P960, which is revealed in the transient hole spectra, is *not* due to excited states that possess a significant contribution from H^- , e.g., $|PB^+H^- \rangle^*$ or $|P^+BH^- \rangle^*$. That is, spectra of the type shown in Fig. 7 can be understood quite well in terms of an electrochromic shift which is consistent with the structure of the $PBHQ^-$ absorption, compare the lower spectrum of Fig. 1 with the upper spectrum of Fig. 7.

In addition to the utilization of white light for reduction, narrow line ($\approx 0.2 \text{ cm}^{-1}$) laser excitation was also used. The upper spectrum of Fig. 8 was obtained with $\lambda_B = 1023.0 \text{ nm}$ from $PBHQ^-$ in glass III. Wavelengths in this region were chosen to provide excitation into the low energy shoulder of the $PBHQ^-$ absorption, Fig. 1, in order to optimize the probability of observing a zero-phonon hole. The spectrum of Fig. 8 was measured with 4 cm^{-1} resolution. A zero-phonon hole is apparent just to the left (blue) of λ_B . Its shift from λ_B is 12 cm^{-1} and its width is $\approx 10 \text{ cm}^{-1}$. The zero-phonon hole is superimposed on a band whose width is $\approx 60 \text{ cm}^{-1}$. This band obviously correlates with the feature at $\approx 9815 \text{ cm}^{-1}$ in the upper spectrum of Fig. 7. For the moment we focus on the 60 cm^{-1} wide band, the band displaced from it by 140 cm^{-1} (at 9956 cm^{-1}) and the broader negative going band whose maximum lies at about 10200 cm^{-1} . For convenience we will refer to these as the α , β , γ features, respectively. The first observation to be made is that these features appear to correlate with those of Fig. 7. Second, narrow line laser excitation has resulted in some line (band) narrowing of α and β . Thus, the low energy shoulder of the $PBHQ^-$ absorption profile is characterized by a degree of inhomogeneous broadening, Γ_{inh} . At the present time it is not

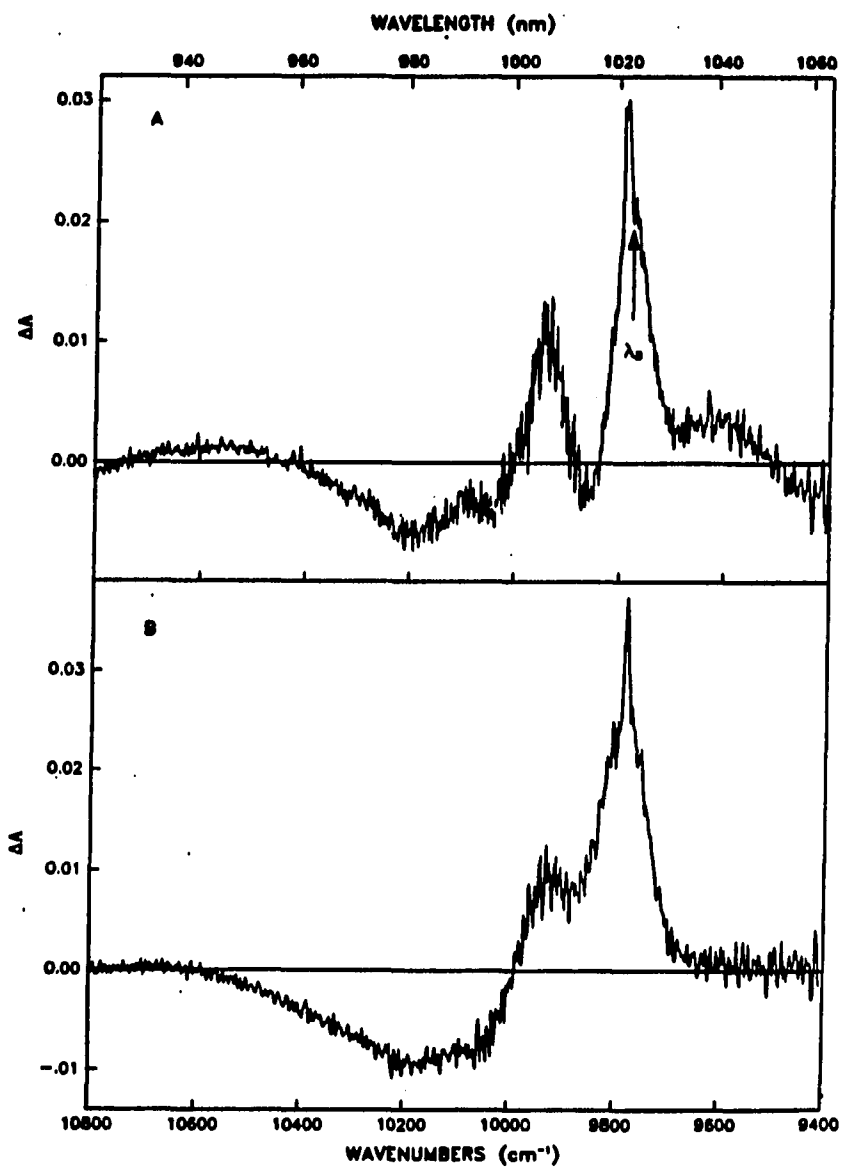


Figure 8.

(A) 4.2 K difference absorption spectrum of chemically reduced RC (PBHQ^-) minus that of PBHQ^- exposed to laser light (1023.0 nm) at ~ 4.2 K, see text. (B) Simulated spectrum which demonstrates that the zero-phonon hole is shifted from the burn wavelength due to an electrochromic shift of hole X, see text

possible to determine the magnitude of Γ_{inh} . For this reason the simulated spectrum, lower trace of Fig. 8, was calculated with the neglect of line narrowing. The simulation provides for the existence of a zero-phonon hole that *would be* coincident with λ_B were it not for a blue electrochromic shift of band a. The lower spectrum of Fig. 8 was calculated in a manner described earlier for the lower spectrum of Fig. 7. However, the electrochromic shift for Fig. 8 was set equal to 6.2 cm^{-1} . A key point is that the zero-phonon hole in the simulated spectrum appears shifted to the blue of λ_B by $\approx 7 \text{ cm}^{-1}$. Thus, our consistent observation that the zero-phonon hole is blue-shifted relative to λ_B is accounted for by a blue electrochromic shift of a broader component of the PBHQ^- absorption profile. The simulated spectrum is not meant to accurately account for the observed spectrum, again because the line narrowing phenomenon has not been sufficiently well characterized. Thus, for example, feature a of the simulated spectrum carries a width of 95 cm^{-1} in comparison with observed value of $\approx 60 \text{ cm}^{-1}$. We note that the width of the a band in the simulated spectrum does depend on the magnitude of the electrochromic shift chosen, see Fig. 7 where its width is $\approx 105 \text{ cm}^{-1}$ for a shift of 20 cm^{-1} .

Finally, we consider Band β in the upper spectrum of Fig. 8. It is particularly well resolved and displaced to higher energy of α by $\approx 140 \text{ cm}^{-1}$. Within experimental error, this displacement is equal to that for bands X and Y of the transient hole burned spectra (120 cm^{-1}), Fig. 3. In addition, bands α and β carry comparable widths. For both of these reasons we believe that there is a significant contribution of the absorbing state associated with hole Y to the β feature of Fig. 8. That is, the spectrum of Fig. 8 is the result of the interplay of electrochromic shifts of three absorption components which correspond to holes X, Y and Z of Fig. 3 for the unreduced RC. In the negative going γ band of the upper

spectrum of Fig. 8, a weak positive band at 10076 cm^{-1} can be discerned. Its displacement from band α is 260 or $2 \times 140\text{ cm}^{-1}$, 140 cm^{-1} being the displacement of band β from α . The observation of the $\alpha - 240\text{ cm}^{-1}$ is reproducible. The simulated spectrum of Fig. 8 provides a hint of its existence.

Because of this, and the correlation between features X-Y and α - γ of the transient and the electrochromic shift spectra, we assign hole Y as a 120 cm^{-1} phononic feature which builds on hole X. With this assignment, the interpretation of the transient hole spectra rests on the assignment of the states associated with the X, Z and zero-phonon holes. It is reasonable to assume that the zero-phonon holes observed in the transient and electrochromic shift spectra are due to the same absorbing state.

DISCUSSION

Broad Structure in the Transient Hole Spectra of P960

Line narrowing achieved by photochemical hole burning has led to the identification of three absorbing states which we refer to as $|X\rangle^*$, $|Y\rangle^*$ and $|Z\rangle^*$. For reasons just presented and given later, $|Y\rangle^*$ is assigned as a 120 cm^{-1} vibration of the electronic state $|X\rangle^*$. Hole X, Fig. 3, has been correlated with the low energy shoulder of the P960 absorption profile, the shoulder having been observed for all three glasses (I-III). Observation of the shoulder in absorption has been made earlier by several groups [12,27,38,39]. Its assignment has been quite controversial and has been variously to $|P^+B^-H\rangle^*$ [12,13] or a feature due to gross RC heterogeneity [39]. The heterogeneity could have several origins, e.g. an artificial protein-pigment configuration resulting from the cooling to cryogenic temperatures. In this picture it would be reasonable to suggest that $|X\rangle^*$ is just $|Z\rangle^*$ of perturbed RC. Whatever the origin of the heterogeneity (associated with structural variation from RC to RC) it is apparent that $|Z\rangle^*$ and $|X\rangle^*$ would be independent and uncoupled states. The hole burning data belie this possibility. The data show that as λ_B varies from the low energy to high energy tails of P960, the ratio of the intensity of hole Z to that of holes X and Y remains the same to within $\approx 20\%$. With reference to Fig. 3, we emphasize again that for $\lambda_B < 1006.2\text{ nm}$ (minimum value used was 947 nm) the hole spectra are identical, for all intent and purposes. This invariance was also observed for glasses II and III. The deconvolution procedure used to arrive at the above percentage did not take into

account the initial loss of line narrowing for holes X and Y as λ_B is decreased from the minimum value used. Taking this loss into account could result in an even greater degree of constancy for the above intensity ratio. Thus, we conclude that bleaching of $|Z\rangle^*$ leads to concomitant bleaching of $|X\rangle^*$ and vice versa. As a result, $|X\rangle^*$ is viewed as a state of the RC that is coupled to $|Z\rangle^*$ in the formation of P^+BHQ^- . The state $|X\rangle^*$ lies about 300 cm^{-1} lower in energy than $|Z\rangle^*$ (vertical energy gap).

An impurity contribution to the P960 absorption profile (e.g., the low-energy shoulder) would also represent heterogeneous broadening and, therefore, can also be eliminated as the origin of the X and Y hole structure. However, because $PBHQ^-$ and/or PBH^-Q^- are potential impurities in the untreated RC, we note that the millisecond gating used to obtain the Δ -transmission transient spectra (see Experimental section) in the A-B mode of the boxcar rules out interferences from them. Their excited state lifetimes [39] are too short to produce population bottleneck hole burning on a millisecond time scale. Of course, the production of PBH^-Q^- from $PBHQ^-$ can lead to persistent hole burning of $PBHQ^-$ at 4.2 K, *vide supra*. However, based on the relatively fast kinetics of formation of PBH^-Q^- [40], any contribution from $PBHQ^-$ would not be expected to appear in the A-B difference spectrum.

The transient hole burned spectra for glasses I-III indicate that $|X\rangle^*$ and $|Z\rangle^*$ are responsible for roughly 30 and 70%, respectively, of the P960 absorption intensity. None of the existing electronic structure calculations [7,8] predict the existence of two close lying states characterized by this intensity distribution. However, these calculations are semi-empirical in nature and continue to undergo refinement.

We proceed now to consider possible assignments for $|X\rangle^*$ and $|Z\rangle^*$. It is reasonable to attempt to interpret $|X\rangle^*$ and $|Z\rangle^*$ as states arising from strong coupling

between P^* (viewed as a special pair state with mixed neutral exciton and charge-transfer (CT) character) and one or more of the CT states $|P^+B^-H\rangle^*$, $|PB^+H^-\rangle^*$ and $|P^+BH^-\rangle^*$. On the basis of the experimental data on the reduced RC (Section III.B), the first two of the above possibilities are not likely. This follows since the production of the stable ground state species PBH^-Q^- would lead to the annihilation of the $|P^+BH^-\rangle^*$ and $|PB^+H^-\rangle^*$ states. The experimental data can be understood on the basis of both $|Z\rangle^*$ and $|X\rangle^*$ undergoing similar electrochromic blue shifts which result from the formation of PBH^-Q^- . These data do not exclude the possibility that $|Z\rangle^*$ and $|X\rangle^*$ are strong admixtures of P^* and $|P^+B^-H\rangle^*$, with P^* being the source of their oscillator strengths. Provided the primary decay channel of $|Z\rangle^*$ is to $|X\rangle^*$ and provided that this decay is faster than the ≈ 1 ps decay of $|X\rangle^*$ to $|P^+BH^-\rangle^*$ (see page 57), such an adiabatic two state model for P960 would be consistent with the low temperature time domain data [17,18] which pertain to the appearance of $|P^+BH^-\rangle^*$. Further discussion of the adiabatic two state model is deferred until page 62.

To conclude this subsection we consider two other possible assignments for $|Z\rangle^*$ and $|X\rangle^*$. The first is that they correspond to the upper and lower exciton (Davydov) components of the special pair. Such an assignment, however, seems unlikely in view of the electronic structure calculations [7,8]. For example, it would be difficult to explain why the lower exciton component is more weakly absorbing than the higher. The second is that $|Z\rangle^*$ and $|X\rangle^*$ are *special pair* states whose origin is the coupling between the neutral excitonic and state and a close lying intra-dimer charge-transfer state. Discussion of this possibility is given in page 59.

*The Zero-phonon Hole
in the Transient Hole Spectra of P960*

The zero-phonon hole (ZPH) coincident with λ_B was only observed when λ_B was located in the near vicinity of the low energy shoulder of the P960 absorption profile, see Figs. 4-6. When λ_B was decreased beyond a certain value (≈ 1016 nm for glass I) the ZPH could not be observed. The ZPH was most pronounced for λ_B located near the peak of hole X. A possible interpretation for the ZPH is that it is due to a photoactive impurity. Such an interpretation we believe to be unlikely since the impurity, in addition to possess a bottleneck state for hole burning with a life time similar to that of P^+BHQ . Furthermore, it is also observed as a feature in the persistent spectra produced by the reduction of $PBHQ^-$ with laser light to PBH^-Q^- when $\lambda_B \approx 1012$ nm, Fig. 8. Arguments which eliminate the possibility that the ZPH in the transient spectra is due to $PBHQ^-$ or PBH^-Q^- have already been given, vide supra. That the ZPH is not due to scattered light was routinely confirmed (see page 36).

We consider two other interpretations: that the ZPH is a feature belonging to the $|Z\rangle^*$ state (hole Z); and that it is associated with the $|X\rangle^*$ state (hole X). The model of Hayes and Small [26,27] admits the possibility that a weak ZPH might be observable for λ_B located on the low energy side of the $|Z\rangle^*$ absorption profile and near the center of the zero-phonon excitation distribution function. However, as will be discussed elsewhere [41], our data are not consistent with the ZPH being associated with $|Z\rangle^*$. The principal reasons are as follows: a coupled deconvolution procedure for the P960 absorption profile and transient hole spectra shows that the contribution of $|Z\rangle^*$ to the absorption near 1020 nm

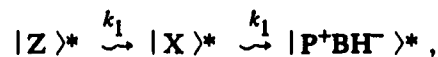
(where the ZPH is observed) is too small to account for the ZPH; and the ZPH should be easier to observe as λ_B decreases from ≈ 1016 nm, in contrast with the experimental observation that it vanishes for $\lambda_B \leq 1016$ nm.

Consider now the possibility that the ZPH is associated with hole X. Fig. 4 shows that as λ_B decreases in the vicinity of 1020 nm the position of the ZPH shifts in a particular manner relative to the maximum of hole X on which it is superimposed. Under the appropriate conditions the behavior seen in Fig. 4 is precisely that predicted by the theory of Hayes and coworkers [27]. Within the framework of this theory, the width of hole X would be associated primarily with electron-phonon coupling and inhomogeneous broadening while the actual relaxation time of $|X\rangle^*$ would govern the width of the ZPH. We note that the 1.8 K fluorescence spectrum of the RC of *Rps. viridis* measured by Maslov et al. [12] bears a mirror symmetry relationship to holes X and Y of Fig. 4 (upper trace). The fluorescence bands which correspond to holes X and Y (by mirror symmetry) are roughly 80 cm^{-1} broader than the holes. This is not surprising since the fluorescence was not measured under line narrowing conditions. The mirror symmetry relationship suggests that at liquid helium temperatures state $|X\rangle^*$ is the emissive state. From our data and those of ref. [12], the Stokes shift is $\approx 150 \text{ cm}^{-1}$. Using the mean phonon approximation, the Stokes shift is given by $2S\omega_m$, where ω_m is the mean phonon frequency. According to refs. [26,27] the intensity of the ZPH relative to the far more intense hole X is given by $\exp(-2S)$. Our transient hole burning measurements on glass I yield a value of ≈ 0.015 for this intensity ratio. Thus, $S \approx 2$. With this value and $2S\omega_m \approx 150 \text{ cm}^{-1}$, one has $\omega_m \approx 35 \text{ cm}^{-1}$. Phonons of this frequency have been observed in the high resolution hole burned spectra of the core antenna and LHCI complexes of photosystem I [42,43]. Both S and ω_m are key parameters in the

above theory and their values given above, together with reasonable values [27] for Γ_{inh} and the width of the one-phonon profile, have led, in preliminary calculations, to spectra that are in reasonable agreement with those of Fig. 4. Refined calculations are now in progress and will be reported on elsewhere [44].

Dynamical Implications of the Zero-phonon Hole (ZPH)

The preceding discussion indicates that the assignment of the ZPH to the $|X\rangle^*$ state is the most reasonable. The widths of the ZPH observed for the three glasses with a read resolution of $\approx 2 \text{ cm}^{-1}$ are $\approx 10 \text{ cm}^{-1}$. This width is an order of magnitude or more larger than those measured for many chromophores imbedded in glasses and polymers at the same temperature [45]. Perhaps more relevant is the observation that the ZPH of Chla in antenna complexes of photosystem I possess widths of $\approx 0.05 \text{ cm}^{-1}$ at 4.2 K [42,43]. Thus, the possibility that the $\approx 10 \text{ cm}^{-1}$ wide ZPH of the RC of *Rps. viridis* is homogeneously broadened due to population decay of the $|X\rangle^*$ state deserves consideration. This width, when viewed as resulting from depopulation of $|X\rangle^*$, corresponds to a decay time of 1 ps. Within our experimental uncertainty this decay time is the same as that measured in the time domain at 10 K (in a glycerol based glass) for the primary electron donor state [17,18]. Therefore, the possibility that $|X\rangle^*$, and not $|Z\rangle^*$, is a precursor state for electron transfer to H is suggested. This suggestion does not appear to conflict with the available time domain data if $k_1 > k_2$ ($k_2^{-1} \approx 1 \text{ ps}$) in the kinetic scheme



where a diabatic description for the oxidized P-reduced H excited state species is used. The fact that $|Z\rangle^*$ and $|X\rangle^*$ are viewed as adiabatic states means that the $|Z\rangle^* \rightarrow |X\rangle^*$ decay would be governed by the nonadiabaticity (nuclear kinetic energy) operator, perhaps through involvement of intermolecular pigment modes of suitably high frequency ($\approx 100 \text{ cm}^{-1}$) [46].

We return now to a discussion of the two models presented earlier for the nature of $|Z\rangle^*$ and $|X\rangle^*$: that they are admixtures of the dimer state P^* and $|P^+B^-H\rangle^*$ (model I); and that they are admixtures of the neutral exciton state of P and a close-lying intra-dimer charge transfer (CT) state (model II). Both models may be oversimplified. Nevertheless, they serve as reasonable starting points for a discussion of the transient hole burning and other data. For both models we assume that the neutral excitation of P is the source of the absorption intensity for P960. We consider model I first. Within this model P^* itself could be considered to possess CT character due to moderate mixing of the neutral exciton state with an intra-dimer CT state (relatively well separated from it) [7,8]. Excitation of $|Z\rangle^*$ or $|X\rangle^*$ would be expected to produce some degree of instantaneous bleaching of the Q_y transition of B due to their $\sim 30\%$ and 70% occupation numbers (vide supra) for $|P^+B^-H\rangle^*$, respectively. This bleaching, however, might be obscured by the concomitant growth of absorption of the Q_y -monomer type expected from P^+ as well as the electrochromic shifting of the Q_y transition of B_M [47]. As mentioned in the introduction, the conclusions drawn from ultrafast transient spectra are, to a degree, dependent on the model employed for data analysis. Another potential problem with model I stems from the fact that the hole associated with $|X\rangle^*$ is significantly sharper by about 3 times than the hole associated with

$|Z\rangle^*$. This suggests that [26,27] the linear electron-phonon coupling¹ associated with $|X\rangle^*$ is significantly weaker than that associated with $|Z\rangle^*$. On the surface this might appear to conflict with the model's tenet that $|X\rangle^*$ has an occupation number for $|P^+B^-H\rangle^*$ which is roughly twice that for $|Z\rangle^*$. However, the relationship between the dipole moment change and the linear electron-phonon coupling strength does depend on the *microscopic* dielectric constant (ϵ_m) [48] which shields the Coulombic interaction between an electron and hole. In part it is this interaction that determines the changes in inter-pigment distances and orientations which occur as a result of excitation to a state possessing significant charge-transfer character [49,50]. Calculations by Warshel [51] do indicate that the ϵ_m appropriate for the internal charge-transfer character of P^* may be significantly smaller than that appropriate for $|P^+B^-H\rangle^*$. Thus, it is conceivable that amino acids and water molecules in the RC could stabilize the charge separation in $|P^+B^-H\rangle^*$ without significant solvent and inter-pigment configurational changes. From ref. [27], an estimate for the solvent reorganization energy ($S\hbar\omega_m$, with ω_m a mean phonon frequency) of $|Z\rangle^*$ is $\approx 300 \text{ cm}^{-1}$, measured relative to the ground state. It is interesting that this value is similar to the energy gap between $|Z\rangle^*$ and $|X\rangle^*$. With the corresponding reorganization energy for $|X\rangle^*$ small in comparison, the difference in linear electron-phonon strengths between $|Z\rangle^*$ and $|X\rangle^*$ would appear to be of magnitude necessary to optimize nonadiabatic decay from $|Z\rangle^*$ to $|X\rangle^*$ via multi-phonon emission. Turning to model II we note first that it does not require an instantaneous bleaching of the Q_y transition of B. However, the problem just discussed for model I is also present for model II. It may be more difficult to reconcile since

¹ The term phonon is meant to include low frequency protein and pigment intermolecular modes.

the varying microscopic dielectric constant argument cannot be used. Nevertheless, model II remains a distinct possibility.

Finally, we mention that the state compositions in both models may be T - and solvent (detergent)-dependent because Stark measurements with polymer hosts at 77 K indicate that the dipole moment (measured relative to the ground electronic state) is constant across the P960 absorption profile [28-30]. Both models would predict this when the occupation numbers of the coupled zero-order states in $|Z\rangle^*$ and $|X\rangle^*$ approach 0.5.

Earlier Related Studies

Meech and coworkers [25] had earlier reported a hole burned spectrum of P960 for *Rps. viridis* RC dissolved in a glycerol/H₂O glass. The spectrum was obtained for $\lambda_B = 980$ nm. The burn laser light was modulated at a couple hundred hertz and the spectrum recorded using phase sensitive detection at a spectral resolution of 7 Å (in contrast with the 1-2 Å resolution of the present work). Despite the lower signal-to-noise ratio of their spectrum, the two-hole structure of Fig. 3 (lower spectrum) is discernible with hole maxima located at 1015 and 987 nm. These positions agree well with those of the lower spectrum of Fig. 3. However, the above workers did not comment on the two-hole structure in their spectrum. The single burn wavelength (980 nm) chosen would preclude observation of the additional structure observed in the present work with higher values of the burn wavelength. In their studies of P960 hole burning with polyvinyl alcohol host films, Boxer and coworkers [24] also utilize phase-sensitive detection but with a laser repetition rate of 10 Hz. A hole reading resolution of about 2 Å was employed. In their work, spectra are reported for

$\lambda_B = 1013, 1001$ and 974.7 nm. The P960 absorption maximum in polyvinyl alcohol occurs at ≈ 995 nm (4.2 K). All three hole spectra are characterized by a single asymmetric hole (width ≈ 400 cm^{-1}) centered near 1000 nm. There appears to be no indication of the additional hole structure (hole X and Y) observed in the present work, even in the $\lambda_B = 1013$ nm spectrum. The signal-to-noise ratio of their spectra would have precluded observation of a ZPH as weak as those reported here. The absence of holes X and Y in the spectra of ref. [24] may be due, in part, to the fact that at 4.2 K the absorption linewidth of P960 in polyvinyl alcohol is about 80 cm^{-1} broader than those reported here for glasses I-III. This additional width would make the hole structure more difficult to discern. Furthermore, the energy separation between the $|Z\rangle^*$ and $|X\rangle^*$ states could reasonably be expected to exhibit solvent dependence. It is suggested that further hole burning studies of P960 in polyvinyl alcohol may prove fruitful.

Interestingly, Ganago et al. [52] have recently reported on the observation of a weak ZPH superimposed on the broad hole observed earlier for P870 of *Rb. sphaeroides*. Only a single burn wavelength located near the absorption maximum was utilized in ref. [52]. Thus, additional studies are required in order to provide a suitably detailed understanding of the hole burning and electronic structure of P870.

Finally, if one accepts the premise that two states contribute to the P960 absorption profile, it becomes necessary to refine the procedure used by Hayes and coworkers [27] to obtain theoretical fits to the hole spectra reported by Boxer and coworkers [24]. In their calculations, a single absorbing electronic state was assumed and furthermore, the determination of the Huang-Rhys factor S and mean phonon frequency, ω_m , was based on an analysis of thermal broadening and Stokes shift data which also assumed a single state model.

Nevertheless, the basic conclusion reached by Hayes et al. [27] that strong linear electron-phonon coupling and inhomogeneous broadening are important contributors to the P960 absorption profile is unlikely to be negated by more elaborate calculations.

CONCLUDING REMARKS

The important conclusion from this work is that two close lying electronic states contribute significantly to the P960 absorption profile. The zero-phonon hole data in combination with the time domain data suggest that the lower energy and less strongly absorbing state is the emitting and precursor state for the formation of $|P^+B^-H\rangle^*$ (at least at low temperatures). The data indicate that the coupling between P^* and another close lying state of the RC is strong. In view of the data presented, the most reasonable candidate for the latter state is $|P^+B^-H\rangle^*$ (model I) and an intra-dimer CT state (which couples with the neutral excitonic state of P, model II). For model I the diabatic description of the initial phase of charge separation (in which the electron is initially located on P) is not appropriate and the question of whether $|P^+B^-H\rangle^*$ serves as a real intermediate or virtual state is not particularly relevant. This is not the case for model II. Since in both models $|Z\rangle^*$ and $|X\rangle^*$ are adiabatic states, the relaxation (rate constant k_1) from $|Z\rangle^*$ to $|X\rangle^*$ would be governed by the nuclear kinetic energy operator. The promoting mode(s) could be a relatively large amplitude inter-pigment vibration which modulates electron exchange between P and B. The 120 cm^{-1} mode of the $|X\rangle^*$ state may be a candidate since such a mode is absent in the Q_y absorption spectra of chlorophyll monomers in antenna complexes [42,43]. The vibrational period of the 120 cm^{-1} mode is 0.28 ps which would set a lower limit for k_1 of $3.6 \times 10^{12}\text{ s}^{-1}$. Within this picture, the 120 cm^{-1} mode could derive its absorption intensity through vibronic coupling between $|Z\rangle^*$ and $|X\rangle^*$.

Experiments designed to further test the adiabatic two state model for P960 (P870) of

Rps. viridis (*Rb. sphaeroides*) are planned.

Note Added in Proof

We have recently succeeded in observing the X-Z hole structure for P870 of *Rb. Sphaeroides* and will report these results in the near future. Hole structure for P680 of PS II, which is similar to that of hole X for P960, has also been observed [53].

ACKNOWLEDGEMENT

Ames Laboratory is operated for the U.S. Department of Energy by Iowa State University under contract No. W-7405-Eng-82. This research was supported by the Director for Energy Research, Office of Basic Energy Science. The research at Argonne Laboratory was supported by the Division of Chemical Sciences, Office of Basic Energy Sciences, U.S. Department of Energy under contract No. W-31-109-Eng-38. One of us (G.J.S.) would like to thank G. R. Fleming, W. W. Parson and A. Warshel for several stimulating discussions and G. R. Fleming for making available to us refs. [16,17].

REFERENCES

1. Budil, D. E.; Gast, P.; Chang, Ch. H.; Schiffer, M.; Norris, J. *Ann. Rev. Phys. Chem.* 1987, 38, 561;
Kirmaier, C.; Holten, D. *Photosynthesis Research* 1987, 13, 225.
2. Deisenhofer, J.; Epp, O.; Miki, K.; Huber, R.; Michel, H. *J. Mol. Biol.* 1984, 180, 385.
3. Deisenhofer, J.; Epp, O.; Miki, K.; Huber, R.; Michel, H. *Nature* 1985, 318, 618.
4. Michel, H.; Epp, O.; Deisenhofer, J. *EMBO J.* 1986, 5, 2445.
5. Allen, J. P.; Feher, G.; Yeates, T. O.; Rees, D. C.; Deisenhofer, J.; Michel, H.; Huber, R. *Proc. Natl. Acad. Sci. USA* 1986, 83, 8589.
6. Chang, C. H.; Tiede, D.; Tang, J.; Smith, U.; Norris, J.; Schiffer, M. *FEBS Lett.* 1986, 205, 82.
7. Warshel, A.; Parson, W. W. *J. Am. Chem. Soc.* 1987, 109, 6143
8. Scherer, P. O. J.; Fisher, S. F. *Biochim. Biophys. Acta* 1987, 891, 157 and refs. therein.
9. Michel-Beyerle, M. E.; Plato, M.; Deisenhofer, J.; Michel, H.; Bixon, M.; Jortner, J. *Biochem. Biophys. Acta* 1988, 932, 52 and refs. therein.
10. Marcus, R. A. *Chem. Phys. Lett.* 1987, 133, 471.
11. Bixon, M.; Jortner, J.; Michel-Beyerle, M. E.; Ogrodnik, A.; Lersch, W. *Chem. Phys. Lett.* 1987, 140, 626.
12. Maslov, V. G.; Klevanik, A. V.; Ismailov, M. A.; Shuvalov, V. A. *Dokl. Akad. Nauk SSSR* 1983, 269, 1217.

13. Shuvalov, V. A.; Klimov, W. A. *Biofizika* 1987, 32(5), 814.
14. Kirnaier, C.; Holten, D.; Parson, W. W. *FEBS Lett.* 1985, 185, 76.
15. Breton, J.; Martin, J.-L.; Antonetti, A.; Orszag, A. *Proc. Natl. Acad. Sci. USA* 1986, 83, 5121.
16. Wasielewski, M. R.; Tiede, D. M. *FEBS Lett.* 1986, 204, 368.
17. Breton, J.; Martin, J. L.; Fleming, G. R.; Lambry, J. C. *Biochemistry*, submitted for publication.
18. Martin, J. L.; Breton, J., Lambry, J. C. and Fleming, G. R., *The photosynthetic bacterial reaction center*, eds. Breton J. and A. Vermeglio, NATO ASI series, Series A: Life sciences (Plenum Press, New York, 1988) p. 195, to be published; Fleming, G. R.; Martin, J. L.; Breton, J., *Nature* 1988, 27, 8276.
19. Martin, J. L.; Breton, J.; Hoff, A. J.; Migus, A.; Antonetti, A. *Proc. Natl. Acad. Sci. USA* 1986, 83, 957.
20. Fisher, S. F.; Scherer, P. O. J. *Chem. Phys.* 1987, 115, 151.
21. Chekalin, S. V.; Matveetz, Ya. A.; Skuropatov, A. Ya.; Shuvalov, V. A.; Yartzer, A. P. *FEBS Lett.* 1987, 216, 245.
22. Boxer, S. G.; Lockhart, D. J.; Middendorf, T. R. *Chem. Phys. Lett.* 1986, 123, 476.
23. Meech, S. R.; Hoff, A. J.; Wiersma, D. A. *Chem. Phys. Lett.* 1985, 121, 287.
24. Boxer, S. G.; Middendorf, T. R.; Lockhart, D. J. *FEBS Lett.* 1986, 200, 237.
25. Meech, S. R.; Hoff, A. J.; Wiersma, D. A. *Proc. Natl. Acad. Sci. USA* 1986, 83, 9464.
26. Hayes, J. M.; Small, G. J. *J. Phys. Chem.* 1986, 90, 4928.
27. Hayes, J. M.; Gillie, J. K.; Tang, D.; Small, G. J. *Biochim. Biophys. Acta* 1988, 932,

- 287.
28. Lösche, M.; Feher, G.; Okamura, M. Y. *Proc. Natl. Acad. Sci. USA* 1987, 84, 7537.
 29. Boxer, S. G.; Lockhart, D. J.; Middendorf, T. R. in *Proc. in Physics, Primary Processes in Photobiology* (Kobayashi, T., ed.) 1987, 20, 80; Springer-Verlag, NY.
 30. Lockhart, D. J.; Boxer, S. G. *Proc. Natl. Acad. Sci. USA* 1988, 85, 107.
 31. Won, Y.; Friesner, R. A. *Proc. Natl. Acad. Sci. USA* 1987, 84, 5511.
 32. Tang, D.; Jankowiak, R.; Gillie, J. K.; Small, G. J.; Tiede, D. M. *J. Phys. Chem.*, 1988, 92, 4012.
 33. Dan Blanken, H. J.; Hoff, A. J. *Biochim. Biophys. Acta* 1982, 681, 365.
 34. Tiede, D. M.; Prince, R. C.; Dutton, P. L. *Biochim. Biophys. Acta* 1976, 449, 447.
 35. Netzel, T. L.; Rentzepis, P. M.; Tiede, D. M.; Prince, R. C.; Dutton, P. L. *Biochim. Biophys. Acta* 1977, 460, 467.
 36. Prince, R. C.; Tiede, D. M.; Thornber, J. P.; Dutton, P. L. *Biochim. Biophys. Acta* 1977, 462, 467.
 37. Tiede, D. M.; Kellog, E.; Breton, J. *Biochim. Biophys. Acta* 1987, 892, 294.
 38. Vergmelio, A.; Paillotin, G. *Biochim. Biophys. Acta* 1982, 681, 32.
 39. Den Blanken, H. J.; Jongenelis, A. P. J. M.; Hoff, A. J. *Biochim. Biophys. Acta* 1985, 725, 472.
 40. Holten, D.; Winsor, M.; Parson, W. W.; Thornber, J. P. *Biochim. Biophys. Acta* 1978, 501, 112;
Schopes, R. J.; Wraight, C. A.; Levine, L. M. A.; Holten, D. *Biophys. J.* 1986, 49A, 23;
Shuvalov, V. A.; Parson, W. W. *Biochim. Biophys. Acta* 1981, 638, 50.

41. Tang, D.; Jankowiak, R.; Small, G. J., to be published.
42. Gillie, J. K.; Hayes, J. M.; Small, G. J.; Golbeck, J. H. *J. Phys. Chem.* 1987, 91, 5524.
43. Gillie, J. K., Small, G. J.; Golbeck, J. H. *J. Phys. Chem.*, in press.
44. Hayes, J. H.; Small, G. J. *J. Phys. Chem.*, to be submitted for publication.
45. Moerner, W. E. (Ed.), *Persistent Spectral Hole-Burning: Science and Application*, in: *Topics in Current Physics 1988*, Vol. 44, Springer-Verlag, New York. Chs. 2, 3 and 5.
46. Warshel, A. *Proc. Natl. Acad. Sci. USA* 1980, 77, 3105.
47. Kirmaier, C.; Holten, D. in: *Structure of Bacterial Reaction Centers: X-Ray Crystallography and Optical Spectroscopy with Polarized Light*, eds. Breton, J. and Vermeglio, A., Plenum, New York, to be published.
48. Warshel, A.; Russell, S. T. *Quart. Rev. Biophys.* 1984, 17, 283.
49. Haarer, D. *J. Chem. Phys.* 1977, 67, 4076.
50. Beckman, R. L.; Small, G. J. *Chem. Phys.* 1978, 30, 19.
51. Warshel, A., private communication.
52. Ganago, A. O.; Melkozernov, A. N.; Shuvalov, V. A. *Biophysics* 1986, 31, 481.
53. Small et al., *J. Chem. Phys.*, in press.

**PAPER II. STRUCTURE AND MARKER MODE OF THE PRIMARY
ELECTRON DONOR STATE ABSORPTION OF PHOTO-
SYNTHETIC BACTERIAL: HOLE BURNED SPECTRA**

**STRUCTURE AND MARKER MODE OF THE PRIMARY
ELECTRON DONOR STATE ABSORPTION OF
PHOTOSYNTHETIC BACTERIA: HOLE BURNED SPECTRA**

D. Tang, S. G. Johnson, R. Jankowiak, J. M. Hayes,

G. J. Small and D. M. Tiede

in *Perspective in Photosynthesis* (J. Jortner and B. Pullman, Eds),

pp 23-38, Dordrecht/Boston/London: Kluwer Academic Press

ABSTRACT

Structured photochemical hole burned spectra are presented for P870 and P960 of the reaction centers (RC) of *Rhodobacter sphaeroides* and *Rhodospseudomonas viridis*. A special pair marker mode (ω_{sp}) Franck-Condon progression is identified for both P870 and P960. Zero-phonon holes are reported which yield P870* and P960* decay times in good agreement with the time domain values. This agreement suggests that vibrational thermalization occurs prior to the primary charge separation process. The theory of Hayes and Small [1], embellished for the marker mode progression, is shown to account for the primary donor state absorption and burn-wavelength dependent hole spectra. Site excitation energy selection is used to establish correlation between a higher energy RC state and P* for both bacteria.

INTRODUCTION

The recently revealed structures of the reaction center (RC) of *Rps. viridis* [2-4] and *Rb. sphaeroides* [5-7] have led to even greater activity [8,9] directed towards understanding the primary charge separation process which is triggered by excitation of the primary electron donor states P960* and P870*, respectively. It is generally accepted that the lowest energy component of the special pair Q_y transition contributes significantly to the electronic structure of P*. This component is often referred to as P₋ since the Q_y transition dipoles of the monomers, which comprise the pair (P_L, P_M), would be anti-parallel in the simplest model. It should be noted, however, that agreement on the structures of the higher energy Q_y states of the six-pigment RC has not been arrived at on the basis of semi-empirical calculations [10,11].

In this paper we present new photochemical hole burned (PHB) spectra for P960 and P870 which reveal that their underlying structures are very similar, identify a low frequency marker mode for both special pairs, reveal the origin of the homogeneous broadening for the P960 and P870 absorption profiles and determine the decay times of P960* and P870* from their zero-point levels at 4.2 K. The decay times are used to address the question of whether or not thermalization of vibrational modes occurs prior to charge separation. In addition, a site excitation energy correlation effect for *Rps. viridis* and *Rb. sphaeroides* is observed which identifies an excited RC state that is correlated with P₋. An assignment of the former to a state which is significantly contributed to by P₊ (upper special pair component) is suggested.

The λ_B (burn-wavelength)-dependent PHB spectra of Boxer and his group [12,13] first

revealed that there is a significant homogeneous broadening contribution to the P870 and P960 absorption profiles. This result attracted considerable attention [14] since the broad ($\sim 400 \text{ cm}^{-1}$) unstructured holes observed could be a manifestation of ultra-fast electronic relaxation [15,16] and/or significant protein-pigment geometry changes [1,17] which accompany electronic excitation of P. We present further evidence [18,19] that proves that the latter is the correct model.

We recently reported structured transient PHB spectra (4.2K) for P960 for three glass-detergent host systems [18,19]. The structure included two relatively broad ($\sim 100 \text{ cm}^{-1}$) holes denoted as X and Y, with Y assigned as a $\sim 130 \text{ cm}^{-1}$ ($\equiv \omega_{sp}$ in what follows) vibronic hole which builds to higher energy on X. The ω_{sp} mode was also identified from the spectrum of PHB^-Q^- (B = BChl monomer, H = BPheo, Q = quinone) produced by narrow line laser irradiation into P960 of PBHQ^- [19]. We note that the ω_{sp} feature in the $(\text{PB}^-\text{HQ}^- - \text{PBHQ}^-)$ difference spectrum had been observed much earlier by Vermeglio and Paillotin [20] under non-line narrowing conditions; however, it was not assigned as a vibration. In addition, in refs. [18,19] a weak but relatively sharp ($\sim 10 \text{ cm}^{-1}$) zero-phonon hole (ZPH) coincident with λ_B was observed when λ_B is located in the vicinity of the low energy shoulder (see below) of the P960 absorption profile for PBHQ^- . It was concluded that X correlates with this shoulder and, furthermore, that the 10 cm^{-1} hole is the ZPH of X. Hole X was assigned as the intramolecular zero-point level (ω_{sp}^0) of P960. The ZPH width of $\sim 10 \text{ cm}^{-1}$ yielded a P960* decay time of 1 ps at 4.2 K which is in reasonable agreement with the 0.7 ± 0.1 ps value measured in the time domain at 10 K [21,22]. The weak intensity of the ZPH relative to X ($\sim 1:100$) was ascribed to moderately strong linear electron-phonon coupling (Huang-Rhys factor $S \sim 2$) involving low frequency protein phonons [1,17].

Arguments, based mainly on the experimental gating employed and the λ_p -dependence of the hole spectra, were presented for the PHB structure (incl. the ZPH) not being due to impurity, e.g., stable $PBH^{\cdot-}Q^{\cdot-}$ afforded by irradiation of $PBHQ^{\cdot-}$ in the presence of cytochrome. Observation of the same structure for P870 of *Rb. sphaeroides* would provide an even stronger argument against impurity since the cytochrome is absent and especially if the ZPH hole width were to yield a decay time for P870* in good agreement with the time domain value of 1.2 ± 0.1 ps at 10 K [21,22]. The results presented here provide definitive proof that the low energy shoulder of P870 and P960 absorption profiles as well as the structure reported in refs. [18,19] for the PHB spectra of P960 are intrinsic to the RC.

EXPERIMENTAL

Sample Preparation

Fresh samples of reaction centers (RC) from *Rps. viridis* and *Rb. sphaeroides* were prepared by dissolving RC crystals in suitably buffered hosts. Details concerning crystallization procedure can be found in Ref. [5]. *Rps. viridis* and *Rb. sphaeroides* were prepared either in glycerol:water glass (2:1, hereafter referred to as glycerol glass) with 0.1% LDAO detergent, 10 mM Tris, $pH = 8.0$ and/or in glycerol glass in the presence of 0.8% n-octyl- β -D glucopyranoside detergent, 10 mM Tris, 1 mM BDTA, $pH = 8.0$. RC samples in polyvinyl alcohol films (PVOH) (~ 0.1 mm thick) were also utilized. The optical density (OD) of the samples utilized in this paper was less than 0.5 at the peak of the primary donor state absorption.

Measurements

The block diagram of the experimental system employed is shown and described in Fig. 1. Burn irradiation (linewidth 0.2 cm^{-1}) was provided by the Raman shifted (H_2 gas) output of an excimer-pumped dye laser, Lambda Physik EMG 102 and FL-2002, respectively. A pulse repetition rate of 16 and 20 Hz was utilized for *Rb. sphaeroides* and *Rps. viridis*, respectively. Raman shifted pulse energies utilized were < 0.4 mJ (focused to either a 0.3 cm diameter spot or a 0.2 cm x 0.8 cm spot). Samples were mounted and cooled to $T = 4.2$ K.

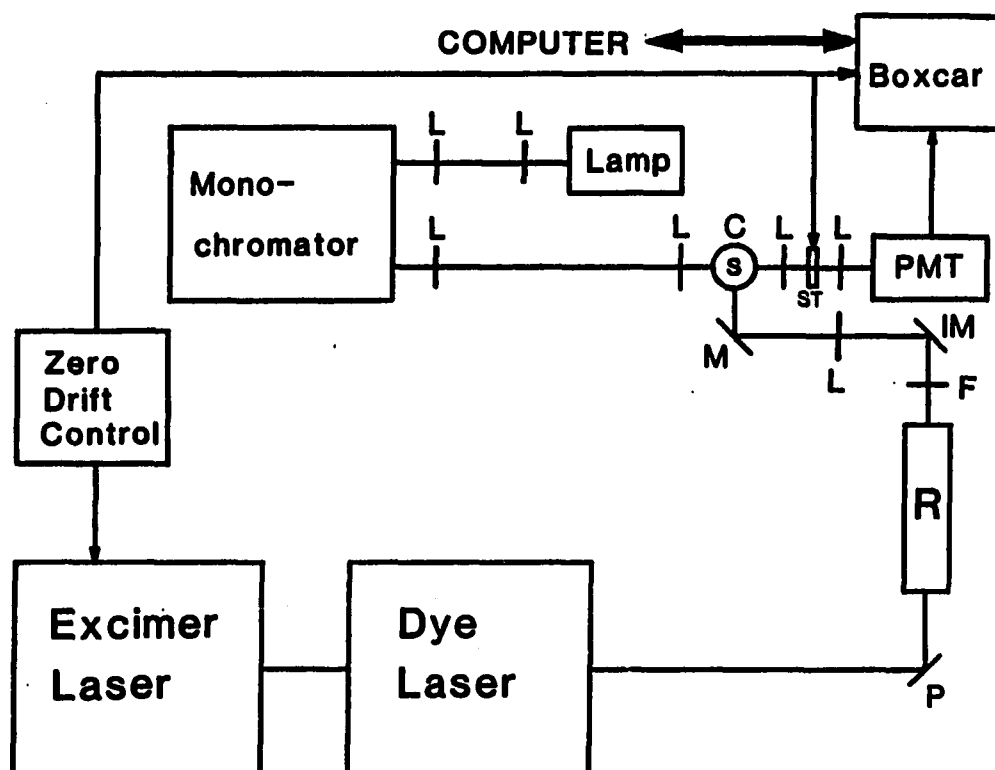


Figure 1. Block diagram of experimental apparatus. L = lens, M = mirror, IM = infrared mirror, ST = mechanical shutter, R = Raman shifter, S = sample, P = prism, C = liquid helium cryostat, F = filter, PMT = photomultiplier tube

in a Janis model 8-DT super vari-temp liquid helium cryostat. All PHB spectra reported here for P870 and P960 are for delta transmission (ΔT) changes $< 20\%$, although by utilizing higher pulse energies bleaching of $\sim 80\%$ could be obtained. Measurements were made by employing a Stanford Research SR250 boxcar averager interfaced with a IBM-PC compatible computer. The gate delay (triggered by the 10 ns laser pulse) for the boxcar was 2-3 ms and the gatewidth was 150 ms. The ΔT and ΔA (absorbance) spectra were obtained by subtracting laser-on and laser-off spectra. Interference from the laser was eliminated by the gating and by using a mechanical shutter between the sample and the photomultiplier tube. In addition, any laser scatter would be detected as a broad range baseline deviation and specific interference with any sharp features would be negligible. By varying the gate delay it was determined that the lifetimes of the charge separated bottleneck state P^+BHQ^- for *Rps. viridis* and *Rb. sphaeroides* (4.2 K) are 8 ± 1 ms and 34 ± 3 ms, respectively. A large number of burn wavelength values were employed, only several examples of representative spectra are shown. Absorption spectra were obtained with a Bruker IFS 120 HR Fourier-transform infrared (visible) spectrometer operating at a resolution of 4 cm^{-1} .

RESULTS AND DISCUSSION

Transient PHB spectra for the Q_y -region of *Rps. viridis* and *Rb. sphaeroides* will be presented for two host/detergent combinations; glycerol/LDAO and PVOH/LDAO for the former and glycerol/NGP and PVOH/NGP for the latter. The 4.2 K absorption spectra are shown in frames A and B of Fig. 2. The FWHM of P960 and P870 are given in the caption. These spectra and those for *Rps. viridis* in glycerol/NGP and PVOH/NGP (not shown) show that PVOH produces a significant blue shift and increase in the FWHM of the PED state absorption profile relative to glycerol [17] host. In spectrum 1 of frame A the bands at 810 and 790 nm are labeled in the usual way as H_L and H_M while the band at 835 nm is labeled as B_L and B_M (unresolved). Of course such assignments should be viewed as approximate since electronic structure calculations suggest significant coupling between the Q_y -transitions of the six-pigment aggregate [11]. The shoulder at ~ 852 nm of spectrum 1 has been assigned by Vermeglio et al. [20] to P_+ , the upper dimer component of the Q_y -transition of the special pair. We present data later that are consistent with this assignment. Comparison of the frame A and B spectra shows that the H_L and H_M transitions are not resolved for *Rb. sphaeroides* and, furthermore, that the " P_+ " transition, which appears on the low E side of the (B_M, B_L) band, is difficult to discern for *Rb. sphaeroides*. It is also evident that the reduction in inhomogeneous broadening provided by glass hosts (relative to PVOH) leads to improved spectral resolution. This is also the case for the transient PHB spectra, vide infra.

Absorption profiles of P960 and P870 are shown in Fig. 3 for glycerol/NGP and glycerol/LDAO glass solvents, respectively. The low E shoulder of P960 is more evident than

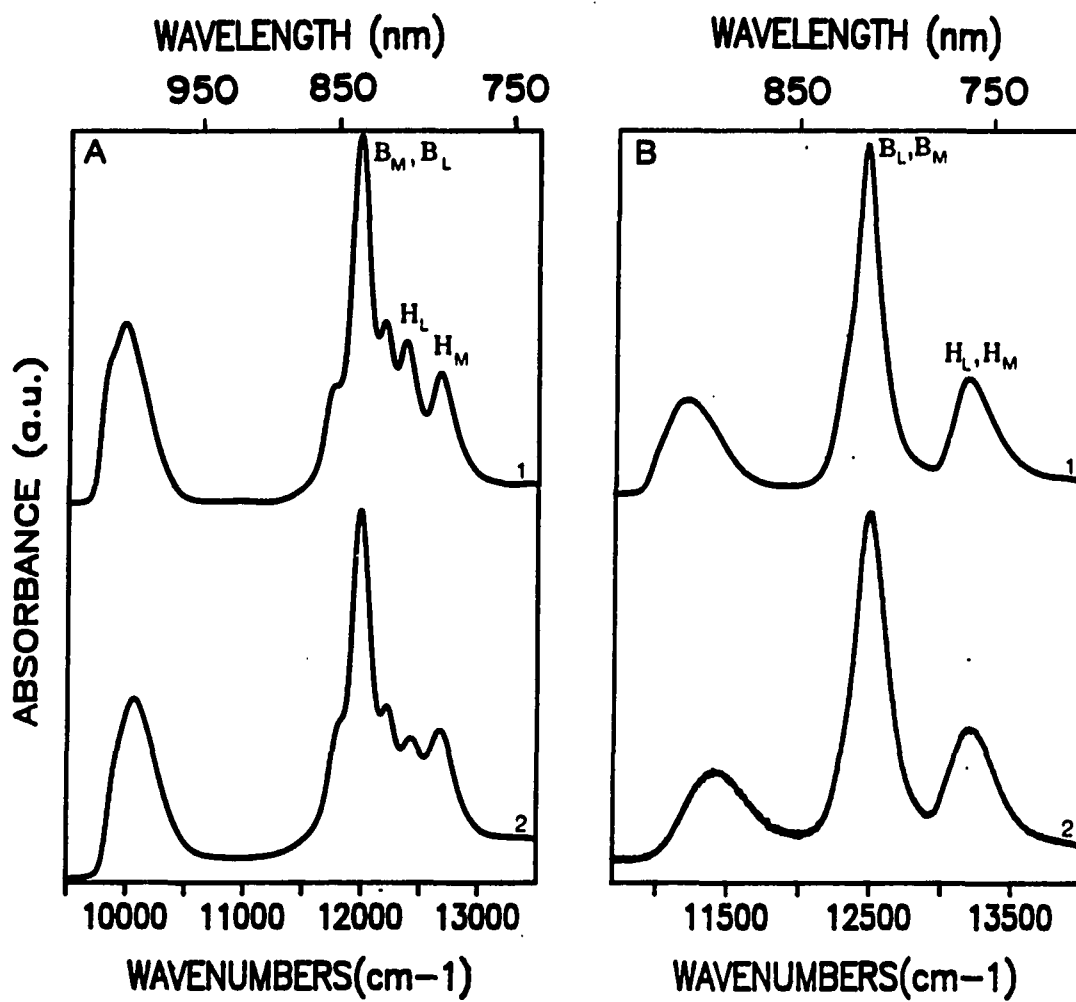


Figure 2. Absorption spectra of the Q_y region, $T = 4.2$ K: A) *Rps. viridis*: 1.) glycerol/LDAO (FWHM = 420 cm^{-1}), 2.) PVOH/LDAO (470 cm^{-1}). B) *Rb. sphaeroides*: 1.) glycerol/NGP (470 cm^{-1}), 2.) PVOH/NGP (550 cm^{-1})

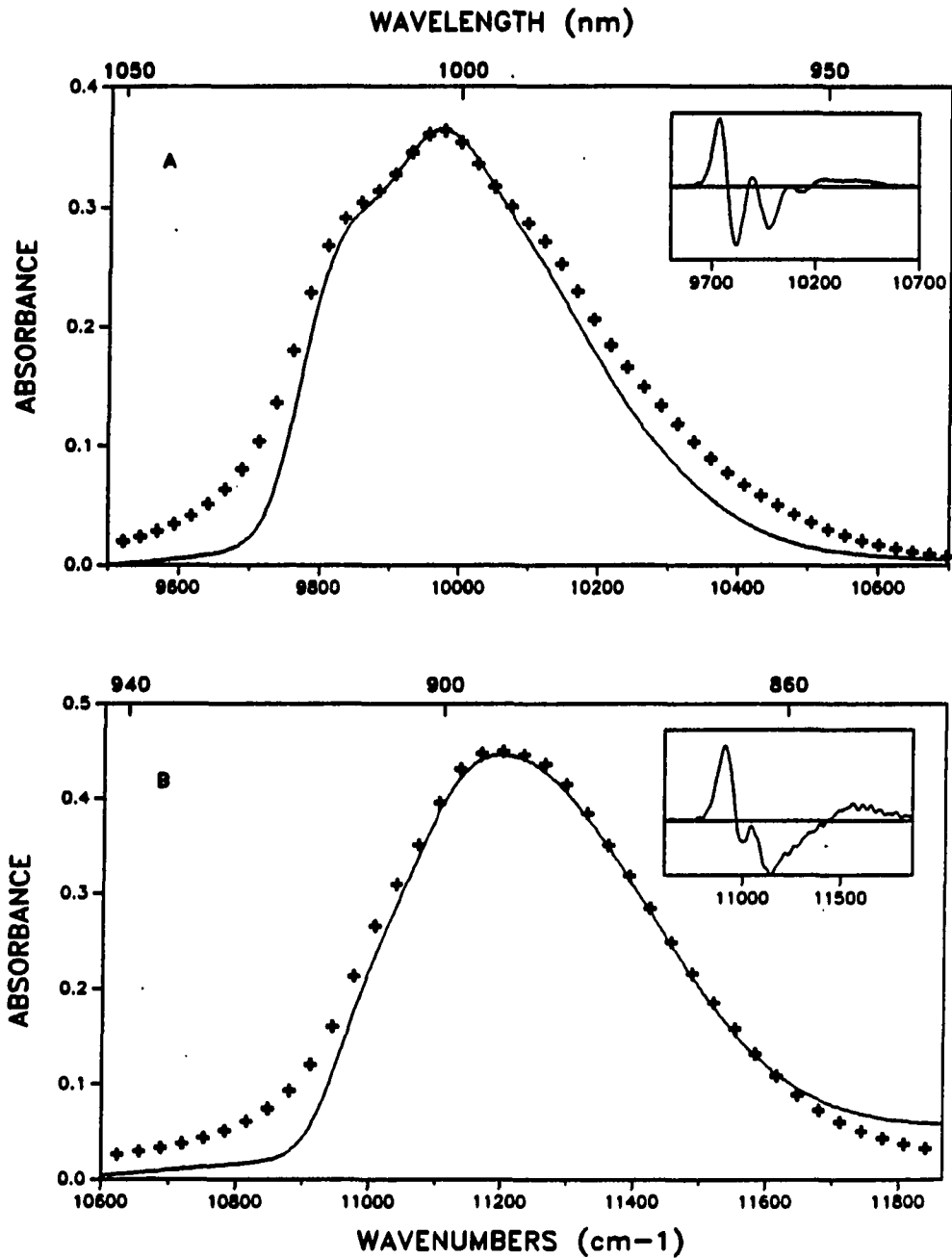


Figure 3.

Calculated and experimental absorption spectra for: A) P960. Parameters for calculated spectrum (++++): Γ (one phonon profile width) = 50 cm^{-1} , ω_m (mean phonon frequency) = 40 cm^{-1} , S (Huang-Rhys factor) = 1.5, Γ_I (inhomogeneous linebroadening) = 120 cm^{-1} , ω_{sp} = 150 cm^{-1} , S_{sp} = 1.1. B) P870. Parameters for calculated spectrum: Γ = 50 cm^{-1} , ω_m = 35 cm^{-1} , S = 2.0, Γ_I = 130 cm^{-1} , ω_{sp} = 125 cm^{-1} , S_{sp} = 1.55. Four overtones of ω_{sp} were utilized in both cases. Insets showing the 2nd-derivative spectra

for P870 (the second derivative spectrum of the P870 profile clearly reveals the shoulder, see insert spectrum). Further evidence [18,19] for the shoulder being the origin (ω_{sp}^0) band of the PED state absorption profile is presented below.

Transient Hole Burned Spectra of P870 and P960

Transient ΔA FHB spectra for P870 (glycerol/NGP) are shown in Fig. 4 for four λ_B -values. ΔT spectra are also presented for $\lambda_B = 907$ and 910 nm in order to illustrate the improved resolution provided by the ΔT -mode when the absorbance is sufficiently high. The ZPH coincident with λ_B becomes more pronounced as λ_B is decreased from the optimum value. Such behavior is consistent with the theory of hole burning in the presence of moderately strong linear electron-phonon coupling and inhomogeneous broadening [1,17], vide infra. The ZPH widths and their relationship to the depopulation decay time of P870* are discussed in section III.B. In spectra 2a and 2b of Fig. 4 one observes a broader hole (indicated by the dashed arrow) which is displaced by $\sim 125 \text{ cm}^{-1}$ to higher energy of the ZPH (λ_B). It is hole Y (ω_{sp}^1) for P870.

The vibronic hole structure associated with ω_{sp} is more apparent for P960, as shown by Fig. 5 (glycerol/LDAO), primarily because ω_{sp} (P960) is significantly higher than for P870 (by about $\sim 20\%$) and the P960 absorption profile is narrower than the P870 profile (420 vs. 475 cm^{-1} FWHM, glycerol/glass). In Fig. 5 three quanta of $\omega_{sp} \sim 150 \text{ cm}^{-1}$ are discernible (see dashed arrows) and the ZPH coincident with λ_B is observable in spectra 2 and 3b. The ZPH for P960 is generally more difficult to detect than for P870 because it is considerably broader, see page 95.

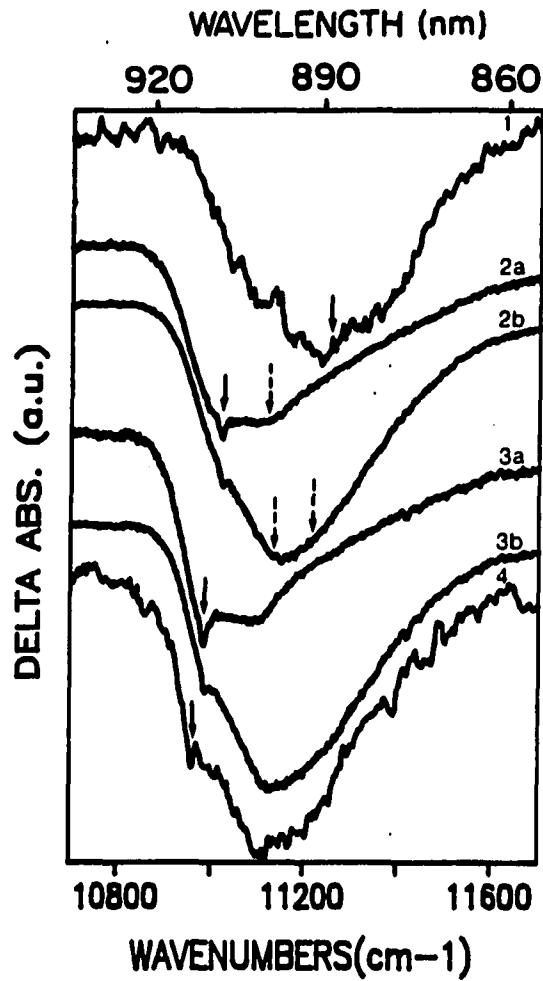


Figure 4.

Hole burned spectra for P870, $T = 4.2$ K. Solid arrows locate $\lambda_B = 890, 907, 910,$ and 912 nm for spectra 1-4. All spectra are ΔA except for 2a and 3a which are ΔT spectra corresponding to 2b and 3b, respectively. Resolution < 8 cm^{-1} . Dashed arrows in 2a and 2b indicate approximate positions of ω_{sp}^1 and ω_{sp}^2 satellites

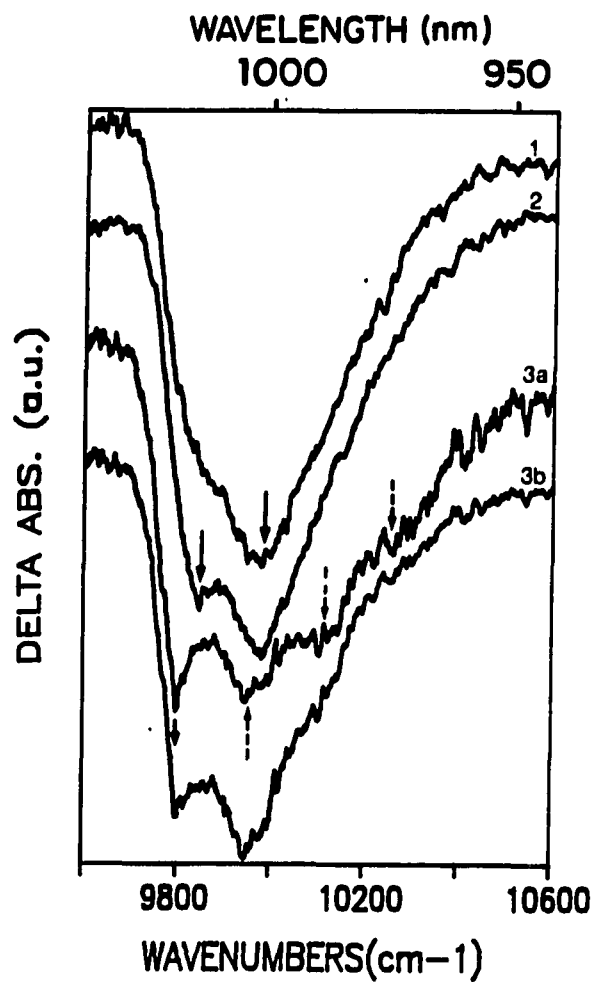


Figure 5. Hole burned spectra for P960, $T = 4.2$ K. Solid arrows locate $\lambda_B = 1000, 1015, 1020$ nm for spectra 1-3. All spectra are ΔA except for 3a which is ΔT spectrum corresponding to 3b. Resolution = 8 cm^{-1} . Dashed arrows in 3a indicate 1st, 2nd, and 3rd quanta of ω_{sp} satellite holes

The spectra of Figs. 3-5 demonstrate that the underlying structure of the PED state absorption profile for photosynthetic bacteria is strongly contributed to by the ω_{sp} -progression with a Huang-Rhys factor, S_{sp} , in the vicinity of unity. However, the weakness of the ZPH belonging to the broader ω_{sp}^0 (origin) hole indicates that the coupling of the $P_- \leftarrow P$ transition to lower frequency phonons must be moderately strong. As discussed in Section III.B., the suggestion that P_- undergoes ultra-fast electronic relaxation into CT states prior to formation of F^+BH^- [15] finds no support from our data. Thus, we proceed to investigate the degree to which the theory of Hayes et al. [17] can account for the absorption and PHB spectra of P870 and P960. This theory was developed to explain the previously reported [12,13] unstructured hole spectra of P870 and P960 and, to this end, the mean phonon frequency (ω_m) approximation was utilized. Because the Franck-Condon factors for the intramolecular modes of BChl are very small (≤ 0.04) [23,24], they were reasoned to be unimportant for understanding the principal features of the PHB spectra of P_- [17]. However, with the observation of the ω_{sp} -progression, the theory must be augmented to include the electron-vibration coupling due to ω_{sp} . The procedure for doing so is straightforward and is briefly outlined in what follows.

Within the mean phonon frequency approximation Hayes et al. [17] express the low temperature absorption profile of a single site as

$$L(\Omega - \nu) = e^{-S} l_0(\Omega - \nu) + \sum_{r=1}^{\infty} \frac{S^r e^{-S}}{r!} l_r(\Omega - \nu - r\omega_m) \quad (1)$$

where ν is the zero-phonon transition frequency and ω_m is the mean frequency for phonons which couple to the electronic transition. The Huang-Rhys factor is S and the Franck-Condon factors for the $r = 0, 1, \dots$ phonon transitions are governed by the Poisson distribution $(S^r e^{-S}/r!)$. Thus, the Franck-Condon factor for the zero-phonon transition is $\exp(-S)$; its profile is a Lorentzian (l_0) with a FWHM = γ , which is the homogeneous linewidth of the zero-phonon line. The lineshape for the one-phonon profile is l_1 and is centered at $\nu + \omega_m$ with a FWHM of Γ . It is well known that the one-phonon profiles for electronic transitions of molecules imbedded in amorphous solids carry a width of about 30 cm^{-1} and the profiles for antenna Chl *a* and Chl *b* are no exception [23]. To a good approximation the profile can be taken to be a Gaussian. Equation 1 is valid for coupling to a pseudo-localized phonon or a distribution of host phonons governed by a suitable density of states. For the latter case and a one-phonon profile governed by a Gaussian, the width of the r -phonon profile (centered at $\nu + r\omega_m$) is given by $\Gamma_r = r^{1/2}\Gamma$. In order to derive an analytic expression for the hole profile Lorentzians for l_r ($r > 1$) were used [1] with widths governed by the Gaussian values, i.e. $r^{1/2}\Gamma$. Since that work it has been shown that the differences in the hole spectra calculated with Lorentzians and Gaussians are small [25].

Now Eq. 1 is readily modified to include coupling to the ω_{sp} -mode:

$$L(\Omega - \nu) = \sum_{j=0}^{\infty} \frac{S_{sp}^j e^{-S_{sp}}}{j!} [e^{-S} l_0^j(\Omega - \nu - j\omega_{sp})] + \sum_{r=1}^{\infty} \frac{S^r e^{-S}}{r!} l_r^j(\Omega - \nu - r\omega_m - j\omega_{sp}) \quad (2)$$

where S_{sp} is the Huang-Rhys factor for ω_{sp} . In writing Eq. 2 the reasonable assumption that the electron-phonon coupling (S) is independent of the ω_{sp} -mode occupation number j is made. Similarly, the mean phonon frequency ω_m and Γ , the width of the one-phonon profile, are to be considered independent of j . However, the homogeneous linewidths γ_j of the zero-phonon I_0^j functions may differ due, for example, to rapid vibrational relaxation of the ω_{sp}^j ($j > 1$) levels.

For disordered hosts a Gaussian distribution of zero-phonon transition frequencies of width Γ_I is the appropriate choice but in order to obtain an analytic expression for the hole profile a Lorentzian is utilized, $N_0(v-v_m)/N$ where N is the total number of absorbers and v_m is the mean zero-phonon frequency. The absorption spectrum is calculated as the convolution of this distribution function with the single site absorption profile $L(\Omega-v)$. We define the absorption cross-section, laser intensity and photochemical quantum yield as σ , I and ϕ . Then following a burn for time τ

$$N_\tau(v-v_m) = N_0(v-v_m) e^{-\sigma I \phi \tau L(\omega_B - v)} \quad (3)$$

where ω_B is the laser burn frequency and $L(\omega_B - v)$ is given by Eq. 2. To obtain the absorption spectrum, A_0 , following the burn we must convolve Eq. 3 with $L(\Gamma - \gamma)$ and integrate over v . For notational simplicity, Eq. 1 rather than Eq. 2 is employed in what follows. The modifications of the resulting hole shape function necessary to take into account the ω_{sp} -progression will simply be stated. Thus,

$$A_\tau(\Omega) = \sum_{r=0}^{\infty} \frac{S^r e^{-S}}{r!} \int d\nu N_0(\nu - \nu_m) e^{-\sigma I \phi \tau L(\omega_B - \nu)} l_r(\Omega - \nu - r\omega_m) \quad (4)$$

For simplicity the short-burn-time limit is employed so that the exponential can be expanded as $1 - \sigma I \phi \tau L(\omega_B - \nu)$. This approximation need not be made, although the resulting expressions are very cumbersome if it is not. The hole spectrum in the short-burn-time limit is simply

$$A_0(\Omega) - A_\tau(\Omega) = \sigma I \phi \tau \sum_{r,r'=0}^{\infty} \left(\frac{S^r e^{-S}}{r!} \right) \left(\frac{S^{r'} e^{-S}}{r'!} \right) \int d\nu N_0(\nu - \nu_m) l_r(\Omega - \nu - r\omega_m) l_{r'}(\omega_B - \nu - r'\omega_m) \quad (5)$$

Because we are interested in holes whose widths are comparable to Γ_I we cannot assume that $N_0(\nu - \nu_m)$ is constant in Eqn. 5. Integration of Eqn. 5 yields

$$[A_0 - A_\tau(\Omega)] = \frac{\sigma \phi \tau}{3(2\pi)^2} \sum_{r,r'=0}^{\infty} \left[\left(\frac{S^r e^{-S}}{r!} \right) \left(\frac{S^{r'} e^{-S}}{r'!} \right) \right] \cdot \left\{ \frac{\Gamma_I + \Gamma_r}{(\Omega - \nu_m - r\omega_m)^2 + \left[\frac{\Gamma_I + \Gamma_r}{2} \right]^2} \right\} \left\{ \frac{\Gamma_r + \Gamma_{r'}}{(\Omega - \omega_B + \omega_m(r' - r))^2 + \left[\frac{\Gamma_r + \Gamma_{r'}}{2} \right]^2} \right\} + \left\{ \frac{\Gamma_I + \Gamma_{r'}}{(\omega_B - \nu_m - r'\omega_m)^2 + \left[\frac{\Gamma_I + \Gamma_{r'}}{2} \right]^2} \right\} \left\{ \frac{\Gamma_r + \Gamma_{r'}}{(\Omega - \omega_B + \omega_m(r' - r))^2 + \left[\frac{\Gamma_r + \Gamma_{r'}}{2} \right]^2} \right\} + \left\{ \frac{\Gamma_I + \Gamma_{r'}}{(\omega_B - \nu_m - r'\omega_m)^2 + \left[\frac{\Gamma_I + \Gamma_{r'}}{2} \right]^2} \right\} \left\{ \frac{\Gamma_r + \Gamma_r}{(\Omega - \nu_m + r\omega_m)^2 + \left[\frac{\Gamma_r + \Gamma_r}{2} \right]^2} \right\} \quad (6)$$

The qualitative implications of Eqn. 6 are discussed by Hayes et al. [17]. Model calculations with realistic values for Γ , ω_m , γ and Γ_l are given in the same paper for various values of S ranging from 0.5 (weak coupling) to 8.0 (strong coupling). In Eqn. 6, $\Gamma_0 = \gamma$ and $\Gamma_r = r^{1/2}\Gamma$ ($r \geq 1$). For strong coupling ($S \geq 2$) and $\omega_B \sim \nu_m$, the intensity of the ZPH relative to the broad hole is given approximately by $\exp(-2S)$. For this value of ω_B , the ZPH is located near the center of the broad and more intense hole upon which it is superimposed. For $\Gamma_l \geq S\omega_m$ a burn with ω_B located on the low and high energy sides of the absorption profile produces broad hole profiles that are shifted to the blue and red, respectively, of ω_B .

The modifications of Eqn. 6 required to take into account the ω_{sp} -progression are as follows: first, an additional double summation $\sum_{j,j'=0}^{\infty} \left(\frac{S^j e^{-S}}{j!}\right) \left(\frac{S^{j'} e^{-S}}{j'!}\right)$ must be included and Γ_r, Γ_r' replaced everywhere by Γ_{rj} and $\Gamma_{rj'}$, respectively. The latter damping constants are defined as $\Gamma_{rj} = \Gamma_r$ for $r \geq 1$ and $= \gamma_j$ for $r = 0$. Thus, γ_j determines the relaxation frequency of the zero-phonon level associated with the j th member of the ω_{sp} -progression; second, the energy denominators are modified by the replacements $r\omega_m \rightarrow r\omega_m + j\omega_{sp}$ and $r'\omega_m \rightarrow r'\omega_m + j'\omega_{sp}$.

For the calculations it was found sufficient to terminate the j - and r -sums at 4 and 10, respectively. It should be emphasized that the PHB spectra provide good first approximations for the values of ω_{sp} , S_{sp} , and S (since the ratio of the intensity of the ZPH to the more intense ω_{sp}^0 phonon sideband hole (hole X) is $\sim \exp(-2S)$ for $\omega_B \sim \nu_m$ [17]) and a direct measurement of γ_0 , cf. section III.B. Furthermore, the Stokes shift is given by $\sim 2S\omega_m$. Our absorption data (specifically the energy of the ω_{sp}^0 low energy shoulder for P870 and P960) together with the low temperature fluorescence spectra for P870 [26] and P960 [27] provide approximate values of 140 and 150 cm^{-1} for the Stokes shift of P870 and P960. Thus, an

estimate for ω_m is available. Furthermore, the low temperature absorption linewidth of the PED state is given roughly by $S\omega_m + S_{sp}\omega_{sp} + \Gamma_I$ so that an estimate for Γ_I can be made. The point is that in fitting the absorption and PHB spectra one cannot vary the values for ω_{sp} , S_{sp} , ω_m , S and Γ_I too far from the estimated values.

The calculated λ_B -dependent hole spectra for P870 (glycerol/NGP) and P960 (glycerol/LDAO) are given in Figs. 6 and 7, respectively. The parameter values utilized are given in the captions. We note in particular that $\omega_{sp} = 125$ and 150 cm^{-1} for P870 and P960, respectively. Spectra 1, 4, 5, 6 of Fig. 6 can be directly compared with spectra 1, 2b, 3b, 4 of Fig. 4 while spectra 2, 3, 4 of Fig. 7 can be compared with spectra 1, 2, 3b of Fig. 5. The λ_B -dependence of the PHB spectra is reasonably well accounted for by the theory; in particular, the loss of line narrowing and elimination of the ZPH as λ_B is decreased from the value corresponding to $\sim \nu_m$. These features of the λ_B -dependence are principally the consequence of an increasing probability for multi-phonon excitation (non-line narrowing) as λ_B is decreased from the ν_m -value. For a sufficiently low value of λ_B , essentially all the structure in the spectrum is lost and further reduction of λ_B produces no further change in the spectrum. In the calculations, allowance was made for sub-ps decay of the ω_{sp}^j ($j > 1$) levels with the decay proportional to $j-1$ (Fermi-Golden rule prediction with cubic intermolecular anharmonicity). The decay times of ω_{sp}^1 for P870 and P960 were set equal to 260 and 350 fs but no significance should be attached to the difference in these values. In the absence of sub-ps decay the calculations predict that vibronic satellite ZPH [28] associated with the ω_{sp} -progression should be observed for λ_B -values that produce a ZPH in the ω_{sp}^0 band. Repeated attempts to observe such features met with no success for both P870 and P960. Additional arguments for sub-ps decay are given in the following sub-section.

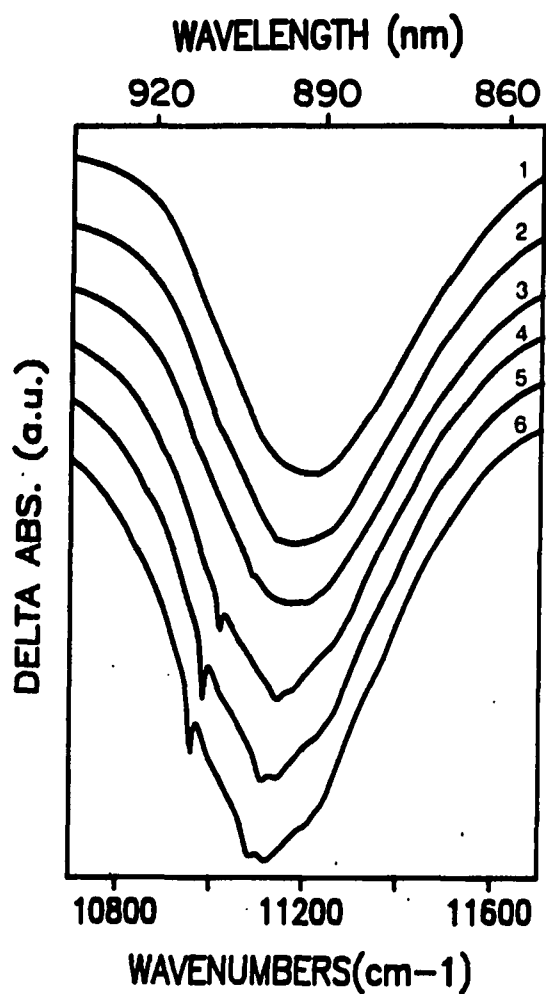


Figure 6. Calculated hole burned spectra for P870 using the same parameters as in Fig. 3B. $\lambda_B =$ 1.) 240 cm^{-1} , 2.) 150 cm^{-1} , 3.) 100 cm^{-1} , 4.) 30 cm^{-1} , 5.) -5 cm^{-1} , 6.) -30 cm^{-1} . λ_B given relative to maximum of zero site distribution function (SDF). Maximum of SDF, 10995 cm^{-1}

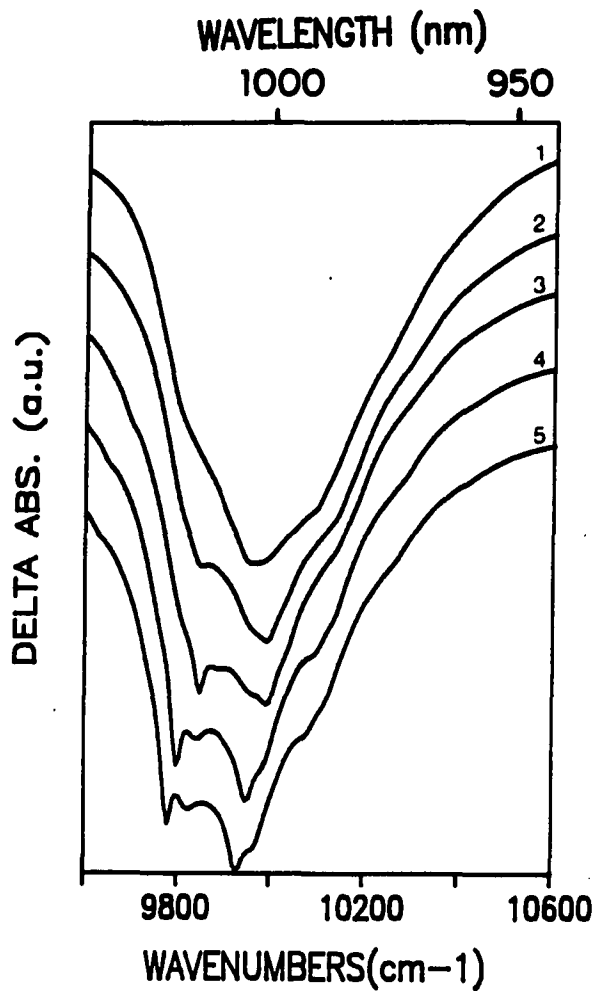


Figure 7. Calculated hole burned spectra for P960 using the same parameters as in Fig. 3A. $\lambda_B =$ 1.) 300 cm^{-1} , 2.) 195 cm^{-1} , 3.) 50 cm^{-1} , 4.) 0 cm^{-1} , 5.) -20 cm^{-1} . Maximum of SDF, 9799 cm^{-1} (See Fig. 6.)

The calculated absorption spectrum for P870 and P960, which correspond to the PHB spectra of Figs. 6 and 7, are given in Fig. 3 where they are compared with the experimental spectra. Agreement is reasonable except on the low energy tail. The disagreement on the low energy tail is primarily the result of utilizing a Lorentzian for the Γ_1 -distribution function. Unfortunately, utilization of a Gaussian precludes derivation of an analytic expression for the hole profile and, as a consequence, would lead to a significant increase in computation time. A comparable disagreement on the low energy side between the calculated and observed PHB spectra exists for the same reason. We hasten to add, however, that the important features of the absorption and λ_B -dependent hole spectra are accounted for by the theory and that calculations with a Gaussian for the Γ_1 -distribution function are not expected to lead to significant changes in the values of the parameters given in the captions to Figs. 6 and 7. Thus, we conclude that approximately 70% and 30% of the P870 and P960 absorption widths are due to homogeneous broadening (from the linear electron-phonon and $-\omega_{sp}$ mode coupling) and inhomogeneous broadening, respectively.

Zero-phonon Holewidths

For P870 (glycerol/NGP) an average of several scans (2 cm^{-1} read resolution) for λ_B in the range 907-912 nm, see Fig. 3, yielded a ZPH width of $8.5 \pm 2.0 \text{ cm}^{-1}$ (corrected for read resolution). Typical profiles are shown in Fig. 8a. This width yields a P870* decay time of $1.3 \pm 0.3 \text{ ps}$, which is in good agreement with the time domain value of $1.2 \pm 0.1 \text{ ps}$ at 10 K [21,22]. A similar procedure for P960 (glycerol/LDAO) with λ_B in the range 1016-1021 nm, see Fig. 8, yielded a P960* decay time of $0.8 \pm 0.1 \text{ ps}$ (ZPH width of $13.0 \pm 1.5 \text{ cm}^{-1}$).

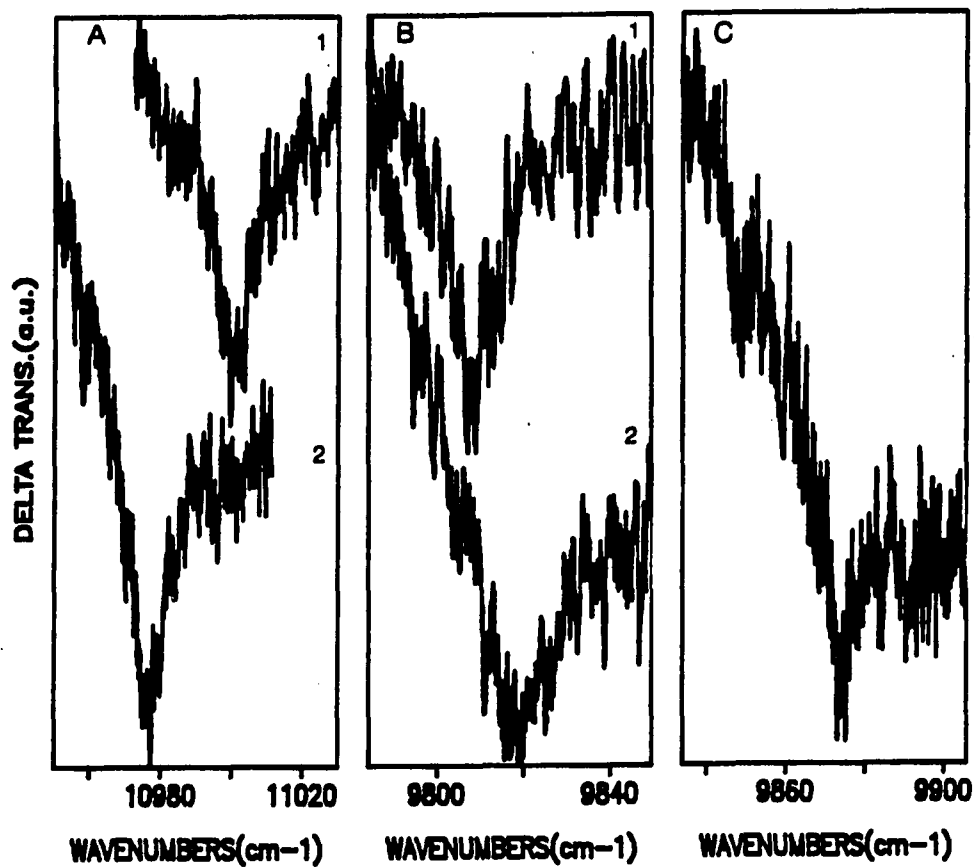


Figure 8. ZPH at 4.2 K for A) P870 1.) $\lambda_B = 909$ nm (11001 cm^{-1}), 2.) $\lambda_B = 911$ nm (10977 cm^{-1}); B) P960 (glycerol/LDAO) 1.) $\lambda_B = 1019.6$ nm (9808 cm^{-1}), 2.) $\lambda_B = 1018.3$ nm (9820 cm^{-1}); C) P960 (PVOH/LDAO) $\lambda_B = 1012.6$ nm (9876 cm^{-1}) (PVOH). Resolution = 2 cm^{-1} for all spectra

A typical ZPH profile is given in Fig. 8 along with profiles for glycerol/NGP and PVOH/LDAO.

The close agreement between the PHB and time domain decay times is interesting since the ZPH width measures decay from zero-point while the time domain experiments initially prepare P* vibrationally excited. If charge separation occurred to a significant extent prior to thermalization (at 10 K), one would not expect agreement [29,30]. The observed agreement suggests that thermalization occurs on a sub-ps time scale. This suggestion is consistent with the photon echo results of Meech et al. [31]. These results and the absence of vibronic satellite holes associated with the ω_{sp} -progression provide justification for inclusion of sub-ps decay of the ω_{sp}^j ($j > 1$) zero phonon levels in the calculations of the P870 and P960 PHB spectra. It should be emphasized that it was carefully determined that scattered laser light (0.2 cm⁻¹ linewidth) did not interfere with the observed ZPH (see experimental section).

Site Excitation Energy Correlation Effects in the Transient Spectra

Recently nonphotochemical hole burning experiments on the antenna complex of the green algae *Prosthecochloris aestuarii* have proven that there is a high degree of site excitation energy correlation between different exciton components of a subunit characterized by strong excitonic interactions [32]. It is with this in mind that we consider the PHB spectra for *Rps. viridis* (PVOH/LDAO) and *Rb. sphaeroides* (PVOH/NGP) shown in Figs. 9 and 10, respectively. For all of the host/detergent systems utilized only one feature of the Q_y-region

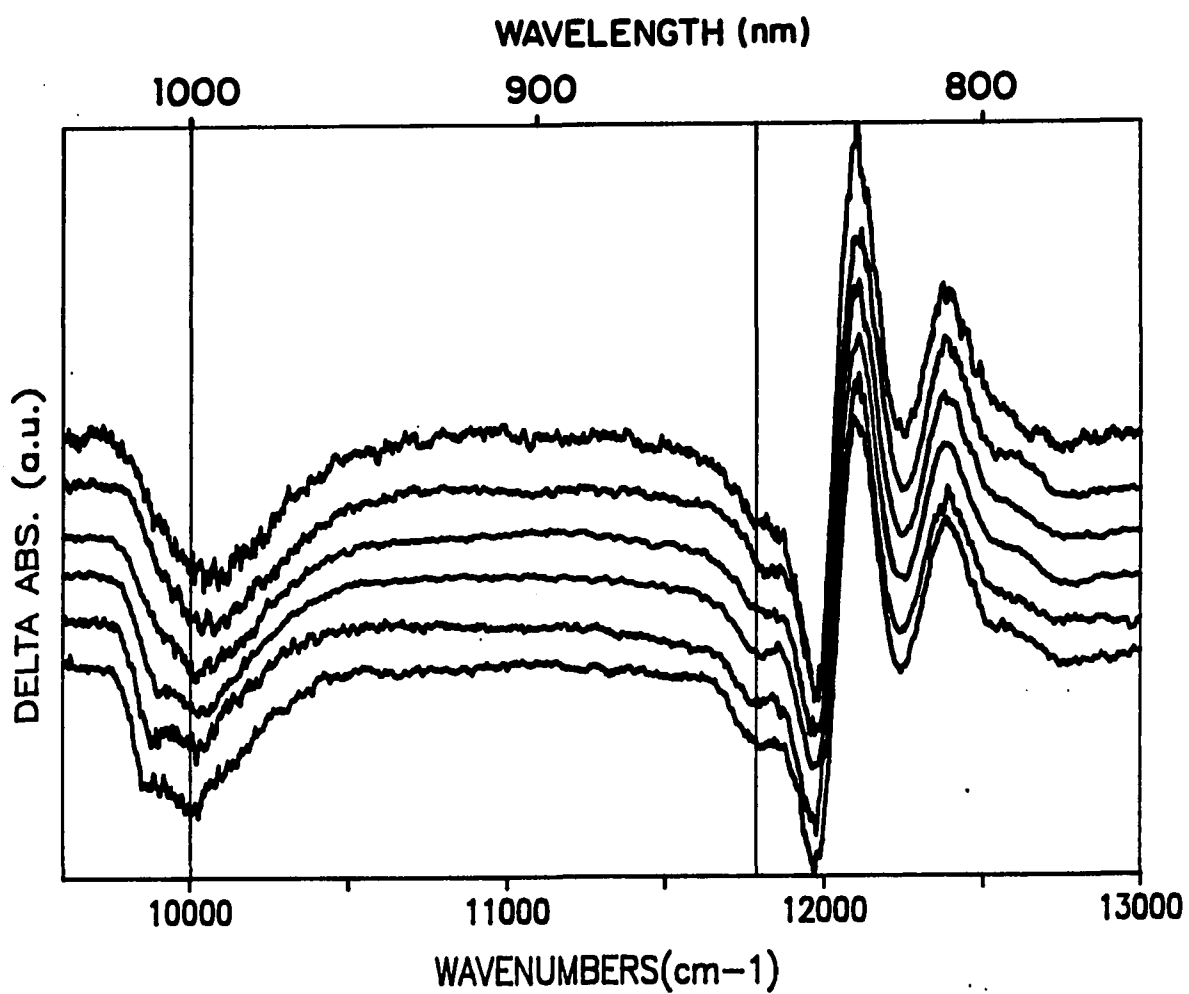


Figure 9. Hole burned spectra for *Rps. viridis* (PVOH/LDAO), $T = 4.2$ K, $\lambda_B = 965, 980, 1000, 1010, 1012, 1015$ nm (ordered from top to bottom). Resolution = 8 cm^{-1}

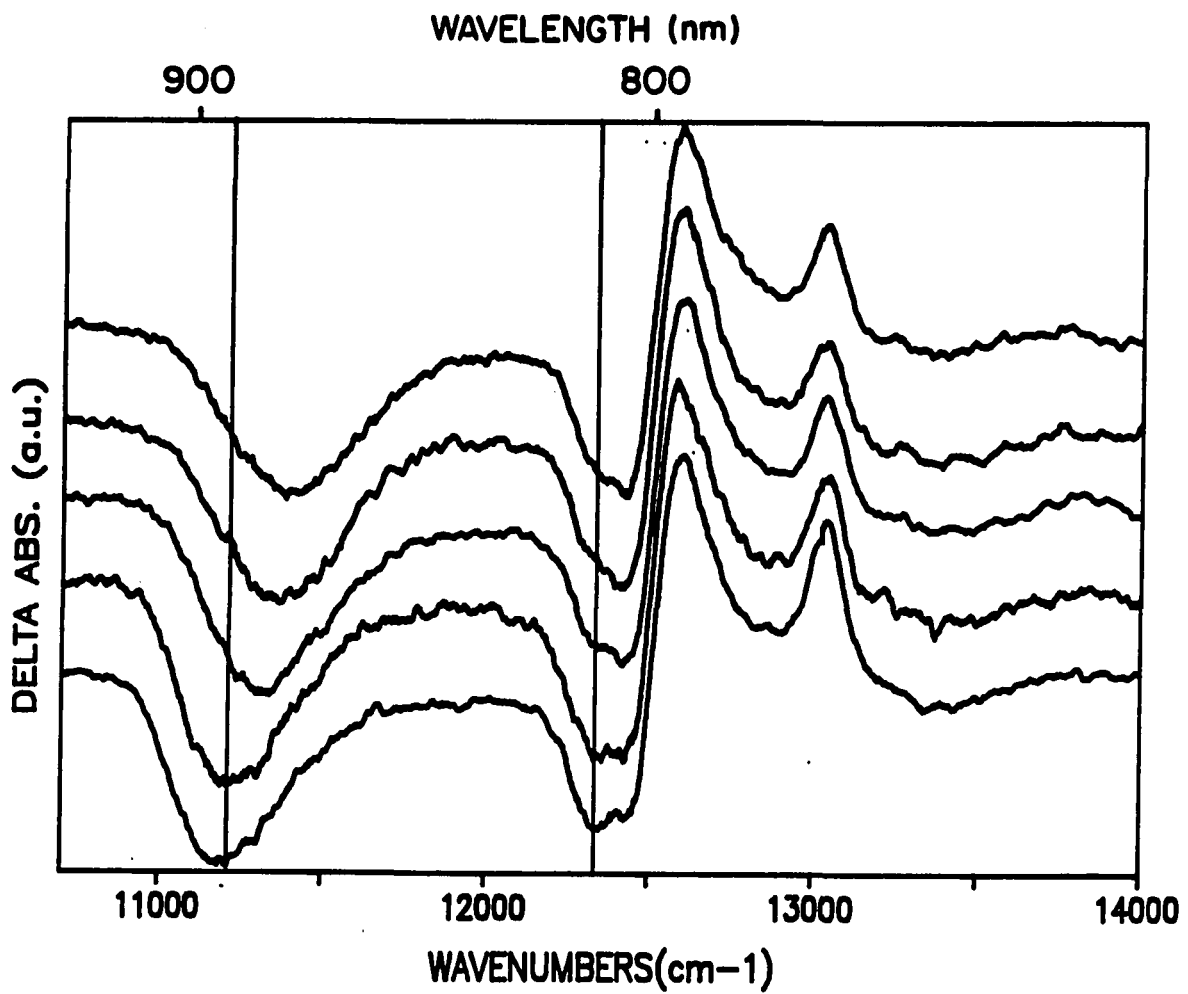


Figure 10. Hole burned spectra for *Rb. sphaeroides* (PVOH/LDAO), $T = 4.2$ K, $\lambda_B = 860, 875, 885, 900, 905$ nm (ordered from top to bottom). Resolution = 8 cm^{-1}

of the transient spectra lying higher in energy than P960 and P870 exhibits an observable dependence on λ_B . It is the hole (bleach [20]) that corresponds to the low E shoulder (LES) of the (B_M, B_L) "monomer" absorption band. The λ_B -dependence is most pronounced for PVOH host films because of the additional $\sim 120 \text{ cm}^{-1}$ of inhomogeneous broadening they provide relative to the glass hosts. In both Figs. 9 and 10 the right and left vertical lines are centered at the centroids of the LES and P_- holes for the highest λ_B -value used. The LES holes for *Rps. viridis* and *Rb. sphaeroides* are located at 848.0 nm (11790 cm^{-1}) and 811.3 nm (12330 cm^{-1}) for this λ_B -value. It is apparent that the LES hole tracks λ_B in a similar manner to the P_- hole for both bacterial RC. Therefore, there is a significant degree of positive correlation between the site excitation energies of the P_- and LES states. The LES state for *Rps. viridis* has been assigned by Vermeglio et al. [20] to P_+ , the upper dimer component of the Q_y -transition of the special pair. For both bacterial RC our linearly polarized transient spectra (not shown) have confirmed that the LES state carries a polarization that is close to opposite of the polarization for P_- [33]. Because of the aforementioned studies on *P. aestuarii* and because we are not aware of any line narrowing studies on molecular systems that establish any correlation for excited states of different electronic parentage, we suggest that our results provide support for the LES state assignment of Vermeglio et al. [20]. The bands in Figs. 9 and 10 lying to higher energy of the LES hole are due to the electrochromic shifting of the "accessory" B and H pigment absorption bands produced by formation of P^+BHQ^- . It is interesting that these bands are independent of λ_B . At this time, however, one cannot conclude that the apparent lack of correlation between the "accessory" states and P_- means that the accessory states are relatively pure, i.e., that they contain only a small contribution from the special pair. The reason is that the accessory bands

(see Fig. 2) may, to a large extent, be homogeneously broadened due to ultra-fast downward electronic energy transfer processes [34,35]. Further PHB experiments are planned which should resolve this issue.

FURTHER DISCUSSION

We consider first the question of the nature of the ω_{sp} mode for P870 and P960. We assign it as a special pair intermolecular Franck-Condon marker mode for the following reasons: recent hole burned spectra for the antenna Chl *a* and Chl *b* for photosystem I have shown that [23] the intramolecular *S*-factors for all modes are ≤ 0.04 . With these data and the fluorescence excitation spectra of BChl *a* reported in ref. [24], the *S*-factors for BChl *a* modes possessing a frequency of $\leq 200 \text{ cm}^{-1}$ can be estimated to be ≤ 0.02 in sharp contrast is the value of $S_{sp} \sim 1.1$ and 1.55 for ω_{sp} reported here. Furthermore, no intramolecular BChl *a*, Chl *a* and Chl *b* monomer modes with frequencies close to the ω_{sp} values reported here have been observed [23,24]. Since the ω_{sp} values reported are for $P^*(P_-)$, it would be worthwhile to attempt resonance Raman or coherent 4-wave mixing experiments on P870 and P960 in order to determine the corresponding ground state frequencies. More important for future work, however, are the questions of the dynamical nature of the ω_{sp} mode associated with the special pair and a possible role for the geometry change associated with ω_{sp} , which accompanies electronic excitation of P, in the primary charge separation process.

We have recently reported structured hole spectra for P680, the primary electron donor state absorption of the RC of PSII [36]. The RC structure of PSII has not been determined. However, the RC of PSII appears to share structural and functional similarities with the RC of the purple bacteria [37,38,39] and the Nanba-Satoh preparation [40] of the PSII RC binds 4-5 Chl *a* and two Pheo *a* molecules. Interestingly, the P680 hole profiles are quite similar in appearance to the origin (ω_{sp}^0) hole (with its ZPH) spectra reported here for P870 and

P960. However, the P680 hole spectra show *no* evidence for the ω_{sp} -marker mode progression. This suggests that if a special pair does exist for the PSII RC, its structure is very different than the special pair structure for the bacterial RC.

The basic conclusion from our earlier work [17], which interpreted the unstructured hole spectra for P870 and P960 reported in refs. (12,13), was that the spectra can be satisfactorily understood in terms of inhomogeneous broadening (resulting from RC to RC heterogeneity) and the Franck-Condon principle (linear electron-vibrational coupling involving low frequency modes). The results reported here, even without consideration of the theoretical calculations, prove that this interpretation is correct. The assertion of Won and Friesner [15] that P* undergoes ultra-fast (≤ 100 fs) electronic relaxation prior to formation of P⁺BH⁻ finds no support from our experimental results. The calculations of Won and Friesner do not yield the ZPH reported here because of the ultra-fast electronic dephasing imposed on the primary electron donor state.

The assertion in ref. [19] that a charge transfer (CT) state, lying ~ 300 cm⁻¹ higher in energy than the low energy shoulder of P960 (i.e., the origin (ω_{sp}^0) band), figures importantly in the PHB spectrum is brought into question by the present results. This assertion was mainly based on a ΔT PHB spectrum (Fig. 3) for which the OD of P960 was sufficiently high (0.6) to render the ΔT spectrum an unfaithful representation of the ΔA spectrum at higher energies (confirmed by measurements on the same but diluted sample) [41]. The present work establishes that the principal features of the PHB spectra can be accounted for without invoking a CT state although the possibility that a weakly absorbing CT state does contribute to the high energy side of the primary donor state absorption profile cannot be excluded.

In conclusion, the results presented here reveal the origin of the homogeneous

broadening associated with the primary donor state absorption profile of bacterial RC, identify a special pair marker mode (the dynamical nature of which is yet to be determined), further establish [19,36] the utility of PHB for determining electron transfer dynamics from zero-point level and establish the potential of site excitation energy selection for the determination of correlation between different RC states.

ACKNOWLEDGEMENT

Ames Laboratory is operated for the U.S. Department of Energy by Iowa State University under Contract No. W-7405-Eng-82. The research was supported by the Director for Energy Research, Office of Basic Energy Science. The research at Argonne Laboratory was supported by the Division of Chemical Sciences, Office of Basic Energy Sciences, U.S. Department of Energy under Contract No. W-31-109-Eng-38.

REFERENCES

1. Hayes, J.M.; Small, G.J. *J. Phys. Chem.* 1986, 90, 4928-4931.
2. Deisenhofer, J.; Epp, O.; Miki, K.; Huber, R.; Michel, H. *J. Mol. Biol.* 1984, 180, 385-398.
3. Deisenhofer, J.; Epp, O.; Miki, K.; Huber, R.; Michel, H. *Nature (London)* 1985, 318, 618-624.
4. Michel, H.; Epp, O.; Deisenhofer, J. *EMBO J.* 1985, 5, 2445-2451.
5. Chang, C. H.; Tiede, D.; Tang, J.; Smith, U.; Norris, J. *FEBS Lett.* 1986, 205, 82-86.
6. Allen, J. P.; Feher, G.; Yeates, T. O.; Rees, D. C.; Deisenhofer, J.; Michel, H.; Huber, R. *Proc. Natl. Acad. Sci. USA* 1986, 83, 8589-8593.
7. Yeates, T. O.; Komiyama, H.; Chirino, A.; Rees, D. C.; Allen, J. P.; Feher, G. *Proc. Natl. Acad. Sci. USA* 1988, 85, 7993-7997.
8. Kirmaier, C.; Holten, D. *Photosynthe. Res.* 1987, 13, 225-260.
9. Budil, D. E.; Gast, P.; Chang, C. H.; Schiffer, M.; Norris, J. *Ann. Rev. Phys. Chem.* 1987, 38, 561-583.
10. Warshel, A.; Parson, W. W. *J. Am. Chem. Soc.* 1987, 109, 6143-6152.
11. Scherer, P. O. J.; Fischer, S. *J. Phys. Chem.* 1989, 93, 1633-1637.
12. Boxer, S. G.; Lockhart, D. J.; Middendorf, T. R. *Chem. Phys. Lett.* 1986, 123, 476-482.
13. Boxer, S. G.; Middendorf, T. R.; Lockhart, D. J. *FEBS Lett.* 1986, 200, 237-241.
14. Meech, S. R.; Hoff, A. J.; Wiersma, D. A. *Proc. Natl. Acad. Sci. USA* 1986, 83,

9464-9468.

15. Won, Y.; Friesner, R. A. *J. Phys. Chem.* 1988, 92, 2214-2219.
16. Won, Y.; Friesner, R. A. *J. Phys. Chem.* 1989, 93, 1007.
17. Hayes, J. M.; Gillie, J. K.; Tang, D.; Small, G. J. *Biochim. Biophys. Acta* 1988, 932, 287-305.
18. Tang, D.; Jankowiak, R.; Gillie, J. K.; Small, G. J.; Tiede, D. *J. Phys. Chem.* 1988, 92, 4012-4015.
19. Tang, D.; Jankowiak, R.; Small, G. J.; Tiede, D. *Chem. Phys.* 1989, 131, 99-113.
20. Vermeglio, A.; Paillotin, G. *Biochim. Biophys. Acta* 1982, 681, 32-40.
21. Fleming, G. R.; Martin, J. L.; Breton, J. *Nature (London)* 1988, 333, 190-193.
22. Breton, J.; Martin, J. L.; Fleming, G. R.; Lambry, J.-C. *Biochem.* 1988, 27, 8276-8284.
23. Gillie, J. K.; Small, G. J.; Golbeck, J. H. *J. Phys. Chem.*, 1989, 93, 1620-1627.
24. Renge, I.; Muring, K.; Avarmaa, R. *J. Lumin.* 1987, 37, 207-214.
25. Lee, I.-J.; Hayes, J. M.; Small, G. J. *J. Chem. Phys.* 1989, to be published.
26. Angerhofer, A., thesis (Ph.D.), 1987, Universitat Stuttgart, Stuttgart, West Germany.
27. Maslov, V. G.; Klevanik, A. V.; Ismailov, M. A.; Shuvalov, V. A. *Dokl. Akad. SSSR* 1983, 269, 1217-1221.
28. Hayes, J. M.; Fearey, B. L.; Carter, T. P.; Small, G. J. *Int. Rev. Phys. Chem.* 1986, 5, 175-184.
29. Jortner, J. *Biochim. Biophys. Acta* 1980, 594, 193-230.
30. Bixon, M.; Jortner, J. *Faraday Discuss. Chem. Soc.* 1982, 74, 17-29.
31. Meech, S. R.; Hoff, A. J.; Wiersma, D. A. *Chem. Phys. Lett.* 1985, 121, 287-292.

32. Johnson, S. G. and Small, G. J. *Chem. Phys. Lett.* 1989, 155, 371-375.
33. Johnson, S. G.; Tang, D.; Jankowiak, R.; Hayes, J.M.; Small, G. J.; Tiede, D., 1989, to be published.
34. Breton, J.; Martin, J.-L.; Migus, A.; Antonetti, A.; Orszag, A. *Proc. Natl. Acad. Sci. USA*, 1986, 83, 5121-5125.
35. Martin, J.-L.; Breton, J.; Hoff, A. J.; Migus, A.; Antonetti, A. *Proc. Natl. Acad. Sci. USA* 1986, 83, 957-961.
36. Jankowiak, R.; Tang, D.; Small, G. J.; Seibert, M. *J. Phys. Chem.* 1989, 93, 1649-1654.
37. Michel, H.; Deisenhofer, D. in *Encyclopedia of Plant Physiology: Photosynthesis III* (Staelin, A.C. and Arntzen, C. J., eds.), 1986, Springer-Verlag, Berlin, pp. 371-381.
38. Michel, H.; Deisenhofer, J. *Chemica Scripta* 1987, 27B, 173-180.
39. Trebst, A., *Z. Naturforsch* 1986, 41C, 240-245.
40. Nanba, O.; Satoh, K. *Proc. Natl. Acad. Sci. USA* 1987, 84, 109-112.
41. Also, experiments performed on the undiluted sample yielded PHB spectra that agree with the ΔT spectra obtained earlier [18,19], yet result in ΔA spectra that are consistent with those presented here. The feature in Fig. 3 (which should be labeled as a ΔT spectrum) of ref. 19 assigned to a CT state is actually the ω_{sp}^2 satellite hole.

**PAPER III. PRIMARY DONOR STATE MODE STRUCTURE AND ENERGY
TRANSFER IN BACTERIAL REACTION CENTERS**

**PRIMARY DONOR STATE MODE STRUCTURE AND ENERGY
TRANSFER IN BACTERIAL REACTION CENTERS**

D. Tang, S. Johnson, R. Jankowiak, J. M. Hayes,

G. J. Small and D. M. Tiede

Journal of Physical Chemistry 1990, in press.

ABSTRACT

Temperature-dependent photochemical hole burning data for P870 of *Rb. sphaeroides* reaction centers (RC) are reported which lead to a determination for the mean frequency of the protein phonons which couple to the optical transition. Utilization of this frequency, $\omega_{sp} \sim 25\text{-}30\text{ cm}^{-1}$, together with improved functions for the single site (RC) absorption lineshape and inhomogeneous broadening are shown to lead to significant improvement in the theoretical fits to the hole and absorption spectra (including those of P960 of *Rhodospseudomonas viridis*). Time-dependent P870 hole spectra are reported which provide additional evidence that the previously observed zero-phonon hole is an intrinsic feature of P870 for active RC. Transient spectra obtained by laser excitation into the accessory Q_y -absorption bands of the RC are presented which show an absence of both line narrowing and a dependence on the location of the excitation frequency. These results, which are consistent with ultrafast energy transfer processes from the accessory states, are discussed in terms of earlier time domain data.

INTRODUCTION

Recently the underlying structures of the primary donor state (special pair) absorption profiles P870 and P960 of the bacterial reaction centers (RC) from *Rhodospseudomonas viridis* and *Rb. sphaeroides* were revealed by transient photochemical hole burning experiments [1,2]. Both are dominated by a fairly lengthy Franck-Condon progression in an intermolecular special-pair marker mode (ω_{sp}) which exhibits an intensity maximum for the one-quantum transition. For P870 and P960 the theoretical fits to the structured hole spectra led to ω_{sp} -values of ~ 150 and 125 cm^{-1} for P960 and P870, respectively [2]. The corresponding S (Huang-Rhys)-factors are $S_{sp} = 1.1$ and 1.5 . The origin (ω_{sp}^0) of the ω_{sp} -progression in the hole spectra for P870 and P960 correlates with the low energy shoulder of the low temperature absorption profile which is readily observed for glass solvents that minimize inhomogeneous broadening, Fig. 1. Although the dynamical nature of the marker mode has not been determined, the fact that it is intermolecular [1,2] and that the primary donor state (P870*, P960*) is believed to possess significant intra-dimer charge-transfer character [3-6], suggest that it is highly localized on the special pair.

The primary donor state also exhibits appreciable coupling to low frequency protein phonons (mean frequency ω_m , Huang-Rhys factor S) as evidenced by the weakness of the zero-phonon hole (ZPH) associated with the ω_{sp}^0 band. Simulations of the hole spectra presented in refs. 1 and 2 were performed with an analytical expression for the hole profile which takes into account coupling to both the marker mode and protein phonons. This expression is valid in the short burn time approximation [7] and, for example, a zero-phonon

excitation frequency distribution function (SDF, width Γ_1) governed by a Lorentzian. Although the principal features of the spectra (including their burn wavelength dependence) could be accounted for, significant deviations occurred on the low energy tails of both the absorption and hole spectra. These deviations were suggested to be due mainly to the utilization of a Lorentzian for the SDF. Although good initial estimates for many of the theoretical parameters (e.g., ω_{sp} , S_{sp} , S , Γ_1) could be obtained from the spectra, this was not the case for ω_m . Thus, we report here a direct determination of ω_m . This value is used in simulations which avoid the approximations employed in refs. 1 and 2. The results reported here provide significantly improved agreement with experiment. Nevertheless, the basic physical model remains unchanged. The refinement of the values for the physical parameters presented is viewed as important for future studies directed towards determination of the marker mode frequency in the ground electronic state, its dynamical nature and the role of the special pair geometry change in the excited state in primary charge separation.

The ZPH widths reported earlier [1,2] yielded P870* and P960* decay times in good agreement with those determined earlier [8,9] by time domain measurements at 10 K, thus proving that there is no ultrafast electronic relaxation [10,11] from zero-point of P* which precedes formation of the charge separated state P^+BPheo^- , where BPheo is bacteriopheophytin. We present here time-dependent hole burning data for P870 which show that the decay kinetics of the ZPH and the broader and more intense hole upon which it is superimposed are the same within experimental uncertainty. This experiment was performed to provide even more convincing evidence [1] that the ZPH is an intrinsic feature of the spectra for functioning RC.

The last part of the paper presents the results of experiments stimulated by the reports

that the line narrowing feature of hole burning could be used to study site excitation energy correlation effects between different Q_y -absorption bands of the bacterial reaction centers [1,2]. In these experiments transient spectra for the entire Q_y -region of *Rb. sphaeroides* and *Rps. viridis* were obtained as a function of laser burn frequency (ω_B) tuned across P870 and P960. Significant positive correlation was observed between the primary donor state absorption band and the band that appears as a low energy shoulder on the BChl monomer band (near 850 and 810 nm for *Rps. viridis* and *Rb. sphaeroides*, respectively). Since such correlation is only expected between states which have similar electronic parentages, it was argued that [1,2] the positive correlation is consistent with the assignment for the "shoulder state" of Vermeglio and Paillotin [12] to the upper dimer component (P_+) of the special pair. Pertinent to the present paper is the observation that the other features in the transient ΔA hole spectra are invariant to ω_B -tuning. These features are due to electrochromic shifts of the so-called BChl and BPheo monomer bands, the shifts arising from the formation of the P^+Q^- (Q = quinone) state which serves as the bottleneck for the hole burning. We will refer to these bands as accessory. There are two apparent explanations for the invariance: one is that the accessory bands correspond to states that have little contribution from the Q_y -states of the monomers comprising the special pair; the other is that these bands are largely homogeneously broadened. Spectra are presented here which were obtained by burning directly into accessory Q_y -bands. The results are shown to be consistent with the second explanation and support the findings of the femtosecond studies which show that energy transfer from the accessory states occurs in < 100 fs [8,9].

EXPERIMENTAL

Fresh samples of RC from *Rb. sphaeroides* were prepared by dissolving RC crystals in a suitably buffered host. Details concerning the crystallization procedure can be found in ref. 13. The RC were prepared in glycerol:water glass (2:1) with 0.8% n-octyl- β -D-glucopyranoside detergent (NGP), 10 mM Tris, 1 mM EDTA, $pH = 8.0$. The optical density (OD) of the samples utilized in this study was 0.25 at the peak of the primary donor state absorption.

The experimental apparatus is described fully in ref. 1. Briefly, burn irradiation (linewidth 0.2 cm^{-1}) was provided by Raman shifted (H_2 gas) output of an excimer-pumped dye laser, Lambda Physik EMG 102 and FL-2002, respectively. A pulse repetition rate of 16 Hz or less was used. A Stanford Research SR 250 boxcar averager was utilized to obtain the gated spectra (gate width of 150 ns). The ΔT (transmission) spectra were obtained by subtracting laser-on and laser-off spectra. ΔA (absorbance) spectra were obtained by subtracting the logarithms of the laser-off transmission spectra and the laser-on transmission spectra. Samples were mounted and cooled in a Janis model 8-DT super vari-temp liquid helium cryostat. Temperature measurements were made with a Lakeshore Cryotronics DTC-500K calibrated silicon diode.

For the study of the temporal decay of the P870 hole profile the position of the 150 ns observation window was varied relative to the laser pulse by adjusting the gate delay of the boxcar. Delay times of 2, 5, 10, 15 and 20 ns were employed. A decay time of $21 \pm 2 \text{ ns}$ for the P^+Q^- bottleneck state had been determined earlier [14].

RESULTS

*Simulations and Temporal Evolution of
the P870 and P960 Hole Profiles*

The theory of Hayes and Small [15] for the hole profile, which is valid for arbitrarily strong linear electron-phonon coupling, was developed to interpret the first hole burned spectra reported for P870 and P960 [16,17]. These important early experimental results demonstrated that there is a significant homogeneous broadening contribution to the absorption profiles but that the maximum of the single broad ($\sim 400 \text{ cm}^{-1}$) hole exhibits a weak dependence on the location of ω_B within the primary donor absorption profile. Since the marker mode progression was not observed, Hayes et al. [7] utilized a single mean phonon frequency approximation to account for the results of refs. (16,17). The single site (RC) absorption profile has the form

$$L(\Omega - \nu) = e^{-S} l_0(\Omega - \nu) + \sum_{r=1}^{\infty} \frac{S^r e^{-S}}{r!} l_r(\Omega - \nu - r\omega_m) \quad (1)$$

where ν is the zero-phonon transition frequency and ω_B is the mean frequency for phonons which couple to the electronic transition. The Huang-Rhys factor is S and the Franck-Condon factors for the $r = 0, 1, \dots$ phonon transitions are governed by the Poisson distribution $(S^r e^{-S}/r!)$. Thus, the Franck-Condon factor for the zero-phonon transition is $\exp(-S)$; its profile is a Lorentzian (l_0) with a FWHM = γ , which is the homogeneous linewidth of the

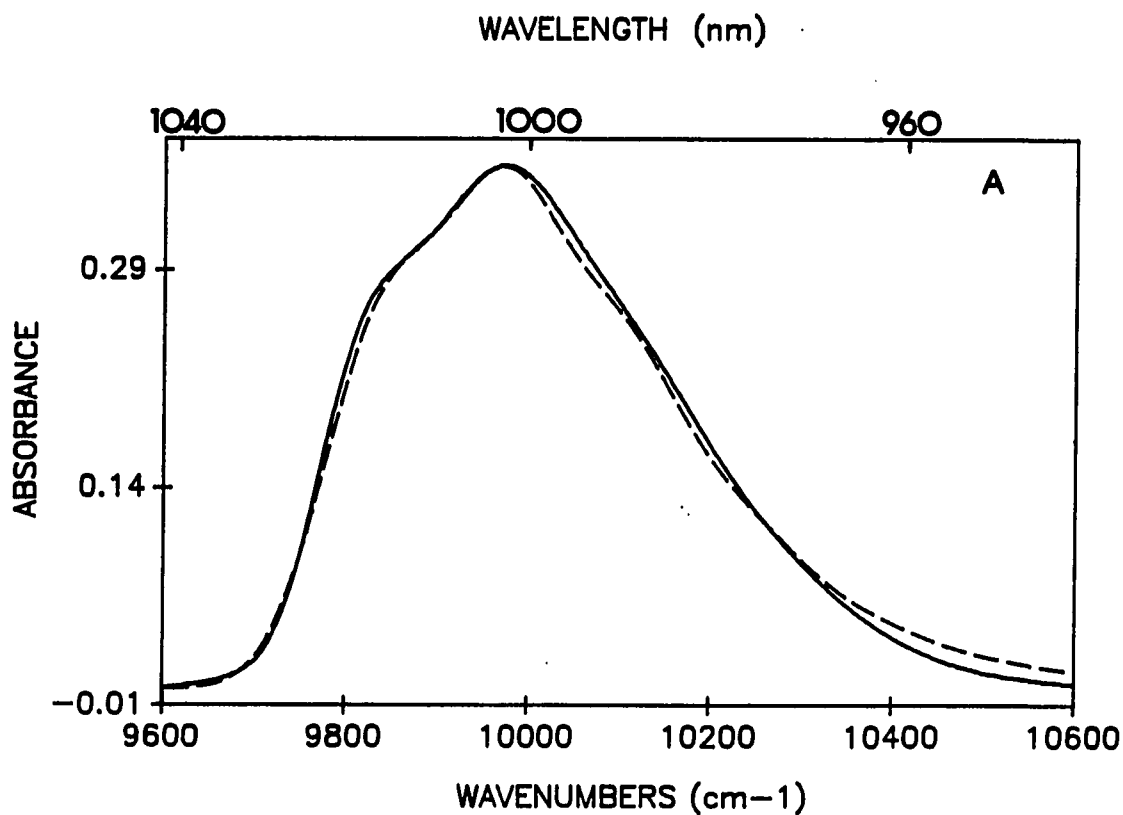


Figure 1. Calculated and experimental absorption spectra for P870 and P960. $T = 4.2$ K, resolution = 4 cm^{-1} . (A) P960 in glycerol glass (LDAO detergent). (B) P870 in glycerol glass (NGP detergent)

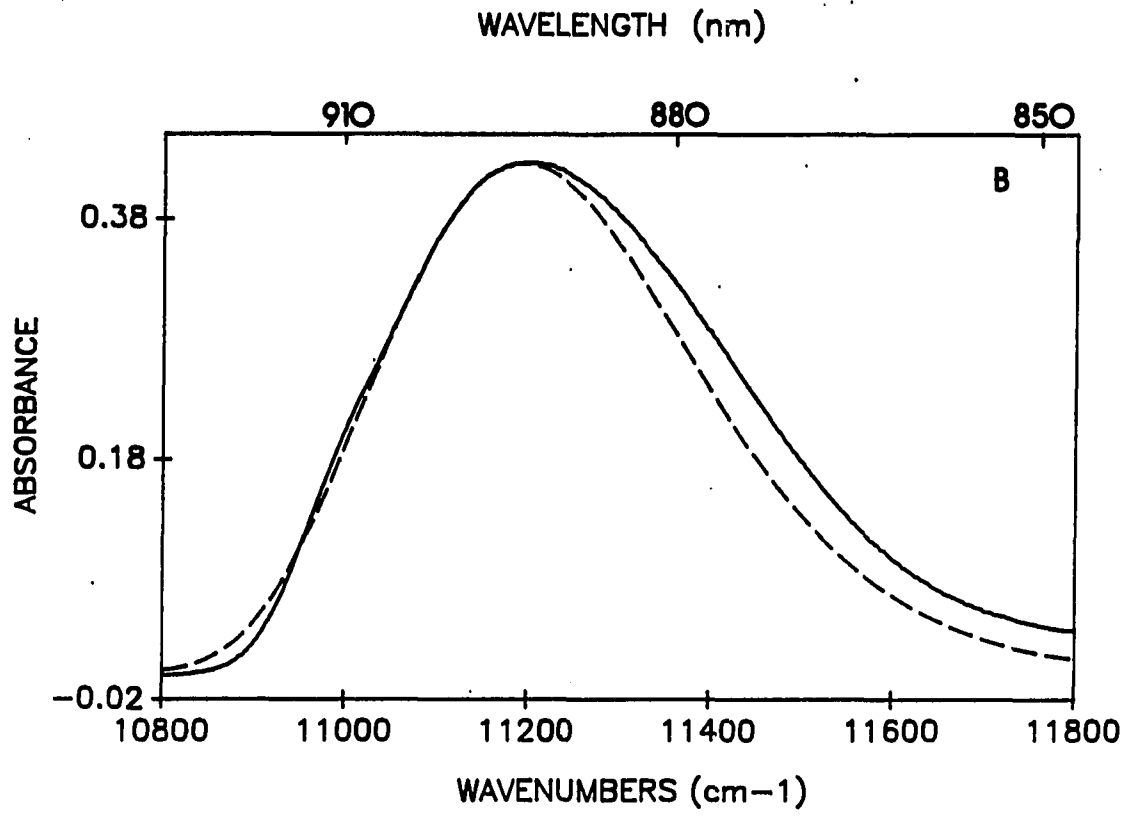


Figure 1. Continued

Table I. Parameters for theoretical fit

| | ω_{sp}^a | S_{sp} | ω_m | S | Γ | Γ_I | S_{tot} | $\Sigma S_i \omega_i$ | FWHM(P) |
|------|-----------------|----------|------------|-----|----------|------------|-----------|-----------------------|---------|
| P960 | 134 | 1.1 | 25 | 2.1 | 40 | 120 | 3.2 | 200 | 390 |
| P870 | 115 | 1.5 | 30 | 2.2 | 30 | 170 | 3.7 | 240 | 410 |
| P960 | 150 | 1.1 | 40 | 1.5 | 50 | 120 | 2.6 | 225 | 460 |
| P870 | 125 | 1.5 | 35 | 2.0 | 50 | 130 | 3.5 | 260 | 495 |
| P960 | --- | --- | 80 | 4.5 | 40 | 150 | 4.5 | 360 | 530 |
| P870 | --- | --- | 80 | 4.5 | 50 | 350 | 4.5 | 360 | 680 |

^aAll frequencies and widths are in cm^{-1} .

zero-phonon line. The lineshape for the one-phonon profile is l_1 and is centered at $\nu + \omega_m$ with a FWHM of Γ . It is well known that the one-phonon profiles for electronic transitions of molecules imbedded in amorphous solids carry a width of about 30 cm^{-1} and the profiles for antenna Chl *a* and *b* are no exception [18]. When the one-phonon profile is taken to be a Gaussian the width of the *r*-phonon profile (centered at $\nu + r\omega_m$) is given by $\Gamma_r = r^{1/2}\Gamma$. In order to derive an analytic expression for the hole profile Lorentzians for $l_r (r > 1)$ were used [7] with widths governed by the Gaussian values, i.e., $r^{1/2}\Gamma$.

Equation 1 is readily modified to include coupling to the ω_{sp} -mode:

$$L(\Omega - \nu) = \sum_{j=1}^{\infty} \frac{S_{sp}^j e^{-S_{sp}}}{j!} [e^{-S} l_0^j(\Omega - \nu - j\omega_{sp})] + \sum_{r=1}^{\infty} \frac{S^r e^{-S}}{r!} [l_r^j(\Omega - \nu - r\omega_m - j\omega_{sp})] \quad (2)$$

where S_{sp} is the Huang-Rhys factor for ω_{sp} . In writing Eq. 2 the reasonable assumption that the electron-phonon coupling (S) is independent of the ω_{sp} -mode occupation number j is made. Similarly, the mean phonon frequency ω_m and Γ , the width of the one-phonon profile, are considered independent of j . However, the homogeneous linewidths γ_j of the zero-phonon l_j functions may differ due, for example, to rapid vibrational relaxation of the ω_{sp}^j ($j > 1$) levels.

We define $N_0(\nu - \nu_m)/N$ where N is the total number of absorbers and ν_m is the mean zero-phonon frequency. The absorption spectrum is calculated as the convolution of this distribution function with the single site absorption profile $L(\Omega - \nu)$. The integrated absorption cross-section, laser intensity and photochemical quantum yield are denoted by σ , I and ϕ .

Following a burn for time τ

$$N_{\tau}(v-v_m) = N_0(v-v_m) e^{-\sigma I \phi \tau L(\omega_B - v)} \quad (3)$$

where ω_B is the laser burn frequency and $L(\omega_B - v)$ is given by Eq. 2. To obtain the absorption spectrum, A_{τ} , following the burn we must convolve Eq. 3 with $L(\Omega - v)$ and integrate over v , i.e.,

$$A_{\tau}(\Omega) = \int dv N_0(v-v_m) e^{-\sigma I \phi \tau L(\omega_B - v)} L(\Omega - v) \quad (4)$$

With Eq. 4 the hole spectrum following a burn for time τ is given by $A_0(\Omega) - A_{\tau}(\Omega)$. In our previous calculations Eq. 4 was simplified by making the short burn time approximation where the exponential is expanded as $1 - \sigma I \phi \tau L(\omega_B - v)$ so that an analytic expression for the hole spectrum could be obtained. We do not do so here because a physically reasonable Gaussian is employed for the zero-phonon excitation energy distribution function of width Γ_1 and a more realistic line shape given to the one-phonon profile. In regard to the latter we note that the one-phonon profile for Chl *a* of the antenna complex of PS I exhibits a single maximum at $\omega_m \sim 25 \text{ cm}^{-1}$ and is asymmetric, with the higher energy half broader (and more tailing) than the lower energy half [18]. For Chl *a* the width (Γ) of the one-phonon profile is $\sim 30 \text{ cm}^{-1}$ and its shape is determined by the product of the protein phonon density of states and a frequency dependent electron-phonon coupling function [19]. The profile can be approximated by a Gaussian for the low energy half and a broader Lorentzian for the high energy half and, thus, we have employed such a profile for the present P870 and P960 calculations.

Unfortunately the phonon sidebands cannot be resolved in the P870 and P960 hole

spectra. Thus, in refs. 1 and 2 the Stokes shifts were used to estimate ω_m . This is less than satisfying and so we report here, for P870, a direct determination of ω_m . Our approach involves measuring the intensity of the ZPH; cf. Section I, as a function of burn temperature. As discussed in ref. 7 and as can be seen by making the short burn time approximation in Eq. 4, the effective Franck-Condon factor for the ZPH is, to a good approximation, given by $\exp(-2S)$ at 0 K (when $\omega_B \approx \nu_m$, as is the case for our experiments). Using long established theory [20], it follows that $\exp[-2S\langle n_x \rangle_T + 1]$ is the effective Franck-Condon factor for the ZPH at temperature where $\langle n_x \rangle_T = [\exp(\hbar\omega_m/kT) - 1]^{-1}$ is the phonon occupation number (x is defined here to be ω_m). The results of our experiment are shown in Fig. 2. The fit to the data points (ZPH with acceptable signal/noise ratio could not be measured for $T_B > 14$ K) with the T-dependent Franck-Condon factor leads to $\omega_m = 23 \pm 4$ cm⁻¹. We note that this value is in the range observed for pigments in antenna complexes [18, 21, 22] and, thus, it appears that protein phonons of this mean frequency are ubiquitous in coupling to electronic transitions.

Examples of our improved simulations to the ω_B -dependent P870 and P960 ΔA (absorbance) hole spectra are shown in Fig. 3. The upper spectra are the corresponding ΔT (transmission) spectra. The values of the parameters used for the simulation are given in Table I. For the spectra shown, ω_B is located near the center of the marker mode origin band (low E shoulders of Fig. 1) and provides optimum line narrowing [1,2]. By comparing the results in Fig. 3 to those of refs. 1 and 2 it can be seen that employment of a Gaussian for the inhomogeneous line broadening contribution in the present work has led to significantly improved fits. For convenience, the significant deviations of our earlier fits on the low energy tail of the spectra are also shown in Fig. 3. The magnitude of the deviations between the low

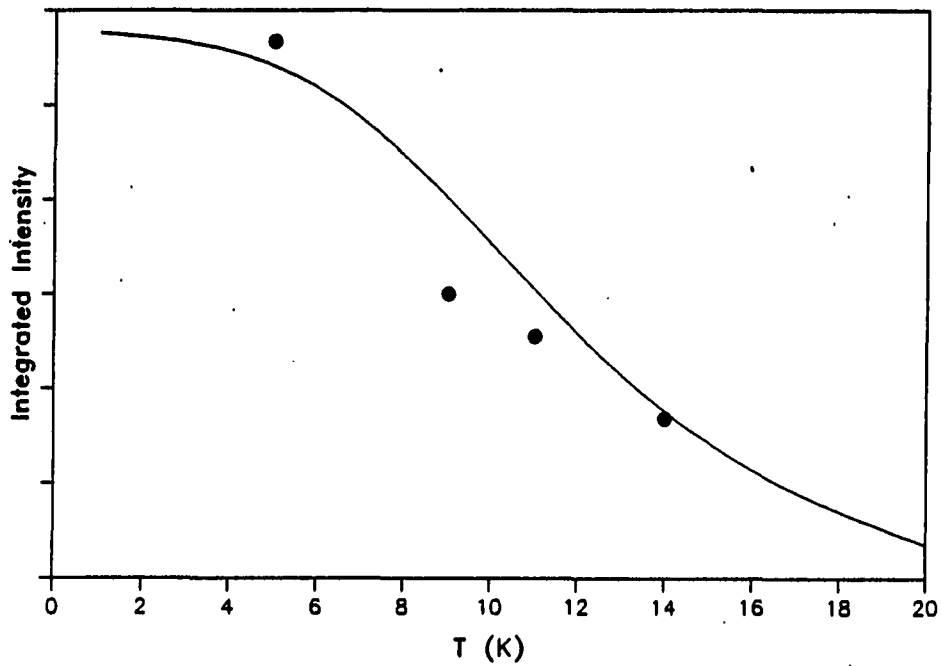


Figure 2. Temperature dependence of the integrated intensity of the zero phonon hole of P870: experimental data (dots with experimental error bars) and theoretical fit (smooth curve). $\lambda_B = 909.5$ nm. (See text for details)

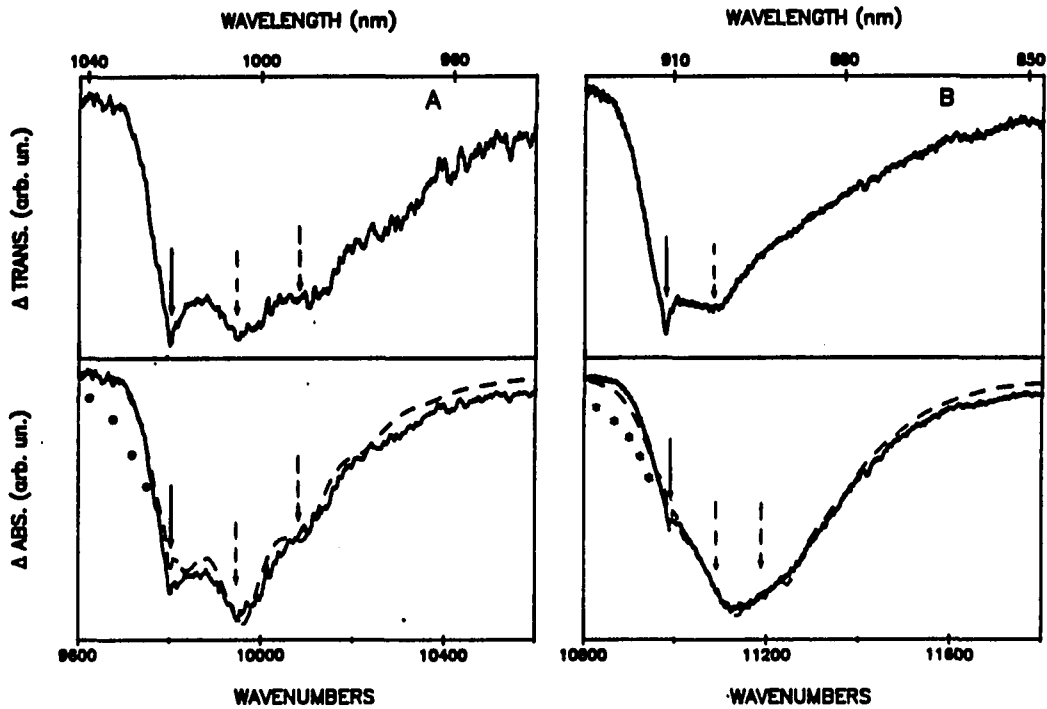


Figure 3. Transient photochemical hole burned spectra (solid line) and theoretical fits (dashed line). (A) *Rps. viridis* (glycerol glass/LDAO), $\lambda_B = 1020$ nm; ΔT spectrum (upper frame), ΔA spectrum and fit (lower frame). (B) *Rb. sphaeroides* (glycerol glass/NGP), $\lambda_B = 910$ nm; ΔT spectrum (upper frame), ΔA spectrum and fit (lower frame). See Table I and text for details of fits. First five overtones of ω_{sp} were included in the calculations. $T = 4.2$ K, resolution = 8 cm^{-1} for all spectra. Solid arrows indicate burn frequency. Dashed arrows indicate first and second quantum ω_{sp} -satellite holes. The low energy portion of the earlier theoretical fits from ref. 1 and 2 are present as dots (P960) and stars (P870) in the lower two frames

low energy sides of the experimental and simulated absorption spectra reported in ref. 2 are comparable. The present calculations also provide a more accurate description of the ω_B -dependence of the hole spectra than that given in ref. 2 [23,24]. This is also true for the absorption spectra, Fig. 1.

To conclude this sub-section we show in Fig. 4 results of an experiment designed to determine whether the ZPH coincident with ω_B for P870 exhibits the same decay kinetics as those for the broad hole upon which it is superimposed. The amplitude of the broad hole decreases by 37% as the delay time is increased from 2 to 10 ms (the decay time of $P870^+Q^-$ is 21 ± 2 ms). The corresponding percentage for the ZPH is estimated to be ~40%. The agreement is reasonable and provides further evidence that the ZPH is an intrinsic feature of the primary donor state.

Transient Spectra for Excitation into Accessory Pigment

Bands, Absence of Line Narrowing

With reference to the last two paragraphs of the Introduction, Fig. 5 shows some of a series of transient spectra for the accessory pigment Q_y -region of *Rb. sphaeroides* obtained for a series of ω_B -values ranging from the high to low energy sides of the BPheo absorption band at 760 nm, see absorption spectrum given in Fig. 6. The contributions to this band from the BPheo of the M and L branches [2] are not resolved but are responsible, in part, for its asymmetry. Figure 5 demonstrates that the electrochromically shifted (red) BPheo feature near $13,000 \text{ cm}^{-1}$ due to P^+Q^- is invariant to ω_B . Furthermore, this feature is essentially identical to that obtained by exciting directly into P870, Fig. 7. Thus, the BPheo band does

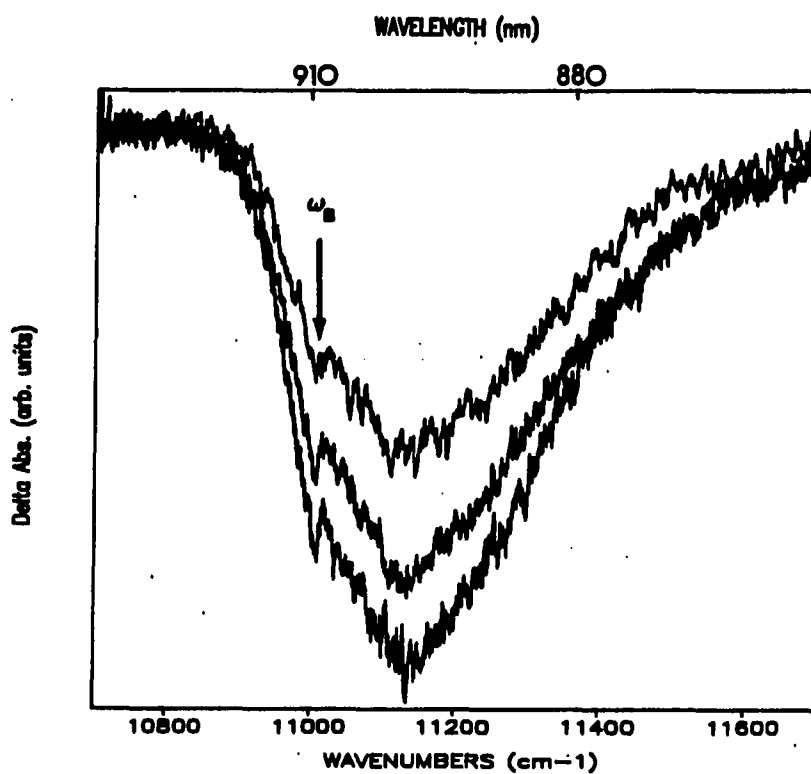


Figure 4. Transient hole burned spectra for P870 using variable gate delay. 2 ms, 5 ms, and 10 ms delay holes are shown with 2 ms being the largest and 10 ms being the smallest change in absorbance. $T = 4.2$ K, resolution = 3 cm^{-1} . $\lambda_B = 908$ nm. Approximately 15% change in transmission was obtained with a delay of 3 ms

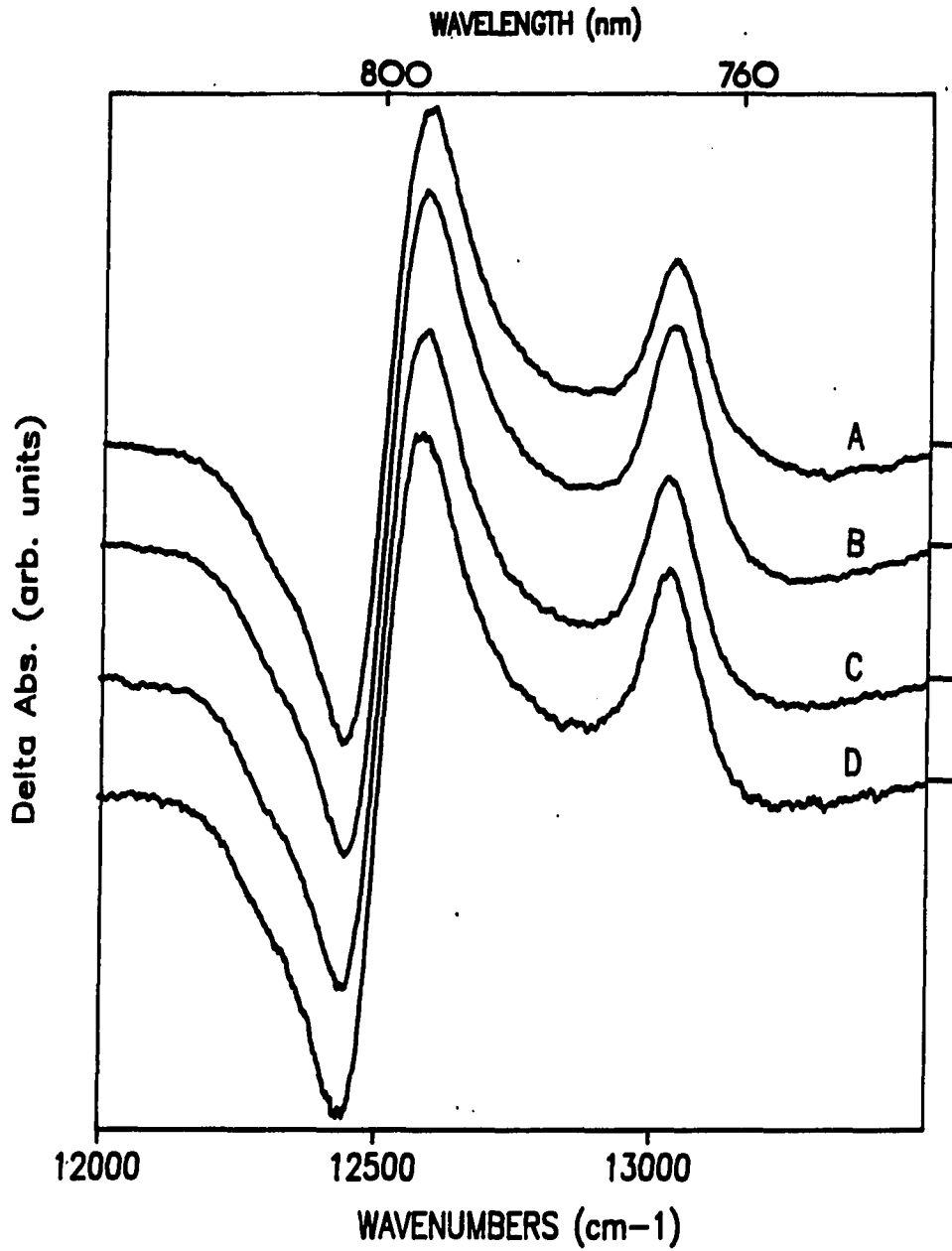


Figure 5. ΔA (absorbance) spectra for hole burning in the pheophytin Q_y bands. Burn wavelength: (A) 750 nm. (B) 760 nm. (C) 765 nm. (D) 770 nm. $T = 4.2$ K. Resolution = 3 cm^{-1} . Dashes on right vertical axis indicate $\Delta A = 0$ for each spectrum

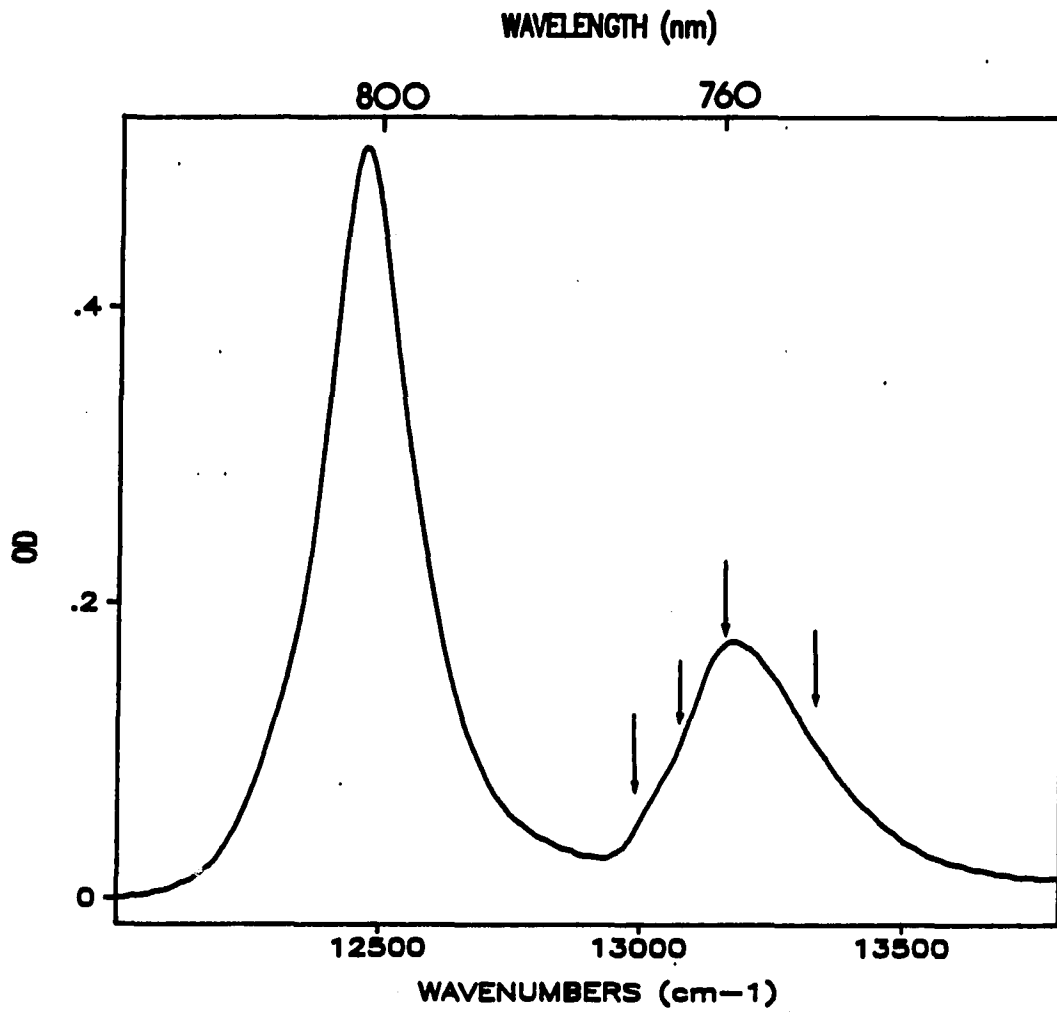


Figure 6.

Absorption spectrum for *Rb. sphaeroides* (glycerol glass/NGP) in accessory pigments Q_y region. $T = 4.2$ K. Resolution = 4 cm^{-1} . Burn frequencies indicated by solid arrows. The peak at ~ 12500 cm^{-1} (802 nm) is the BChl *a* monomer (B_L , B_M) band and the peak at ~ 13200 cm^{-1} (760 nm) is the BPheo *a* monomer (H_L , H_M) band

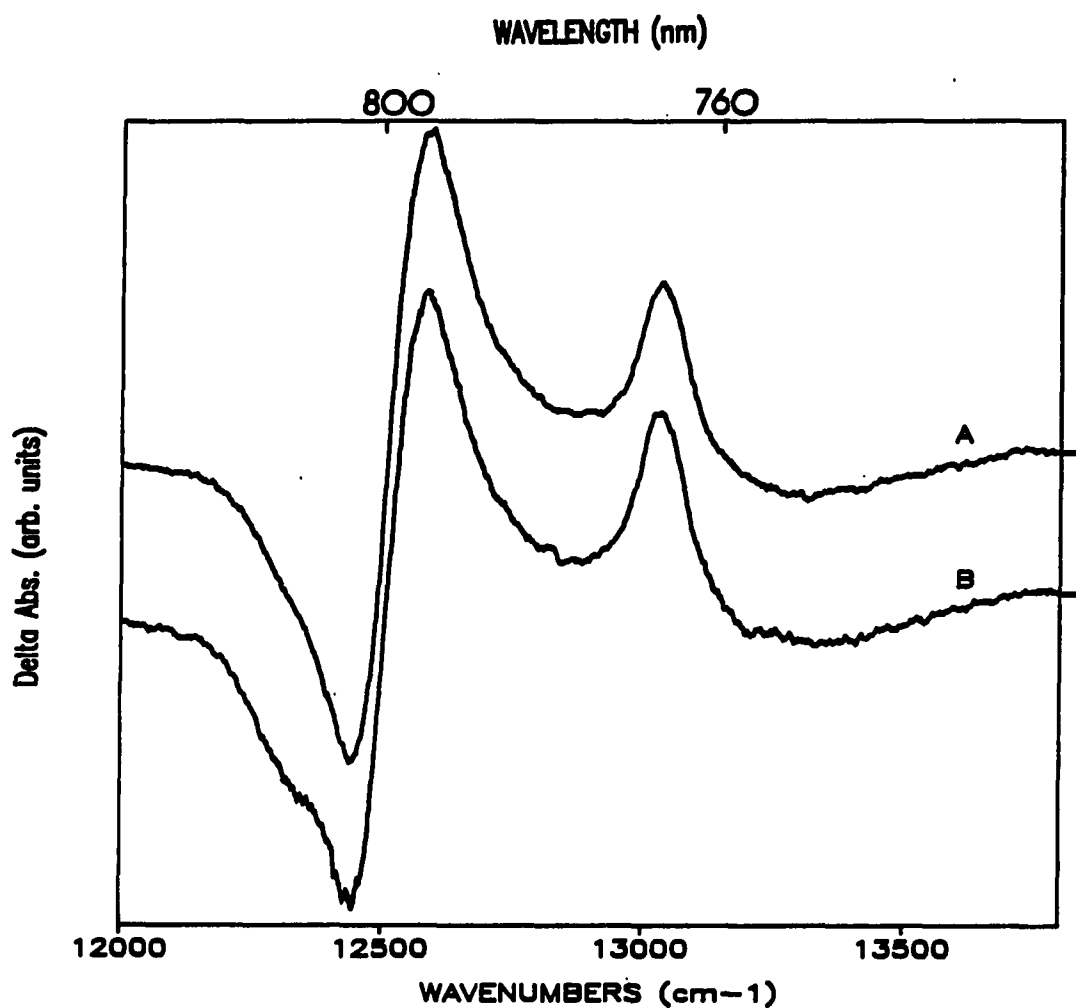


Figure 7. Hole burned spectra in accessory Q_y region for (A) $\lambda_p = 750$ nm. (B) $\lambda_p = 907$ nm. $T = 4.2$ K. Resolution = 3 cm^{-1} . Dashes on right vertical axis indicate $\Delta A = 0$ for each spectrum

not exhibit the line narrowing expected for a band whose width is dominated by inhomogeneous broadening. A similar result has been observed for the BChl accessory band of *Rps. viridis* [23]. The absence of line narrowing for the bacterial RC accessory bands provides a striking contrast to the RC of PS II [21], for which intense and persistent nonphotochemical ZPH and resolved phonon-sideband holes are observed for the Chl and Pheo accessory pigments. The width of the asymmetric BPheo band in Fig. 6 is 290 cm^{-1} which sets a lower limit of $\sim 20\text{ fs}$ for the decay time of BPheo* (on either the M- or L-side). We note that the intramolecular modes in the $700\text{-}1100\text{ cm}^{-1}$ region which build on the accessory Bchl band at 802 nm can be expected to contribute to the tailing on the high energy side of the BPheo band. Using the recently determined Franck-Condon factors for Chl *a* [18] in the above region we estimate a FWHM of $\sim 250\text{ cm}^{-1}$ from the two quasi-degenerate BPheo. Accepting that there is a large homogeneous lifetime broadening contribution to the BPheo band, we draw upon our calculations on the ω_B -dependence of the P870 and P960 hole spectra to estimate the contribution from inhomogeneous broadening to the above 250 cm^{-1} BPheo bandwidth. In order that a change of the electrochromically shifted BPheo spectrum not be observed as ω_B is tuned across the absorption band it is necessary that the inhomogeneous width be about one-half or less of the homogeneous width. Taking one-half as the upper limit, we obtain from 250 cm^{-1} inhomogeneous and homogeneous contributions of ~ 80 and 170 cm^{-1} , respectively. The latter yields a BPheo* lifetime of 30 fs [25]. An immediate question is whether a value of 80 cm^{-1} for the inhomogeneous broadening is reasonable since we have determined an inhomogeneous linewidth of 170 cm^{-1} for P870, Table I. We believe it is since the lowest exciton state of the special pair should be far more sensitive to structural variations from RC to RC. It is germane to note that the width of the BChl_{M,L} band in Fig. 6

at 802 nm is 200 cm^{-1} and that from the sharpest low temperature absorption spectrum for the RC of *Rps. viridis* we are aware of [26], the widths of the $\text{BChl}_{\text{M,L}}$, BPheo_{M} and BPheo_{L} bands are 205, 240, and 260 cm^{-1} , respectively. From Table I the inhomogeneous linewidth of P960 is 120 cm^{-1} . If it is assumed that this inhomogeneous width is also reduced by about one-half for the *Rps. viridis* accessory bands, one obtains ~ 30 fs lifetimes for $\text{BChl}_{\text{M,L}}$, BPheo_{M} , and BPheo_{L} . Although the above arguments are approximate, we believe that ~ 30 fs lifetimes are very reasonable estimates for the accessory pigment states of both RC. If the lifetimes of BPheo^* of *Rb. sphaeroides* and BChl^* of *Rps. viridis* were as long as 100 fs, a change of their electrochromically shifted profiles with ω_{B} or line narrowing should have been observed.

DISCUSSION

Having studied the hole spectra of P870 and P960 in several different glass-detergent systems we think it is unlikely that their resolution can be improved significantly with glassy hosts beyond that shown here and in refs. 1 and 2. The linear electron-phonon and -marker mode coupling are fundamental properties of the RC, only Γ_1 (inhomogeneous width) is subject to experimental manipulation. It is unlikely that Γ_1 can be appreciably reduced from our values for glass hosts given in Table I. It is appropriate, therefore, to consider the evolution of our simulations which have been stimulated by improvements in resolution of the hole spectra. The P870/P960 parameter set values given in Table I are given in chronological order, from the bottom up. From the outset [15] our model was based on the premise that the large homogeneous broadening of P870 and P960, indicated by the earliest hole burning experiments [16,17], was due to linear electron-phonon coupling, and not ultra-fast electronic relaxation of P^* [10,11,16,17]. The structured hole spectra discussed here and in refs. 1 and 2 prove that the former is the correct picture (the marker mode is, strictly speaking, a localized or resonant phonon [27] since it is intermolecular and of low frequency relative to the intramolecular modes). The lowest entries in Table I do not contain values for ω_{sp} and S_{sp} because the hole spectra available at that time were unstructured, i.e., a single mean phonon frequency approximation was utilized with $\omega_m = 80 \text{ cm}^{-1}$ and $S = 4.5$ for both P870 and P960. These values and those for Γ_1 led to calculated spectra (for different ω_D -values) in reasonable agreement with the spectra of Boxer and his group [16,17]. The value of $\Gamma_1 = 150 \text{ cm}^{-1}$ for P960 is similar to those determined later while the value of 350 cm^{-1}

is considerably higher. The latter is a consequence of the fact that the P870 absorption width reported in ref. 16 for a polyvinyl alcohol film was unusually large ($\sim 630 \text{ cm}^{-1}$). It is instructive to compare the value of $\omega_m = 80 \text{ cm}^{-1}$ with the values of ω_m and ω_{sp} determined later. From Table I one observes that the mean of $(\omega_m + \omega_{sp})$ is roughly equal to 80 cm^{-1} . Furthermore $S_{\text{total}} = S_{sp} + S$ from the two upper pairs of entries is not so different from 4.5. These rough agreements are not surprising since, in the theory (irrespective of the number of modes employed), the sensitivity of the centroid frequency of the total hole profile on ω_B depends on the ratio of Γ_1 to $\sum S_j \omega_j$. The spectra of Boxer and his group [16,17] give a good indication of the sensitivity. In the limit as $\Gamma_1 \rightarrow 0$ the hole spectrum becomes independent of ω_B .

In comparing the two upper P870/P960 entries of Table I it should be noted that the parameter values were determined by fitting to the same experimental spectra. The middle set was determined with the short burn time limit of the theory and Lorentzians for the inhomogeneous distribution and multi-phonon profiles, see page 116, were employed. The present calculations (upper set in Table I) avoid the short burn time approximation, employ more physically realistic inhomogeneous and phonon lineshape functions and utilize mean phonon frequency (ω_m) values in the range determined by experiment. The latter are similar to those observed for pigments of antenna complexes [18,21,22]. According to our analysis, it is the utilization of the improved spectral functions that is primarily responsible for the better agreement with experiment. Nevertheless, the important aspects of the physics remain the same. We note that the ultrafast relaxation times for the ω_{sp}^j ($j > 1$) ZPH levels given in the caption to Table I are discussed in ref. 1. It was the failure to observe, in the experimental spectra, the ω_{sp}^j ($j > 1$) ZPH satellite holes associated with the ZPH (at ω_B) of ω_{sp}^j

that indicated the ultrafast relaxation. Without such relaxation, the simulations clearly show the satellite ZPH structure. Furthermore, experiments in which ω_B was located in the vicinity of the ω_{sp}^1 component of the absorption profile failed to produce a ZPH at ω_B [23,24]. The implication that marker mode relaxation occurs faster than primary charge separation is consistent with the agreement between the time domain and hole burning decay times for P*.

In condensed phase spectroscopy the demarcation between weak and strong linear electron-phonon coupling is traditionally set at $S_{total} = 1$. For $S_{total} = 1$, the Franck-Condon factors for the zero-phonon and one-phonon transitions are equal. From Table I one observes that the coupling for P870 and P960 is strong, e.g., for $S_{total} = 3$ the Franck-Condon factor for the zero-phonon line of the origin band is only 0.05.

Earlier it had been stated that reasonable estimates for several of the theoretical parameters were afforded by the experimental data. Obviously ω_{sp} and S_{sp} are two. But S is also since, according to the theory [7,15], the ratio of the integrated intensity of the ZPH to that of the broader ω_{sp}^0 hole it is superimposed on is $\approx \exp(-2S)$. Furthermore, an experimental determination for ω_m of $23 \pm 4 \text{ cm}^{-1}$ is available (Fig. 2). With these estimates and the observed width of the primary donor absorption profile, one can estimate Γ_1 . From our simulations we have found that the optimal parameter values are within about 20% of the original estimates. Thus the simulations are best viewed as a refinement procedure for the experimental estimates. Turning now to the energy transfer properties of the higher energy Q_y -states of the bacterial RC we note that Jean et al. [28] have shown that Forster theory falls far short of accounting for the remarkably short (<100 fs) lifetimes of the "accessory" pigment states or the upper special pair state (P_+). Inadequate spectral overlap and large energy spacings between the relevant states make it very unlikely that Forster theory, even if

modified, will work. In fact, it is incorrect to apply this "weak coupling" theory to relaxation from P_+ to P_- (primary donor state) since the excitonic splitting far exceeds the energy fluctuations of these states due to pure dephasing from bath fluctuations. An alternative mechanism is afforded by the theory of Davydov [27]. Here one would start with zero-order pigment aggregate states which are diagonal with respect to the excitonic Hamiltonian, $H_{ex}(0)$, for a suitable static aggregate geometry. Relaxation between eigenstates of $H_{ex}(0)$ would be induced by variations of H_{ex} produced by intermolecular displacements associated with modes Q , i.e. $(\partial H_{ex}/\partial Q)_0 Q$ and higher order terms. The modes expected to be most effective are those involving rotational displacements of the pigments [29]. Such a mechanism is known to lead to decay of the upper triplet dimer (Davydov) state to the lower (by 25 cm^{-1}) Davydov state of the anthracene crystal (by one-phonon emission) in 5 ps [30]. Recently, hole burning studies on the antenna complex of *Prosthecochloris aestuarii* have been performed [22,31]. Pair-wise excitonic interactions in the basic subunit of this complex, which contains 7 BChl molecules, are as large as $\sim 200 \text{ cm}^{-1}$ [32]. The experimentally observed exciton structure in absorption occurs over a $\sim 500 \text{ cm}^{-1}$ wide spectral region. The shortest exciton level decay times for this system are $\sim 250 \text{ fs}$ [22,31]. This value can be viewed as consistent with that for anthracene under the expectation that decay is proportional to the exciton bandwidth squared and that in *P. aestuarii* the relaxation occurs by two-phonon emission. The excitonic interactions between pigments in the RC (other than that between the two Bchl of the special pair) are no larger than those in the *P. aestuarii* subunit [33]. With this in mind and a consideration of the RC accessory state level spacings, it is not apparent that one can reconcile the fact that decay of the accessory states of the RC is an order of magnitude faster than in *P. aestuarii*. The problem is more evident when one attempts to understand a $< 100 \text{ fs}$ direct

decay from the upper (P_+) to lower (P_-) dimer states of the special pair. In *Rps. viridis* the dimer or exciton splitting is $\sim 2000 \text{ cm}^{-1}$, which is larger than the marker mode or intramolecular vibrational frequencies. Thus, one is in the strong coupling limit [34-36] of the Davydov theory. If, for example, one were to invoke only the marker mode for $P_+ \Rightarrow P_-$ relaxation, creation of ~ 20 quanta of this mode would be necessary for the process. This is a very high order and improbable event (as in Herzberg-Teller vibronic coupling theory [37], a 2-quantum process is one to two orders of magnitude less probable than a 1-quantum process, etc.) Invoking a high frequency ($\sim 1500 \text{ cm}^{-1}$) intramolecular mode plus several quanta of a low frequency intermolecular dimer mode would not appear to be a solution either since the former would not be expected to provide significant modulation of the resonance energy transfer matrix element. Although approximate, the above scaling argument indicates that the Davydov mechanism cannot account for the ultrafast energy transfer processes of the RC.

A third possibility is that the "dark" charge-transfer (CT) states, which have been invoked to explain the primary charge separation process [38], provide a broad distribution of level structure through the Q_y -region which serves as a conduit for energy transfer from the higher energy optically allowed states to P_- . The fact that such CT states would be characterized by very high S -values for intermolecular modes is consistent with a broad distribution. Within this model decay would be viewed in terms of a breakdown of the Born-Oppenheimer approximation. Hopefully, electronic structure calculations may eventually be able to speak to the viability of this model.

CONCLUSION

An experimental determination of the mean frequency for protein phonons which couple to the primary donor state together with the avoidance of approximations to the theory of Hayes and Small made earlier have led to a significant improvement of the theoretical fits to the absorption and hole spectra of P870 and P960. The optical reorganization energies for P870 and P960 due to low-frequency modes (phonons, marker mode) are about one-third the value determined for the 100% CT state of the anthracene-pyromellitic acid dianhydride crystal [39] but an order of magnitude greater than for Chl in antenna complexes [18,22,31]. This result provides strong support for the suggestion from Stark data that [4,5,6] the primary donor state possesses significant CT character. The reported marker mode frequencies of 115 and 134 cm^{-1} are for P870* and P960*; determination of the corresponding ground state frequencies would be important for elucidation of the dynamical nature of the special pair mode.

New experimental results are used to determine decay times of ~ 30 fs to the accessory Q_y -states of the bacterial RC due to downward energy transfer. An approximate scaling argument is presented which indicates that the Davydov energy transfer mechanism, like the Forster mechanism [28], cannot account for the ultrafast decays. An alternative mechanism, which invokes intermediacy of a broad distribution of level structure due to charge-transfer states, is suggested for future consideration.

ACKNOWLEDGEMENT

Research at the Ames Laboratory was supported by the Division of Chemical Sciences, Office of Basic Energy Sciences, U.S. Department of Energy. Ames Laboratory is operated for the U.S. Department of Energy by Iowa State University under Contract No. W-7405-Eng-82. Research at Argonne National Laboratory was supported by the Division of Chemical Sciences, Office of Basic Energy Sciences, under Contract No. W-31-109-Eng-38.

REFERENCES

1. Johnson, S.G.; Tang, D.; Jankowiak, R.; Hayes, J.M.; Small, G.J.; Tiede, D.M. *J. Phys. Chem.* 1989, 93, 5953.
2. Tang, D.; Johnson, S.G.; Jankowiak, R.; Hayes, J.M.; Small, G.J.; Tiede, D.M. In *Perspectives in Photosynthesis*, Jortner, J., Pullman, B., Eds.; Kluwer Academic: Dordrecht, 1990, p 99.
3. Warshel, A.; Parson, W.W. *J.A.C.S.* 1987, 109, 6143.
4. Lösche, M.; Feher, G.; Okamura, M.Y. *Proc. Natl. Acad. Sci. USA* 1987, 84, 7537.
5. Boxer, S.G.; Lockhart, D.J.; Middendorf, T.R. In *Proceedings in Physics, Primary Processes in Photobiology*, Kobayashi, T., Ed.; Springer-Verlag: New York, 1987, Vol. 20, p 80.
6. Lockhart, D.J.; Boxer, S.G. *Proc. Natl. Acad. Sci. USA* 1988, 85, 107.
7. Hayes, J.M.; Gillie, J.K.; Tang, D.; Small, G.J. *Biochim. Biophys. Acta* 1988, 932, 287.
8. Fleming, G.R.; Martin, J.L.; Breton, J. *Nature (London)* 1988, 85, 190.
9. Breton, J.; Martin, J.L.; Fleming, G.R.; Lambry, J.-C. *Biochemistry* 1988, 27, 8276.
10. Won, Y. and Friesner, R.A. *J. Phys. Chem.* 1988, 92, 2214.
11. Meech, S.R.; Hoff, A.J.; Wiersma, D.A. *Chem. Phys. Lett.* 1985, 121, 287.
12. Vermeglio, A.; Paillotin, G. *Biochim. Biophys. Acta* 1982, 681, 32.
13. Chang, C.H.; Tiede, D.; Tang, J.; Smith, U.; Norris, J. *FEBS Lett.* 1986, 205 82.
14. This was inadvertently misstated in ref. 1 as 34 ± 3 ms and corrected here to

21 ± 2 ms.

15. Hayes, J.M.; Small, G.J. *J. Phys. Chem.* (1986), 90, 4928.
16. Boxer, S.G.; Lockhart, D.J.; Middendorf, T.R. *Chem. Phys. Lett.* 1986, 123, 476.
17. Boxer, S.G.; Middendorf, T.R.; Lockhart, D.J. *FEBS Lett.* 1986, 200, 237.
18. Gillie, J.K.; Small, G.J.; Golbeck, J.H. *J. Phys. Chem.* 1989, 93, 1620.
19. Rebane, K.K. *Impurity Spectra of Solids*, Plenum Press, New York, 1970.
20. Richards, J.L.; Rice, S.A. *J. Chem. Phys.* 1971, 54, 2014.
21. Jankowiak, R.; Tang, D.; Small, G.J.; Seibert, M. *J. Phys. Chem.* 1989, 93, 1649.
22. Johnson, S.G.; Small, G.J. *Chem. Phys. Lett.* 1989, 155, 371.
23. Tang, D. Ph.D. dissertation, Iowa State University, 1990.
24. Johnson, S.G. Ph.D. dissertation, Iowa State University, 1990.
25. The origin of the homogeneous contribution to the linewidth is assigned to an ultrafast excited state lifetime and not to strong linear electron-phonon coupling ($S \sim 6$, $S\omega_m \approx 190 \text{ cm}^{-1}$). For strong coupling to account for the large homogeneous width the zero phonon hole (ZPH) would have to be relatively narrow, at most a few cm^{-1} in width, in order to fulfill the conditions of strong coupling (i.e., integrated area of ZPH ≈ 0.002 relative to total integrated area and a totally suppressed ZPH). A ZPH of a few cm^{-1} (FWHM) would indicate an excited state lifetime in the picosecond range which would be inconsistent with energy transfer occurring in $\sim 100 \text{ fs}$ [8,9].
26. Fig. 2 of ref. 2. The solvent is glycerol/H₂O (2:1) with LDAO.
27. Davydov, A.S. *Theory of Molecular Excitons*; Plenum Press: New York, 1971.
28. Jean, J.M.; Chan, C.-K.; Fleming, G.R. *Israel J. Chem.* 1988, 28, 169.
29. Dissado, L.A. *Chem. Phys.* 1975, 8, 289.

30. Port, H.; Rund, D.; Small, G.J., Yakhot, V. *Chem. Phys.* 1979, 39, 175.
31. Johnson, S.G. and Small, G.J. *J. Phys. Chem.* 1990, to be published.
32. Pearlstein, R.M. In *Photosynthetic Light-Harvesting Systems*, Scheer, H., Schneider, S., Eds.; De Gruyter: Berlin, 1988, p 555.
33. Knapp, E.W.; Fischer, S.F.; Zinth, W.; Sander, M.; Kaiser, W.; Deisenhofer, J.; Michel, H. *Proc. Natl. Acad. Sci. USA* 1985, 82, 8463.
34. Witkowski, A. and Moffit, W. *J. Chem. Phys.* 1960, 33, 873.
35. McClure, D.S. *Can. J. Chem.* 1958, 36, 59.
36. Gregory, A.R.; Henneker, W.H.; Siebrand, W.; Zgierski, M.Z. *J. Phys. Chem.* 1975, 63, 5475.
37. Fischer, G., *Vibronic Coupling, The Interaction between the Electronic and Nuclear Motions*, Academic Press: New York, 1984.
38. Friesner, R.A.; Won, Y. *Biochim. Biophys. Acta* 1989, 977, 99.
39. Haarer, D. *J. Chem. Phys.* 1977, 67, 4076.

CONCLUSIONS

Transient spectral hole burning studies have been performed on P960 (PED state of *Rps. viridis*) and P870 (PED state of *Rb. Sphaeroides*) [38-42]. The hole profiles obtained in both RCs revealed an important low frequency Franck-Condon progression [40]. This progression has been assigned to intermolecular vibrational modes of the PED in the reaction center which serve as a true marker for the structure of the special pair for purple bacteria [40]. The implication of this marker mode in the charge separation dynamics, however, is still not clear. For appropriate burn wavelengths, zero phonon holes were observed (with exception of *Rb. Sphaeroides* in PVOH film) for samples embedded in various hosts [38-42] with good agreement with time domain data [19,21]. Such observation strongly supports the proposal by Hayes and coworkers [36,37] that the broad and intense component(s) of the resulting PED hole profile is due to the combined effect of linear electron-phonon coupling and site inhomogeneous line broadening rather than ultrafast decay of the primary donor state [30-35]. Hole burning technique measures the decay from the zero-point of P* and time domain experiments initially prepare P* vibrationally excited. Thus, good agreement between the results achieved by both methods allows us to suggest that thermalization occurs on a subpicosecond time scale. If charge separation occurred to a significant extent prior to thermalization, one would not expect such agreement. Calculated hole profiles utilizing the theory by Hayes and Small [36,37] modified for the marker mode, have yielded quite respectable agreement. The theory of Won and Friesner [34,35] found no support from our results. On the basis of the total electron-phonon coupling strength ($S_{\text{total}} \sim 3.5$), it is natural

for us to view P^* possessing significant charge-transfer character. Such assumption are in agreement with the previous hole burning [30-33], accumulated photon echo [31,33] and Stark measurements [45-47]. Questions regarding the early time dynamics arise as the ~ 30 fs downward energy transfer time from the accessory pigments to P^* was measured [42]. The "dark" charge-transfer states invoked for charge separation have been speculated [48] to carry the responsibility for such ultrafast process. Recent experiments performed on the RC of PS II have indicated that the energy transfer decay times of the accessory pigment Q_y -states are of three orders of magnitude slower [49-51]. Further discussions will be presented in the next section.

It has been demonstrated here that hole burning spectroscopy can be effectively used to provide us the data essential for understanding the electronic structure of the primary donor states as well as its coupling to the phonons of the protein-pigment complex. A more complete understanding of nature of the charge separation, however, still awaits further investigation.

REFERENCES

1. Deisenhofer, J.; Epp, O.; Miki, K.; Huber, R.; Michel, H. *J. Mol. Biol.* 1984, 180, 385.
2. Deisenhofer, J.; Epp, O.; Miki, K.; Huber, R.; Michel, H. *Nature(Lodon)* 1985, 318, 618.
3. Michel, H.; Epp, O.; Deisenhofer J. *EMBO J.* 1986, 5, 2445.
4. Allen, J. P.; Feher, G.; Yeates, T. O.; Rees, D. C.; Deisenhofer, J.; Michel, H.; Huber, R. *Proc. Natl. Acad. Sci. USA* 1986, 83, 8589.
5. Allen, J. P.; Feher, G.; Yeates, T. O.; Komiya, H.; Rees, D. C. *Proc. Natl. Acad. Sci. USA* 1986, 84, 5730.
6. Allen, J. P.; Feher, G.; Yeates, T. O.; Komiya, H.; Rees, D. C. *Proc. Natl. Acad. Sci. USA* 1986, 84, 6162.
7. Allen, J. P.; Feher, G.; Yeates, T. O.; Komiya, H.; Rees, D. C. *Proc. Natl. Acad. Sci. USA* 1986, 84, 6438.
8. Allen, J. P.; Feher, G.; Yeates, T. O.; Komiya, H.; Rees, D. C. *Proc. Natl. Acad. Sci. USA* 1986, 85, 8487.
9. Chang, C. H.; Tiede, D. Tang, J.; Smith, U.; Norris, J.; Schiffer, M. *FEBS Lett.* 1986, 205, 82.
10. Budil, D.; Gast, P.; Chang, C. H.; Schiffer, M.; Norris, J. R. *Ann. Rev. Phys. Chem.* 1987, 38, 561.
11. Yeates, T. O.; Koyima, H.; Chirino, A.; Rees, D. C.; Allen, J. P.; Feher, G. *Proc. Natl. Acad. Sci. USA* 1988, 85, 7993.

12. Kirmaier, C.; Holten, D. *Photosynthe. Res.* 1987, 12, 225.
13. Maroti, P.; Kirmaier, C.; Wraight, C.; Holten, D.; Pearlstein, R. M. *Biochim. Biophys. Acta* 1985, 810, 132.
14. Holten, D.; Kirmaier, C.; Levine, L. in *Progress in Photosynthesis Research, Vol. I.*, J. Biggins, Ed., The Hague: Martinus Nijhoff, 1987, pp. 169-175.
15. Bylina, E. J.; Youvan, D. C. *Z. Naturforsch.*, 1987, 42C, 769.
16. Bylina, E. J.; Youvan, D. C. *Proc. Natl. Acad. Sci. USA* 1988, 85, 7226.
17. Bylina, E. J.; Jovine, R.; Youvan, D. C. in *Photosynthetic Bacterial Reaction Center: Structure and Dynamics, Vol. 149*, J. Breton and A. Vermèglio, Eds., Plenum: New York, 1988, pp. 113-118.
18. Kirmaier, C.; Holten, D.; Bylina, E. J.; Youvan, D. C. *Proc. Natl. Acad. Sci. USA* 1988, 85, 7562.
19. Martin, J. L.; Breton, J.; Lambry, J. C.; Fleming, G. in *Photosynthetic Bacterial Reaction Center: Structure and Dynamics, Vol. 149*, J. Breton and A. Vermèglio, Eds., Plenum: New York, 1988, pp. 198-203.
20. Fleming, G. R.; Martin, J. L.; Breton, J. *Nature*, 1988, 333, 190.
21. Breton, J.; Martin, J. L.; Fleming, G. R.; Lambry J.-C. *Biochemistry* 1988, 27, 8276.
22. Martin, J. L.; Breton, J. Hoff, A. J.; Migus, A.; Antonetti, A. *Proc. Natl. Acad. Sci. USA* 1986, 83, 5121.
23. Breton, J.; Martin, J. L.; Migus, A.; Antonetti, A.; Orszag, A. *Proc. Natl. Acad. Sci.* 1986, 83, 5121.
24. Breton, J.; Martin, J. L.; Petrich J.; Migus, A.; Antonetti, A. *FEBS Lett.* 1986, 209, 37.

25. Wasliewski, M.; Tiede, D. *FEBS Lett.* 1986, 204, 368.
26. Kirmaier, C.; Holten, D. *FEBS Lett.* 1988, 239, 211.
27. Woodbury, N.; Becker, M.; Middendorf, D.; Parson, W. W. *Biochemistry* 1985, 24, 7516.
28. Chekalin, S. V.; Matveetz, Ya. A.; Skuropatov, A.; Shuvalov, V. A.; Yartzer, A. P. *FEBS Lett.* 1986, 123, 476.
29. Holzapfel, W.; Finkle, U.; Kaiser, W.; Oesterhelt, D.; Scheer, H.; Stilz, H. U.; Zinth, W. *Chem. Phys. Lett.* 1989, 160, 1.
30. Boxer, S. G.; Middendorf, T. R.; Lockhart, D. J.; *FEBS Lett.* 1986, 200, 237.
31. Meech, S. R.; Hoff, A. J.; Wiersma, D. A. *Proc. Natl. Acad. Sci. USA* 1986, 83, 9464.
32. Boxer, S. G.; Lockhart, D. J.; Middendorf, T. R.; *Chem. Phys. Lett.* 1986, 123, 476.
33. Meech, S. R.; Hoff, A. J.; Wiersma, D. A. *Chem. Phys. Lett.* 1985, 121, 287.
34. Won, Y.; Friesner, R. A. *J. Phys. Chem.* 1988, 92, 2214.
35. Won, Y.; Friesner, R. A. *Proc. Natl. Acad. Sci. USA* 1987, 84, 5511.
36. Hayes, J. M.; Small, G. J. *J. Phys. Chem.* 1986, 90, 4928.
37. Hayes, J. M.; Gillie, J. K.; Tang, D.; Small, G. J. *Biochim. Biophys. Acta* 1988, 932, 287.
38. Tang, D.; Jankowiak, R.; Small, G. J.; Tiede, D. M. *J. Phys. Chem.* 1988, 92, 4012.
39. Tang, D.; Jankowiak, R.; Small, G. J.; Tiede, D. M. *Chem. Phys.* 1989, 131, 99.
40. Tang, D.; Johnson, S. G.; Jankowiak, R.; Small, G. J.; Tiede, D. M. in *Perspective in Photosynthesis*, J. Jortner and B. Pullman, Eds., Kluwer Academic Press: Dorecht/Boston/London, 1989, pp. 23-38.

41. Johnson, S. G.; Tang, D.; Jankowiak, R.; Hayes, J. M.; Small, G. J.; Tiede, D. M. J. *Phys. Chem.* 1989, 93, 5953.
42. Johnson, S. G.; Tang, D.; Jankowiak, R.; Hayes, J. M.; Small, G. J.; Tiede, D. M. J. *Phys. Chem.* 1990, accepted.
43. Tiede, D. M. *Biochemistry* 1987, 26, 397.
44. Chang, C.-H.; Schiffer, M.; Tiede, D.; Smith, U.; Norris, J. J. *Mol. Biol.* 1985, 186, 201.
45. Lösche, M.; Feher, G.; Okamura, M. Y. *Proc. Natl. Acad. Sci. USA* 1987, 84, 7537.
46. Lockhart, D. J.; Boxer, S. J. *Biochemistry* 1987, 26, 664.
47. Lockhart, D. J.; Boxer, S. J. *Proc. Natl. Acad. Sci. USA* 1988, 85, 107.
48. Friesner, R. A.; Won, Y. *Biochim. Biophys. Acta* 1989, 977, 99.
49. Tang, D.; Jankowiak, R.; Yocum, C. F.; Seibert, M., Small, G. J. *J. Phys. Chem.* 1990, submitted.
50. Tang, D.; Jankowiak, R.; Small, G. J.; Seibert, M. *Photosynthe. Res.*, submitted.
51. Small, G. J.; Jankowiak, R.; Seibert, M.; Yocum, C. F.; Tang, D. in *Proceedings of the Feldafing II Workshop on Structure and Function of Bacterial Reaction Centers*, Michel-Byerle, Ed., Springer-Verlag, submitted.

SECTION II.

**PHOTOCHEMICAL HOLE BURNING STUDIES
OF REACTION CENTER OF PHOTOSYSTEM II**

INTRODUCTION

Photosystem II is a membrane-protein complex where primary charge separation and subsequent electron transfer for oxygen production are its major functions. It is composed of various kinds of proteins, chlorophylls (Chl), pheophytins (Pheo), carotenoids, lipids, quinones and inorganic ions. The primary charge separation is originated in the reaction center (RC) of Photosystem II. Upon direct or indirect excitation of the RC, a primary electron donor (PED) called P680 (named after the absorption maxima) rapidly donates an electron to a pheophytin molecule [1-4]. Two plastoquinones are the subsequent electron acceptors. An electron is then donated to the P680⁺ by a nearby tyrosine molecule [5,6] constituting the secondary electron transfer process. Although the crystal structure of RC of PS II is yet to be determined, recent developments have suggested that structural and functional similarities between PSII RC and of bacterial RCs [3,4,7-11] exist. In 1984, a RC complex of PS II was first isolated by Nanba and Satoh [12] containing only D1 (32 kDa), D2 (34 kDa) and cytochrome *b*-559 proteins. Pigment analysis utilizing reverse-phase HPLC yielded 4-5 Chl *a*, 2 Pheo *a*, and a single β -carotene molecule. No bound quinone molecule was found in the analysis which may have been lost as a result of the isolation procedure [12]. A later work by Barber et al. [13] has obtained a ratio of 4:2:1 (Chl *a*:Pheo *a*: β -carotene) following a similar procedure. In comparison to the bacterial RCs [14-20], the pigment content reflects striking resemblance. Two polypeptides, D1 and D2, have shown significant homologies to the L and M apoproteins of bacterial RC [3-5,21-24] by nucleotide and amino acid sequence analysis. In addition, recent spectroscopic evidence has shown that the primary charge

separation and electron transfer kinetics are also similar [1,25-28].

Recently, a report on several other preparations [11,29-37] brought controversy concerning the pigment composition as well as the origin of instability of the isolated D1-D1-cyt *b*-559 complex. Significant changes of the optical absorption spectrum of PSII RC upon the addition of Triton X-100 detergent [26,27,35-37] have raised a question of whether the integrity of the RC complex was preserved during the preparation in which high concentration of detergent was used. A compilation of several recent preparations are tabulated in Table I. The shaded boxes indicate the samples utilized for spectroscopic investigation in this work.

Hole burning experiment was first performed by Vink et al. in an attempt to probe the early time optical dynamics [38] of PS II RC. A broad 110 cm^{-1} hole was observed with no indication of a ZPH. The maxima of the broad hole, however, does indicate slight burn-wavelength dependence. The failure to observe the ZPH may have been due to poor signal-to-noise of the instrument and background laser scattering. However, the broad hole together with observed burn-wavelength dependence of its maxima, may be a manifestation of strong linear electron-phonon coupling [1,39,40]. PAPER IV [3] in this section presents the first report on the charge separation kinetics of PS II RC at 4.2 K utilizing transient photochemical hole burning technique. The decay time of P680* was found to be 1.9 ± 0.2 ps. Time domain experiments performed by Wasielewski et al. [4,7] obtained a electron transfer time to Pheo of 1.4 ± 0.2 ps at 15 K [4] and 2.6 ± 0.6 ps at 4°C [5]. The hole profile obtained showed no evidence of a Franck-Condon marker mode which indicates that the structure of PED for P680 may be significantly different from that for the special pair of the bacteria RCs. Theoretical calculations without employing the coupling of low-frequency marker mode indicate that the theory of strong linear electron-phonon coupling and inhomogeneous line

Table I. Comparison of several recent PS II RC preparations

| PS II RC Preparations | Chl <i>a</i>/Pheo <i>a</i> Ratio | Detergent Used |
|--|---|--|
| Nanba & Satoh (1987) Ref. 12 | ~ 4-5/2 | Triton X-100 |
| Kobayashi et al. (1990) Ref. 34 | ~ 6/2 | Digitonin |
| Barber et al (1987) Ref. 13 (Method used similar to Nanba & Satoh preparation) | ~ 4/2 | Triton X-100 |
| Gounaris et al. (1989) Ref. 31 | ~ 16/2 | Triton X-100 |
| Seibert et al. (1989) Ref. 29 McTavish et al. (1989) Ref. 30 (Modified Nanba & Satoh preparation) | no data available | Triton X-100 (but removed with PEG in final step) |
| Breton (1990) Ref. 37 | no data available | Triton X-100 (final elution used dodecyl maltoside) |
| Dekker et al. (1989) Ref. 32 Ghanotakis et al. Ref. 33 | ~ 10-12/2-3 | Dodecyl maltoside |

broadening by Hayes and Small can be successfully used to account for the experimental results.

PAPER V [26] and PAPER VI [27] offered detailed study on the energy transfer dynamics of different preparations [29,30,32,33] as well as the nature of the detergent effect. Utilizing the technique of steady-state triplet bottleneck hole burning [26,27], the location of P680* was accurately determined and found to be quasi-degenerate with Pheo Q_y state [26-28]. The difference of energy transfer dynamics between PS II RC and that of bacterial RC is also discussed in this section.

EXPERIMENTAL METHODS

Sample Preparation

The isolation of the reaction center of PS II follows the procedure described by McTavish et al. [30]. Briefly, the D1-D2-cyt *b*-559 RC complex of PS II was prepared from spinach PS II membrane fragments [12,29,30] which were solubilized in 4% Triton X-100 (TX), 50 mM Tris-HCl (*pH* 7.2) for 1 hour with stirring. The material was then centrifuged for 1 hour at 100,000 x *g*. The supernatant was then loaded onto a TSK-GEL DEAE-Toyopearl 650S (Supelco, Bellefonte, PA) column pre-equilibrated with 50 mM Tris-HCl (*pH* 7.2), 30 mM NaCl, and 0.05% Triton X-100. The column was washed with the same buffer until the eluent was colorless, and the RC fraction was eluted with a 30 to 200 mM NaCl gradient containing 50 mM Tris-HCl (*pH* 7.2) and 0.05% TX. RC were then concentrated by precipitation with polyethylene glycol (PEG). After 90 min incubation, the suspension was centrifuged at 31,300 x *g* for 15 min. The pellet was resuspended in 50 mM Tris-HCl (*pH* 7.2) with no detergent and then centrifuged again at 1,100 x *g* for 90 sec to pellet mostly colorless material containing PEG aggregates. The pellet material was discarded, and the RC fraction was stored at -80°C until use. All of the above procedures were performed in the dark at 4°C. In several early experiments, PS II RC complexes prepared by the original Nanba and Satoh [12] were used. The details are described in ref. [3]. Prior to experiment, the RC complexes was thawed in the dim light and at 4°C. A flash light with a interference filter center around 550 nm was used. The host used consists of 60% glycerol

and 40% H₂O with 10 mM Tris-HCl. Various amounts of detergent (ranging from 0.01% to 0.2%) such as Triton X-100 or dodecyl maltoside were added to the host upon need.

For the experiments involving extraction of TX from a sample to which TX had been added, 0.05% TX was added to a solution containing the PS II RC complex (stored as described above) and the solution incubated for 20 min in the dark at ice temperature. A fraction of the sample was then removed and stored in the dark at -80°C for later use as the control. The remaining sample was centrifuged at 20,000 x g for 30 min and then at 50,000 x g for another 30 minutes. Supernatant was carefully removed and the pellet resuspended in 50 mM Tris-HCl buffer (pH 7.2) and subsequently stored in the dark at -80°C. Prior to the spectroscopic experiments, samples were unfrozen and diluted with 60/40 Glycerol/H₂O (buffered with Tris-HCl) to achieve the appropriate optical density. TX was added to the solvent used for dilution of the sample which had been previously incubated with TX in order to maintain the desired 0.05% concentration.

Cryogenic Equipment

Samples were contained in polystyrene centrifuge tubes (path length ~ 1 cm) in a brass sample holder and cooled to 4.2 K in a Janis Model 8-DT Super Vari-Temp liquid helium cryostat described in detail in SECTION I.

Experimental Techniques

Absorption spectra of the PS II complex were obtained with a Bruker IFS 120 HR Fourier-transform Visible-IR spectrometer operating at a resolution of either 2 or 4 cm⁻¹. In

the earlier experiments described in PAPER IV, transient hole spectra were measured with a 1 m monochromator (McPherson, Model 2061) with a experimental setup shown in Figure 1 at a spectral resolution of 2 cm^{-1} . In this setup the probe source was a Xenon model 437 B nanopulser ($\sim 25 \text{ ns}$ pulse width) whose output was focused and passed through a 2 mm aperture at the sample. The transmitted beam from the nanopulser was passed through the monochromator and detected with a Tracor Northern TN-6134 intensified gateable diode array comprised of 1024 diodes spanning a spectral window of $\sim 12 \text{ nm}$. Gated detection was accomplished using a Lambda Physik EMG-97 zero-drift control to synchronize the sync out pulse from a Lambda Physik excimer laser (vide infra) to within a few nsec of the laser pulse. A Berkeley Nucleonic Corporation model 8010 pulse generator was used to synchronize the probe pulse with the observation window of the optical multichannel analyzer (Tracor Northern TN-6500). A second delay generator (ORTEC model 416A) was used to simultaneously delay the probe pulse and the gate of the OMA relative to the laser pulse. The gate width of the OMA was set at $\sim 30 \text{ ns}$ using an Avtech model AVL-TN-1 high voltage pulse generator. Control spectra were routinely obtained to ensure that laser light scatter did not provide spectral artifacts. The transient spectra reported are averages of 10 scans of the diode array with 10 seconds per scan.

An excimer (Lambda Physik EMG 102) pumped dye laser (Lambda Physik FL-2002) was utilized with a linewidth of 0.2 cm^{-1} and pulse width of 10 ns for transient hole burning. Oxazine 720 was used as the dye. The excimer laser (XeCl) was operated at a repetition rate of 15 or 50 Hz. Pulse energies were $\sim 2 \text{ mJ}$ with the pump beam focused to a rectangular spot of area 0.3 cm^2 .

In the later experiments which are presented in PAPER V and PAPER VI, the Bruker

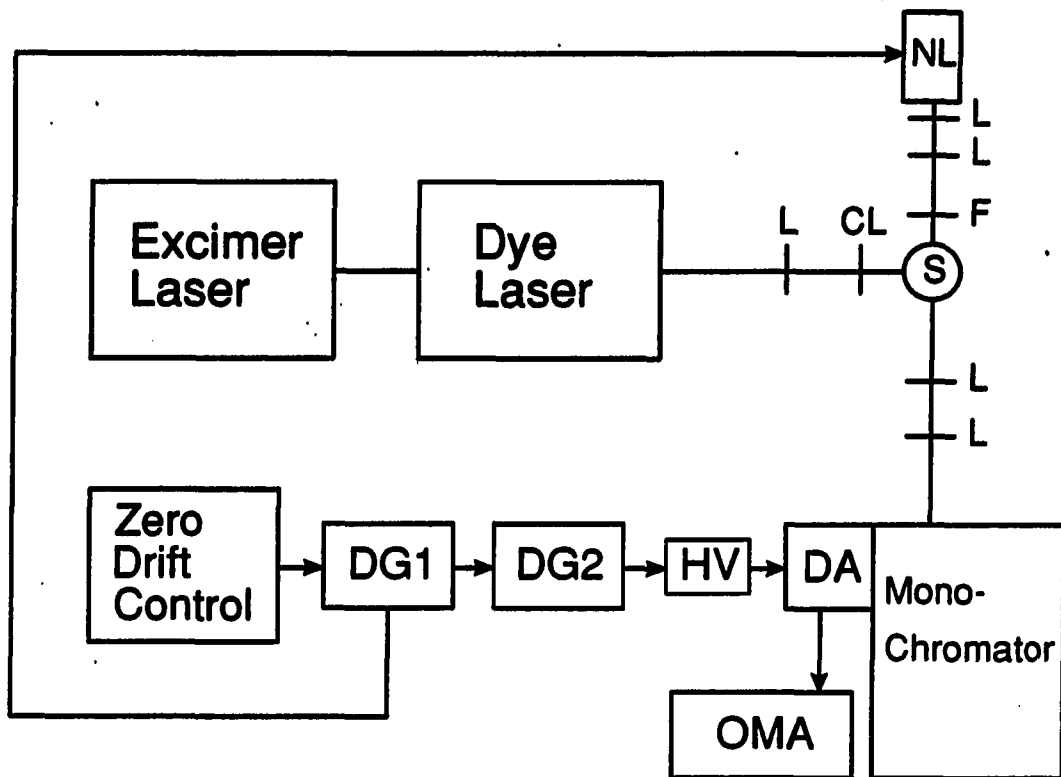
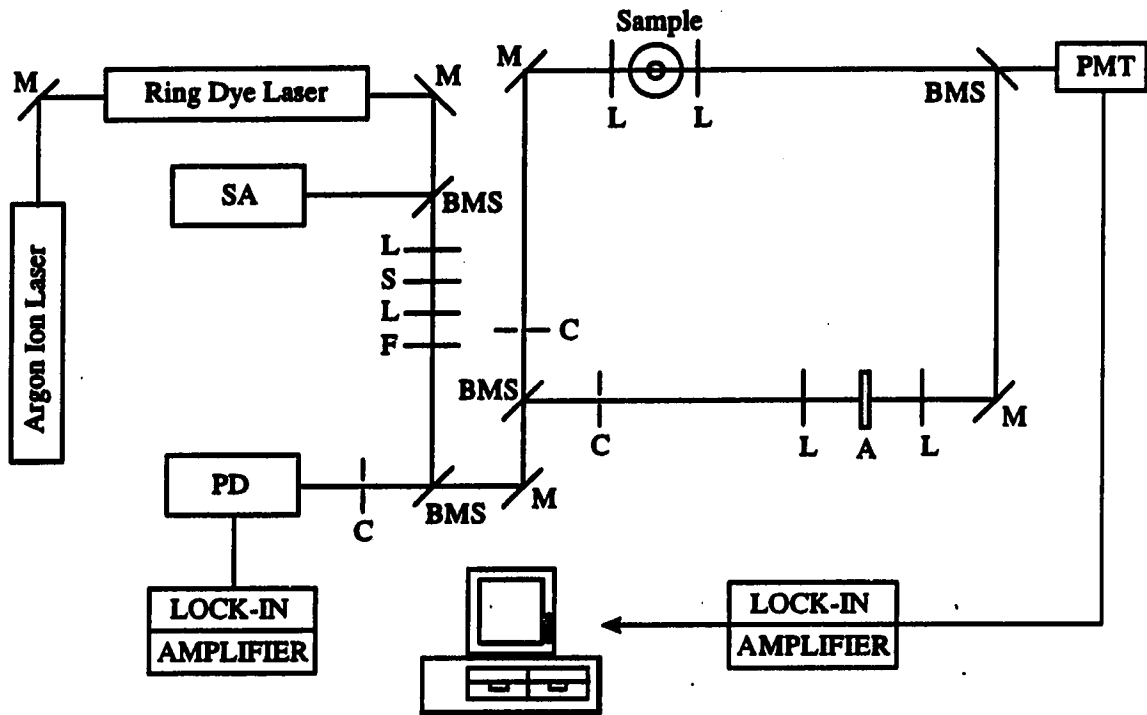


Figure 1. Block diagram of the transient hole-burning experiment showing excimer laser, dye laser, liquid helium cryostat (C), sample (S), monochromator, Zero-drift Control, delay generators (DG1, DG2), high voltage switch (HV), Diode Array (DA), Optical Multichannel Analyzer (OMA), Nanopulse lamp (NL), cylindrical focusing lens (CL), filters (F) and focusing lenses (L)

IFS 120 HR Fourier-transform Visible-IR spectrometer was utilized at resolutions from 0.1 to 4 cm^{-1} . The transient P680* hole burned spectra were obtained by subtracting the laser-on from the laser-off spectrum after the persistent hole spectrum had been saturated. The interference due to the laser light scatter was readily identifiable since it appeared as a sharp spike relative to the sharpest P680 feature observed and could be easily corrected.

A Coherent 699-21 ring dye laser (DCM dye) pumped by an Innova 90-5 argon ion laser was used for the CW persistent hole burning studies. The linewidth of the laser was $\sim 0.07 \text{ cm}^{-1}$.

In the study of energy transfer in the PS II RC complex at the presence of Triton X-100, it was necessary to operate the ring dye laser in a much narrower width. Such narrow linewidth ($<0.002 \text{ cm}^{-1}$) was achieved with two low finesse intra-cavity etalons having free spectral ranges of 10 GHz and 100 GHz in combination with a birefringent filter ($\sim 380 \text{ MHz}$). The output of the ring laser was monitored for single frequency operation by directing a portion of the laser beam to a confocal spectrum analyzer (Spectra-Physics Model 470-40, FSR= 8 GHz). The output of the spectrum analyzer was displayed on an oscilloscope. The laser wavelength was roughly determined by a 1/3 m monochromator (McPherson Model 218). Laser powers were set using a variable attenuator and neutral density filters. Part of the attenuated beam was modulated by a mechanical chopper (PAR Model 125) and monitored for intensity with a photodiode and lock-in amplifier (PAR Model 124 with a Model 118 preamplifier). The remaining portion of the beam was then directed to a double beam spectrometer and split into sample and reference beams by an beam-splitter. Both beams are modulated at different frequencies with two separate mechanical choppers (Laser Precision Model CTX-534). After attenuating the reference beam for compensating the losses caused



BMS: Beam Splitter
C: Chopper
L: Lens
M: Mirror
PD: Photodiode
PMT: Photomultiplier tube
S: Shutter
SA: Spectrum Analyzer
F: Filters
A: Attenuator

Figure 2. Experimental setup for the single-frequency scan experiment

in the sample beam by scattering from the cryostat and sample, two beams were recombined and sent to a cooled photomultiplier tube (RCA C31034 in a PFR PR-1400-RF thermoelectrically cooled housing). The signal was then detected by two lock-in amplifiers (Ithaco Model 97EO). The output from the lock-in amplifiers was integrated and digitized with an integrator/coupler (Ithaco Model 385EO-2) and interfaced to a microcomputer (Digital Equipment Corporation Micro PDP-11/23+ with RT-11 operating system). The computer is also used to drive the scanning of the ring dye laser. To resolve the persistent zero-phonon holes associated with the accessory Chl *a* for TX-containing samples it was necessary to probe the profiles in transmission by scanning the dye laser over 30 GHz (maximum scanning range of the ring dye laser by an intra-cavity angle tuned brewster plate). The probe intensity was reduced 3-4 orders of magnitude lower than the burn intensity in order to eliminate hole burning during the scan. Data collected were then transferred to a 20 MHz IBM compatible 386 computer with a 10 MHz 287 math coprocessor for analysis as described in Section I.

**PAPER IV. TRANSIENT AND PERSISTENT HOLE BURNING OF REACTION
CENTER OF PHOTOSYSTEM II**

**TRANSIENT AND PERSISTENT HOLE BURNING OF
THE REACTION CENTER OF PHOTOSYSTEM II**

**Deming Tang, Ryszard Jankowiak, Gerald J. Small
and Michael Seibert**

Journal of Physical Chemistry, 1989, 93, 1649

ABSTRACT

Transient hole burned spectra for the primary donor state, P680*, of the photosystem II (PS II) reaction center (RC) are reported. The RC complex was prepared by a modification of the Nanba and Satoh procedure. The P680* hole profile at 4.2 K consists of a weak but relatively sharp zero-phonon hole (width 5-6 cm^{-1}) superimposed on a broad hole (width $\sim 130 \text{ cm}^{-1}$). This structure is successfully analyzed using the theory of Hayes and coworkers for hole burning in the presence of arbitrarily strong linear electron-phonon coupling. The zero-phonon hole width yields a decay time for P680* of $1.9 \pm 0.2 \text{ ps}$ at 4.2 K. Persistent spectral hole burning is also reported for the accessory pigments of PS II RC that absorb in the near vicinity of P680. In contrast with the hole spectra of P680*, which are characterized by strong linear electron-phonon coupling, the persistent hole spectra are characterized by weak coupling (strong zero-phonon hole and weak phonon sideband hole).

INTRODUCTION

The photosystem II (PS II) reaction center (RC) of plants and the RC of purple bacteria appear to share structural and functional similarities [1,2]. For example, nucleotide and amino acid sequence homology exists between the D1 and D2 protein subunits of the PS II RC and the L and M subunits of the bacterial reaction center. Recently, Nanba and Satoh [3] isolated a complex from PS II that contains only D1, D2 and cytochrome *b*-559 proteins. This preparation binds 4-5 Chl *a* molecules, 2 pheophytin *a* (Pheo) molecules and a single *b*-carotene molecule. Immunological characterization [4,5] and other data [3,5,6] have confirmed the identification of the D1 and D2 proteins as the RC of PS II. Although this RC has yet to be crystallized, the crystal structures for the RC of *Rhodospseudomonas viridis* (*Rps. viridis*) [7-9] and *Rhodobacter sphaeroides* (*Rb. sphaeroides*) [10,11] have been determined. The structures reveal that, in the RC, two pigment branches (related by an approximate C₂-rotation axis) extend from the special bacterialchlorophyll (BChl) pair (P), each containing a BChl monomer (B) in closest proximity to P followed by a bacteriopheophytin (H) monomer and a quinone (Q) molecule. In the Nanba and Satoh preparation, the quinone acceptors are absent (not bound). The above structure determinations have stimulated an even greater activity directed towards understanding the primary charge separation process which leads to the production of the excited state | P⁺BH⁻ >* associated with the active L protein branch [12,13]. Very recently, ~ 100 fs resolution experiments have led to a complete characterization of the temperature dependence for the primary charge separation kinetics for *Rps. viridis* and *Rb. sphaeroides* [14,15]. However, no direct time

domain or frequency domain data that characterize such kinetics for the RC of PS II have been reported at any temperature.

In this paper we present transient spectral hole burning data for the primary electron donor state of PS II RC which determine its decay time at 4.2 K and the protein reorganization energy associated with its optical excitation from the ground state. By convention, the primary donor state is referred to as P680* (P680 denoting the pigment that absorbs at 680 nm). The primary charge separated state of PS II will be denoted in this work as $|P680^+ Pheo^- \rangle^*$. The transient hole burned spectra for P680* will be compared with those obtained very recently [16,17] for the primary donor state of *Rps. viridis*, P960* (P again denoting pigment rather than pair). For appropriate burn wavelengths the P960* spectra exhibit a four hole structure at 4.2 K (including a zero-phonon hole (ZPH) with a width of $\sim 10 \text{ cm}^{-1}$) [16,17]. Further discussion of the spectra are presented later but we note that the spectra establish that two excited states, $|X \rangle^*$ and $|Z \rangle^*$, contribute significantly to the P960 absorption profile. The lower energy (by $\sim 300 \text{ cm}^{-1}$) state is $|X \rangle^*$ and it is this state with which the ZPH is associated. The data were shown to be consistent with a model in which $|X \rangle^*$ and $|Z \rangle^*$ are viewed as adiabatic states resulting from strong exchange coupling between P^* (lowest excited state of the special pair) and $|P^+B^-H \rangle^*$ associated with the active L branch [12,13]. $|X \rangle^*$ was assigned as the precursor state in the formation of $|P^+BH^- \rangle^*$.

The P680* hole spectra are shown here to bear a striking resemblance to those associated with the $|X \rangle^*$ state of P960 and are characterized by a weak ZPH, which possesses a width of $5\text{-}6 \text{ cm}^{-1}$, superimposed on a more intense hole (width $\sim 130 \text{ cm}^{-1}$). The P680* hole spectra are analyzed in terms of the theory of Hayes and coworkers [18,19]

developed for hole burning in the presence of arbitrarily strong linear electron-phonon coupling and large site inhomogeneous line broadening. Earlier transient hole burning studies on P680* by Vink and coworkers [20] led only to the identification of the broad hole. Their experimental setup precluded observation of the ZPH due to interfering laser light scatter. Companion time domain experiments were inconclusive [20] concerning the kinetics of primary charge separation. However, the possibility that the broad hole associated with P680* is a manifestation of strong linear electron-phonon coupling, as discussed in refs. 18 and 19, was raised [20].

In this paper, an experimental transient hole burning apparatus, which eliminates background interference due to scattered laser light and fluorescence, is described and shown to provide transient hole spectra for P680 possessing a high S/N ratio at a resolution of 2 cm^{-1} . This experimental system allowed for the identification of a persistent hole burning contribution from the accessory pigments (not to be confused with residual antenna pigments) belonging to the PS II RC complex. Data for the persistent hole burning obtained with a CW burn laser are also presented and discussed.

EXPERIMENTAL

Preparation of the PS II Reaction Center Complex

The RC complex of PS II was prepared from spinach PS II membrane fragments [21,22] by a modification of the Nanba and Satoh procedure [3] since the RC obtained by their procedure is rather unstable (see ref. 23 and 24 for details). PS II membranes were solubilized in 4% Triton X-100, 50 mM Tris-HCl (*pH* 7.2) for 1 hour with stirring. The material was then centrifuged for 1 hr at 100,000 x g, and the resultant supernatant was loaded onto a TSK DEAE-650S (Supelco, Bellefonte, PA) column pre-equilibrated with 50 mM Tris-HCl (*pH* 7.2), 30 mM NaCl, and 0.05% Triton X-100. The column was then washed with the same buffer until the eluent was colorless, and the RC fraction was eluted with a 30 to 200 mM NaCl gradient containing 50 mM Tris-HCl (*pH* 7.2) and 0.05% Triton. Reaction Centers were immediately concentrated by precipitation with poly(ethylene) glycol (PEG) at this point [23,24]. PEG (32.5% wt/vol; MW = 3300) was added slowly and dispersed with a soft paintbrush. After 90 min incubation, the suspension was centrifuged at 31,300 x g for 15 min. The pellet was resuspended in 50 mM Tris-HCl (*pH* 7.2) with no detergent and then centrifuged again at 1,100 x g for 90 s to pellet mostly colorless material containing PEG aggregates. The pellet material was discarded, and the RC fraction was stored at -80°C until use. All above manipulations were done at 4°C in the dark.

It should be noted that the experiments which led to the results presented here were preceded (by several months) by hole burning studies of PS II RC complexes prepared by the

original Nanba and Satoh procedure. The results of those experiments are in essential agreement with those presented here. Different aliquots from the sample of the stabilized preparation yielded identical results.

Measurements

Reaction center samples for spectroscopy (90 mg Chl/ml) were unfrozen in dim light, and 0.04% Triton X-100 (final concentration) was added immediately to keep the material from aggregating [24]. Samples, to which glycerol was added (buffered, dilution factor H10), were placed rapidly into polystyrene centrifuge tubes (path length ~ 1 cm) and cooled immediately to 4.2 or 1.6 K in a Janis model 8-DT Super Vari-Temp liquid helium cryostat. Absorption spectra of the PSII complex were obtained using a Bruker IFS 120 HR Fourier transform spectrometer operating at a resolution of 2 cm^{-1} . The absorbance at 680-682 nm was typically ~ 0.2 .

Transient hole spectra were measured with a 1-m focal length McPherson 2061 monochromator ($F=7.0$) at a spectral resolution of 2 cm^{-1} . The probe source was a Xenon model 437 B nanopulser (~ 25 ns pulse width) whose output was focused and passed through a 2 mm aperture at the sample. To avoid photo-induced damage of the sample during the course of a run, appropriate optical density and cut-off filters were utilized. The transmitted beam from the nanopulser was passed through the monochromator and detected with a Tracor Northern TN-6134 intensified gateable diode array comprised of 1024 diodes spanning a spectral window of ~ 12 nm. Gated detection was accomplished using a Lambda Physik EMG-97 zero-drift control to synchronize the sync out pulse from a Lambda Physik excimer

laser (vide infra) to within a few nsec of the laser pulse. A Berkeley Nucleonic Corporation model 8010 pulse generator was used to synchronize the probe pulse with the observation window of the optical multichannel analyzer (Tracor Northern TN-6500). A second delay generator (ORTEC model 416A) was used to simultaneously delay the probe pulse and the gate delay of the OMA relative to the laser pulse. The transient spectra reported here are due to a population bottleneck state which has been suggested to be the triplet state of the primary electron donor [25]. Data presented in ref. 25 indicate that the bottleneck state has a decay constant of roughly 20 s^{-1} . Typical gate delay times (relative to the laser pulse) used in the present work were in the range 1 to 100 ms (longest delay time for the apparatus). Thus, the decay kinetics of the above bottleneck state could not be studied with our transient apparatus. The gate width was set at $\sim 30 \text{ ns}$ using an Avtech model AVL-TN-1 high voltage pulse generator. Control spectra were routinely run to ensure that laser light scatter did not provide spectral artifacts. The above gated detection and OMA system allowed for automatic subtraction of fluorescence from the transient spectra. The transient spectra reported are averages of 10 scans of the diode array, 10 sec/scan.

An excimer (Lambda Physik EMG 102) pumped dye laser (Lambda Physik FL-2002) was utilized with a linewidth of 0.2 cm^{-1} and pulse width of 10 ns for transient hole burning. Oxazine 720 was used as the dye. The excimer laser (XeCl) was operated at a repetition rate of 15 or 50 Hz. Pulse energies were $\sim 2 \text{ mJ}$ with the pump beam focused to a rectangular spot of area 0.3 cm^2 .

A Coherent 699-21 ring dye laser (DCM dye) pumped by an Innova 90-5 argon ion laser was used for the CW persistent hole burning studies. The linewidth of the laser was

~ 0.07 cm⁻¹. Pre-burn and hole burned spectra were read using the aforementioned Fourier-transform spectrometer operating at resolution of 0.1 cm⁻¹.

RESULTS

Figure 1 shows the 4.2 K absorption spectrum (Q_y region) of the PS II RC. At this temperature the absorption maximum and low energy shoulder were consistently observed to occur at ~ 671 and ~ 680 nm, in agreement with the findings of van Dorssen et al. [26]. The clear resolution at 4.2 K of the shoulder due to P680 is the result of a significant red shift of P680 (relative to the Q_y transitions of the accessory pigments) with decreasing temperature which is comparable to those observed for the primary donor states of *Rps. viridis* [19,27] and *Rb. sphaeroides* [19,27]. The Q_y transitions of the primary electron donor, accessory Chl, and Pheo pigments all lie within the 420 cm^{-1} broad absorption profile of Fig. 1. Thus, the interpretation of this spectrum represents a more formidable challenge than for those of the RC for *Rps. viridis* and *Rb. sphaeroides* which display accessory pigment Q_y absorptions which are resolved from the primary donor state absorption. Data presented later show that a considerable fraction of the absorption at ~ 680 nm is due to P680. However pigments, other than the Chl *a* of P680, also contribute to the absorption at 680 nm.

Transient photochemical hole burned spectra have been obtained for a large number of burn wavelength (λ_B) values located in the low energy side of the absorption profile. Transient hole spectra were obtained in transmission as the difference of spectrum a (laser blocked) and spectrum b (laser unblocked). To determine whether persistent changes in the absorption spectrum occurred in the course of obtaining the a - b hole spectrum, a third spectrum c (laser blocked) was routinely obtained after the a - b spectrum was acquired. For each λ_B value a fourth spectrum d (laser unblocked, probe blocked) was also acquired to

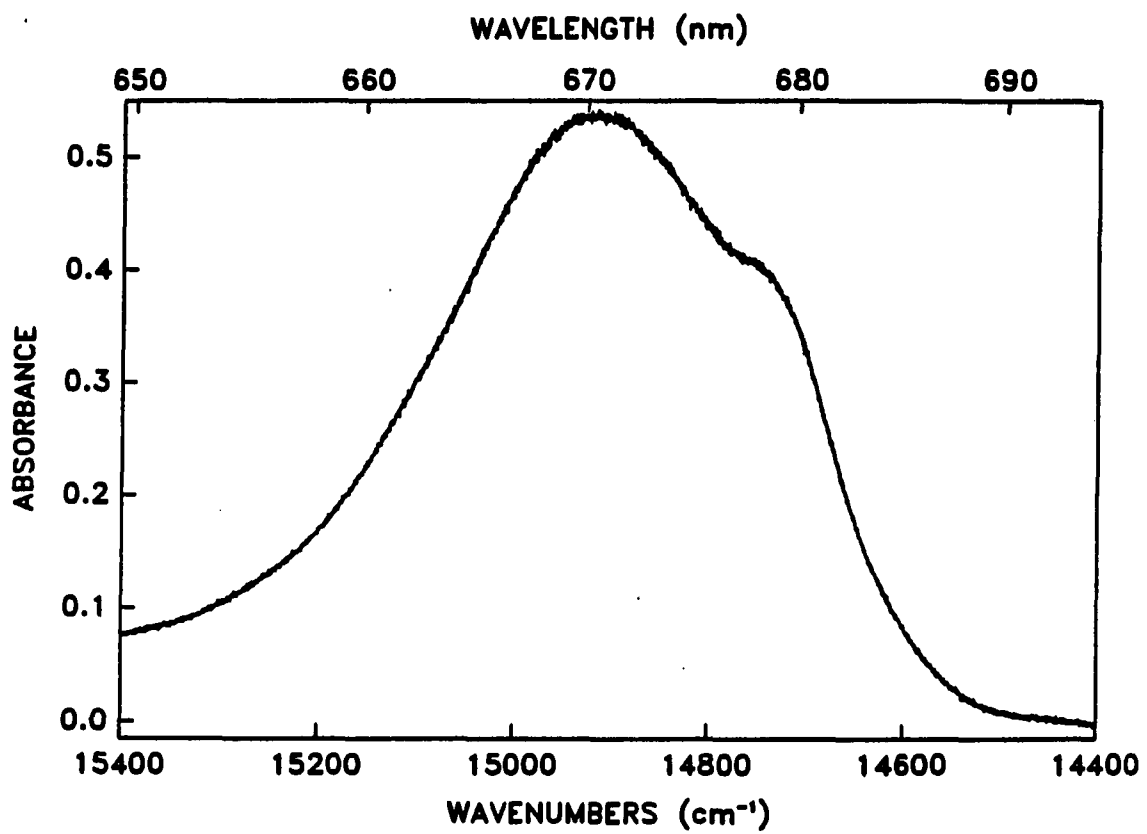


Figure 1. Absorbance spectrum of the Q_y region of the PSII RC at T = 4.2 K

ensure that sharp features in the a-b or c-b spectra were not artifacts due to laser scatter.

Transient difference spectra obtained with $\lambda_p = 680.9$ nm are shown in the upper two traces of Fig. 2. Spectra 1 and 2 correspond to a-b and c-b, vide supra. The a-b transient hole burned (THB) spectrum, however, is contaminated by a contribution from persistent hole burning (PtHB) as will become clear shortly. The PtHB interferes mainly with the transient ZPH, evident in the a - b (1) spectrum. In view of the protocol discussed above, it might be concluded that the c - b spectrum represents the "true" THB spectrum. However, this would be the case only if spontaneous hole filling of the persistent hole (in particular the ZPH) did not occur to a significant extent during the time interval between the recording of the b and c spectra. Such filling or filling due to white light irradiation are well-known phenomena associated with PtHB of chromophores imbedded in amorphous host media [28,29]. Trace 3 of Fig. 2 is the a - c spectrum, equivalent to spectrum 1 - spectrum 2. Trace 3 represents the PtHB spectrum and features a ZPH possessing a width of ~ 2.5 cm^{-1} (instrument limited) which is about half the width of the ZPH in spectra 1 and 2. It is apparent that the PtHB spectrum does not possess the broad (~ 130 cm^{-1}) hole on which the ZPH in spectra 1 and 2 is superimposed. The PtHB spectrum is similar to those recently observed for Chl a in the antenna complex of PSI [30,31]. Our preliminary studies of the rates of persistent ZPH filling indicate that filling occurs to a significant extent (roughly 20%) during the time scale of the experiment (~ 4 min). Thus, with the procedure used to obtain the c-b spectrum (2) of Fig. 2, it was not possible to exclude contamination of the transient ZPH by the persistent ZPH. Before presenting a methodology which circumvents this interference, some illustrative PtHB spectra obtained with the CW dye laser are presented.

In Fig. 3, spectra obtained with $\lambda_p = 682.05$ nm at 1.6 K are shown for two laser

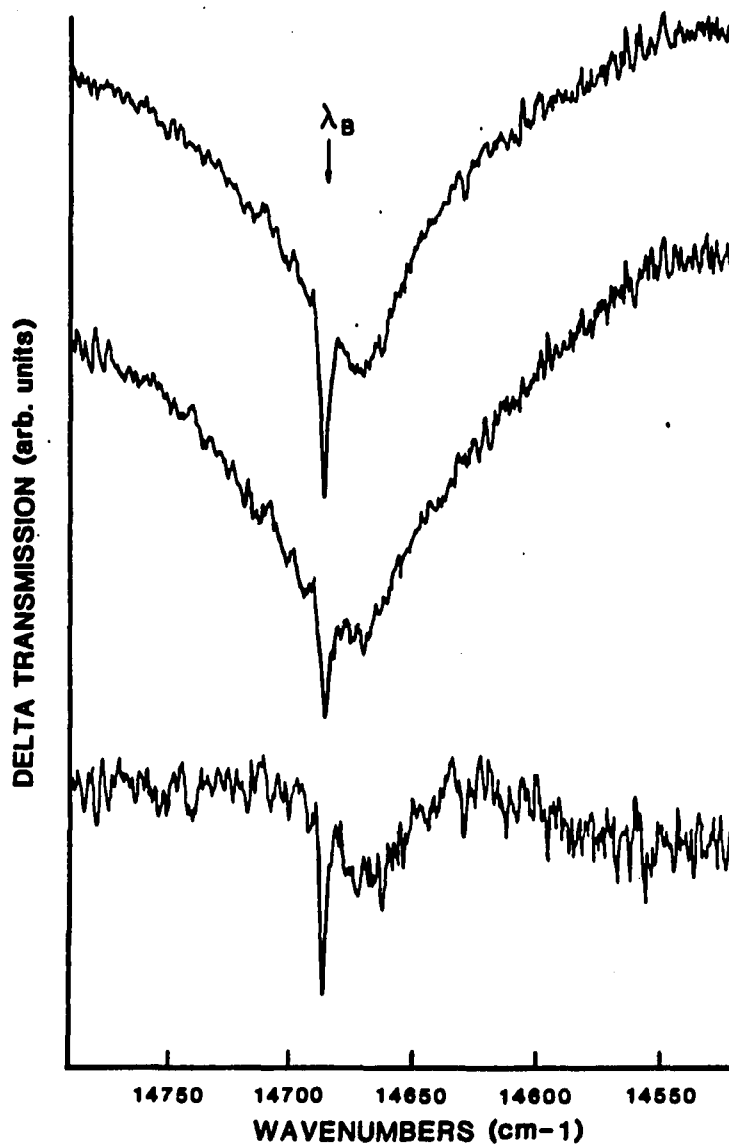


Figure 2. Transient (traces 1 and 2) and persistent (trace 3) hole burned spectra of the RC of PSII. Spectra were obtained for $\lambda_B = 680.9$ nm (laser repetition rate 50 Hz) at $T = 4.2$ K. Read resolution ~ 2 cm^{-1} . 1: (a-b); 2: (c-b) and 3: (a-c) or (1-2). Persistent hole spectrum (trace 3) was scaled by a factor of ~ 3.7 to reveal more details

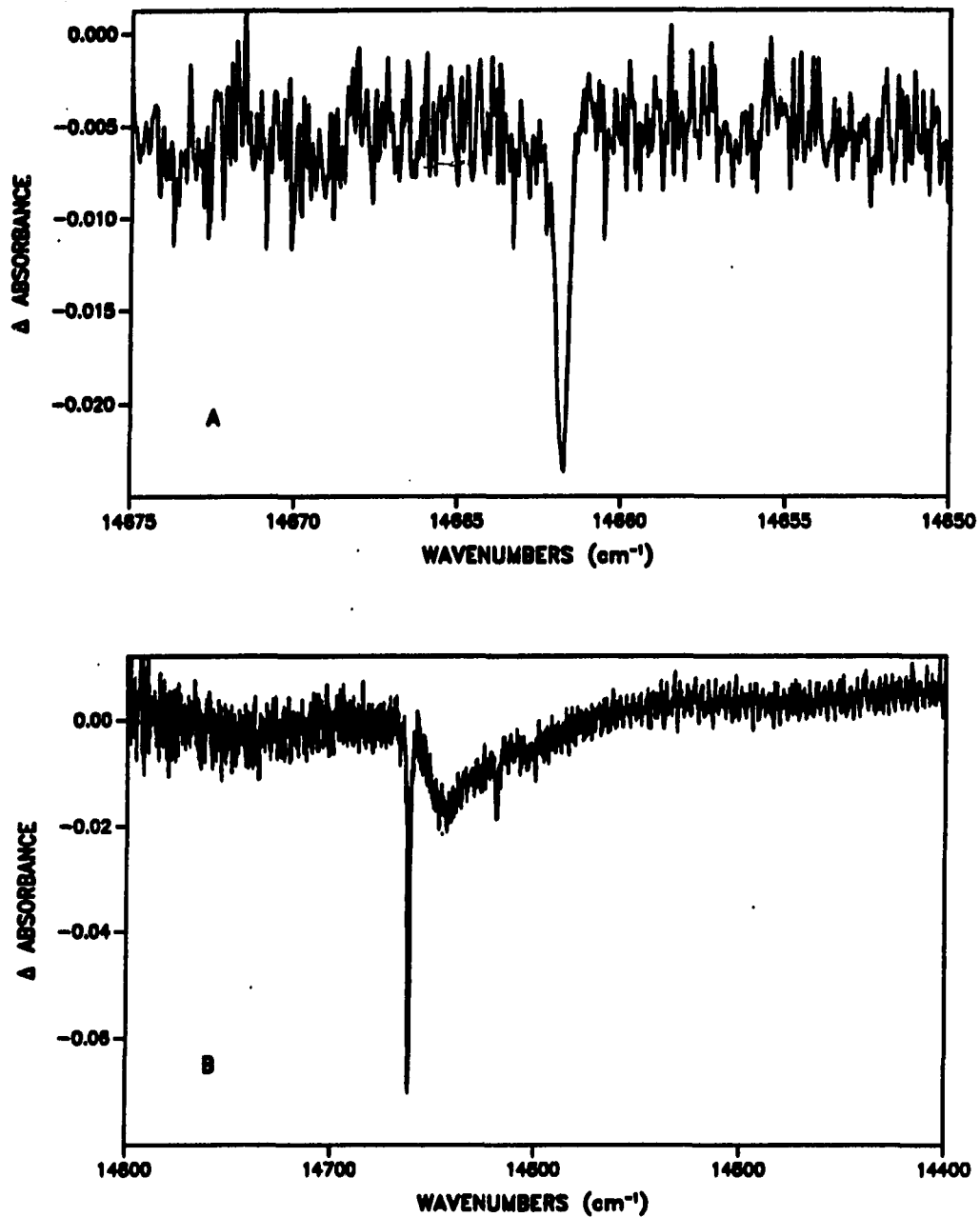


Figure 3. Scans of the persistent holes burned in P680 band (read resolution 0.07 cm^{-1}). Unsaturated hole for A and saturated hole for B were obtained with $\lambda_B = 682.05 \text{ nm}$ at 4.2 K . Burn conditions are 2 min irradiation with 3.3 mW/cm^2 (A); and 16 min irradiation with 120 mW/cm^2 . Hole widths are 0.43 cm^{-1} and 1.1 cm^{-1} , respectively. Percent ΔOD changes are 10% (A) and 30% (B). The pre-burn OD at λ_B was 0.2

fluences. Spectrum A (lower fluence) is dominated by a ZPH which possesses a width of 0.43 cm^{-1} . Spectrum B shows the ZPH burned to saturation. The percent change in OD of the ZPH in spectrum B is $\sim 30\%$. To the right of the ZPH, a pseudo-phonon sideband hole [32,33] due to phonons of frequency $\sim 20 \text{ cm}^{-1}$ is evident. Phonon sideband holes of about this frequency have been observed for Chl *a* in the core antenna complex of PS I [30] and for Chl *a* and *b* in the antenna complex of PS I-200 [31]. Persistent holes can not only be produced in the P680 region but also over a wide range of λ_B values spanning the absorption profile in Fig. 1. To illustrate this, a PtHB spectrum obtained with $\lambda_B = 668.1 \text{ nm}$ is presented in Fig. 4.

Returning now to the problem of the interference of the transient ZPH by the persistent ZPH, we note that recent spontaneous hole filling studies of persistent holes in glassy hosts indicate that such filling is characterized by a slower initial rate (percent filling per unit time) for holes that are saturated [34]. This interesting result, which may have its origin in dispersive kinetics, suggested that, prior to the acquisition of spectrum a, the sample should be burned at λ_B with a fluence sufficiently high to ensure that the persistent hole due to the accessory pigments (not P680) is saturated. Subsequently, the protocol used to obtain the results of Fig. 2 would be followed. The results obtained with $\lambda_B = 682.4 \text{ nm}$ are given in Fig. 5. The key observation to be made is that the *c* - *a* (3) trace is devoid of hole structure. This proves that no significant filling of the PtHB spectrum has occurred in the time interval between the acquisition of spectrum a and c. As a consequence, one can confidently assign the upper two (identical) spectra to transient photochemical hole burning of photoactive P680. Based on these spectra and others not shown, the transient ZPH width is $5\text{-}6 \text{ cm}^{-1}$. The ZPH always appeared superimposed on a far more intense and broad ($\sim 130 \text{ cm}^{-1}$) hole.

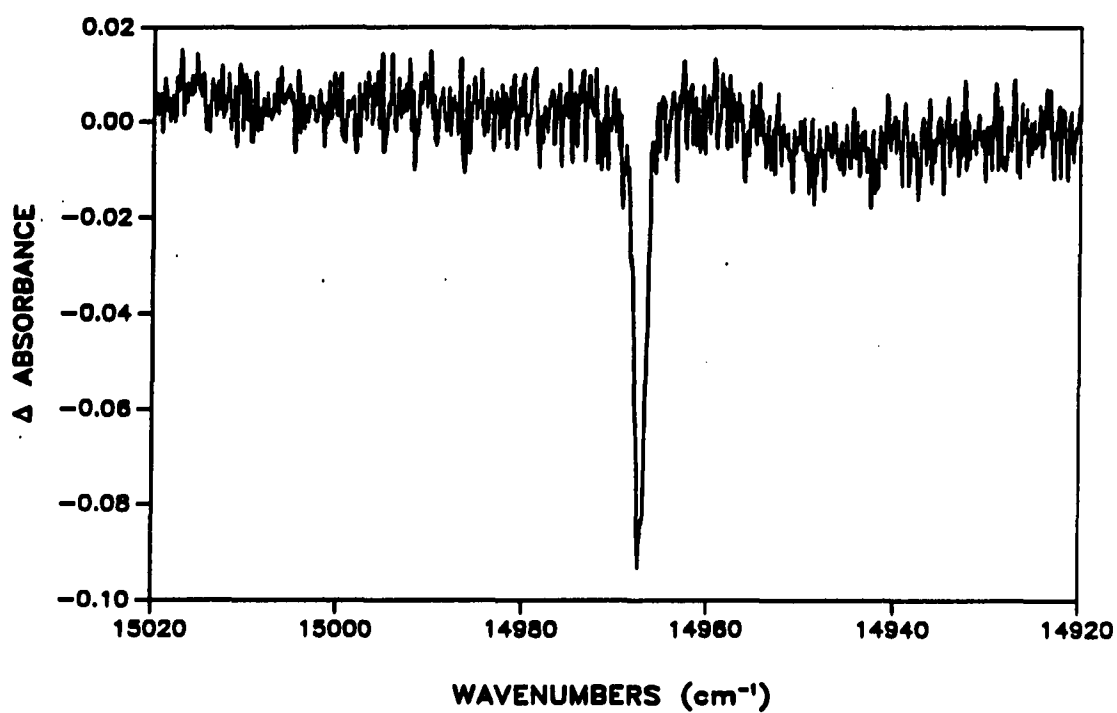


Figure 4. Persistent hole on the high energy side of the 671 nm band obtained with $\lambda_B = 668.1$ nm at 4.2 K. Burn conditions: 10 min irradiation with 400 mW/cm^2 . Width of the hole is ~ 1.2 cm^{-1} and ΔOD change is $\sim 20\%$. The pre-burn OD at λ_B was 0.5

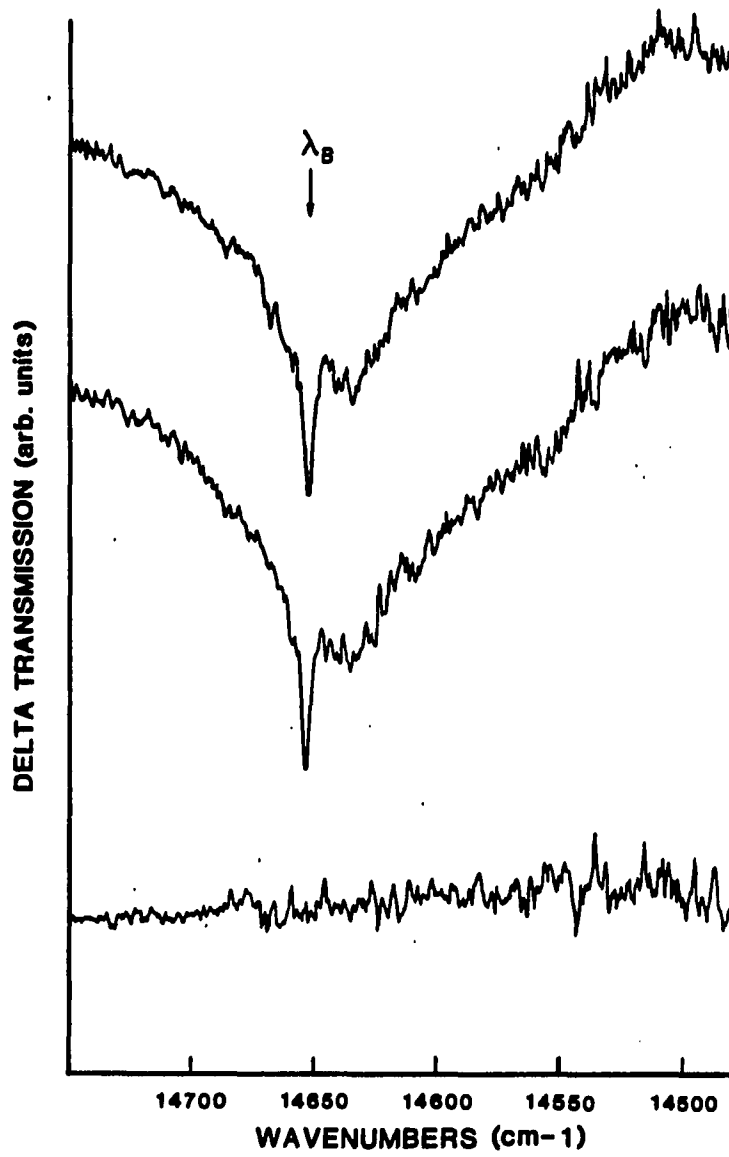


Figure 5. Transient hole burned spectra (traces 1 and 2) of the RC of PSII obtained at 4.2 K with $\lambda_B = 682.4$ nm (laser repetition rate 15 Hz). Trace 1: (a-b), trace 2: (c-b). Note that no persistent hole is present on trace 3, see text

DISCUSSION

This section will focus mainly on the transient hole spectra in the vicinity of 680 nm. We begin, however, with a brief discussion of the persistent holes. The ZPH/pseudo-phonon side hole structure seen in Fig. 3B and Fig. 4 is similar to that observed for Chl *a* in the core antenna complex of PS I [30] and for Chl *a* and *b* in PS I-200 [31]. For the latter two systems, the linear electron-phonon coupling strength associated with the Q_y transition of Chl *a* has been determined to be weak with S (Huang-Rhys factor) ~ 0.8 [30,31]. From a comparison of the spectra given here with those of ref. 31, one can conclude that the coupling is also weak ($S < 1$) for the Q_y transitions of the pigments responsible for the persistent holes of PS II RC. In contrast, the coupling for P680* to phonons is considerably stronger; vide infra. For the antenna systems of PS I, the mechanism for persistent hole burning is nonphotochemical [29], as proven in ref. 30 and 31. This may also be the case for the RC of PS II but further experiments are required to determine whether this is so.

In the transient experiments on PS II, it has been observed that the contribution of the persistent hole structure to the transient spectrum increases as λ_B is decreased from H681 nm (data not shown). This and the weak coupling suggest that the persistent structure is due to the accessory Chl *a* and Pheo *a* pigments. As noted earlier, there is uncertainty as to whether the RC preparation contains 4 or 5 Chl *a*. If the RC pigment composition (Chl, Pheo) is identical to that of bacterial RC, a Chl *a* content of 5 would indicate the presence of an antenna Chl *a* in the preparation. The antenna Chl *a* could be expected to contribute to the

persistent hole burning. However, spectra of the type (saturated) shown in Fig. 3B, together with a consideration of the Huang-Rhys factor, lead to the conclusion that more than 50% of the pigments (not associated with P680), whose zero-phonon transition frequency is coincident with λ_B , undergo hole burning. Thus, the PiHB must, to a significant extent, be associated with the accessory Chl *a* and Pheo *a* which belong to the RC. Preliminary persistent vibronic satellite hole burning studies with $\lambda_B = 630.1$ nm have identified excited state intramolecular modes at 745, 980, 1060 and 1170 cm^{-1} . Although these frequencies are in reasonable agreement with those observed for Chl *a* of PS I-200 [31], more detailed satellite hole studies are required before mode assignments for Chl *a* and Pheo *a* can be made. Finally, it was noted earlier that the observed widths for the persistent ZPH are ~ 0.4 cm^{-1} . Higher resolution measurements in the short burn time and low intensity limits may lead to narrower widths [35-37]. In refs. 30 and 31, ZPH widths of ~ 0.02 - 0.04 cm^{-1} were reported for antenna Chl *a* (1.6 K). A ZPH width of 0.03 cm^{-1} , when viewed as due to population decay, corresponds to a decay time of ~ 300 ps. However, one might expect widths broader than 0.03 cm^{-1} for accessory pigments of the RC if they efficiently transfer their excitation energy to P680 at 1.6 K.

Turning now to the transient hole burned spectra, we assign the broad hole (FWHM ~ 130 cm^{-1}) apparent in the upper two traces of Figs. 2 and 5 to P680* [26]. This assignment is in accord with the assignment made by Vink and coworkers [20] on the basis of their transient hole burned spectra; cf. Introduction. Because of the transient nature of the ZPH in Fig. 5 and other factors to be discussed, we also assign the ZPH to P680*. We note that the transient ZPH could not be observed when λ_B was tuned much lower than 680 nm, e.g., to ~ 675 nm. Furthermore, the frequency of the maximum of the broad hole generally depends

on λ_B , Figs. 2 and 5. Spectra not given here show that as λ_B is reduced below ~ 680 nm, the broad hole undergoes further broadening. For example, with $\lambda_B = 678.4$ nm its width is ~ 150 cm^{-1} . Under the appropriate conditions the above characteristics are precisely those predicted by Hayes and co-workers [18,19] who developed a theory for hole burning in the presence of arbitrarily strong linear electron-phonon coupling and site inhomogeneous line broadening, Γ_{inh} . In its simplest form the theory requires for calculation of the hole spectrum knowledge of Γ_{inh} , S (Huang-Rhys factor), the mean phonon frequency (ω_m), the width of the one-phonon profile (Γ) and the homogeneous linewidth for the zero-phonon optical transition (γ). The latter is just half the ZPH width which we determined to be $5\text{-}6$ cm^{-1} . Therefore, $\Delta\gamma = 2.5\text{-}3.0$ cm^{-1} . The S parameter is readily determined from spectra exhibiting a ZPH [19]. For the spectra of Fig. 5 the ratio of the ZPH intensity to the broad hole intensity is $\exp(-2S)$ [which may be viewed as the ZPH Franck-Condon factor], which we measure to be 0.023. This leads to a value of 1.9 for S . The Stokes shift between the absorption and fluorescence maxima of P680* is $2S\omega_m$. Barber et al. [38] have determined that the P680* fluorescence maximum lies at 684 nm at 77 K. Our own measurements yield a value of ~ 685 nm at 4.2 K. The absorption maximum for P680 was determined to lie at 680.3 nm at 4.2 K based on hole burned spectra obtained under non-line-narrowing conditions (e.g., high energy excitation at 630.1 nm) (spectrum not shown). The width of the P680 bleach in these spectra was ~ 170 cm^{-1} . Choosing 680 and 685 nm as the absorption and fluorescence maxima leads to $2S\omega_m \sim 100$ cm^{-1} , which with $S \sim 1.9$ yields a value of ~ 26 cm^{-1} for the mean phonon frequency. This frequency is similar to those observed in the persistent hole structure for PS II RC (Fig. 3B) and for Chl a in the core antenna complex of PS I [30] and in PS I-200 [31]. The 30 cm^{-1} phonons were utilized for the calculation of the hole burned spectra

associated with P700, the primary donor state of PS I [39]. For Γ we choose a value of 25 cm^{-1} , which is consistent with Fig. 3B. Calculated hole spectra for $\Gamma_{\text{inh}} = 120 \text{ cm}^{-1}$ are given in Fig. 6. The three spectra shown were calculated for different values of the burn frequency (ω_B) measured relative to the center of distribution for the zero-phonon excitation frequency. The extent to which the ZPH loses intensity as ω_B is tuned to the blue of the center of this distribution should be noted. This is consistent with the fact that the ZPH could not be observed with $\lambda_B = 675 \text{ nm}$; vide supra. The agreement between the spectrum calculated with $\lambda_B = 25 \text{ cm}^{-1}$ and the observed spectrum in Fig. 5 is reasonable. The low-temperature width of the P680 absorption profile calculated with the parameter values used for Fig. 6 is 180 cm^{-1} , in reasonable agreement with the experimental value of $\sim 170 \text{ cm}^{-1}$; vide supra.

The transient ZPH width of $5\text{-}6 \text{ cm}^{-1}$ is considerably broader than those of the persistent ZPH and is too large to be ascribed to pure dephasing [29]. For these reasons we attribute the $5\text{-}6 \text{ cm}^{-1}$ hole width to population decay of P680* arising from electron transfer. The holewidth (cm^{-1}) is given by $(\pi c \tau)^{-1}$ where τ is the decay time and c is the speed of light. Thus, we determine that $\tau \approx 1.9 \pm 0.2 \text{ ps}$ at 4.2 K . Importantly, this value can be compared with the recent 500 fs resolution time domain data of Wasielewski and coworkers [40] obtained on samples from the same batch used in this work. At ice temperatures these workers have determined that $\tau = 2.6 \pm 0.6 \text{ ps}$ and that the rise time for $| \text{P680}^+ \text{Pheo}^- \rangle^*$ is $3 \pm 0.6 \text{ ps}$. Comparison of the τ values suggests that the temperature-dependence for the primary charge separation process may be slightly weaker than that of *Rb. sphaeroides* which exhibits a factor of ~ 2.5 decrease in τ as the temperature is decreased from room temperature to 10 K [14,15]. At room temperature the decay and appearance times for the primary donor

and charge separated states of *Rb. sphaeroides* are both equal to 2.8 ps [14,15]. The similarity between the primary charge separation kinetics for PS II and *Rb. sphaeroides* and their weak temperature dependence suggest that their structures probably are similar also.

With reference to that part of the Introduction which dealt with the results of recent transient photochemical hole burning experiments on P960 of *Rps. viridis* [16,17], we remark that the hole spectra of $|X\rangle^*$ are strikingly similar to those for P680*. The $|X\rangle^*$ state exhibits a weak ZPH possessing a width of $\sim 10\text{ cm}^{-1}$ (4.2 K) superimposed on a broad hole possessing a width of $\sim 130\text{ cm}^{-1}$. Calculations of the type presented here for P680* have yielded the following parameter values for $|X\rangle^*$ [41]: $S = 2$, $\omega_m = 35\text{ cm}^{-1}$, $\Gamma_{\text{inh}} = 150\text{ cm}^{-1}$ and $\Gamma = 30\text{ cm}^{-1}$. At this stage of refinement the slight differences between these values and those for P680* should not be considered to be significant. The ZPH width of $\sim 10\text{ cm}^{-1}$ for $|X\rangle^*$ yielded a decay time of 1 ps that is, within experimental uncertainty, equal to the time domain measurement of the appearance time for $|P^+BH^-\rangle^*$ at 10 K [14,15]. Preliminary experiments on PS II RC to determine whether the state analogous to $|Z\rangle^*$ of P960 exists have, thus far, been inconclusive. For P960, $|Z\rangle^*$ lies $\sim 300\text{ cm}^{-1}$ higher in energy than $|X\rangle^*$. If this were also the case for PS II (and P680* is the analogue of $|X\rangle^*$), $|Z\rangle^*$ for PS II RC would lie at $\sim 15,000\text{ cm}^{-1}$ which is close to the maximum of the absorption (Fig. 1) to which the accessory pigments contribute significantly. Further experiments designed to determine the existence or nonexistence of $|Z\rangle^*$ in PS II are planned and are obviously important since they speak to the question of whether or not the special pair exists in PS II.

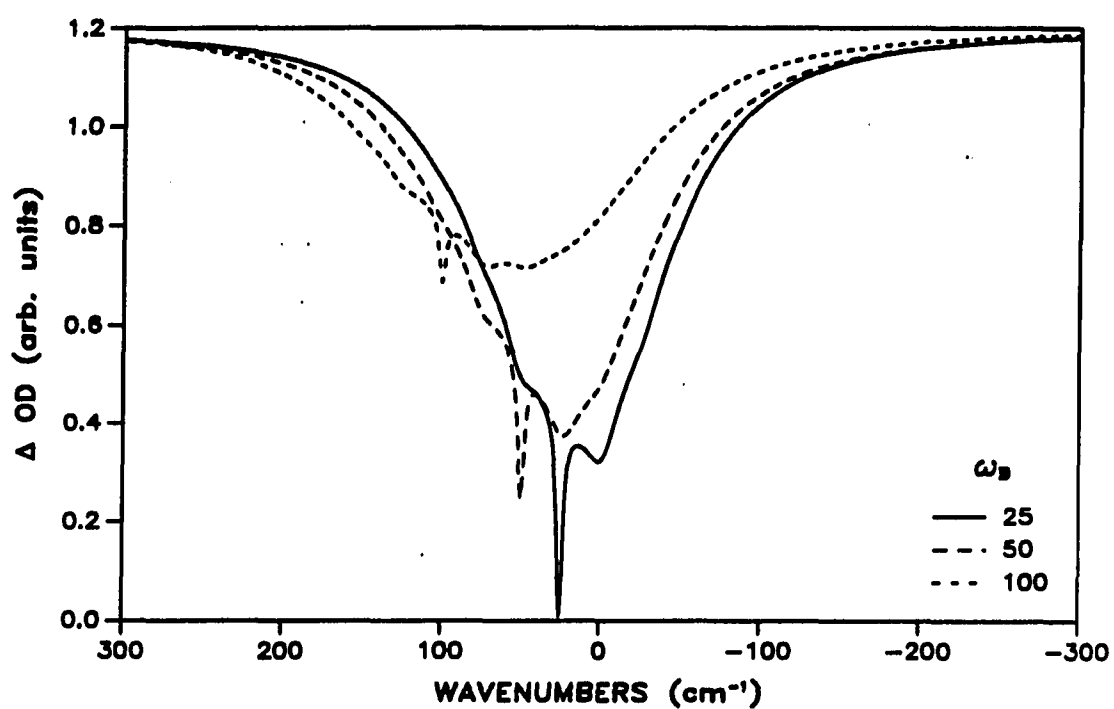


Figure 6. Computed transient hole spectra for $S = 1.9$, $\omega_m = 26 \text{ cm}^{-1}$, $\gamma = 2.5 \text{ cm}^{-1}$, $\Gamma = 25 \text{ cm}^{-1}$ and $\Gamma_{inh} = 120 \text{ cm}^{-1}$. The three spectra shown were calculated for different values of the burn frequencies $\omega_B = 25, 50$ and 100 cm^{-1} measured relative to the center of the distribution for the zero-phonon excitation frequency

CONCLUDING REMARKS

Photosystem II provides the second example (after *Rps. viridis*) for the utility of spectral hole burning for determining the decay time of the primary electron donor state of the RC at liquid helium temperatures. Of course, time domain spectroscopies are more versatile in this regard since they can also probe the appearance of the charge separated state, e.g., $|P680^+ Pheo^- \rangle^*$, and can provide kinetic data over a wide temperature range. However, hole burning can provide the data important for understanding the electronic structure of the primary donor state as well as its coupling to the phonons of the protein-pigment complex. Both are necessary input for dynamical calculations of the primary charge separation process. The observation of the ZPH for P960 of *Rps. viridis* and now P680 of PS II provides strong support for the proposal of Hayes and coworkers [18,19] that the broad and intense component(s) of the hole profile of the primary donor state is due to the combined effect of strong linear electron-phonon coupling and site inhomogeneous line broadening, rather than ultrafast (< 100 fs) dephasing of the primary donor state [42,43].

The observation for PS II RC of persistent hole burning associated with the accessory Chl *a* (Pheo *a*) was not anticipated and suggests that persistent hole burning of the accessory pigments in the RC of *Rps. viridis* and *Rb. sphaeroides* may be possible. Such experiments are planned as well as more detailed studies of the persistent hole burning of PSII RC since they could lead to the determination of the rate constants for excitation transport from the accessory pigments to the primary donor state at low temperatures. However, one can suggest at this time that low frequency phonons are important acceptor modes for this excitation

transport in PS II RC. This follows since the linear electron-phonon coupling for the accessory pigments and P680* is weak and strong, respectively, and since the Q_y states of the accessory pigments lie only slightly higher in energy than P680*. Recently, spectral hole burning and time domain data and multiphonon excitation transport calculations for the core antenna complex of PS I have led to the conclusion that phonons (and not intramolecular modes) mediate excitation transport within the antenna and from the antenna to the RC [31].

ACKNOWLEDGEMENT

Ames Laboratory is operated for the U.S. Department of Energy by Iowa State University under contract No. W-7405-Eng-82. This research was supported by the Director for Energy Research, Office of Basic Energy Science. Work at SERI was supported by the Energy Biosciences Division, Office of Basic Energy Sciences, U.S. Department of Energy under contract 18-006-88. The authors would like to thank John M. Hayes for providing us with the program used to calculate the hole burned spectra of P680* and Hugh McTavish for assistance in the preparation of the RC used in this study.

REFERENCES

1. Trebst, A., *Z. Naturforsch.* 1986, 41C, 240.
2. Michel, H.; Deisenhofer, P., in *Encyclopedia of Plant Physiology: Photosynthesis III*, eds. Staehelin, A. C.; Arntzen, C. J. 1986 (Springer, Berlin), pp. 371-381.
3. Nanba, O.; Satoh, K., *Proc. Natl. Acad. Sci. USA* 1987, 84, 109.
4. Satoh, K.; Fujii, Y.; Aoshima, T.; Tado, T., *FEBS Lett.* 1987, 216, 7.
5. Marder, J. B.; Telfer, A.; Barber, J., *BBA* 1988, 932, 363.
6. Yeates, T.-O.; Komiya, H.; Rees, D. C.; Allen, J. P.; Feher, G., *Proc. Natl. Acad. Sci. USA* 1987, 84, 6438.
7. Deisenhofer, J.; Epp, O.; Miki, K.; Huber, R.; Michel, H., *J. Mol. Biol.* 1984, 180, 385.
8. Deisenhofer, J.; Epp, O.; Miki, K.; Huber, R.; Michel, H., *Nature* 1985, 318, 618.
9. Michel, H.; Epp, O.; Deisenhofer, J., *EMBO J.* 1986, 5, 2445.
10. Allen, J. P.; Feher, G.; Yeates, T. O.; Rees, D. C.; Deisenhofer, J.; Michel, H.; Huber, R., *Proc. Natl. Acad. Sci. USA* 1986, 83, 8589.
11. Chang, C. H.; Tiede, D.; Tang, J.; Smith, U.; Norris, J.; Schiffer, M., *FEBS Lett.* 1986, 205, 82.
12. Kirmaier, C.; Holten, D., *Photosynthesis Research* 1987, 13, 225.
13. Budil, D. E.; Gast, P.; Chang, Ch. H.; Schiffer, M.; Norris, J., *Ann. Rev. Phys. Chem.* 1987, 38, 561.
14. Breton, J.; Martin, J. L.; Fleming, G. R.; Lambry, J.C., *Biochemistry*, submitted.

15. Fleming, G. R.; Martin, J. L.; Breton, J., in Proceedings of NATO ARW, Cadarache 1987.
Fleming, G. R.; Martin, J. L.; Breton, J., Nature (in press).
16. Tang, D.; Jankowiak, R.; Gillie, J. K.; Small, G. J.; Tiede, D. M., J. Phys. Chem., in press.
17. Tang, D.; Jankowiak, R.; Small, G. J.; Tiede, D. M., Chem. Phys., accepted.
18. Hayes, J. M.; Small, G. J., J. Phys. Chem. 1986, 90, 4928.
19. Hayes, J. M.; Gillie, J. K.; Tang, D.; Small, G. J., Biochim. Biophys. Acta 1988, 932, 287.
20. Vink, K. J.; de Boer, S.; Plijter, J. J.; Hoff, A. J.; Wiersma, D. A., Chem. Phys. Lett. 1987, 142, 433.
21. Kuwabara, T.; Murata, N., Plant & Cell Physiol. 1982, 76, 829.
22. Dunahay, T. G.; Staehelin, L. A.; Seibert, J.; Ogilvie, P. D.; Berg, S. P., Biochim. Biophys. 1984, 764, 179.
23. Seibert, M.; Picorel, R.; Rubin, A. B.; Connolly, J. S., Plant Physiol. 1988 (in press).
24. McTavish, H.; Picorel, R.; Seibert, M., Plant Physiol. 1988, to be submitted.
25. Okamura, M. Y.; Satoh, K.; Isaacson, R. A.; Feher, G., in Progress in Photosynthesis Research, Proceedings of the VIIth International Conference on Photosynthesis, Biggins, J.; ed. Vol. I, pp. 379.
26. van Dorssen, R. J.; Breton, J.; Plijter, J. J.; Satoh, K.; van Gorkom, H. J.; Amesz, J., BBA 1987, 893, 267.
27. Kirmaier, C.; Holten, D., in: Structure of Bacterial Reaction Centers: X-ray Crystallography and Optical Spectroscopy with Polarized Light, J. Breton and A.

Vermeglio (eds.) Plenum, New York, 1987.

28. Fearey, B. L.; Small, G. J., *Chem. Phys.* 1986, 101, 269.
29. Jankowiak, R.; Small, G. J., *Science* 1987, 237, 618 and references therein.
30. Gillie, J. K.; Hayes, J. M.; Small, G. J.; Golbeck, J. H., *J. Phys. Chem.* 1987, 91, 5524.
31. Gillie, J. K.; Small, G. J.; Golbeck, J. H., *J. Phys. Chem.*, submitted.
32. Friedrich, J.; Swalen, J. D.; Haarer, D., *J. Chem. Phys.* 1980, 73, 705.
33. Hayes, J. M.; Small, G. J., *Chem. Phys.* 1978, 27, 151.
34. Elschner, A.; Bässler, H., *Chem. Phys.* 1988, 123, 305.
35. Friedrich, J.; Haarer, D., *Angew. Chem. Int. Eds. Engl.* 1984, 23, 113.
36. van den Berg, R.; Völker, S., *Chem. Phys. Lett.* 1986, 127, 525.
37. Jankowiak, R.; Shu, L.; Kenney, M. J.; Small, G. J., *J. Lumin.* 1987, 36, 293.
38. Barber, J.; Chapman, D. J.; Telfer, A., *FEBS Lett.* 1987, 220, 67.
39. Gillie, J. K.; Fearey, B. L.; Hayes, J. M.; Small, G. J.; Golbeck, J. H., *Chem. Phys. Lett.* 1987, 134, 316.
40. Wasielewski, M. R.; Johnson, D. G.; Seibert, J.; Govindjee, *Proc. Natl. Acad. Sci. USA*, submitted.
41. Hayes, J. M.; Small, G. J., to be submitted.
42. Meech, S. R.; Hoff, A. J.; Wiersma, D. A., *Chem. Phys. Lett.* 1986, 121, 287.
43. Won, F.; Friesner, R. A., *J. Phys. Chem.* 1988, 92, 2214; *ibid* 92, 2208.

**PAPER V. EXCITED STATE STRUCTURE AND ENERGY TRANSFER
DYNAMICS OF TWO DIFFERENT PREPARATIONS OF THE
REACTION CENTER OF PHOTOSYSTEM II: A HOLE BURNING
STUDY**

**EXCITED STATE STRUCTURE AND ENERGY TRANSFER
DYNAMICS OF TWO DIFFERENT PREPARATIONS OF THE
REACTION CENTER OF PHOTOSYSTEM II:
A HOLE BURNING STUDY**

D. Tang, R. Jankowiak, M. Seibert,

C. F. Yocum and G. J. Small

Journal of Physical Chemistry, 1990, Submitted

ABSTRACT

Two distinctly different preparations of the photosystem II reaction center (RC) are shown to exhibit very similar 4.2 K absorption and hole burned spectra in glasses. Absorption profiles for P680 and the active pheophytin are fully characterized with the mean zero-point energy of P680* lying $\approx 25 \text{ cm}^{-1}$ lower in energy than the Q_y -state of the latter. Decay of the accessory chlorophyll and pheophytin Q_y -states due to energy transfer is shown to be about three orders of magnitude slower than in bacterial RC.

The structure-function relationships which govern the dynamics of energy transfer and primary charge separation in photosynthetic reaction centers (RC) have, for many years, attracted considerable attention. The X-ray structure determination of the bacterial RC from *Rhodospseudomonas viridis* [1-3] and, later, for *Rhodobacter sphaeroides* [4-6] sparked even greater theoretical and experimental activity [7,8]. The L and M protein subunits of the bacterial RC bind 4 BChl (bacteriochlorophyll), 2 BPheo (bacteriopheophytin) and 2 quinones. Despite the existence of a pseudo- C_2 symmetry axis, which relates the monomers of the pair and the other pigments belonging to the L and M branches, charge separation occurs almost exclusively along the L branch [7,8] to produce $P^+BPheo_L^-$ in $\approx 3 \text{ ps}$ at room temperature [9-12]. This intriguing one-sided electron transfer and the role of the BChl monomer which forms a "bridge" between P and BPheo pose but two of several problems which await definitive solution. Another stems from the observation that primary charge separation

accelerates as the temperature is reduced [13,14]. Still another is provided by the time domain measurements which show that the accessory pigment (BChl, BPheo) Q_y -states decay to P^* in < 100 fs [13,14]. These decays are not strongly dependent on temperature and, recently, spectral hole burning was used to determine that they occur in ≈ 30 -50 fs [15]. It seems clear that excited electronic state structure calculations, which accurately account for stabilization of the pertinent dark charge-transfer states by the polarizable protein, are necessary for solution of most, if not all, of the above problems.

While further theoretical and experimental studies of the bacterial RC are clearly warranted, it is also important to study charge separation and energy transfer in the photosystem I (PS I) and photosystem II (PS II) RC of green plants. The latter RC is particularly interesting from the point of view of comparison with the bacterial RC since its primary pigments are Chl *a*, Pheo *a* and quinones (analogous to those of the bacterial RC) and both structural and functional similarities with the bacterial RC have been suggested [16,17]. The original Nanba and Satoh preparation of the isolated D1-D2-Cyt b-559 RC of PS II [18] was reported to contain 4-5 Chl and 2 Pheo [19]. The correct pigment composition is now subject to debate. For example, Kobayashi et al. [20] have purified the D1-D2-Cyt b-559 complex by isoelectric focusing in digitonin rather than using Triton X-100 and reported a Chl/Pheo ratio of 6:2. Earlier, Dekker et al. [21] reported on a distinctly different preparation which involves the isolation of the core antenna complex CP47-D1-D2-Cyt b-559 and utilization of dodecyl maltoside as the detergent. For this preparation (referred to hereafter as preparation B) the Chl/Pheo ratio was found to be 10-12 Chl:2-3 Pheo and it was suggested that utilization of Triton X-100 might extract pigments from the RC. Still earlier, Seibert and coworkers [22] had reported on a modified Nanba-Satoh preparation (referred to hereafter as

preparation A) with improved stability which results from the removal of excess Triton X-100 following the final elution step. The primary charge separation kinetics of this preparation have been studied by time domain [23,24] and spectral hole burning [25] spectroscopies and found to be similar to those of *Rb. sphaeroides* (incl. the temperature dependence).

We are particularly interested in a comparison of the bacterial and PS II RC from the viewpoints of excited state level structure and early time dynamical events. In this letter we report the results of spectral hole burning studies which speak to the former and the kinetics of energy transfer from the accessory pigment Q_y -states. In so doing we are able to determine whether primary charge separation, which occurs on a picosecond time scale, goes hand in hand with ultra-fast energy transfer of the type observed for the bacterial RC. Given the above discussion of the different preparations for the PS II RC, the importance of studying samples from different isolation procedures is apparent. To this end we studied both preparation A and B of the PS II RC.

The PS II RC samples were prepared as described in refs. 22,26 (preparation A) and ref. 21 (preparation B). Excess Triton X-100 was removed from the former. Samples were stored at $-80\text{ }^{\circ}\text{C}$ until use and all sample preparation procedures for hole burning were performed at ice temperature in dim light. Samples with appropriate optical density were prepared by dilution with buffered glycerol/ H_2O (60:40) in polystyrene centrifuge tubes (path length ~ 1 cm) and cooled rapidly to liquid He temperatures in a Janis Model 8-DT Super Vari-Temp cryostat. Importantly, the low RC concentrations employed did not require detergent addition to the solvent for formation of glasses with high optical quality. We note that dodecyl maltoside was not removed from the preparation B samples used in the experiments. Elsewhere we report on studies which show that dodecyl maltoside addition to the solvent

does not significantly affect the low temperature absorption and hole burned spectra of the RC from preparation A [27,28]. Thus, a comparison of preparations A and B is meaningful. Absorption and hole burned spectra were obtained with a Bruker IFS 120 HR Fourier-transform spectrometer operating at a resolution of 2 cm^{-1} and 0.05 cm^{-1} for extended scans and high resolution scans of the zero-phonon holes, respectively. A Coherent 699-21 CW ring dye laser (DCM dye) pumped by an Innova 90-5 argon-ion laser with a linewidth of $< 0.002\text{ cm}^{-1}$ was used for hole burning. Burn intensities and times are given in the figure captions.

The 4.2 K absorption spectra of the Q_y -region for preparation A (dashed) and B (solid) are shown in Fig. 1. The two spectra are very similar with the lowest energy band at 679 nm due to the primary electron donor state, P680*, and the higher energy band at 673 nm (referred to hereafter as band A) due primarily to the accessory Chl *a* pigments. The full width-half-maximum of the Q_y -profile and the P680:band A intensity ratio are the same for the two preparations. Closer inspection reveals that the spectrum of preparation B is blue-shifted by $\approx 0.3\text{ nm}$ and exhibits slightly less tailing on the low energy side of the absorption profile. We attach no significance to these differences since samples from only a limited number of preparations have been studied. In our studies of bacterial RC samples prepared by the same procedure but at different times, we have observed shifts in the low temperature absorption spectra. Shifts due to "aging" of samples stored in the dark at -80°C have also been observed. The persistent nonphotochemical hole burned (NPHB) spectra [29,30] shown at the bottom of Fig. 1 provide additional support for the equivalence of the two preparations. The sharp zero-phonon holes (ZPH) near $15,000\text{ cm}^{-1}$ are coincident with the laser burn frequencies (ω_B) employed (the low dispersion monochromator used for

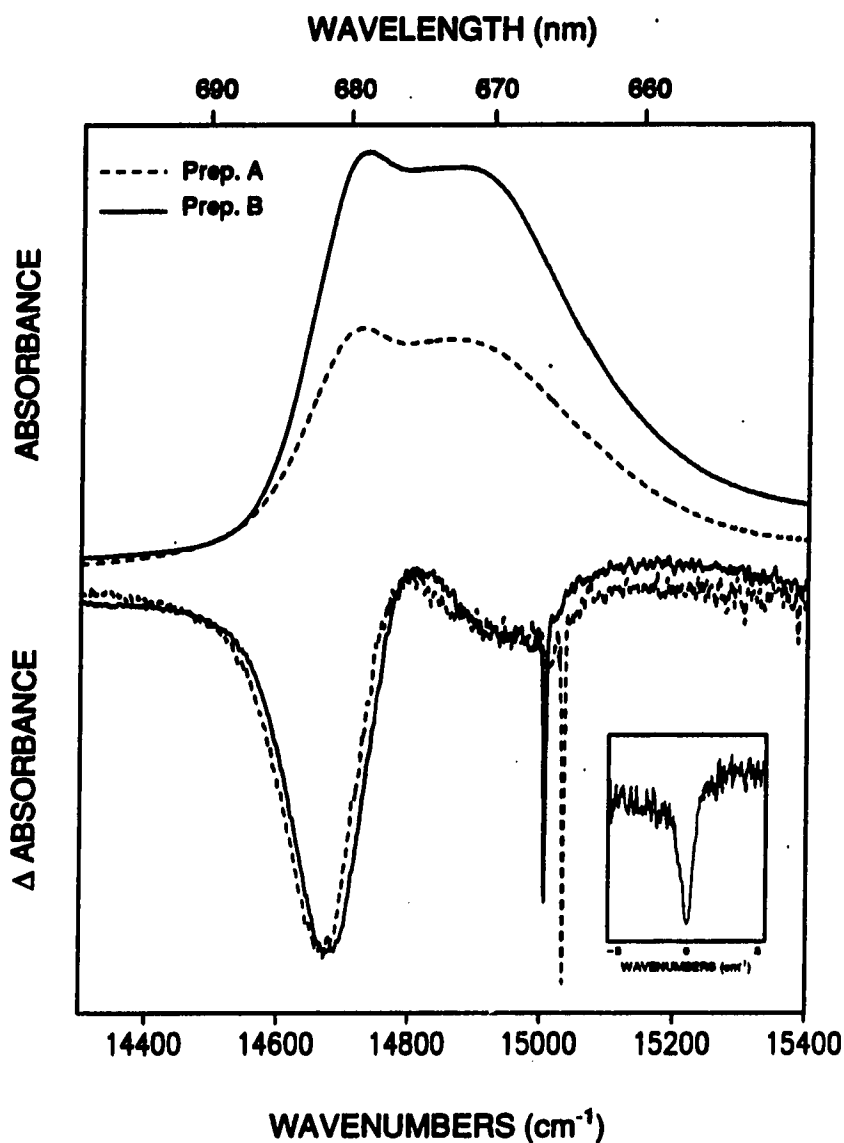


Figure 1.

PS II reaction center low temperature spectra. Top: 4.2 K absorption spectrum of preparation A (dashed line) and B (solid line). Optical density at P680 maximum is 0.2 and 0.5, respectively. Bottom: persistent hole burned spectrum of preparation A (dashed line) and preparation B (solid), 4.2 K. Burn wavelength (λ_b) for each spectrum is coincident with the sharp zero-phonon hole near ~ 665 nm. The broad (~ 120 cm^{-1}) Pheo *a* satellite holes at 681.6 nm (preparation A) and 681.3 nm (preparation B) are due to energy transfer from the Chl *a* pigments excited at λ_b . The Pheo *a* holes represent a peak percentage ΔA change of 7%. Hole burning conditions: $I_B = 200$ mW/cm^2 ; $\tau_B = 20$ min; $T_B = 4.2$ K. Inset: high resolution (0.1 cm^{-1}) scan of zero-phonon hole at 665 nm. Hole width = 0.85 cm^{-1} , $T_B = 1.6$ K.

the initial selection of ω_B prevented utilization of precisely the same ω_B for both samples; the slight difference in ω_B -values is of no consequence). We note that the burn fluences used to obtain both NPHB spectra were the same within $\approx \pm 10\%$ (which uncertainty may explain, at least in part, the slightly different ZPH depths for the two preparations). Striking is the appearance of the broad ($\sim 120 \text{ cm}^{-1}$) lower energy satellite hole near 681.3 nm (14678 cm^{-1}). For both preparations we determined that the peak position of the satellite hole is invariant to tuning of ω_B (and the coincident ZPH) within band A [27]. We note that the Pheo satellite hole for preparation B is blue-shifted by 0.3 nm and that this shift is identical to that observed in absorption (relative to preparation A).

The satellite hole is a consequence of downward energy transfer from the pigments excited at ω_B to acceptor pigments at 681.3 nm. Such behavior has been observed for phycobilisomes of *Masticogladus laminosus* and ascribed to energy transfer from phycocyanin to allophycocyanin [31]. A key question is the identity of the pigment that serves as the trap for the accessory Chl *a*? Germane to this question is the observation, from experiments involving dithionite plus white light reduction of Pheo to Pheo^- , that the Pheo Q_y -state active in charge separation lies in the near vicinity of P680 [32]. We performed such a bleaching experiment for preparation A at 4.2 K and found that the bleaching profile due to formation of Pheo^- is, for all intent and purposes, identical to that of the broad satellite hole shown in Fig. 1. We conclude, therefore, that the 120 cm^{-1} wide satellite hole is contributed to by the Pheo active in charge separation (the nature of the 120 cm^{-1} width is considered later). Further support for this assignment is provided by Fig. 3, vide infra.

Figure 2 shows ω_B -dependent NPHB spectra for preparation B (the same behavior was observed for preparation A [22,26]). For spectra 1 and 2, ω_B is located well into the

accessory Chl absorption band, cf. absorption spectra of Fig. 1. For all spectra the relatively sharp ZPH is coincident with ω_B . For spectra 3 and 4, ω_B is located in the valley between P680 and band A at ~ 672 nm. In comparing these spectra with 1 and 2 one observes that the ZPH of the former are more intense and accompanied by real- and pseudo-phonon sideband holes [33-36] at ± 20 cm⁻¹. Furthermore, the active Pheo satellite hole at 682 nm is weaker in spectra 3 and 4. Spectrum 5 was obtained with $\lambda_B = 683$ nm, near the maximum of P680 where absorption from band A is weak. The Pheo satellite hole is absent in spectrum 5, which consists of only the ZPH plus the well-resolved phonon sideband holes. The hole profile of spectrum 5 was observed for several ω_B -values which lie to lower energy of ω_B utilized for spectrum 5. Such hole profiles are assigned to the Pheo Q_y-state (P680* does not yield measurable NPHB due, in part, to its short life time). The observation of sharp ZPH coincident with ω_B for Pheo proves that the 120 cm⁻¹ width of the Pheo satellite hole shown in Fig. 1 is due mainly to inhomogeneous line broadening. The appearance of the 120 cm⁻¹ width in Fig. 1 (also spectra 1 and 2 of Fig. 2) is due to the absence of correlation between the site excitation energy distribution functions of the accessory Chl and active Pheo Q_y-states [31].

With this lack of correlation between different pigment states in mind and the fact that the ω_B -value for spectrum 5 of Fig. 2 provides for optimum excitation of P680*, a possible explanation for the absence of the broad Pheo hole in spectrum 5 emerges. It is that at 4.2 K P680* lies lower in energy than the Q_y-state of Pheo, i.e., P680* cannot transfer energy to the latter. The spectra in Fig. 3, together with linear electron-phonon coupling (optical reorganization energy) data, vide infra, confirm that this is the case. Spectrum A is the non-line narrowed persistent NPHB spectrum of the active Pheo obtained with ω_B located

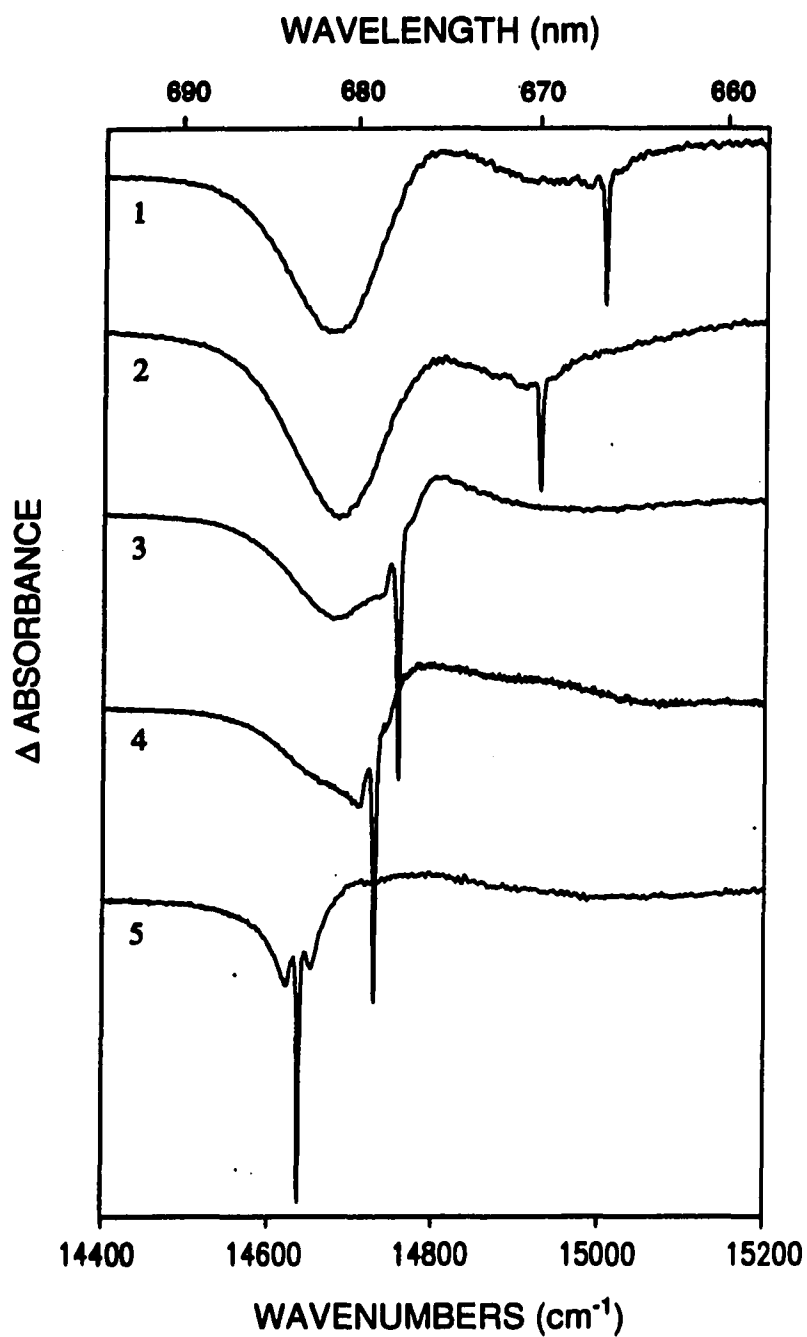


Figure 2. Burn wavelength dependence of the nonphotochemical hole burned spectrum of preparation B. From the top $\lambda_B = 666.4, 669.9, 677.6, 678.9$ and 684.2 nm. The % ΔA changes for the sharp zero-phonon holes are (from the top) 4, 6, 15, 19 and 31%. Burn conditions are identical to those of Fig. 1

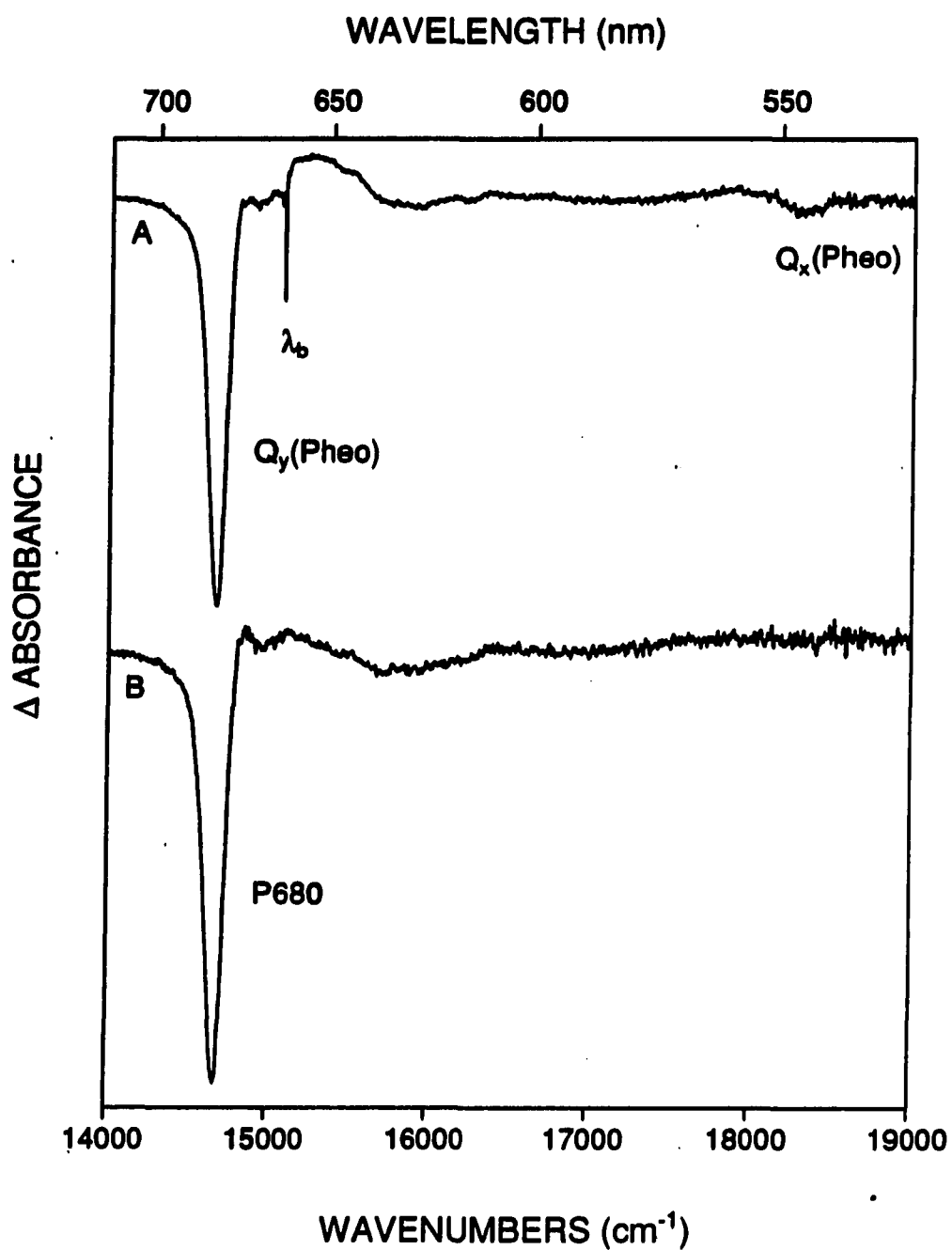


Figure 3. Non-linear narrowed hole spectrum of the Pheo α Q_y -state (upper) and P680 (lower) for preparation A, 4.2 K, $\lambda_B = 663$ nm. In the upper spectrum the satellite hole at 545.7 nm is due to the Q_x -state of Pheo α . The P680 and Pheo α Q_y -state maxima are essentially degenerate at 681.5 nm

in band A. In addition to the Pheo Q_y -satellite hole one observes a hole at 546 nm due to the Q_x -state of Pheo (such an effect has recently been reported for a tetraphenyl porphyrin [36]). Its observation proves that the 120 cm^{-1} wide hole at 681.3 nm is due to Pheo. Following the procedure of ref. (27), the transient non-line narrowed spectrum (B) of P680 was obtained by subtracting laser-on and laser-off spectra following saturation of the persistent NPHB spectrum due to Pheo. The transient P680 spectrum is due to population hole burning arising from population of the metastable $^3\text{P680}^*$ state [37]. The absence of the Pheo Q_x -hole in spectrum B proves that the transient P680 spectrum is not significantly interfered with by Pheo. The width of the P680 hole is 140 cm^{-1} and, like the Pheo Q_y -hole of spectrum A, is an accurate reflection of the absorption spectrum. Within experimental uncertainty, the $^3\text{P680}^*$ and Pheo Q_y -hole maxima are isoenergetic. However, the hole maxima do not accurately reflect the mean zero-point energies of the $^3\text{P680}^*$ and Pheo Q_y -states. Transient hole burned spectra of P680 obtained under line narrowing conditions have shown that the optical reorganization energy ($S\omega_m$, where ω_m is the mean phonon energy = 20 cm^{-1}) is $\approx 40 \text{ cm}^{-1}$ [25,27]. Our analysis of line-narrowed NPHB Pheo hole spectra of the type shown as spectrum 5 of Fig. 2 lead to a value of $\approx 15 \text{ cm}^{-1}$ for the reorganization energy of Pheo. Thus, the mean zero-point level of $^3\text{P680}^*$ lies lower in energy than that of the Pheo Q_y -state by $\approx 40 - 15 = 25 \text{ cm}^{-1}$. This explains why $^3\text{P680}^*$ cannot transfer energy to the Q_y -state of Pheo at 4.2 K. It follows also that the inhomogeneous line broadening contribution to the P680 and Pheo holes (absorption profiles) in Fig 3 is ≈ 100 and $\approx 105 \text{ cm}^{-1}$, respectively since the observed width is given approximately by $\Gamma_{\text{inh}} + S\omega_m$ [35].

We have performed high resolution scans for shallow (< 4%) ZPH burned into the Pheo and accessory Chl Q_y -absorption regions. A profile for the latter is shown in the insert

of Fig. 1; it possesses a width of 0.85 cm^{-1} at 1.6 K. The width of the ZPH of Pheo (not shown) is 0.2 cm^{-1} . The extensive literature on spectral hole burning of π -molecular systems in amorphous hosts indicates that the contribution to the ZPH-width from pure dephasing and spectral diffusion is typically $< 0.02 \text{ cm}^{-1}$ at 1.6 K [38]. Thus we ascribe both holewidths to lifetime broadening and use the standard formula [38], $T_1 = (\pi\Gamma c)^{-1}$, for a determination of the lifetime (T_1). Here Γ is the holewidth in cm^{-1} and c is the speed of light. For the accessory Chl and the Pheo Q_y -state, $T_1 = 12$ and 50 ps , respectively. These lifetimes are determined by downward energy transfer. A plausible candidate for the state that serves as the trap for the Pheo Q_y -state is P680* itself.

The present work leads to the following conclusions. First, the pigment compositions of the two preparations are the same. This conclusion is based on the close similarity of the low temperature absorption spectra (the main difference being a 0.3 nm shift) and ω_p -dependent hole spectra of the type shown in Fig. 2. A more detailed comparison of the hole spectra is given in ref. 28. It is important to realize that the nonphotochemical hole growth kinetics for the accessory Chl *a* and active Pheo *a* depend in a very sensitive way on their excited state lifetimes. The hole growth rate depends on the induced absorption rate, which is linearly proportional to the lifetime, and on the quantum efficiency, which is determined by the rate constants for excited state decay and hole burning. This is nicely illustrated by our experiments on the effects of Triton X-100 addition to the solvent on preparation A of the PS II RC [27]. This detergent disrupts energy transfer from Chl *a* to Pheo *a* (without pigment extraction) and the decrease in the energy transfer rate is accompanied by a comparable increase in the NPHB efficiency for the accessory Chl *a* (due to the concomitant increase in the lifetime of its Q_y -state). Since the excited state lifetimes

are determined by energy transfer, reaction centers with different pigment compositions must be expected to have significantly different energy transfer dynamics. This is not the case for the two preparations studied in this work. We cannot exclude, however, the possibility that the two preparations differ slightly in protein-pigment structure or concentration of damaged (inactive) RC. Given that the isolation procedures are distinctly different, small differences of this type should be anticipated. Second, the mean zero-point levels of P680* and the active Pheo Q_y -state are nearly degenerate with the latter lying only $\approx 25 \text{ cm}^{-1}$ higher in energy at liquid helium temperatures. Third, the inhomogeneous line broadening contribution to the P680 and Pheo absorption profiles (140 and 120 cm^{-1} widths) is ≈ 100 and $\approx 105 \text{ cm}^{-1}$, respectively, with the remaining contribution to the widths derived from electron-phonon coupling ($\omega_m = 20 \text{ cm}^{-1}$ and $S \approx 2.0$ and 0.7 for P680* and the Pheo Q_y -state, respectively). Fourth, the P680* and Pheo Q_y -state energy transfer decay times at 1.6 K are 12 and 50 ps.

We conclude by emphasizing that while the primary charge separation kinetics for the PS II and bacterial RC are very similar [14,25], the energy transfer decay times of the accessory pigment Q_y -states for the former are about three orders of magnitude longer than those of the bacterial RC. Given that the Q_y -state level spacing is much denser for the PS II RC than the bacterial RC (which exhibit a relatively sparse level structure), this result is puzzling when viewed in terms of conventional Förster and Davydov energy transfer theories. It might be suggested that the markedly slower energy transfer kinetics of the PS II RC is the result of disruptive protein-pigment structural perturbations introduced by the isolation procedure. However, we have observed the same slow energy transfer for the PS II RC from two distinctly different isolation procedures. It has recently been speculated that [15] one and the same "dark" charge-transfer states which have been invoked for charge separation in

bacterial RC [39] may be important for the ultra-fast decays of the accessory Q_y -states. However, a convincing theoretical argument for this mechanism has not been presented. It is clear from the present study, however, that ultra-fast (< 100 fs) energy transfer is not a necessary condition for primary charge separation to occur in a couple of picoseconds.

ACKNOWLEDGEMENT

Research at the Ames Laboratory was supported by the Division of Chemical Sciences, Office of Basic Energy Sciences, U.S. Department of Energy. Ames Laboratory is operated for the U.S. Department of Energy by Iowa State University under Contract No. W-7405-Eng-82. Work at SERI was supported by the same division of USDOE under Contract No. DE-AC02-83CH-10093. The research of C.F.Y. was supported by an NSF grant DCB 89-04075. We would like to thank Steve Toon and Scott Betts for assistance in the isolations of preparations A and B of the PS II RC.

REFERENCES

1. Deisenhofer, J.; Epp, O.; Miki, K.; Huber, R.; Michel, H. *J. Mol. Biol.* 1984, 180, 385-398.
2. Deisenhofer, J.; Epp, O.; Miki, K.; Huber, R.; Michel, H. *Nature (London)* 1985, 318, 618-624.
3. Michel, H.; Epp, O.; Deisenhofer, J. *EMBO J.* 1986, 5, 2445-2451.
4. Chang, C. H.; Tiede, D. M.; Tang, J.; Smith, U.; Norris, J.; Schiffer, M. *FEBS Lett.* 1986, 205, 82-86.
5. Allen, J. P.; Feher, G.; Yeates, T. O.; Rees, D. C.; Deisenhofer, J.; Michel, H.; Huber, R. *Proc. Natl. Acad. Sci. USA* 1986, 83, 8589-8593.
6. Yeates, T. O.; Komiyama, H.; Chirino, A.; Rees, D. C.; Allen, J. P.; Feher, G. *Proc. Natl. Acad. Sci. USA* 1988, 85, 7993-7997.
7. Kirmaier, C.; Holten, D. *Photosynthe. Res.* 1987, 13, 225-260.
8. Budil, D. E.; Gast, P.; Chang, C. H.; Schiffer, M.; Norris, J. *J. Annu. Rev. Phys. Chem.* 1987, 38, 561-583.
9. Woodbury, N. W.; Becher, M.; Middendorf, D.; Parson, W. W. *Biochemistry* 1985, 24, 7516-7521.
10. Martin, J. L.; Breton, J.; Hoff, A.; Migus, A.; Antonetti, A. *Proc. Natl. Acad. Sci. USA* 1986, 83, 957-961.
11. Breton, J.; Martin, J. L.; Migus, A.; Antonetti, A.; Orszag, A. *Proc. Natl. Acad. Sci. USA* 1986, 83, 5121-5125.

12. Wasielewski, M. R.; Tiede, D. M. *FEBS Lett.* 1986, 204, 368-372.
13. Fleming, G. R.; Martin, J. L.; Breton, J. *Nature* 1988, 333, 190-192.
14. Breton, J.; Martin, J. L.; Fleming, G. R.; Lambry, J. C. *Biochemistry* 1988, 27, 8276-8284.
15. Johnson, S. G.; Tang, D.; Jankowiak, R.; Small, G. J. *J. Phys. Chem.*, accepted.
16. Trebst, A. Z. *Naturforsch., C: Biosci.* 1986, 41C, 240-245.
17. Michel, H.; Deisenhofer, P. in *Encyclopedia of Plant Physiology: Photosynthesis III*; Staehelin, A. C.; Arntzen, C. J., Eds.; Springer: Berlin, 1986, pp 371-381.
18. Nanba, O.; Satoh, K. *Proc. Natl. Acad. Sci. USA* 1987, 84, 109-112.
19. Barber, J.; Chapman, D. J.; Tedfer, A. *FEBS Lett.* 1987, 220, 67-73.
20. Kobayashi, M.; Maeda, H.; Watanabe, T.; Nakane, H.; Satoh, K. *FEBS Lett.* 1990, 260, 138-140.
21. Dekker, J. P.; Bowlby, N. R.; Yocum, C. F. *FEBS Lett.* 1989, 254, 150-154.
22. Seibert, M.; Picorel, R.; McTavish, H. *Plant Physiol.* 1989, 89, 452-456; Seibert, M.; Picorel, R.; Rubin, A. B.; Connolly, J. S. *Plant Physiol.* 1988, 87, 303.
23. Wasielewski, M. R.; Johnson, D. G.; Seibert, M.; Govindjee. *Proc. Natl. Acad. Sci. USA* 1989, 86, 524-528.
24. Wasielewski, M. R.; Johnson, D. G.; Govindjee, Preston; C., Seibert, M. *Photosynthe. Res.* 1989, 22, 89-99.
25. Jankowiak, R.; Tang, D.; Small, G. J.; Seibert, M. *J. Phys. Chem.* 1989, 93, 1649-1654.
26. Tetenkin, V. L.; Gulyaev, B. A.; Seibert, M.; Rubin, A. B. *FEBS Lett.* 1989, 250, 459-463.

27. Tang, D.; Jankowiak, R.; Small, G. J.; Seibert, M., *Photosynthesis Research*, submitted.
28. Small, G. J.; Tang, D.; Jankowiak, R.; Seibert, M.; Yocum, C. F. in *Proceedings of the Feldafing II Workshop on Structure and Function of Bacterial Reaction Centers*, Michel-Byerle, Ed., Springer-Verlag, submitted.
29. Jankowiak, R.; Small, G. J. *Science*, 1987, 237, 618-625 and references therein.
30. See Hayes, J. M.; Jankowiak, R.; Small, G. J. in *Topics in Current Physics, Persistent Spectral Hole Burning: Science and Applications*, W. E., Moerner, Ed. (Springer-Verlag, New York, 1987), Chap. 5, and other chapters therein.
31. Köhler, W.; Friedrich, J.; Fisher, R.; Scheer, H., *J. Chem. Phys.* 1988, 89, 871-874.
32. Breton, J. in *Perspectives in Photosynthesis* (J. Jortner and B. Pullman, Eds.) pp. 23-38, Kluwer Academic Publishers, Dordrecht/Boston/London.
33. Friedrich, J.; Swalen, J. D.; Haarer, D. *J. Chem. Phys.* 1980, 73 (2), 705-711.
34. Friedrich, J.; Haarer, D. *J. Chem. Phys.* 1982, 76, 61-68.
35. Hayes, J. M.; Gillie, J. K.; Tang, D.; Small, G. J. *Biophys. Biochem. Acta* 1988, 932, 287-305.
36. Lee, I-J; Small, G. J.; Hayes, J. M. *J. Phys. Chem.*, accepted.
37. Rutherford, A. W.; Satoh, K.; Mathis, P. *Biophys. J.* 1983, 41, 40a.
38. Völker, S. *Annu. Rev. Phys. Chem.* 1989, 40, 499-530.
39. Friesner, R. A.; Won, Y. *Biochim. Biophys. Acta* 1989, 977, 99-122.

PAPER VI. EFFECTS OF DETERGENT ON THE EXCITED STATE STRUCTURE AND RELAXATION DYNAMICS OF THE PHOTOSYSTEM II REACTION CENTER: A HIGH RESOLUTION HOLE BURNING STUDY

**EFFECTS OF DETERGENT ON THE EXCITED STATE
STRUCTURE AND RELAXATION DYNAMICS OF THE
PHOTOSYSTEM II REACTION CENTER:
A HIGH RESOLUTION HOLE BURNING STUDY**

**Deming Tang, Ryszard Jankowiak, M. Seibert,
and Gerald J. Small**

Photosynthesis Research, 1990, Submitted

ABSTRACT

Low temperature (4.2 K) absorption and hole burned spectra are reported for a stabilized preparation (no excess detergent) of the photosystem II reaction center complex. The complex was studied in glasses to which detergent had and had not been added. Triton X-100 (but not dodecyl maltoside) detergent was found to significantly affect the absorption and persistent hole spectra and to disrupt energy transfer from the accessory chlorophyll *a* to the active pheophytin *a*. However, Triton X-100 does not significantly affect the transient hole spectrum and lifetime (1.9 ps at 4.2 K) of the primary donor state, P680*. Data are presented which indicate that the disruptive effects of Triton X-100 are not due to extraction of pigments from the reaction center, leaving structural perturbations as the most plausible explanation. In the absence of detergent the high resolution persistent hole spectra yield an energy transfer decay time for the accessory Chl *a* Q_y-state at 1.6 K of 12 ps, which is about three orders of magnitude longer than the corresponding time for the bacterial RC. In the presence of Triton X-100 the Chl *a* Q_y-state decay time is increased by at least a factor of 50.

Abbreviations: PS I - photosystem I, PS II - photosystem II, RC - reaction center, P680, P870, P960 - the primary electron donor absorption bands of photosystem II, *Rhodobacter sphaeroides*, *Rhodospseudomonas viridis*, NPHB - nonphotochemical hole burning, TX - Triton X-100, DM - dodecyl maltoside, Chl - chlorophyll, Pheo-pheophytin, ZPH - zero phonon hole

INTRODUCTION

The isolation by Nanba and Satoh of the D1-D2-Cyt *b*-559 reaction center (RC) complex of photosystem (PS II) from spinach [1] has stimulated questions about structural and functional similarities between PS II and bacterial RC [2]. We are particularly interested in comparison from the viewpoints of energy transfer, primary charge separation and high resolution hole burned spectra. Recently, time domain [3,4] and hole burning [5] studies have shown that the primary charge separation kinetics for formation of P680⁺ Pheo⁻ are very similar to those of *Rhodobacter sphaeroides* [6]. However, the special pair intermolecular marker mode progression, which dominates the hole (absorption) spectra of the primary electron donor (PED) state P870* and P960* of *Rb. sphaeroides* and *Rhodospseudomonas viridis* [7-9], is absent in the hole burned spectra of the corresponding state of PS II, P680*. (The mode frequencies for P870 and P960 are 115 and 135 cm⁻¹, respectively.) Thus it was suggested that if P680 is a special pair, its geometric and/or excited state electronic structure must be significantly different from those of the bacterial RC [7]. Energy transfer dynamics also appear to be different for the PS II and bacterial RC. Time domain measurements have shown that the accessory Q_y-states of the bacterial RC decay and transfer energy to the PED state in < 100 fs [6,10]. Hole burning studies have led to ≈ 30-50 fs decay times for the accessory states at 4.2 K [9]. In sharp contrast, the moderate resolution (~ 1 cm⁻¹) persistent hole burned spectra for the PS II RC indicated that the energy transfer times of the accessory pigment Q_y-states might be significantly longer at liquid helium temperatures [5].

The above hole burning and time domain studies on the PS II RC were performed

with samples prepared from spinach by a modified Nanba-Satoh procedure which improves stability by removal of excess Triton X-100 (TX) following the final elution step [11,12] (see page 215). However, TX was added ($\approx 0.05\%$) to the glass forming solvent to prevent aggregation of the RC particles. Given that the enhanced stability of the above preparation has been attributed to the removal of TX and in view of other reports [13-15] on the effects of TX on the PS II RC, it is important to examine the effects of detergent addition to the glass forming solvent on the excited state structure and relaxation dynamics of the PS II RC. Fortunately, and because of the low concentrations of the RC required for hole burning, it has been possible for us to study the RC in glasses devoid of detergent. As a result, we have recently shown that the two distinctly different isolation procedures of Seibert and coworkers [11,12] and Dekker et al. [16] yield complexes that, for all intent and purposes, are identical in pigment composition and structure [17]. This finding is significant because the pigment analysis of Dekker et al. [16] yielded a Chl *a*/Pheo *a* ratio of 10-12 : 2-3, which is different from the ratio of 4-5 Chl *a* : 2 Pheo *a* reported for the Nanba-Satoh preparation [1]. At present the situation concerning the pigment composition (including hemes and carotenoids) is unclear. For example, Kobayashi et al. [18] have purified the D1-D2-cyt *b*-559 by isoelectric focusing in digitonin rather than using TX and report a Chl *a* / Pheo *a* ratio of 6 : 2. Breton [19] has recently reported on a modification of the isolation procedure of McTavish et al. [12] which utilizes dodecyl maltoside instead of TX in the final chromatographic elution step. His low temperature absorption spectrum is very similar to those reported [17] for the preparations of Seibert and coworkers, McTavish et al., and Dekker et al.. The absorption spectrum of the former preparation is discussed in Results section. Thus, we are of the opinion that there are now three different isolation procedures which yield

RC complexes with identical Chl *a* and Pheo *a* compositions.

In this paper we report the results of experiments on the effects of solvent addition of TX and the less polar detergent dodecyl maltoside (DM) on the absorption, hole burned spectra, energy transfer and primary charge separation kinetics of the PS II RC. The preparation studied was that of McTavish et al. [12].

EXPERIMENTAL

Following the procedure of McTavish et al. [12], the D1-D2-cyt *b*-559 RC complex of PS II was prepared from spinach PS II membrane fragments which were solubilized in 4% Triton X-100 (TX), 50 mM Tris-HCl (*pH* 7.2) for 1 hour with stirring. The material was then centrifuged for 1 hour at 100,000 x g. The supernatant was then loaded onto a TSK-GEL DEAE-Toyopearl 650S (Supelco, Bellefonte, PA) column pre-equilibrated with 50 mM Tris-HCl (*pH* 7.2), 30 mM NaCl, and 0.05% Triton X-100. The column was washed with the same buffer until the eluent was colorless, and the RC fraction was eluted with a 30 to 200 mM NaCl gradient containing 50 mM Tris-HCl (*pH* 7.2) and 0.05% TX. RC were then concentrated by precipitation with polyethylene glycol (PEG). After 90 min incubation, the suspension was centrifuged at 31,300 x g for 15 min. The pellet was resuspended in 50 mM Tris-HCl (*pH* 7.2) with no detergent and then centrifuged again at 1,100 x g for 90 sec to pellet mostly colorless material containing PEG aggregates. The pellet material was discarded, and the RC fraction was stored at -80°C until use. All of the above procedures were performed in the dark at 4°C.

For the experiments involving extraction of TX from a sample to which TX had been added, 0.05% TX was added to a solution containing the PS II RC complex (stored as described above) and the solution incubated for 20 min in the dark at ice temperature. A fraction of the sample was then removed and stored in the dark at -80°C for later use as the control. The remaining sample was centrifuged at 20,000 x g for 30 min and then at 50,000 x g for another 30 minutes. Supernatant was carefully removed and the pellet

resuspended in 50 mM Tris-HCl buffer (*pH* 7.2) and subsequently stored in the dark at -80°C. Prior to the spectroscopic experiments, samples were unfrozen and diluted with 60/40 Glycerol/H₂O (buffered with Tris-HCl) to achieve the appropriate optical density. TX was added to the solvent used for dilution of the sample which had been previously incubated with TX in order to maintain the desired 0.05% concentration.

Samples were contained in polystyrene centrifuge tubes (path length ~ 1 cm) and cooled rapidly to 4.2 K in a Janis Model 8-DT Super Vari-Temp liquid helium cryostat. Absorption and hole spectra in Figs. 1-3 were obtained with a Bruker IFS 120 HR Fourier-transform Visible-IR spectrometer operating at a resolution of 2 cm⁻¹. The resolution used to obtain the P680* transient hole burned spectrum of Fig. 4 was 0.1 cm⁻¹. This spectrum is the result of the population bottleneck provided by the lowest triplet state of P680 [20, 21]. It was obtained by subtracting the laser-on from the laser-off spectrum after the persistent hole structure had been saturated [5]. The interference due to laser light scatter was readily identifiable since it appeared as a sharp spike (0.1 cm⁻¹ width) relative to the sharpest P680 feature observed (5-6 cm⁻¹). The laser spike was subtracted to yield the spectrum in Fig. 4.

A Coherent 699-21 CW ring dye laser (DCM dye) pumped by an Innova 90-5 Ar-ion laser was used for hole burning (linewidth < 0.002 cm⁻¹). To resolve the persistent zero-phonon holes associated with the accessory Chl *a* for TX-containing samples it proved necessary to probe the profiles in transmission by scanning the dye laser over 20 GHz. The probe intensity was reduced 3-4 orders of magnitude lower than the burn intensity in order to eliminate hole burning during the scan. The double-beam apparatus used to obtain the

Δ OD hole profiles is described elsewhere [22]. Burn intensities and times are given in the figure captions.

RESULTS

The 4.2 K absorption spectrum of the RC complex without detergent exhibits maxima at 679.5 (P680) and 672.8 nm (referred to hereafter as band A), Fig. 1. The 4.2 and 77 K spectra (latter not shown) yielded a red shift for P680 due to temperature reduction of only $\sim 10 \text{ cm}^{-1}$, which is significantly smaller than the corresponding shifts for P870 and P960 [23]. However, the narrowing of P680 leads to improved resolution of P680 and band A at 4.2 K. Band A is due to accessory Chl *a* (and possibly Pheo) pigments. At a level of 0.03%, TX has a significant effect on the absorption, Fig. 2. P680 and band A blue shift to 678.4 and 671.4, respectively, and P680 has the lower peak intensity (see also Ref. 13). These effects become more pronounced as the concentration of TX is increased [24].

Persistent hole burning provides for greater insight on the effect of TX addition to the solvent. First, Fig. 1 shows results obtained in the absence of detergent with λ_B (burn wavelength) = 665.2 nm. A sharp zero-phonon hole (ZPH), with a width determined primarily by the read resolution of 2 cm^{-1} , is observed at λ_B . The ΔA value for the ZPH (not saturated) represents a $\sim 7\%$ absorbance change. The most striking feature is the broad ($\sim 120 \text{ cm}^{-1}$) satellite hole at $681.6 \pm 0.1 \text{ nm}$ (solid arrow). This is a consequence of downward energy transfer from the pigments excited at λ_B to acceptor pigments at 681.6 nm. Such behavior has been observed for phycobilisomes of *Mastigocladus laminosus* and ascribed to energy transfer from phycocyanin to allophycocyanin [25]. Dithionite plus white light bleaching experiments, in which Pheo is reduced to Pheo^- , have shown that the band due to active Pheo is in close proximity to P680 [19]. At 4.2 K we found that the bleaching

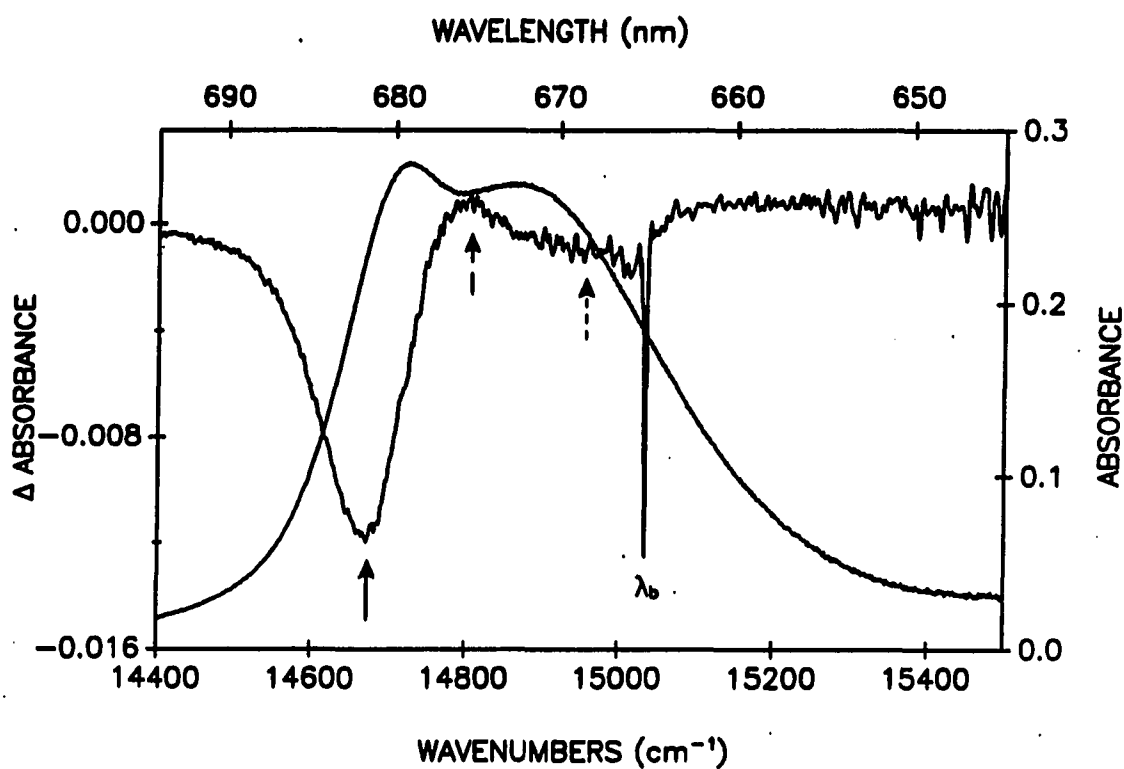


Figure 1. Absorption and persistent hole burned spectra of PS II RC in the absence of detergent, 4.2 K. Hole burning conditions: burn intensity = 200 mW/cm²; burn time = 20 min; λ_b = 665.2 nm (coincident with sharp ZPH). Broad satellite hole at 681.6 nm (solid arrow) is a manifestation of downward energy transfer from pigments excited at λ_b , see text

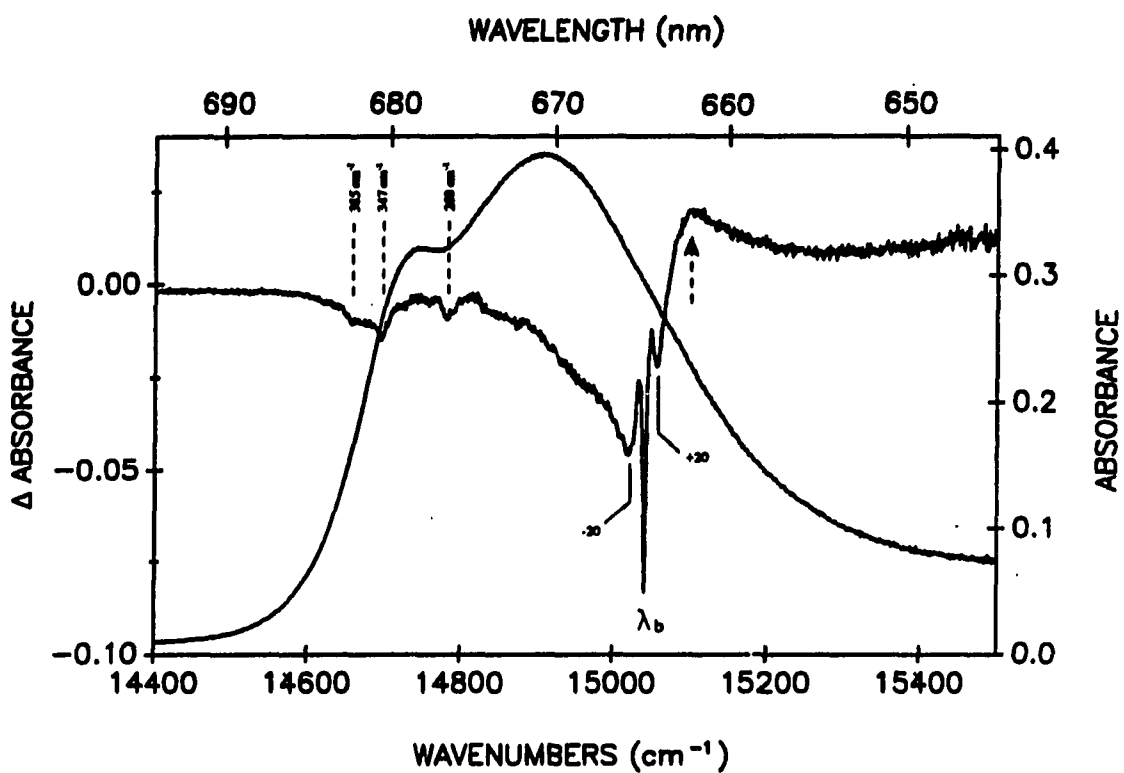


Figure 2. Absorption and persistent hole burned spectra of PS II RC in the presence of 0.03% Triton X-100, 4.2 K. Hole burning conditions: see Fig. 1; $\lambda_b = 664.8$ nm. Note marked diminution in intensity of broad satellite hole at 681.6 nm, cf. Fig. 1. Features (hole) at 260, 347 and 385 cm^{-1} are Chl *a* vibronic satellite holes associated with the ZPH at λ_b , see text

due to formation of stable Pheo⁻ is very similar to the 681.6 nm hole of Fig. 1 [24]. The former is slightly blue shifted ($\sim 5 \text{ cm}^{-1}$) due to an accompanying electrochromic shift of P680. The persistent 681.6 nm hole of Fig. 1 was found to be independent of the location of λ_B within band A and an identical hole was obtained for excitation of the weaker vibronic absorption bands near 632 nm. For λ_B located throughout the band A profile a sharp ZPH (with weak phonon sideband hole structure) is observed coincident with λ_B [24], proving that band A is largely inhomogeneously broadened. These results and the observation that hole burning of the Q_x-Pheo absorption band accompanies production of the 681.6 nm hole [17] indicate that the 681.6 nm hole of Fig. 1 is contributed to by the Pheo active in charge separation.

At the same burn intensity and time conditions, the persistent hole burned spectrum of the RC complex with TX is markedly different, Fig. 2.¹ First, the hole burning efficiency at λ_B is significantly higher since the absorbance change for the ZPH is $\sim 27\%$ and pronounced pseudo- and real-phonon sideband holes [26-29] at $\omega_B - 20 \text{ cm}^{-1}$ and $\omega_B + 20 \text{ cm}^{-1}$ are observed. The holes are sufficiently intense to produce an observable anti-hole characteristic of nonphotochemical hole burning which is peaked at 675.5 nm (dashed arrow). Second, the Pheo satellite hole at 681.6 nm is markedly suppressed. The sharp features (e.g., 347 cm^{-1}) are vibronic satellite holes associated with the ZPH at λ_B and of the type which has been extensively studied for Chl *a* and *b* of the light harvesting complex of PS I [30, 31]. The frequencies of 260, 347 and 385 cm^{-1} correlate well with excited state Chl *a* mode

¹ The λ_B -value for Fig. 2 (and 3) is slightly different than the value of 665.2 nm for Fig. 1 because of the low dispersion of the monochromator used for initial calibration. Such small differences ($\sim 1 \text{ nm}$) do not affect hole structure at and in the near vicinity of λ_B or the Pheo satellite hole.

frequencies [31, 32]. Thus, Chl *a* is a significant contributor to the absorption at λ_p . The hole burned spectra of Figs. 1 and 2 establish that TX disrupts an energy transfer pathway from the accessory Chl *a* Q_y -state.

In contrast, detergent dodecyl maltoside does not significantly perturb the RC. Figure 3 shows the absorption spectrum and persistent hole burned spectrum for a sample to which 0.02% DM was added. The latter was obtained under the same conditions used in Figs. 1 and 2. Comparison of Figs. 1 and 3 shows that the absorption spectra are very similar as are the hole burned spectra [17, 14], even at the level of percentage absorbance change for the ZPH at λ_p and the Pheo satellite hole. Addition of as much as 0.12% DM did not alter the situation. Thus, the integrity of the preparation is maintained in the presence of DM.

That TX alters energy transfer raises the question of whether it has a comparably large effect on the transient hole burned spectrum of P680 (persistent hole burning of P680 is not observed due, in part, to the short lifetime of P680*, vide infra) and the primary charge separation process. Figure 4 shows the transient hole spectrum of P680 obtained in the absence of detergent. In this case, the long lived triplet state of the primary donor serves as the population bottleneck for hole burning [33, 5]. This spectrum is very similar to those reported earlier [5] and exhibits a ZPH width of 5.5 cm^{-1} , which leads again [5] to a 1.9 ps lifetime for P680* at 4.2 K. The phonon sideband hole structure is characterized by an *S*-factor of ≈ 2 and a mean phonon frequency (ω_m) of 20 cm^{-1} [5]. At the level of 0.05% TX, the structure of the transient P680 hole spectrum is not significantly perturbed even though P680 undergoes a blue shift, vide supra.

In order to understand why the hole burning efficiency at λ_p is significantly higher in the presence of TX (Fig. 2), ZPH widths were carefully measured to determine the rates

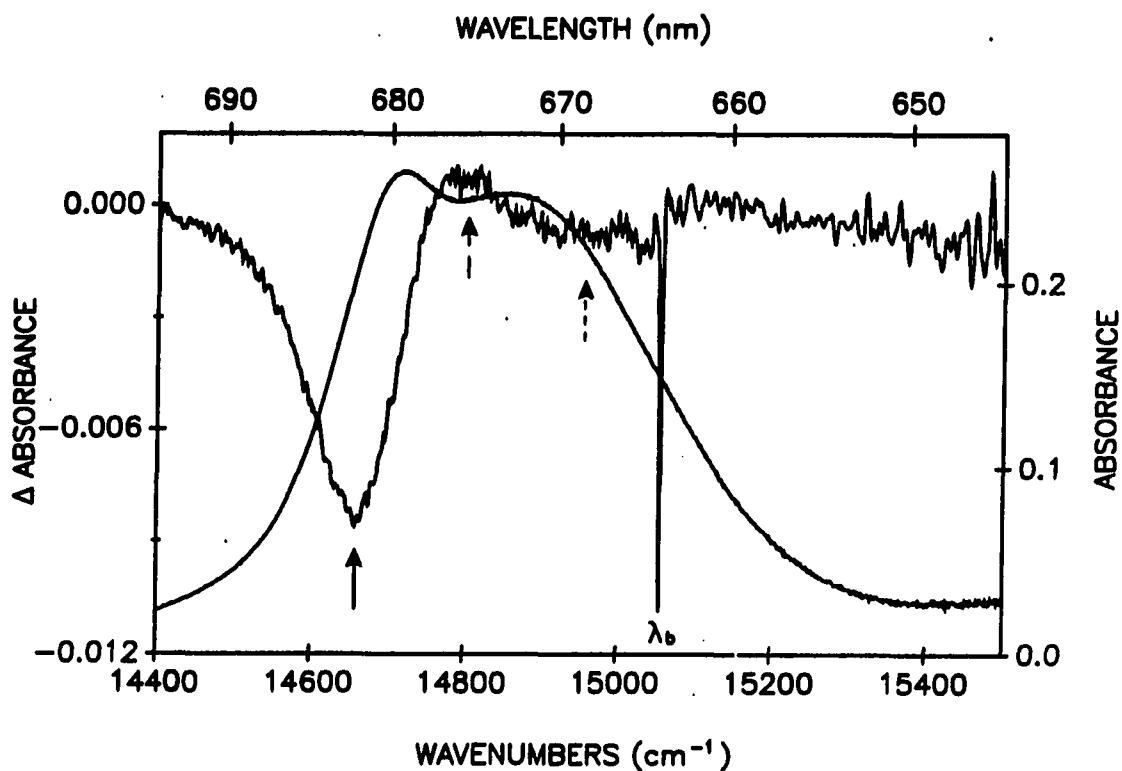


Figure 3. Absorption and persistent hole burned spectra of PS II RC in the presence of 0.02% dodecyl maltoside, 4.2 K. Hole burning conditions: see Fig. 1; $\lambda_b = 664.3$ nm. Note similarity of the spectra with those of Fig. 1

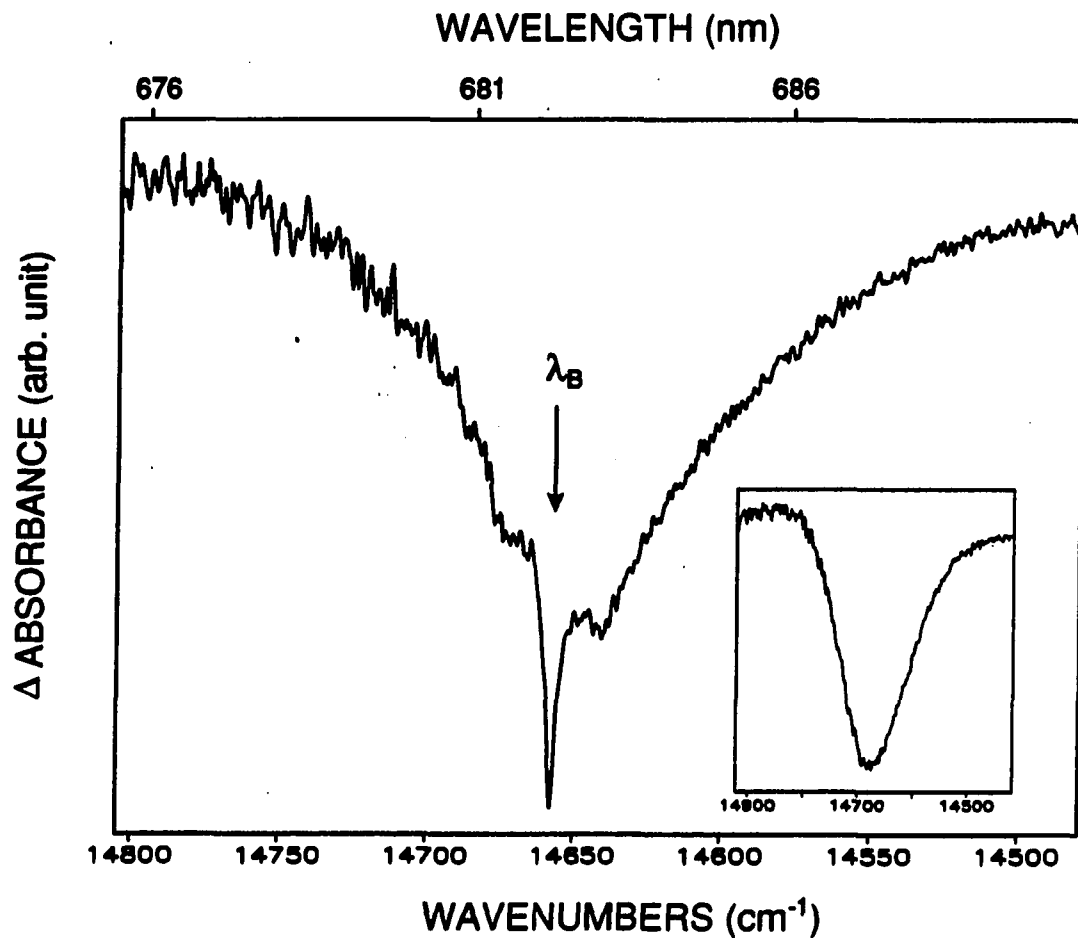


Figure 4.

Transient hole burned spectrum of P680 obtained in the absence of detergent, 4.2 K and $\lambda_b = 682.3$ nm. The ZPH at λ_b has a width of ≈ 5.5 cm^{-1} . Broader features at $\lambda_b \pm 20$ cm^{-1} are phonon sideband holes. Inset spectrum: P680 hole profile obtained under non-line narrowing conditions with $\lambda_b = 665$ nm. This profile is shifted relative to center of gravity of the structured P680 hole since the latter was obtained under line narrowing conditions

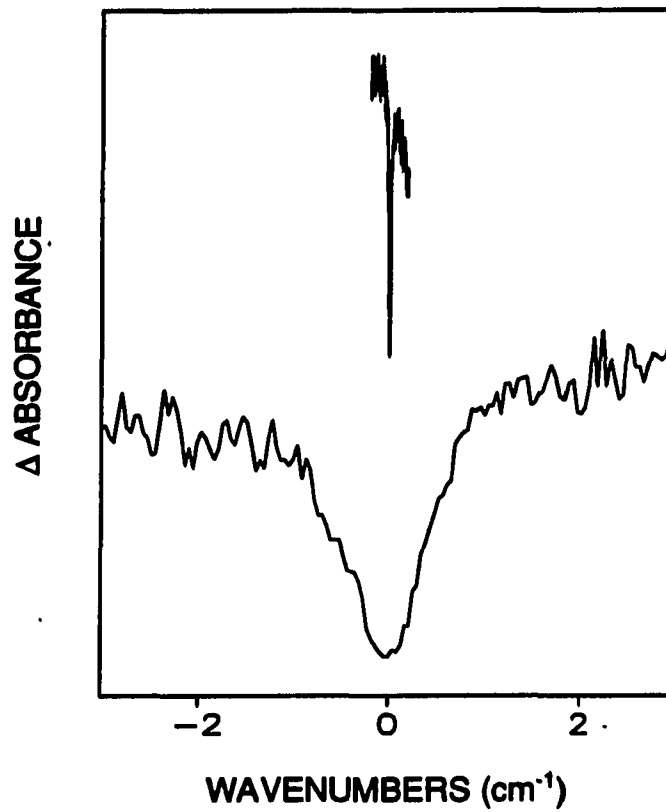


Figure 5.

Persistent zero-phonon holes of PS II RC with (top) and without (bottom) Triton X-100 at 1.6 K. Hole widths were measured as 0.018 cm^{-1} (top) with read resolution of 0.002 cm^{-1} and 0.85 cm^{-1} (bottom) with read resolution of 0.1 cm^{-1} . Hole depths were less than 5% in both cases

of energy transfer. Figure 5 shows the persistent hole burned spectra of PS II RC at 1.6 K with and without TX. At a read resolution of 0.1 cm^{-1} , the width of the ZPH coincident with λ_B ($\sim 665 \text{ nm}$) is 0.85 cm^{-1} in the absence of TX. But, in its presence ($\sim 0.03\%$), the width is reduced to 0.018 cm^{-1} (read resolution $< 0.002 \text{ cm}^{-1}$). In order to avoid artificial broadening processes [34], these measurements were made on ZPH with absorbance changes of $< 5\%$.

The question of whether TX alters the absorption spectrum and disrupts energy transfer in the PS II RC by extracting pigments or by producing structural changes was addressed by TX-extraction experiments (cf. Section II). The upper and middle spectra of Fig. 6 are the absorption of the control (no TX) and the sample that had been incubated with TX. The effect of TX is similar to that described earlier in terms of Figs. 1 and 2. Spectrum 3 of Fig. 6 is that of the pellet (redissolved) from which TX had been removed by centrifugation. Comparison of the three absorption spectra shows that the centrifugation procedure results in a significant degree of restoration towards the control spectrum. The P680/band A peak intensity ratios for spectra 1-3 are 1.03, 0.80 and 0.98, respectively. The fact that the control spectrum is not completely recovered could be due to incomplete TX-extraction and/or recovery of the original pigment-protein structure. As shown above, the 681.6 nm Pheo *a* satellite hole of samples devoid of TX (see Fig. 1) suffers a marked decrease in intensity upon addition of TX to the solvent (see Fig. 2). The dashed line hole burned spectrum of Fig. 6 (obtained under the same burning conditions used to produce the hole spectra of Figs. 1-3) establishes that TX extraction by centrifugation results in the reappearance of the Pheo *a* satellite hole upon excitation of the band A accessory pigments. In our opinion the results of Fig. 6 provide a strong argument against TX extracting Chl *a* or

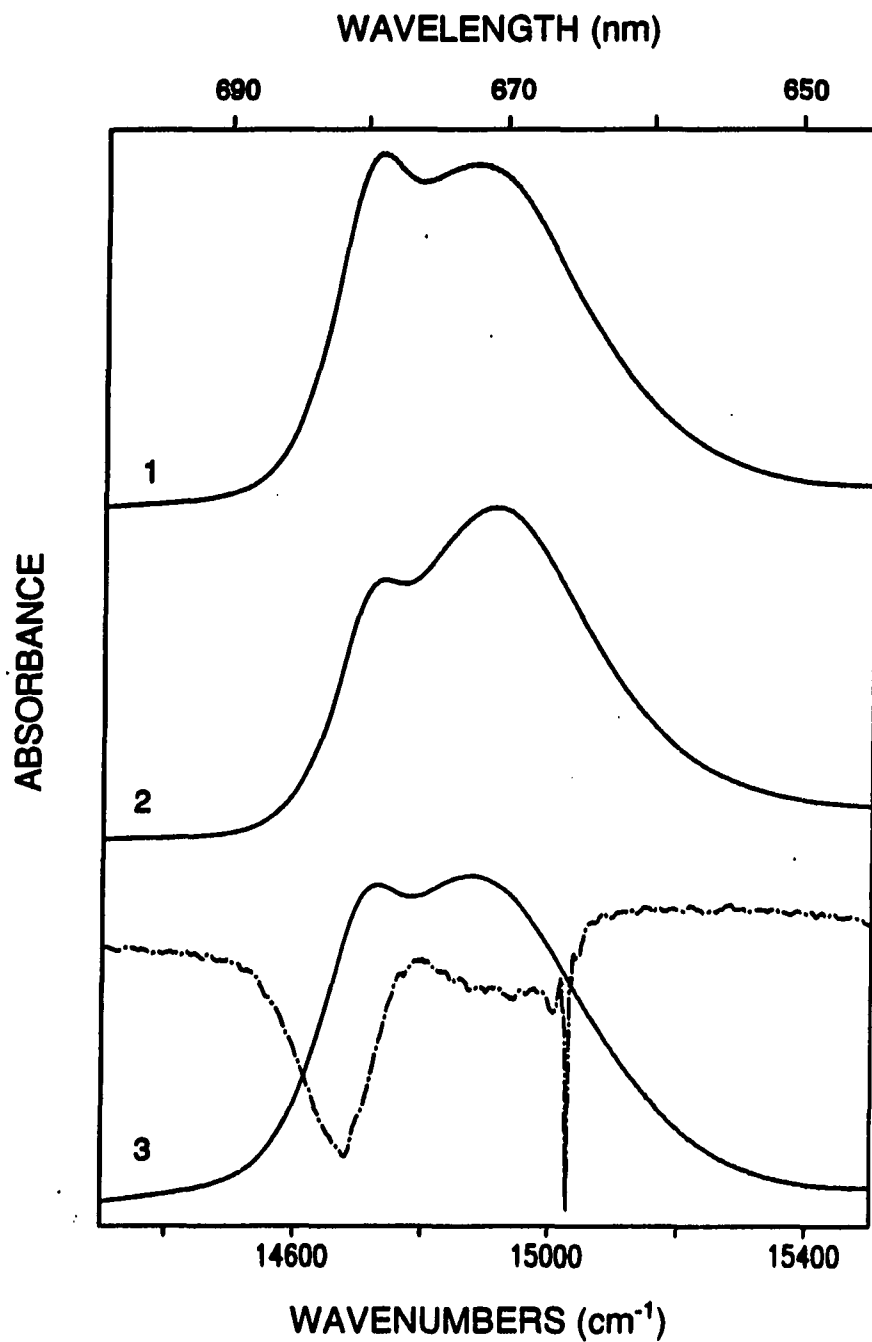


Figure 6. Absorption spectra of 1) Control sample (without TX), 2) Control sample with 0.05% TX, and 3) Pellet resuspended in Tris buffer (after the removal of TX by centrifugation). The dash-dotted hole burned spectrum was obtained by 10 min burning ($I = 200 \text{ mW/cm}^2$) at $\lambda_b \sim 665 \text{ nm}$ on the pellet sample (resuspended in Tris buffer and diluted)

Pheo *a* from the PS II RC since it is unlikely that the RC would be reconstituted with these pigments during centrifugation.

DISCUSSION

Effects of Detergent

Our results show that Triton X-100 (TX) addition to the solvent significantly perturbs the low temperature absorption and hole burned spectra of the stabilized Namba-Sato preparation of the PS II RC [12, 13] and, moreover, disrupts an energy transfer pathway from the accessory Chl *a* to the active Pheo *a*. In sharp contrast, the detergent dodecyl maltoside (DM) does not significantly perturb the spectra or disrupt energy transfer. The extraction experiments (Fig. 6) strongly indicate that TX does not extract Chl *a* or Pheo *a* pigments from the RC. Therefore, we conclude that the disruptive effects of TX are due to protein-pigment structural perturbations. Recently, it was reported that TX disrupts Chl *b* to Chl *a* energy transfer in the light-harvesting complex II of *Dunaliella tertiolecta* without pigment extraction [35]. A similar result has been reported for various PS I core antenna complexes [36] (in their studies DM was observed to have a relatively weak effect).

It was noted earlier that spectral hole burning has been used to establish [17] the equivalence of the preparation studied in this work and that of [16]. Since the latter isolation procedure is distinctly different and one that utilizes DM throughout, it is highly unlikely that TX extracts pigments at earlier stages of the preparation of Seibert and coworkers.

To what extent does TX disrupt the aforementioned energy transfer process? Without detergent, the ZPH at λ_B located in band A (see Fig. 1) exhibits a width of 0.85 cm^{-1} at 1.6 K. With TX this width is reduced to 0.018 cm^{-1} . The extensive literature on spectral hole

burning of π -molecular systems indicates that at 1.6 K the contribution to the holewidth from pure dephasing and spectral diffusion is typically $< 0.02 \text{ cm}^{-1}$ [34]. Thus we ascribe the 0.85 cm^{-1} holewidth to lifetime broadening and use the standard formula [34], $T_1 = (\pi \Gamma c)^{-1}$, for a determination of the lifetime (T_1) of the pigment state(s) that absorbs at λ_B . Here Γ is the holewidth in cm^{-1} and c is the speed of light. The result is $T_1 = 12 \text{ ps}$, which is attributed to downward energy transfer which directly and/or indirectly populates the Pheo state at 681.6 nm (which then undergoes persistent hole burning). For the 0.018 cm^{-1} hole the possibility that pure dephasing and/or spectral diffusion contributes to the width cannot be excluded. Thus, T_1 is increased by at least a factor of 50. The increased persistent hole burning rate produced by TX is presumably due to the increase in the induced absorption rate (due to the decrease in the homogeneous linewidth of the zero-phonon line) and a corresponding increase in the hole burning quantum yield (due to the increase in the excited state lifetime). The increase in lifetime is consistent with the observation that TX addition to the solvent results in an increase in fluorescence from the band A pigments [14].

The question of how the TX-induced structural changes yield a 50-fold (or greater) diminution in the rate of energy transfer from the accessory Chl *a* is most interesting, especially since TX does not appear to affect the lifetime and hole spectra of P680*. The answer to this question may have to await the determination of the X-ray structures of the PS II RC, crystallized in the presence and absence of TX. However, polarized hole burning studies are planned which may provide information on the structural perturbations induced by TX.

Other Aspects of the Hole Burned Spectra

Concerning the mechanism for persistent hole burning, we note first that repeated cycles of hole burning-sample warming to 278 K-cooling to 4.2 K-hole burning did not yield evidence for photodegradation. This suggests that the mechanism is nonphotochemical. Nonphotochemical hole burning (NPHB) has been observed for several antenna systems [37] and is a manifestation of photoinduced protein pigment structural change which persists long after pigment-deexcitation has occurred. For $\pi\pi^*$ excited states, the associated anti-hole (increase in absorption) generally lies predominantly to higher energy of the hole [29]. The onset of the anti-hole in Fig. 2 is indicated by the dashed arrow. The broad interfering minimum to the right of the arrow may be due to unresolved vibronic satellite hole structure associated with excited state vibrations in the 260-400 cm^{-1} region. The difficulties in demonstrating a conservation of absorption intensity between hole and anti-hole structure in NPHB spectra have been recently discussed [28, 29]. The ZPH at λ_B plus its phonon sideband holes in Figs. 1 and 3 are too weak to produce a measurable anti-hole (the anti-hole of a ZPH is generally very broad relative to the ZPH). Similarly, the dashed (long) arrows in Figs. 1 and 3 mark the onset of the anti-hole for the broad Pheo satellite hole at 681.6 nm. This anti-hole is also interfered with by a broad hole (short dashed arrow) whose origin is currently under investigation. Spectra obtained with $\lambda_B = 632$ nm (vibronic excitation) do not exhibit this interference and show more clearly the Pheo anti-hole [24].

The question of why 681.6 nm Pheo hole of Figs. 1 and 3 is so broad (FWHM = 120 cm^{-1}) relative to the ZPH at λ_B is interesting. Persistent hole spectra for λ_B in the

vicinity of the Pheo absorption at 681.6 nm exhibit sharp ZPH (FWHM $< 1 \text{ cm}^{-1}$) with weak phonon sideband holes [17, 24]. The observation of sharp ZPH proves that the Pheo hole shown in Figs. 1 and 3 is largely inhomogeneously broadened (due to statistical structural variations from RC to RC). The 120 cm^{-1} width is attributed to the absence of correlation between the site excitation energy distribution functions for Pheo and the pigments excited at λ_B [25]. Since the Pheo hole obtained with vibronic excitation at $\lambda_B = 632 \text{ nm}$ is identical to that shown in Fig. 1 [24], the hole profile is an accurate reflection of the Pheo absorption profile with a maximum at 681.6 nm ($14,670 \text{ cm}^{-1}$).

Tang et al. [17] have determined the absorption maximum frequency for P680. Since in Fig. 1 the P680 band is interfered with by band A, its true maximum must occur at $\lambda > 679.5 \text{ nm}$, cf. section III. The true maximum was determined from transient hole spectra obtained under non-line narrowing conditions (e.g., $\lambda_B = 665 \text{ nm}$) which yielded a structureless P680 hole at $681.7 \pm 0.1 \text{ nm}$ with a width of $\sim 140 \text{ cm}^{-1}$, inset spectrum of Fig. 4. Under the conditions of the experiment, the Pheo Q_x -band at 542.3 nm exhibited no change proving that the P680 hole is not interfered with by the 681.6 nm persistent Pheo hole (the latter is accompanied by hole burning of the Q_x -band.) Therefore, the P680 and Pheo Q_y -absorption maxima are degenerate to within experimental uncertainty. However when the linear electron-phonon coupling is taken into account, the mean energy of the zero-point level of P680* is actually lower than that for the Pheo Q_y -state by 25 cm^{-1} [17]. Thus, P680* can serve as an excitation trap for Pheo* at 4.2 K.

ACKNOWLEDGEMENT

Ames Laboratory is operated for the U.S. Department of Energy by Iowa State University under Contract No. W-7405-Eng-82. This research was supported by the Division of Chemical Sciences, Office of Basic Energy Sciences, U.S. Department of Energy. Work at SERI was supported by the same division under Contract No. DE-AC-02-83 CH. We thank Steve Toon for assistance in preparation of the RC used in this study.

REFERENCES

1. Nanba, O.; Satoh, K., *Proc. Natl. Acad. Sci. USA* 1987, 84, 109-112.
2. Michel, H.; Deisenhofer, J., *Biochemistry* 1988, 27, 1-7.
3. Wasielewski, M. R.; Johnson, D. G.; Seibert, M.; Govindjee, *Proc. Natl. Acad. Sci. USA* 1989, 86, 524-528.
4. Wasielewski, M. R.; Johnson, D. G.; Govindjee; Preston, C.; Seibert, M., *Photosynthesis Res.* 1989, 22, 89-99.
5. Jankowiak, R.; Tang, D.; Small, G. J.; Seibert, M., *J. Phys. Chem.* 1989 93, 1649-1654.
6. Breton, J.; Martin, J. L.; Fleming, G. R.; Lambry J.-C., *Biochemistry* 1988, 27, 8276-8284.
7. Tang, D.; Johnson, S. G.; Jankowiak, R.; Hayes, J. M.; Small, G. J.; Tiede, D. M., In: *Twenty-second Jerusalem Symposium Quantum Chemistry and Biochemistry: Perspective in Photosynthesis (Jortner, J. and Pullman, B., eds.)*, 1989, pp. 23-38. Dordrecht/Boston/London: Kluwer Academic Press.
8. Johnson, S. G.; Tang, D.; Jankowiak, R.; Hayes, J. M.; Small, G. J.; Tiede, D. M., *J. Phys. Chem.* 1989, 93, 5933-5957.
9. Johnson, S. G.; Tang, D.; Jankowiak, R.; Hayes, J. M.; Small, G. J.; Tiede, D. M., *J. Phys. Chem.* 1990, in print.
10. Fleming, G. R.; Martin, J. L.; Breton, J., *Nature* 1988, 333, 190-192.
11. Seibert, M.; Picorel, R.; Rubin, A. B.; Connolly, J. S., *Plant Physiol.* 1988, 88, 303-

- 306.
12. **McTavish, H.; Picorel, R.; Seibert, M., Plant Physiol. 1989, 89, 452-456.**
 13. **Tetenkin, V. L.; Gulyaev, B. A.; Seibert, M.; Rubin, A. B., FEBS Lett. 1989, 250, 459-463.**
 14. **Scherz, A.; Braun, P.; Greenberg, B. M., Biochemistry 1990, in print.**
 15. **Ghanotakis, D. E.; de Paula, J. C.; Demetrion, D. M.; Bowlby, N. R.; Peterson, J.; Babcock, G. T.; Yocum, C. F., Biochem. Biophys. Acta 1989, 974, 44-53.**
 16. **Dekker, J. P.; Bowlby, N. R.; Yocum, C. Y., FEBS Lett. 1989, 254, 150-154.**
 17. **Tang, D.; Jankowiak, R.; Yocum, C. F.; Seibert, M.; Small, G. J., J. Phys. Chem. 1990, submitted.**
 18. **Kobayashi, M.; Maeda, H.; Watanabe, T.; Nakane, H.; Satoh, K., FEBS Lett. 1990, 260, 138-140.**
 19. **Breton, J., In: Twenty-second Jerusalem Symposium Quantum Chemistry and Biochemistry: Perspective in Photosynthesis (Jortner, J. and Pullman, B., eds.), 1990, pp 23-38. Dordrecht/Boston/London: Kluwer Academic Press.**
 20. **Rutherford, A. W.; Satoh, K.; Mathis, P., Biophys. J. 1983, 41, 40a.**
 21. **den Blanken, H. J.; Hoff, A. J.; Jongenelis, A. P. J. M.; Diner, B. A., FEBS Lett. 1983, 151, 21-27.**
 22. **Gillie, J. K.; Fearey, B. L.; Hayes, J. M.; Small, G. J.; Golbeck, J. H., Chem. Phys. Lett. 1987, 134, 316-322.**
 23. **Hayes, J. M.; Gillie, J. K.; Tang, D.; Small, G., Biochim. Biophys. Acta 1988, 932, 287-305.**
 24. **Small, G. J.; Jankowiak, R.; Seibert, M.; Yocum, C.; Tang, D. (1990) In:**

Proceedings of Feldafing II Workshop on Structure and Functional Bacterial Reaction Centers (Michel-Byerle, M. E., ed.), 1990. Berlin: Springer-Verlag (submitted).

25. Köhler, W.; Friedrich, J.; Fisher, R.; Scheer, H., *J. Chem. Phys.* 1988, 89, 871-874.
26. Friedrich, J.; Swalen, J. D.; Haarer, D., *J. Phys. Chem.* 1980, 73, 705-711.
27. Friedrich, J.; Haarer, D., *J. Chem. Phys.* 1982, 76, 61-68.
28. Lee, J.-L.; Hayes, J. M.; Small, G. J., *J. Chem. Phys.* 1989, 91, 3463-3469.
29. Shu, L.; Small, G. J., *Chem. Phys.* 1990, 141, 447-455.
30. Gillie, J. K.; Hayes, J. M.; Small, G. J.; Golbeck, J. H., *J. Phys. Chem.* 1987, 91, 5524-5229.
31. Gillie, J. K.; Small, G. J.; Golbeck, J. H., *J. Phys. Chem.* 1989, 93, 1620-1627.
32. Avarma, R. A.; Rebane, K. K., *Spectrochim Acta* 1985, 41A, 1365-1380.
33. Meech, S. R.; Hoff, A. J.; Wiersma, D. A., *Chem. Phys. Lett.* 1985, 121, 287-292.
34. Völker, S., In: *Relaxation processes in molecular excited states: optical relaxation processes at low temperature* (Fünfschilling, J., ed.), 1989, p. 113. Dordrecht: Kluwer Academic Press.
35. Sukenik, A.; Falkowski, P. G.; Bennett, J., *Photosynthesis Res.* 1989, 21, 37-44.
36. Nechushtai, R.; Nourizadeh, S. D.; Thornber, J. P., *Biochim. Biophys. Acta* 1986, 848, 193-200.
37. Johnson, S. G.; Lee, I.-J.; Small, G. J., In: *Chlorophylls* (Scheer H. ed.), 1990. CRC Press, Boca Raton, Florida.

CONCLUSIONS

Although the structure of PSII RC is not yet determined, important data concerning its early time charge separation kinetics as well as energy transfer have been obtained via transient and persistent hole burning experiments. Such data are important in addressing the question of structural and functional similarities between the PSII RC and bacterial RC [3-5,9-11].

Based on the earlier experiments presented in PAPER IV and confirmed later with a different approach as shown in PAPER V and PAPER VI, a decay time of 1.6 ps for P680* of PS II RC has been measured. This is consistent with data obtained by time domain experiments [3] at 10 K. The observed temperature dependence of decay kinetics was found to be similar to that of bacterial RCs. Although other similar arguments regarding structural similarity between RC of PS II and of purple bacteria have been raised, it appears that some major differences do exist. The most obvious one would be the lack of evidence of an upper exciton component due to the congestion in the Q_y region. The energy transfer decay times of the accessory pigment Q_y -states are three orders of magnitude longer than those of the purple bacterial RC [41]. It has been shown that the addition of Triton X-100 detergent strongly perturbs the PS II RC. As a result of this perturbation, a 50 fold slow-down of the energy transfer rate was observed. However, our data have shown that the charge separation kinetics still remains unchanged. Such results suggest that ultrafast (< 100 fs) energy transfer may not be a necessary condition for primary charge separation to occur in a couple of picoseconds. Another striking difference between them is the absence of a Franck-Condon

marker mode in the P680* hole profile. Although the geometry change along the marker mode coordinate for P* of bacterial RC may have a role in the primary charge separation process, the existence of this marker mode as indicated by present work, may not be the absolute condition for charge separation. An interesting similarity is provided by the observation that the coupling of P* to low frequency delocalized protein phonons is moderately strong ($S \sim 2$) for both PSII and bacterial RC. The implications of this coupling for the charge separation process, particularly its T-independence, have yet to be considered. This coupling is significantly stronger than that observed for Chl or Pheo monomers and we suggest, therefore, that P680 is a special pair, albeit significantly different than the special pair of the bacteria RC (either in geometry and/or excited state electronic structure). Still another difference between the PS II and bacterial RC is the fact that the Q_y -state of the active Pheo in the former is quasi-degenerate with P* where the separation in the bacterial RC is close to 3000 cm^{-1} . It is intriguing that, while from an energy transfer perspective, the PS II RC behaves like a weakly coupled "Förster" aggregate and the bacterial RC behaves like an extremely strongly interacting aggregate, the primary charge separation kinetics are still so similar. More work is needed to improve the sample preparation procedures for PS II RC to achieve better sample stability and gain further insight in its pigment composition and structural details.

Furthermore, it should be noted that the spectral hole burning technique, which has been successfully applied in the studies of photosynthetic complexes such as antenna complex of PS I, green bacterium *P. aestuarii*, the reaction center of PS I and those of purple bacteria, has again demonstrated its unique capability in probing the excited state structure of a

complicated molecular system, gaining information regarding pigment-protein interaction and providing optical spectra with exceptional high resolution.

REFERENCES

1. Klimov, V. V.; Krasnovsky, A. A. *Photosynthetica* 1981, 15, 592.
2. Klimov, V. V.; Klevanik, A. V.; Shuvalov, V. A.; Krasnovsky, A. A. *FEBS Lett.* 1977, 82, 183.
3. Jankowiak, R.; Tang, D.; Small, G. J.; Seibert, M. *J. Phys. Chem.* 1989, 93, 1649.
4. Wasielewski, M. R.; Johnson, D. G.; Govindjee; Preston, C.; Seibert, M. *Photosynthe. Res.* 1989, 22, 89.
5. Debus R. J.; Barry, B. A.; Babcock, G. T. McIntosh, L. *Proc. Natl. Acad. Sci. USA* 1988, 85, 427.
6. Vermaas, W. F. J.; Rutherford, A. W.; Hansson, Ö. *Proc. Natl. Acad. Sci.* 1988, in press.
7. Wasielewski, M. R.; Johnson, D. G.; Seibert, M.; Govindjee *Proc. Natl. Acad. Sci. USA* 1989, 86, 524.
8. Breton, J.; Martin, J.-L.; Fleming, G. R.; Lambry, J. C. *Biochemistry* 1988, 27, 8276.
9. Trebst, A. *Z. Naturforsch.* 1986, 41C, 240.
10. Michel, H.; Deisenhofer, P. in *Encyclopedia of Plant Physiology: Photosynthesis III*, A. C. Staehelin, C. J. Arntzen, eds., Springer-Verlag: Berlin, 1986, pp. 371-381.
11. Michel, H.; Deisenhofer, J. *Biochemistry* 1988, 27, 1.
12. Nanba, O.; Satoh, K. *Proc. Natl. Acad. Sci. USA* 1987, 84, 109.
13. Barber, J.; Chapman, D. J.; Telfer, A. *FEBS Lett.* 1987, 220, 67.
14. Deisenhofer, J.; Epp, O.; Miki, K.; Huber, R.; Michel, H. *J. Mol. Biol.* 1984, 180,

- 385.
15. Deisenhofer, J.; Epp, O.; Miki, K.; Huber, R.; Michel, H. *Nature (London)* 1985, 318, 618.
 16. Michel, H.; Epp, O.; Deisenhofer, J. *EMBO J.* 1986, 5, 2445.
 17. Allen, J. P.; Feher, G.; Yeates, T. O.; Rees, D. C.; Deisenhofer, J.; Michel, H.; Huber, R. *Proc. Natl. Acad. Sci. USA* 1986, 83, 8589.
 18. Allen, J. P.; Feher, G.; Yeates, T. O.; Komiya, H.; Rees, D. C. *Proc. Natl. Acad. Sci. USA* 1986., 84, 5753.
 19. Allen, J. P.; Feher, G.; Yeates, T. O.; Komiya, H.; Rees, D. C. *Proc. Natl. Acad. Sci. USA* 1986., 84, 6162.
 20. Chang, C. H.; Tiede, D.; Tang, J.; Smith, U.; Norris, J.; Schiffer, M. *FEBS Lett.* 1986, 1987, 38, 561.
 21. Williams, J. C.; Steiner, L. A.; Feher, G.; Simon, M. J. *Proc. Natc. Acad. Sci. USA* 1984, 81, 7303.
 22. Williams, J. C.; Steiner, L. A.; Ogden, R. C.; Simon, M. J. *Proc. Natc. Acad. Sci. USA* 1983, 80, 6506.
 23. Youvan, D. C.; Bylina, E. J.; Alberti, M.; Begusch, H.; Hearst, J. E. *Cell* 1984, 37, 949.
 24. Hearst, J. E.; Sauer, K. *Z. Naturforsch.* 1984, 39C, 421.
 25. Tang, D.; Johnson, S. G.; Jankowiak, R.; Hayes, J. M.; Small, G. J.; Tiede, D. M. in *Perspectives in Photosynthesis* (J. Jortner and B. Pullman, eds.), Kluwer Academic Press: Dordrecht/Boston/London, 1989, pp. 23-38.
 26. Tang, D.; Jankowiak, R.; Yocum, C. F.; Seibert, M.; Small, G. J. *J. Phys. Chem.*

- 1990, submitted.
27. Tang, D.; Jankowiak, R.; Seibert, M.; Small, G. J. *Photosynthe. Res.*, submitted.
 28. Small, G. J.; Jankowiak, R.; Seibert, M.; Yocum, C. F.; Tang, D. in *Proceedings of the Feldafing II Workshop on Structure and Function of Baterial Reaction Centers (Michel-Byerle, Ed.) Springer-Verlag: Berlin*, submitted.
 29. Seibert, M.; Picorel, R.; Rubin, A. B.; Connolly, J. S. *Plant Physiol.* 1988, 88, 303.
 30. McTavish, H.; Picorel, R.; Seibert, M. *Plant Physiol.* 1989, 89, 452.
 31. Gounaris, K.; Chapman, D. J.; Barber, J. *Biochim. Biophys. Acta* 1989, 973, 296.
 32. Dekker, J. P.; Bowlby, N. R.; Yocum, C. F. *FEBS Lett.* 1989, 254, 150.
 33. Ghanotakis, D. E.; de Paula, J. C.; Demetron, D. M.; Bowlby, N. R., Peterson, J.; Babcock, G. T.; Yocum, C. F. *Biochim. Biophys. Acta* 1989, 974, 44.
 34. Kobayashi, M.; Maeda, H.; Watanabe, T.; Nakane, H.; Satoh, K. *FEBS Lett.* 1990, 260, 138.
 35. Scherz, A.; Braun, P.; Greenberg, B. M. *Biochemistry* 1990, in press.
 36. Tetenkin, V. L.; Gulyaev, B. A.; Seibert, M.; Rubin, A. B. *FEBS Lett.* 1989, 250, 459.
 37. Breton, J. in *Perspective in Photosynthesis (J. Jortner, B. Pullman, eds.) Kluwer Academic Press: Dorecht/Boston/London*, 1989, pp. 23-38.
 38. Vink, K. J.; de Boer, S.; Plijter, J. J.; Hoff, A. J.; Wiersma, D. A. *Chem. Phys. Lett.* 1987, 142, 433.
 39. Hayes, J. M.; Small, G. J.; Tiede, D. M.; *J. Phys. Chem.* 1988, 92, 4012.
 40. Hayes, J. M.; Gillie, J. K.; Tang, D.; Small, G. J.; *Biochim, Biophys. Acta* 1988, 932, 287.

41. Johnson, S. G.; Tang, D.; Jankowiak, R.; Hayes, J. M.; Small, G. J.; Tiede, D. M.
J. Phys. Chem. 1990, in press.

ACKNOWLEDGEMENTS

This dissertation is dedicated to my parents for their encouragements, love and support throughout my educational experience. Their guidance during my childhood are most responsible for what I am today.

I would also like to express my sincere thanks and gratitude to Prof. Gerald J. Small for his help, guidance and unfaltering encouragement throughout this work. The completion of this dissertation would not have been possible without his helpful advice and patient discussion.

I would also like to thank Dr. Ryszard Jankowiak and Dr. John M. Hayes for their help and advice with experimental details and theoretical understanding. Dr. Ryszard Jankowiak has assisted me in various aspects of this work and thus deserves a very special thanks. My acknowledgement also goes to Dr. Stephen Johnson for the collaboration on the project of bacterial reaction centers.

I also want to acknowledge and thank Dr. David M. Tiede, Dr. Michael Seibert and Dr. Charles F. Yocum for providing samples for this research.

I am also grateful to my brother Dezheng Tang for his constant encouragement and companionship.

This work was supported by the Ames Laboratory of U.S. Department of Energy and Department of Chemistry.